Biofiltration of Hydrogen Sulphide and Toluene Using a Novel Biological Activated Carbon Biotrickling Filter

Liang Juan

School of Civil & Environmental Engineering

A thesis submitted to the Nanyang Technological University
in fulfilment of the requirement for the degree of
Doctor of Philosophy

2007

ACKNOWLEDGMENTS

The author would like to express her sincere gratitude and great appreciation to her research supervisor, A/P Lawrence C. C. Koe, for his unmatched concern, invaluable suggestions, support and encouragement throughout the project.

The author would like to acknowledge all the Environmental Laboratory staff, especially Mrs. Phang-Tay Beng Choo, Mr. Yong Fook Yew, and Mr. Aw Wah Beng, for their kind assistance throughout the project.

The author would also like to thank her fellow research scholars, especially Mr. Tong Dongjin, Miss Duan Huiqi, for their kind help, co-operation, encouragement and friendship.

The author also wishes to thank her family members for their constant support, encouragement and patience throughout the period of her studies in Singapore.

Finally, the author wishes to express her gratitude to the Nanyang Technological University for awarding the Research Scholarship, which enabled her to pursue a higher degree.

TABLE OF CONTENTS

SUMMARY

In this study, granular activated carbon (GAC) was chosen as the packing material to test potential improvements to current biofiltration processes by investigating the use of a novel support medium for mixture gases removal. Carbon characteristics were investigated to study its feasibility as a packing material for biofiltration. The experimental data showed that GAC had a large surface area, porous structure, neutral pH, high adsorption capacity and uniform shape that were favorable for use as a medium of biofiltration. Immobilization tests indicated that microorganisms grew rapidly and formed a satisfactory biofilm on the carbon surface. The results of this study demonstrated that GAC with biofilm formed a novel packing medium termed in this study as biological activated carbon (BAC).

Experiments were firstly conducted to evaluate the BAC capacity in a bench biofilter. BAC presented a better performance than GAC as a pure gas pollutant adsorbent. The adsorption capacity of GAC for H_2S and toluene was exhausted eventually; however, the performance of BAC was kept at a high and stable level during the operation. Toluene gas at low concentration of 0-200ppmV did not impact the H_2S biodegradation. 1ppmV of H_2S would not influence toluene removal but 5ppmV had an adverse effect. After the biofilter operation, the characteristics changes of the carbon were monitored. It was observed that GAC particles allowed biological growth on the surface of the carbon granules and also in pores that were sufficiently large for microbial cells. The inner portion of the particle was largely inaccessible as the inner pores were smaller than microbial cells.

The application of the novel packing medium for treatment of gas mixer was evaluated in three experimental biotrickling filters—a neutral pH single-stage biotrickling filter, a low pH single-stage biotrickling filter and a two-stage biotrickling filter, to evaluate the capacity of the BAC for the treatment of both H_2S and VOCs. Results demonstrated that BAC biotrickling filters obtained high removal efficiencies for both H_2S and VOCs. At a GRT of 15s and inlet

concentration of 50ppmV, the toluene removal efficiency of the two-stage biotrickling filter, the neutral pH single-stage biotrickling filter and the low pH single-stage biotrickling filter was 96%, 94%, 86%, respectively. The H_2S removal efficiency of the two-stage biotrickling filter (20ppmV inlet), the low pH single-stage biotrickling filter (20ppmV inlet) and the neutral pH single-stage biotrickling filter (5ppmV inlet) was 95%, 92%, 90%, respectively at a GRT of 3.75s. The three biotrickling filters showed a similar behavior regarding the toluene elimination capacity as a function of loading rate, i.e. the elimination capacity increased linearly with the increasing inlet loading until it reached an equilibrium value which is defined as the maximum elimination capacity of the biotrickling filter. The maximum elimination capacities of toluene in the three biotrickling filters were 310g/m^3·h (the two-stage biotrickling filter) > 280g/m^3·h (the neutral pH single-stage biotrickling filter) > 205g/m^3·h (the low pH single-stage biotrickling filter). All the H_2S elimimination capacities of the three biotrickling filters increased linearly with the increasing inlet loading but could not achieve the maximum value due to the low inlet loading rate. However, the H_2S elimimination capacities order of three biotrickling filters was the two-stage biotrickling filter > the low pH single-stage biotrickling filter > the neutral pH single-stage biotrickling filter according to the experimental curves. Based on the experimental results, the two-stage biotrickling filter performance was the best among the three biotrickling filters tested because degrading microorganisms grew in different environments and the two-stage bioreactor allowed for separate media beds of different microorganisms. In a two-stage bioreactor system, most H_2S was degraded in the first stage and this protected the second stage from significant acidification. Toluene was removed chiefly during the second stage which was operated at a neutral pH. GRTs exceeding 3s for H_2S removal or 12s for toluene removal were required to obtain high removal efficiency in the two-stage bioreactor. The main degradation product of H_2S was sulphuric acid while most toluene was converted to carbon dioxide, water and biomass.

The removal mechanisms of the BAC were investigated after the biotrickling filter operation. To a large extent, the performance of the BAC systems was controlled by

the additive contributions of two removal mechanisms (adsorption and biodegradation). During the start-up period, before a fully functional biofilm had been developed, the substrate was removed primarily by adsorption. After the biofilm was established and the steady-state conditions were reached, system performance was dominated by biodegradation. However, under shock loading, the activated carbon could operate like a buffer: it protected the immobilized microorganisms by adsorbing toxic pollutant concentrations and set low quantities of the adsorbed pollutant free for biodegradation gradually. In conclusion, the BAC system combining adsorption and bioregeneration has the following advantages: faster development of the biomass; resistance to shock loading; stable and good performance; allowing the treatment of hydrophobic biodegradable gases. A mathematical model of the two-stage biotrickling filter was also developed in this work to achieve a better understanding about gas mixture treatment.

In general, BAC as a novel packing medium could achieve excellent performance for gas mixture treatment due to the interaction of adsorption and biodegradation. BAC biotrickling filters also overcame many problems of conventional biotrickling filters such as bed compaction, acid decomposition and channeling.

LIST OF TABLES

LIST OF FIGURES

NOTATIONS

a_j Extended Langmuir isotherm parameter (m^3/g)

A_S^* Total surface area available for biolayer formation and adsorption per unit volume of biotrickling filter (m^{-1})

A_{Sj} Biolayer surface area per unit volume of reactor, for VOC j (m^{-1})

b_j Extended Langmuir isotherm parameter (m^3/g)

C_j Concentration of substance j in the air at a position h along the biotrickling filter (g/m^3)

C_j^* Equilibrium pollutant j concentration in the gas phase (g/m^3)

$C_{j,0}$ Value of C_j at t=0 (g/m^3)

C_{ji} Value of C_j at h=0 (g/m^3)

$C_{ji,0}$ Value of C_j at $h=0$ and $t=0$ (g/m^3)

C_{jP} Concentration of substance j on the solid particle (g of pollutant j-adsorbed/g particle)

C_O Oxygen concentration in the air at a position h along the biotrickling filter (g/m^3)

C_{Oi} Oxygen concentration in the air at the inlet of the biotrickling filter (g/m^3)

$\overline{C}_j$ Dimensionless concentration of pollutant j in the air difined as $\overline{C}_j = C_j/C_{ji}$

$\overline{C}_j^*$ Dimensionless equilibrium concentration of pollutant j defined as $\overline{C}_j^* = C_j^* / C_{ji}$

$\overline{C}_{jP}$ Dimensionless concentration of substance j on the solid particle defined as $(1-\upsilon)\,\rho_P\ C_{jP}/\upsilon\ C_{ji}$

$\overline{C}_O$ Dimensionless concentration of oxygen in the air defined as $\overline{C}_O = C_O/C_{Oi}$

D_{jA} Diffusion coefficient of substrates in air (cm^2/s)

D_j Dispersion coefficient of substrates in air (cm^2/s)

D_O Dispersion coefficient of oxygen in air (cm^2/s)

D_{jW} Diffusion coefficient of substrates in water (m^2/s)

D_{OW}	Diffusion coefficient of oxygen in water (m^2/s)
$f(X_V)$	Ratio of diffusivity of a compound in the biofilm to that in water
h	Position in the column (m)
H	Total height of the biotrickling filter bed (m)
k_j	Mass transfer coefficient between the gas and the solid particle (m/h)
k_{jd}	Freundlich isotherm parameter for substrate j
K_O	Constant in the specific growth rate expression of a culture, expressing the effect of oxygen (g/m^3)
K_j	Constant in the specific growth rate expression of a culture growing on compound j (g/m^3)
K_{Ij}	Inhibition constant in the specific growth rate expression of a culture growing on compound j (g/m^3)
m_j	Diffusion coefficient for the substance j/water system
m_O	Diffusion coefficient for the oxygen-in -air/water system
n_j	Freundlich isotherm parameter for substrate j removal
S_j	Concentration of pollutant j at a position x in the biolayer at a point h along the column (g/m^3)
$S_{j,0}$	Value of S_j at $t=0$ (g/m^3)
S_O	Oxygen concentration at a position x in the biolayer at a point h along the column (g/m^3)
$\overline{S}_j$	Dimensionless concentration of pollutant j in the biolayer defined as $\overline{S}_j = S_j/K_j$
t	Time (h)
u_g	Superficial air velocity in the biotrickling filter (m/h)
X_V	Biofilm density (kg/m^3)
X	Position in the biolayer (m)

Y_j	Yield coefficient of a culture on VOC j (g-biomass/g-compound j)
Y_{Oj}	Yield coefficient of a culture on oxygen (g-biomass/g-oxygen)
Z	Dimensionless positon in the biotrickling filter ($Z=h/H$)

Greek Symbols

a	Fraction of total surface area available for biofilm formation
δ	Effective biolayer thickness (m)
ξ	Dimensionless time defined as $u_g\ t/H$
θ	Dimensionless position in the biolayer defined as x/δ
μ_j	Specific growth rate (h^{-1})
μ_j^*	Constant in the specific growth rate expression (h^{-1})
τ	Space time (h)
β_{1j}	Dimensionless group defined as $D_{jW}\ Ha\ A_S^*\ f(X_V)\ K_j/\upsilon\ u_g\ C_{ji}\ \delta$
β_2	Dimensionless group defined as $D_{OW}\ Ha\ A_S^*\ f(X_V)\ K_O/\upsilon\ u_g\ C_{Oi}\ \delta$
χ_j	Dimensionless group defined as $H(1-a)\ A_S^*\ f(X_V)\ K_j/\upsilon\ u_g$
ϕ_{1j}	Dimensionless group defined as $D_{jW}\ H\ f(X_V)\ /\ u_g\ \delta^2$
ϕ_2	Dimensionless group defined as $D_{OW}\ H\ f(X_V)\ /\ u_g\ \delta^2$
η_{1j}	Dimensionless group defined as $H\ \mu_j X_V/\ Y_j\ K_j\ u_g$
η_{2j}	Dimensionless group defined as $H\ \mu_j X_V/\ Y_{Oj}\ K_O\ u_g$
ε_j	Dimensionless Henry's coefficient for j defined as $C_{ji}\ /K_j\ m_j$
Pe_j	Peclet number of substrate j defined as $u_g H/\upsilon\ D_j$
Pe_O	Peclet number of oxygen defined as $u_g H/\upsilon\ D_O$
λ_{1j}	Dimensionless group defined as $\rho_P\ (1-\upsilon)/\upsilon$
λ_{2j}	Dimensionless group defined as $b_j\ C_{ji}$
υ	Packing material porosity
ρ_P	Density of the solid particles (g/m^3)

CHAPTER ONE

INTRODUCTION

1.1 Background

The nuisance impact of air pollutant emissions from Wastewater Treatment Plants (WWTPs) is a major issue of concern to environmental engineers all over the world. WWTPs off-gases usually contain a mixture of odours and VOCs. Odour nuisance and regulations concerning the emission of VOCs require WWTPs to treat these off-gases.

H_2S is the major contributor of odours at WWTPs and is often used as an indicator of the degree of odour by many researchers. Toluene, which is an excellent surrogate for relatively easily biodegradable VOCs, is also widely found among WWTPs off-gases. In this research, therefore, H_2S is chosen as the model odorous compound and toluene as the model VOC.

An emerging, cost-effective technology for air pollution control is biological waste air treatment technology, which uses microorganisms to metabolize the off-gases contaminants and to convert them to benign end products such as water and carbon dioxide (CO_2). One promising and widely used bioreactor for air pollution control is the biotrickling filter.

Biotrickling filters work by passing a stream of contaminated air through a water trickling packed bed of organic or synthetic material on which pollutant-degrading microorganisms are naturally immobilized. As the air passes through the bed, the contaminants in the air phase sorb into the biofilm and onto the filter medium, where they are then biodegraded. The elimination of a gaseous pollutant in a biotrickling filter is the result of a complex combination of different

physicochemical and biological phenomena: absorption, adsorption, degradation, and desorption (Derek and Joseph, 1999).

The overall effectiveness of a biotrickling filter is largely governed by the properties and characteristics of the support medium, which include porosity, degree of compaction, water retention capabilities, and the ability to host microbial populations. Traditional packing media have some problems such as compaction, acid degradation and frequent replacement (Kennes and Veiga, 2001). In this study, GAC, which has adsorbing properties that are not encountered in other materials, is chosen as the packing material for its unique physical and chemical properties. Therefore BAC can produce a system in which both adsorption and biodegradation contribute to pollutants removal. So far limited studies have been published about this novel packing medium for air pollution control. The changes of carbon characteristics during operation are unknown as well. This investigation into the application of BAC will provide new insights on the use of this novel medium for the removal of odorous H_2S and VOCs.

Many studies have explored the use of bioreacters for the removal of H_2S or VOCs, individually (Cox and Deshusses, 1999; Koe and Yang, 1999; Li et al., 2002; Patricio et al., 2003). However, very few studies were carried out to study the biological treatment of off-gases that contain both H_2S and VOCs. The typical metabolic product of H_2S oxidation by *Thiobacillus sp.* is sulphuric acid, which will decrease the pH inside a bioreactor rapidly. Most *Thiobacillus sp.* are autotrophic organisms and thus they do not use VOCs as carbon sources for growth. On the other hand, VOCs are degraded by heterotrophic microorganisms, which are thought to be most effective at a neutral pH. Most biotrickling filter researchers have assumed that removal efficiency for VOCs decreases when pH declines and early researches supported this assumption (Derek and Joseph, 1999; Cox and Yang, 2002). Low pH conditions contribute to organic medium degradation, compaction and flow short-circuiting, which can shorten the medium life span. Buffers, such as oyster shells (Ergas et al. 1995), have been added to the medium to avoid pH decrease. The medium may also be regularly washed to help control pH (Yang and

Allen, 1994). However, in practical applications, it is difficult and expensive to control pH and the medium has to be replaced when its alkalinity is completely exhausted (Webster et al., 1996). In addition, maintaining the uniformity of the neutral pH in the medium may be difficult, because the irrigation water may not trickle through it uniformly. These apparently conflicting pH optima for microbial activity are a challenge for developing bioreactors for simultaneous removal of both H_2S and VOCs.

A two-stage bioreactor may solve these problems. The first stage, where an inert and acid resistant medium can be used, can be designed to remove H_2S at a low pH condition. The second stage is designed to remove VOCs at a neutral pH. Because H_2S removal is confined to the first stage, there is no acid production in the second stage. However, some researchers are still studying the co-treatment of a mixture gas of H_2S and VOCs in a single bioreactor (neutral pH or low pH) and some degree of good performances have been reported.

1.2 Objective and scope

The objective of this research is, therefore, to study the feasibility and application of BAC as a novel biotrickling filter packing medium, especially for co-treatment of gas mixtures such as H_2S and toluene. To evaluate the performances of BAC biotrickling filters for gas mixture treatment under acidic and neutral pH environment and the removal mechanisms of BAC, three horizontal biotrickling filters, comprising two single-stage biotrickling filters (neutral pH and low pH) and a two-stage biotrickling filter, were used in laboratory experiments.

In order to achieve the above objective, the scope of this study will mainly cover:

1. To study the characteristics of GAC as a packing medium;
2. To investigate the feasibility of BAC production;
3. To study the application of BAC in a bench biofilter;

4. To evaluate the removal capacity and mechanisms of BAC for gas mixture treatment using three horizontal biotrickling filters and compare their performances for gas mixture treatment;
5. To develop the mathematical model possibly explaining the co-treatment of H_2S and toluene;

1.3 Contribution

Packing material is a crucial component of a bioreactor as it is the microbial population's habitat. The use of activated carbon as a biotrickling filter packing medium is attractive. The physico-chemical properties such as large surface area and uniform shape favour the use of carbon as a suitable packing medium. The porous structure and good crushing resistant ability prevent it from bed channeling and compaction often encountered in conventional media. The most important feature is its adsorption capacity. BAC, a novel packing material combining biodegradation and adsorption, may show to have high removal efficiency for air pollutants treatment.

A comparative study of three BAC biotrickling filters was conducted to evaluate the application of this novel medium and biotrickling filter capacity for gas mixture removal. The BAC biotrickling filters developed in this study produce better performance than the biotrickling filters treating similar pollutants reported in previous published literature (Todd et al., 1996; Cox and Deshusses, 2001; Cox and Yang, 2002). The two-stage biotrickling filter demonstrated superiority over the two single-stage biotrickling filters. Various optimum operation parameters were provided as references. The experimental data were validated by a complete and complex mathematical model. In summary, this thesis offers a novel packing medium and an effective biotrickling filter style for removal of a gas mixture such as H_2S and toluene.

1.4 Outline of the report

This thesis evaluates the feasibility and application of a novel packing material named as BAC for H_2S and toluene removal. The organization of the thesis is as follows. The significance and background information of this study are summarized in Chapter One. Chapter Two introduces the biofiltration system, microorganisms for H_2S and toluene degradation, GAC as a packing medium, and reviews the history and current status of the biofiltration system. In Chapter Three, the materials and methodologies used in this study are described in detail. Chapter Four investigates the feasibility of BAC development and the performance of BAC in a bench biofilter. Chapter Five discusses the performances of three different horizontal BAC biotrickling filters for gas mixture treatment under acidic and neutral pH conditions, and the removal mechanisms of BAC. A mathematical model to describe the kinetics of gas mixture removal in biotrickling filters is outlined in Chapter Six. Conclusions and recommendations for future studies are presented in Chapter Seven.

CHAPTER TWO

LITERATURE REVIEW

2.1 Characterization of WWTPs waste air contaminants

Wastewater Treatment Plants (WWTPs) are the primary means for treating wastewater. Emission of air pollutants from WWTPs includes odour compounds (such as H_2S and ammonia) and a wide range of Volatile Organic Carbons—VOCs (such as aromatics and chlorinated species). They arise from pump station, bar screens, sludge holding tank and other facilities that handle wastewater and sludge. Odours and VOCs are strongly odorous and hazardous air pollutants, which cause complaints from neighbors. These emissions also cause severe environmental problems such as photochemical smog. The nuisance impact of air pollutant emissions from WWTPs is a major issue of concern to environmental engineers all over the world, and odour nuisance regulations concerning the emission of VOCs require WWTPs to treat their off-gases.

In comparison with air emissions from industrial sources, emissions from WWTPs differ significantly because of the following:

1. Emissions from WWTPs contain compounds at relatively low concentrations. H_2S concentration ranges from ppbV level to several hundred ppmV. VOCs are usually 50ppbV to 10ppmV of a single component (Ergas et al., 1995);

2. Emissions from WWTPs contain mixtures of compounds, including relatively degradable VOCs (methanol, toluene, acetone), relatively nondegradable VOCs (chloroform, MTBE, trichloroethene), H_2S, ammonia (NH_3) and others;

3. Large temporal variations in compound concentrations occur for WWTPs emissions. There is, therefore, a need for control systems to have certain buffering capacities.

2.1.1 Properties and characteristics of H_2S

H_2S is the major contributor of odours and is often used as an indicator to the degree of odour by many researchers. In this research, therefore, H_2S is chosen as the model odorous compound. It is a colourless, flammable, poisonous gas with the odour of rotten eggs. Table 2.1 shows the basic physical and chemical properties of H_2S (Bowker et al., 1989).

Table 2.1 Physical and chemical properties of H_2S

Molecular weight	34.08
Boiling point, °C	-60.2
Melting point, °C	-83.8 to -85.5
Vapour pressure, -0.4°C 25°C	10atm 20atm
Specific gravity (relative to air)	1.192
Auto ignition temperature, °C	250
Explosive range in air, %	4.5 to 45.5

Table 2.2 Effects of H_2S gas on humans

Concentration, in ppmV (parts per million by volume)	Effect
<0.00021	Olfactory detection threshold
0.00047	Olfactory recognition threshold
0.5 to 30	Strong odour
10 to 50	Headache, nausea, and eye, nose, and throat irritation
50 to 100	Eye and respiratory injury
300 to 500	Life threatening (pulmonary edema)
700 or more	Immediate death

H_2S is an extremely toxic substance. It can cause odour nuisance at concentration as low as 8 ppbV (Smet and Langenhove, 1998) and corrosion problems in the sewer systems (Islander et al., 1990). The effects of H_2S gas on humans at different concentrations are shown in Table 2.2 (ASCE, 1989).

2.1.2 Properties and characteristics of toluene

VOCs are liquids or solids that contain organic carbon (carbon bonded to carbon, hydrogen, nitrogen, or sulphur, but not carbonate carbon as in $CaCO_3$ or carbide carbon in CaC_2, CO or CO_2), which vaporize at significant rates. The common VOCs include aromatics (e.g., toluene, benzene, xylene), aldehydes (e.g., acetaldehyde, formaldehyde), ketones (e.g., acetone, methyl ethyl ketone) etc.

VOCs are contributors to the problem of photochemical oxidants (smog, ozone). Some VOCs are also powerful infrared absorbers and thus contribute to the greenhouse problem (de Nevers, 1995). VOCs are readily absorbed by the lung, gastrointestinal tract, and in liquid form, the skin. They may bioaccumulate in lipid tissues in the body. All the VOCs are known to cause both acute and chronic central nervous system (CNS) diseases (Forst and Cornroy, 1998). Since 1990, the control of VOCs in waste gases has become a major air pollution concern.

Toluene, which is widely found among WWTPs off-gases, is an excellent surrogate for relatively easily biodegradable VOCs and so is selected as the model VOC in this study. Toluene is a clear, colorless liquid with a distinctive sweet and pungent smell. Its odour threshold is 2.9 ppmV. It is used as a solvent, in the production of many chemicals, perfumes, medicines, dyes, explosives, and detergents. The physical and chemical properties of toluene are shown in Table 2.3 (Card, 1998).

Toluene ranks among the most toxic and hazardous substances produced, and it is included in the U.S. Environmental Protection Agency Superfund List and the 189 hazardous air pollutants in the 1990 Clean Air Act Amendments (CAAA). Human exposure to small amounts of toluene can irritate the skin, nose, throat, eyes and

cause tiredness, weakness, and loss of appetite. Repeated exposures can damage bone marrow, brain, liver and kidneys, even developing foetus. Short-term exposure to high concentrations can cause one to feel dizzy, light-headed, unconscious, and possible death. No studies have indicated that it can cause cancer, but it may cause mutations.

Table 2.3 Physical and chemical properties of toluene

Molecular formula	C_7H_8
Molecular weight (g/mol)	92.4
Density (g/cm^3)	0.87
Vapour pressure at 25°C (mmHg)	30
Henry's law coefficient ($atm/mol \cdot m^3$)	0.0064201
Henry's law constant (water/gas; unitless)	0.29
Aqueous diffusion coefficient (cm^2/s)	0.0000086
Diffusion coefficient in air (cm^2/s)	0.087
Boiling point (°C)	110.7

2.2 Biological waste gas treatment systems

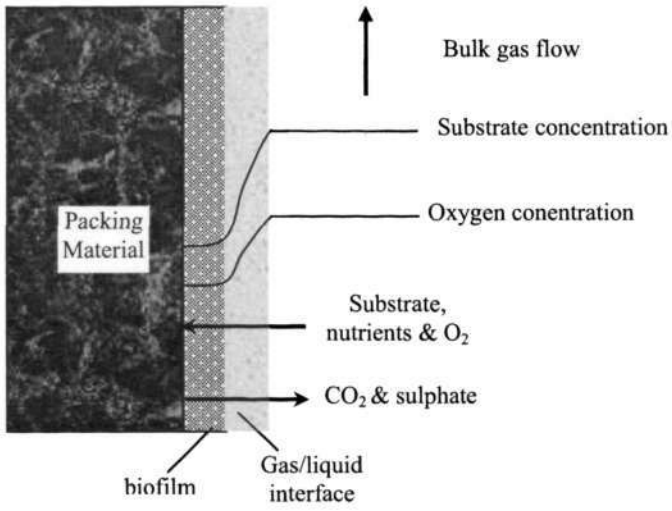

Figure 2.1 Basic principles of a biofilter system

Biological waste gas treatment is an emerging technology for air pollution control. When the waste gases pass through the reactor, the microorganisms attached to the packing material metabolize the contaminants and convert them to benign end products. Figure 2.1 displays the basic principles of a biofilter system (Swanson and Loehr, 1997).

Bioreactors for air pollution control have found most of their success in the treatment of dilute, high flow waste gas streams containing odours or VOCs (Koe et al., 2000; Wu L., 2000; Wu Y., 2000). It offers several advantages such as lower treatment costs, reduced environmental impact, absence of formation of by-products, low energy demand, no need for fossil fuel burning, and low temperature treatment. In the last few decades, the number of application of biological treatment systems for off-gas purification has strongly increased (Abumaizar et al., 1998; Cox et al., 1998; Mason et al., 2000; Koe et al., 2002a).

2.2.1 Classification of biological systems

According to the different behaviors of the liquid phase (which is either continuously moving or stationary in the contact reactor) and of the microorganisms (which are either freely dispersed in the aqueous phase or immobilized on packing materials), biological waste gas treatment technology can generally be categorized into three systems— biofilter, bioscrubber and biotrickling filter, as shown in Table 2.4 (Wu Y., 2000).

Table 2.4 Distinctions of three biological waste gas treatment systems

System	Aqueous phase	Microorganisms
Biofilter	Stationary	Immobilised
Bioscrubber	Mobile	Dispersed
Biotrickling filter	Mobile	Immobilised

Biofilter system includes a bed of packing material in either an open or enclosed container (Figure 2.2). The filter material can be soil, compost, peat, plastic media or other suitable materials. The air stream is humidified to supply moisture before entering the reactor. As the humidified waste gas passes through the biofilter, the air pollutants can be adsorbed by the attached film and then degraded by the microorganisms. In this process, the packing medium provides pH buffer and the necessary nutrient source for microorganisms. Once the buffer or nutrient source is exhausted, the packing material should be re-blended with aqueous solution or nutrient salts and restored into the reactor. For natural organic media, such as compost and peat, replacement of media is needed every two to three years because they will be biodegraded and compacted over time. Acidification (H_2SO_4, HCl) and compression of the packing material over time are the main disadvantages of the biofilter system. From the conventional soil and compost filters, which were used in the early 1950s, a high pressure drop and a non-homogeneous structure were known to exist. In order to reduce energy consumption, the height of such a filter bed was usually 0.5~1.0m, while the initial gas loads applied were usually 5~10 $m^3/m^2 \cdot h$. Fairly long gas retention time (up to several minutes) was needed in order to achieve high removal efficiency (Ottengraf and Diks, 1992). Therefore, this system is efficient in treating air streams containing relatively low concentration gas pollutants.

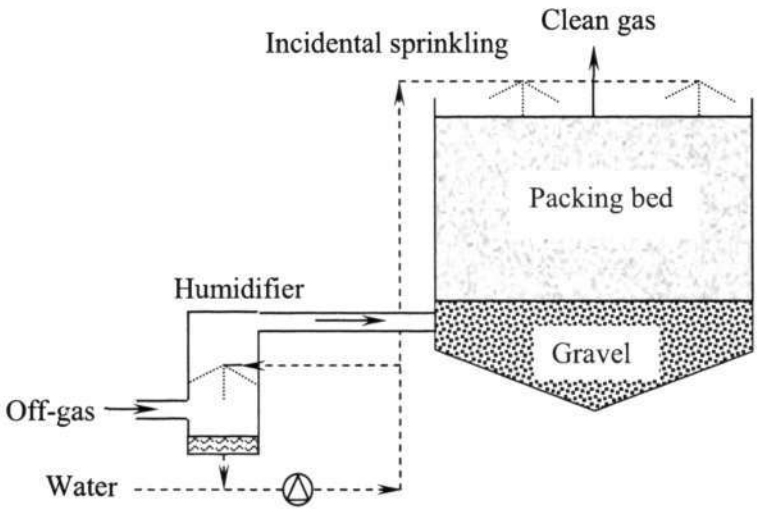

Figure 2.2 Schematic diagram of a biofilter system
(Groenestijn and Hesselink, 1993)

Bioscrubber system normally consists of two interconnected reactors, a scrubber section and a regeneration tank (Figure 2.3). The scrubber section is the contacting unit, where the contaminant is transferred from the gas phase to the liquid phase by bubbling the air up through a mixture of water, support media and biomass. The regeneration tank is the biodegradation unit, where the contaminant undergoes biodegradation. Water-soluble contaminants in the air stream are firstly absorbed into the liquid in the scrubber section, and then passed to the regeneration tank and biodegraded by the employing suspended microorganisms. After the regeneration, the liquid is re-circulated to the scrubber section. Generally, the bioscrubber system is only suitable for treating water-soluble air contaminants, such as H_2S, ammonia, some low-molecular weight amines and alcohol.

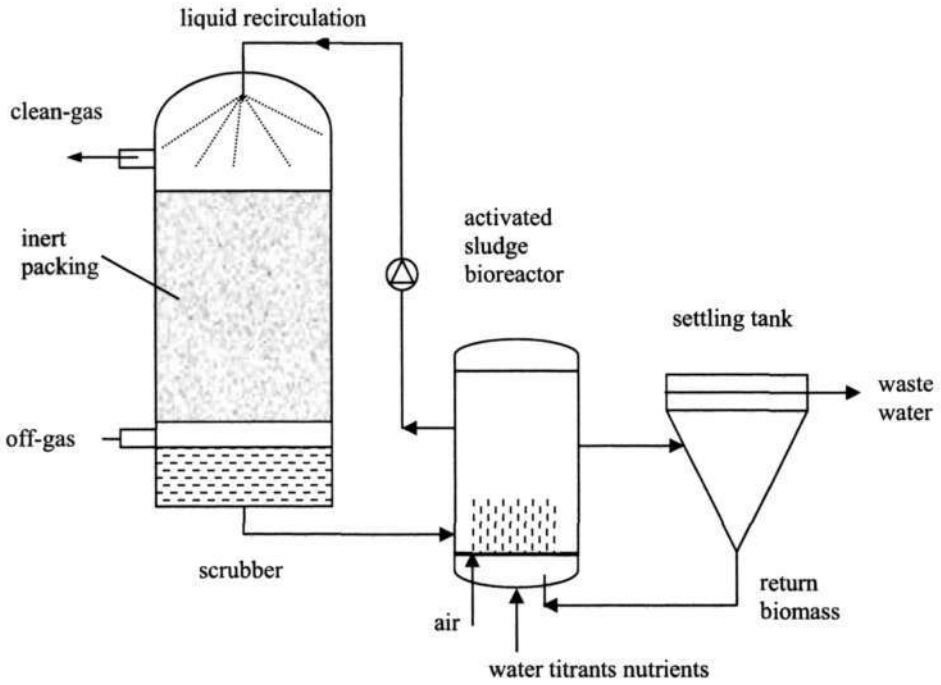

Figure 2.3 Schematic diagram of a bioscrubber system
(Groenestijn and Hesselink, 1993)

Biotrickling filter system is rather similar to a biofilter system. It contains synthetic or inorganic packing materials, such as ceramics, plastics and activated carbon. On the surface of the packing, a biofilm of pollutant degrading microorganisms forms which aerobically degrade the absorbed pollutant. The system is operated with a recycled aqueous phase trickling over the packing media; thus, the nutrients and pH buffering agents can be easily added to the liquid phase. The undesired metabolites can also be easily removed by replacing the re-circulation liquid (Figure 2.4).

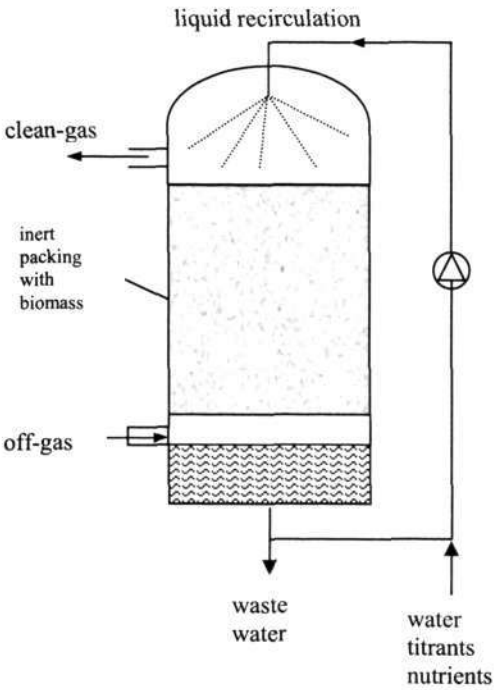

Figure 2.4 Schematic diagram of a biotrickling filter system
(Groenestijn and Hesselink, 1993)

2.2.2 Bacteria for H_2S biodegradation

Like all other biological treatment processes, air biotreatment also relies on microbial reactions for the degradation of waste compounds. Several genera and particular species of microorganisms have been identified as H_2S oxidizers. Genera of the *Chromatiaciae* and *Chlorobiaciae* families use light as an energy source to anaerobically oxidize H_2S to elemental sulfur. *Xanthomonas species*, *Hyphomicrobium species* and *Pseudomonas species* are heterotrophs capable of H_2S oxidation (Anders and Colin, 1995). *Thiobacillus sp.* are probably the most studied genus because of the key role the organisms play in crown corrosion in sewer mains (Islander et al. 1990). They are mostly chemoautotrophic bacteria, using CO_2 as their carbon source and obtaining energy from the oxidation of sulfur compounds. Some species like *T. intermedius* and *T. novellus* are also facultative heterotrophs.

Different Thiobacillus species dominate at different pH ranges. Islander et al. (1990) hypothesized microbial succession in sewer pipes with decreasing pH. At neutral pH, *T. intermedius, T. novellus* and *T. denitrificas* tend to dominate. As the pH decreases to 6, *T. neapolitanus* dominates. When pH declines to 3, *T. thiooxidans*, which grows vigorously between pH 1 to 3, will dominate. Below pH 0.5 acid concentration will become inhibitory even to *T. thiooxidans*. Table 2.5 shows the different pH ranges of the *Thiobacillus sp.* This same microbial succession is expected to occur in biotrickling filters where the initial pH depends on the medium used, which is usually near neutral.

Conversion of H_2S always causes acid accumulation, which results in the pH of the biotrickling filter to fall (down to 2.0). Among these species, only *Thiobacillus thiooxidans* and *Thiobacillus caldus* can thrive in an acidic environment that results naturally from sulphate accumulation. Moreover, they assimilate carbon as carbon dioxide and obtain energy exclusively from the aerobic oxidation of reduced sulphur forms such as H_2S. *Thiobacillus thiooxidan* has, in addition, an outstanding feature for its wide pH range of living environment and high degradation ability of H_2S. These two features help them to occupy a constrained ecological niche that is

characterized by extremely low-pH and low-organic conditions (Padival et al., 1995). Some investigators have seen substantial treatment successes in low pH bioreactors (Yang, 1999; Wu et al., 2001; Koe et al., 2002c).

Table 2.5 Different pH ranges of the *Thiobacillus sp.* (www.dsmz.de)

Thiobacillus sp.	Growth pH range	Optimum pH range
Thiobacillus acidophilus	NA	3.5 - 4.5
Thiobacillus albertis	NA	4.4 - 4.7
Thiobacillus aquaesulis	NA	6.0 - 7.6
Thiobacillus caldus	**1.0 - 5.0**	**1.5 - 2.5**
Thiobacillus cuprinus	3.0 - 7.0	3.5 - 4.0
Thiobacillus denitrificans	NA	6.8 – 7.0
Thiobacillus ferrooxidans	1.4-6.0	2.5 - 5.8
Thiobacillus halophilus	NA	7.3 – 7.5
Thiobacillus hydrothermalis	NA	6.0 – 7.5
Thiobacillus neapolitanus	3.0 - 8.5	6.2 - 7.0
Thiobacillus novellus	5.0 - 9.2	7.8 - 9.0
Thiobacillus plumbophilus	NA	6.0 - 7.0
Thiobacillus prosperus	2.0 - 7.0	2.5 - 3.0
Thiobacillus tepidarius	NA	6.0 – 6.9
Thiobacillus thiooxidans	**0.5 - 6.0**	**2.0 - 3.5**
Thiobacillus thioparus	4.5 - 10	6.6 - 7.2
Thiobacillus thyasiris	NA	7.0 – 7.6
Thiobacillus versutus	NA	7.0 - 8.5

NA: not available

In the process of H_2S biodegradation, H_2S is used as electron donors by the sulphur bacteria. The oxidation of the most reduced sulphur compound, i.e. H_2S, occurs in stages, and the first oxidation step results in the formation of elemental sulphur, S^0. When the supply of H_2S has been depleted, additional energy can be obtained from the oxidation of suphur to sulphate. The final product of oxidation in most cases is sulphate (SO_4^{2-}) and the total number of electrons involved between H_2S (oxidation state, -2) and sulphate (oxidation state, +6) is 8. Less energy is available when the intermediate products are produced like elemental suphur (S^0) and thiosulphate ($S_2O_3^{2-}$) because of limited oxygen (Brock, 1991). Some of these reactions are stated below:

$2HS^- + O_2 \rightarrow 2\,S^0 + 2OH^+$	sulphide	-170.6 KJ/mol
$S^0 + H_2O + 1.5O_2 \rightarrow SO_4^{2-} + 2H^+$	sulphur	-589.1 KJ/mol
$S_2O_3^{2-} + H_2O + 2O_2 \rightarrow SO_4^{2-} + 2H^+$	thiosulphate	-409.4 KJ/mol
$2HS^- + 4O_2 \rightarrow 2SO_4^{2-} + 2H^+$	sulphide	-732.58 KJ/mol

The equations show a two-step process comprising an initial oxidation to elemental sulfur followed by slower additional oxidation to sulfate. The additional oxidization needs much more energy than the initial oxidization. Under oxygen limiting conditions (oxygen concentration is below 0.1mg/L), sulfur is the major end-product of the sulfide oxidation. The accumulation of elemental sulphur in a bioreactor may choke up the small void spaces in fine packing materials like sand media, resulting in the increase of pressure drop and ultimately leading to air channeling. Therefore, satisfactory transportation of mass and oxygen is a great concern in bioreactor design. Note that in the sulphur-oxidation reactions shown above, one of the products is H^+. The sulphuric acid formed by the sulphur oxidizing bacteria would bring about a marked reduction in pH of the medium.

2.2.3 Bacteria for toluene biodegradation

During the past decades, a broad variety of bacteria capable of degrading toluene have been isolated and characterized. A wide range of genera and species are

available and the degradation is found through more than one pathway. The VOCs constitute the main sources of carbon and energy for the metabolism of the aerobic bacteria and are transformed into carbon dioxide, water and biomass. For the degradation of toluene, two approaches are known to be used by different bacteria strains in the initial degradation steps: a methyl group may be oxidized by a monooxygenase to the corresponding alcohol, or the aromatic nucleus may be directly attacked by an oxygenase.

Among the specific species quoted in the literature, pure cultures of *Pseudomonas putida* are undoubtedly the most utilized as good metaboliser of toluene, not only because this microorganism has been proven to be the best for the purpose of metabolic pathway studies but mainly because of its ability to utilize different aromatics, such as toluene, benzene, ethylbenzene, phenol, etc. (Shareefdeen et al., 1993; Zilli et al., 1993; Holden et al., 1997; Villaverde et al., 1997). *P. putida* is unicellular, polar flagellated, aerobic, and gram-negative bacterium, which prefers temperatures ranging from 25~30°C. The cell diameter and length are 0.7~1.1μm and 2.0~4.0μm respectively. Like other pseudomonads, many of its induced enzymes are non-specific and its metabolic pathways contain a high degree of convergence. The convergence of catabolic pathways allows for the efficient utilization of a wide range of growth substrates, while the non-specificity of the induced enzymes allows for the simultaneous utilization of several similar substrates without an excess of redundant genetic coding for enzyme induction (Hutchinson and Robinson, 1988). *P. putida* F1 has also received attention for its ability to co-metabolise the biodegradation of trichloroethene in the presence of toluene and other aromatics (Reardon et al., 2000). Figure 2.5 shows the *P. putida* F1 catabolic pathways for toluene, benzene, and phenol. The aromatic nucleus is deoxygenated at the 2, 3 position, yielding 3-methyl catechol. Finally it enters the Tricarboxylic Acid (TCA) cycle where it is completely oxidized to CO_2, H_2O and biomass.

In most cases, representatives of the genus *Pseudomonas* have very simple nutritional requirements and grow organotrophically at a neutral pH with

temperatures in the mesophilic range. One of the striking properties of the pseudomonads is the wide variety of organic compounds used as carbon sources and as electron donors for energy generation. Some strains utilize over 100 different compounds, and only a few strains utilize fewer than 20. Nutritionally versatile pseudononads typically contain numerous inducible operons because the catabolism of unusual organic substrates often requires the activity of several different enzymes. The pseudononads are ecologically important organisms in soil and water and are probably responsible for the aerobic degradation of many soluble compounds derived from the breakdown of plant and animal materials (Brock and Madigan, 1991).

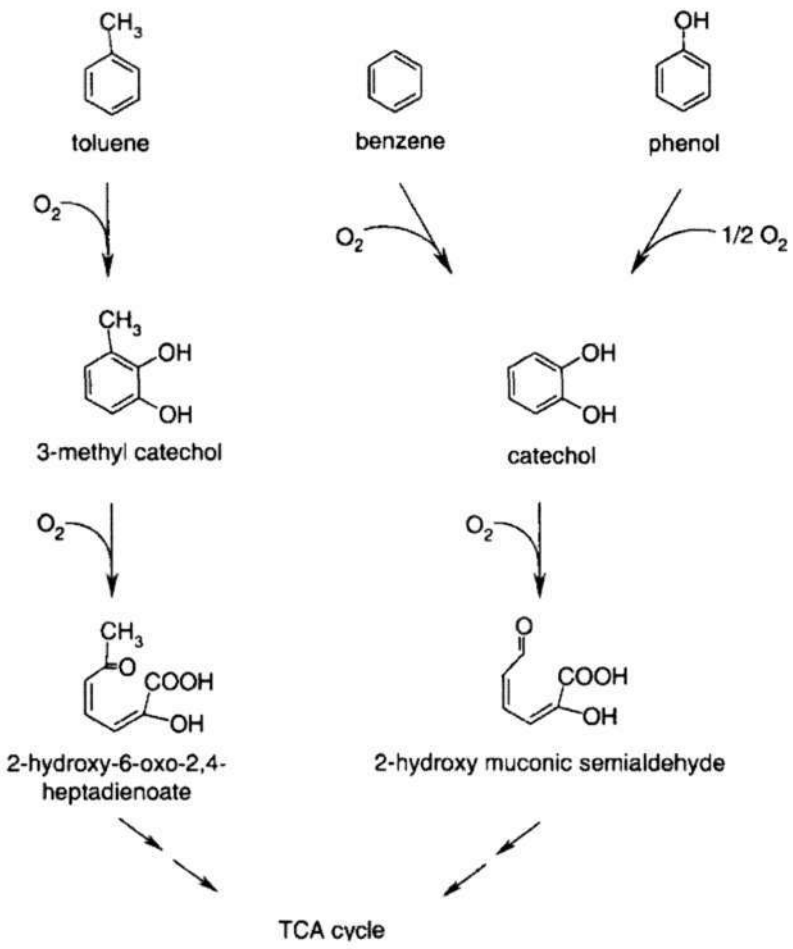

Figure 2.5 *P. putida* F1 catabolic pathways for toluene, benzene and phenol
(Reardon et al., 2000)

Biodegradation of toluene at an extremely low pH condition may be feasible through acclimation of the species present to difficult environmental conditions or by the growth of low-pH-tolerant species. Sewer crowns were found to contain abundant heterotrophs between pH 1.5 to 6. Recent research indicates that these microorganisms may consume VOCs while *Thiobacillus sp.* degrade H_2S (Webster et al. 1997). But limiting values and degradation rates vary from compound to compound. The degradation of aromatic compounds may involve a microbial consortium instead of individual acidophilic bacteria. In the mineralization experiments, Raymond et al. (1998) reported that no defined mixed cultures were able to evolve $^{14}CO_2$ from labeled substrates, while an undefined mixed culture including a fungus, a yeast, and several bacteria successfully metabolized approximately 27% of supplied naphthalene after 1 week. Complete mineralization of the aromatic contaminants at a low pH environment may involve a complex interaction between several distinct groups of microorganisms.

2.2.4 pH control

Medium pH is a key parameter for a biofiltration system, especially important for co-treatment of H_2S and toluene in this study. Biotrickling filter performance is often pH-sensitive because most bacteria grow over the pH range of 4~8. Biodegradation of compounds containing chlorine, sulphur or nitrogen is often expected to cause pH drop through the formation of acidifying products. Some of *Thiobacillus sp.* are able to grow under highly acidic conditions. However, when mixed waste gases are to be treated other than H_2S, the degradation of VOCs might be inhibited under acidic conditions.

Inevitable acid generation will make pH fall to the point where the microbial ecosystem is inhibited. Acidification of the filter bed may also promote decomposition of the organic support medium, which creates channeling and short circuiting problems, resulting in poor performances.

In order to control pH in a biotrickling filter, buffer materials may be added to the medium in the form of calcium carbonate, dolomite or oyster shells. As acid formation continues, buffer capacity can be depleted quickly, requiring replacement of the filter material. The filter bed may also be washed with alkaline solutions. However, the addition of chemicals, such as sodium hydroxide for neutralizing pH is not recommended as it might adversely affect the overall removal efficiency through the accumulation of high salt concentrations and increased ionic strength (Dolfing et al., 1993). Finally, it may be advantageous to operate the biotrickling filter at the low pH. The easiest way to control the pH is to wash it away with an excess of irrigation water. Simple water washing for pH control is not practical at pH 7, but more feasible at pH 1. At pH 1, the water needed to carry the acid away is a million times less.

2.2.5 Packing medium

The packing medium, which supports the microorganisms, is the heart of a biotrickling filter. The medium characteristics affect microbial activity and the biotrickling filter performance. The medium serves to adsorb the contaminants, hence increasing their retention time and chances of oxidation. It is a source of nutrients and humidity for the microorganisms and also serves as a mechanical support for the internal structure of the biotrickling filter (Altaf et al., 1998a). As the nature of the medium will influence both the removal performance and the operational costs, a good packing medium is, therefore, required for a biotrickling filter to provide a stable and high performance. The choice of a good material should be based on the following criteria.

1. Large surface area: the packing medium should provide enough surface area for attachment of microorganisms.
2. Mechanical properties: the filter bed should maintain a stable structure with time. Bed clogging or shrinking due to material decomposition or compaction should be prevented.

3. Sorption capacity: in the event of fluctuating inlet conditions, sorption of the pollutant onto the medium will play an important role in attenuating concentration peaks.
4. Bacterial attachment: the medium should be porous, rough and hydrophilic to enhance microbial attachment and minimize hydraulic shearing.
5. Lifetime: medium replacement is usually necessary for organic media because of its natural decay. Typically, compost lifetime is limited to 3 to 4 years while GAC has an indefinite lifetime (Medina, 1995). In addition, acid production by oxidation of some contaminates can accelerate the decomposition of organic or inorganic media if they contain dissolved elements under acidic conditions.
6. Uniform shape: the ideal filter material should be homogeneous to allow uniform air flow with a low pressure drop.

A large number of materials have been used by many researchers, usually including natural materials such as soil, compost, peat, wood chips and synthetic materials such as ceramic saddles, polyethylene pall rings, activated carbon (Yang and Allen, 1994b; Sorial et al., 1995; Abumaizar et al., 1998; Koe et al., 2001).

The natural media have the advantages of being cheap. However, the media naturally decay over time, causing compaction, channeling and increased pressure head across the bed. The filter media ultimately will need replacement due to decreasing removal efficiency. Synthetic medium is acid resistant, uniform, and has a stable structural integrity and a high porosity. However, it does not contain moisture, nutrients or microorganisms, so these supplements must be added.

Optimization of biotrickling filter media is an ongoing field of research. The characteristics of GAC suggest the potential for an ideal alternative biotrickling filter medium. GAC has a large surface area and porous structure. It is relatively uniform in shape and size, which leads to even distribution of the gas flow. It also has a high adsorptive capacity and so may provide more resistance to shock loading.

2.2.6 Development of activated carbon as a packing medium

Activated carbon has widely been used to remove polluted gases through physical and/or chemical adsorption (Yan et al., 2002). It can also be used to reduce the pollutants concentration variations at the inlet before a biological reactor (Weber and Hartmans, 1995). Essentially, the conventional adsorption technique has two major disadvantages: inadequate exploitation of the adsorptive capacity; the need for thermal regeneration and ultimate disposal of the spent activated carbon (Frank and Peter, 1997). Some researchers found that microorganisms could colonize activated carbon and degrade previously adsorptive contaminants (DiGiano et al., 1984). The lifetime extension and a further increase of cost effectiveness can be achieved if the adsorption process is combined with biological regeneration.

BAC was initially used in water and wastewater treatment. The term BAC was first suggested by Rice and Robson (1982). Figure 2.6 schematically shows the relationships between micropores, macropores and bacteria located in some macropores (Rice and Robson, 1982). GAC contains bacterial colonies on the external surface layer and in some larger macropores. Several studies demonstrate that its use as a biomass carrier produces a system in which both adsorption and biodegradation affect pollutant removal (Zhao et al., 1999; Alexander et al., 2001; Yan et al., 2003).

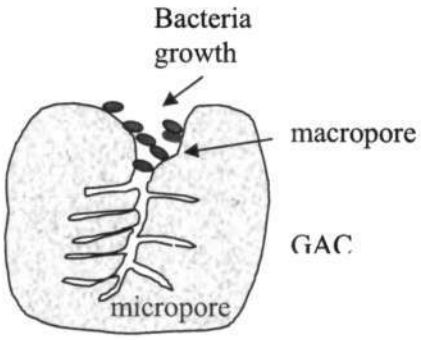

Figure 2.6 Relationships between micropores, macropores and bacteria
(Rice and Robson, 1982)

An advantage of these BAC systems is the faster development of the biomass on the surface of activated carbon than on other material surfaces, which has been experimentally confirmed by Thomas et al. (1992). In his study, the same amount of inoculums was added into two biological systems (GAC with microbial growth system vs. non-activated carbon with microbial growth system) during the start-up period. The time required until effective biodegradation was 200h for GAC biosystem, while the time was 500h for the non-activated carbon biosystem. During the step increases in organic loading, the combination of biological and adsorptive removal capacity resulted in an enhanced pollutant removal and a more stable operation. Many cases have demonstrated that although the adsorption capacity of the activated carbon decreased significantly when a layer of biofilm was formed, the removal efficiency still remained higher than other materials. Zhao et al. (1999) studied the adsorption capacity of biofilm coated activated carbon from a biological fluidized bed reactor. They found that the adsorption capacity of biocoated carbon remained at greater than 70% of initial levels during the first two months, and after six months of operation, the remaining capacity was still over 40%.

The concept of using BAC as a biotrickling filter medium in the field of air pollution control had only been considered in the last ten years. In the investigation of Liu et al. (1994), the BAC biofilter accomplished more than 90% removal efficiency consistently in a gas stream containing 10 to 20ppmV of toluene. In comparison with existing biofilters, this engineered biofilter using synthetic media showed 40 to 80 times greater biodegradation efficiency. Using activated carbon as the packing material of the biofilter provides another advantage, which is the adsorption of gases onto the carbon itself and biofilm instead of the adsorption only onto the biofilm. This allows the treatment of hydrophobic biodegradable gases that would not typically be absorbed into aqueous phase. Activated carbon can be the packing material itself or mixed with other materials. Tang and Hwang (1997) proved that the GAC-compost biofilter had a better transient performance than the chaff-compost and diatomaceous earth (DE)-compost biofilters for toluene gas removal. Combining adsorption and biofiltration technologies is sometimes believed to be a very promising alternative for air pollution control.

2.3 Application of biofiltration for H_2S or/and toluene

2.3.1 Bioreactors for the removal of H_2S/VOCs as single pollutant

Over the past ten years, numerous studies have investigated the effectiveness of biofilters to remove H_2S and VOCs. The following is a non-exhaustive listing of specific compounds that have been removed from waste gas streams with biofiltration: ammonia, H_2S, acetone, benzene, butanol, butyl acetate, dimethyl disulfide, ethanol, hexane, ethylbenzene, acetate, methanol, methyl-ethyl-ketone, styrene, dimethyl sulfide, toluene, xylene isomers, dichloromethane etc. In general, maximum removal performance of compounds in the bioreactor followed the sequence: alcohols > esters > ketones > aromatics > alkanes. Tables 2.6 and 2.7 summarize the operation conditions and performance results for H_2S and toluene removal by different researchers.

As shown in Table 2.6, the relationships between H_2S removal efficiency and operation parameters such as temperature, pH, water content, GRT, loading rate and sulfate concentration (not all listed) have been experimentally determined by several researchers. A variety of packing materials were tested and most of the bioreactors were inoculated with *Thiobacillus sp.*. The maximum elimination capacity reported for H_2S varied from 25 to 140 $g/m^3 \cdot h$ and very high removal efficiency was obtained at a short GRT of about several seconds. The minimum GRT reported for achieving 99% removal efficiency was 5 seconds.

Similar to H_2S, many materials and microorganisms were investigated for toluene biofiltration. GRT for toluene degradation was apparently much longer than H_2S. The reported maximum elimination capacity of toluene was 15~125 $g/m^3 \cdot h$. It was estimated that toluene removal was zero order above inlet gas concentration of 0.7~0.8 g/m^3 and below this concentration toluene removal was roughly first order (Kennes and Veiga, 2001).

Table 2.6 Selected laboratory studies on H_2S removal

Reactor	Filter material	Inoculum	GRT	Removal efficiency	Maximum elimination capacity ($g/m^3 \cdot h$)	Reference
BTF	Pall ring	*Thiobacillus sp.*	5s	99%	—	Koe and Yang, 1999
BTF	Pall ring	*T. thiooxidans*	30s	99%	82	Zhou, 2000
BTF	Pall ring	*T. thiooxidans*	5s	99%	88.3	Wu L., 2000
BTF	Polyurethane foam + activated carbon	Activated sludge	3s	93%	25	Higuchi et al., 1999
BTF	GAC	*Thiobacillus sp.*	5s	> 99%	—	Tong, 2005
BF	compost	No inoculum	23s	> 99%	130	Yang and Allen, 1994a
			7s	93%		
BF	Peat	*T. thioparus*	51s	90%	55	Patricio et al., 2003
BF	GAC	Enrichment culture	5s	> 99%	> 110	Duan et al., 2005a
BF	Lava rock	No inoculum	15s	99%	100	Yang et al., 1999
BF	Beads	*T. novellus*	100s	98%	29.2	Chung et al., 1998

Table 2.7 Selected laboratory studies on toluene removal

Reactor	Filter material	Inoculum	Load ($g/m^3 \cdot h$)	Maximum elimination capacity ($g/m^3 \cdot h$)	GRT	Reference
BTF	—	Rhodococcus sp.	70~220	15~42	1.2s	Kirchner et al.,1989
BTF	Celite pellets	Sample of reactor	60	60	60~120s	Smith et al., 1996
BTF	Pall rings	Enrichment culture	6~150	35	0.53~2.4min	Pedersen and Arvin, 1995
BTF	PP Pall rings	Pseudomonas corrugata	35~225	71~83	56s	Cox and Deshusses, 1999
BTF	Pall rings	Pseudomonas putida	10~2500	>125 (RE=99%)	15s	Wu Y., 2000
BTF	Conditioned biomass	Four specific microorganisms	0~280	165	20~50s	Karim et al., 1997
BF	Celite	Enrichment culture	0~102.2	>101.2	60s	Sorial et al., 1995
BF	Compost	No inoculum	0~65	55	65~165s	Marie et al., 2002
BF	GAC, soil, sewage sludge	Commercial seeding	90	64	1.8min	Medina et al., 1995
BF	GAC	Enrichment culture	30~170	150	25~75s	Li et al., 2002

Note: BTF—biotrickling filter; BF—biofilter

2.3.2 Co-treatment of H_2S and VOCs

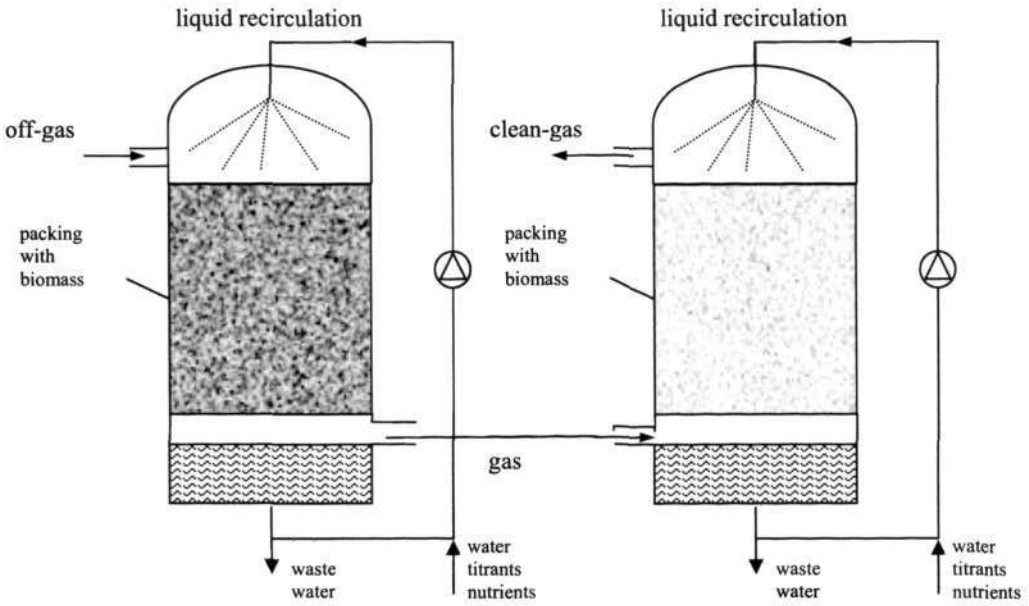

Figure 2.7 Schematic diagram of a two-stage biotrickling filter

Many studies have explored the use of biofilters and biotrickling filters for the removal of H_2S or VOCs as single pollutant (Koe et al., 2002b). However, relatively little is known on the treatment of off-gases that contain both H_2S and VOCs. A major problem is that the product of H_2S oxidation (sulphuric acid) will influence the VOCs removal (preference at a neutral pH). Cox and Yang (2002) studied the odour and VOCs control from a wastewater treatment plant and observed that the removal of VOCs was much higher at a near neutral pH than at a low pH. Several strategies have been suggested for biofiltration of mixture gases. A two-stage biotrickling filter might be used, with the first stage at a low pH to remove H_2S, and the second stage at a neutral pH to remove VOCs. Figure 2.7 shows the schematic diagram of a two-stage biotrickling filter. It is believed that the most optimal way to treat polluted air mixture is to divide the bioreactor into different stages allowing optimal activity of different organisms under different environmental conditions. Alternatively, a single-stage biotrickling filter could be

operated, with extensive efforts to maintain the pH at neutral level. Finally, for some mixtures of compounds, a single low-pH biotrickling filter, using inorganic materials that are unaffected by acid, may remove most of these pollutants.

Derek and Joseph (1999) suggested that a two-stage bioreactor might prevent the interaction of H_2S or VOCs. They designed a full-scale, two-stage biofilter (two tanks) at a wastewater treatment plant. The first stage, called an acid gas biofilter (AGB), was an enclosed system with a medium of small, inert, porous stones (lava rock). The second stage was a traditional open biofilter filled with wood chips. A conventional wood chip biofilter was also designed to compare the removal efficiency. The two-stage and single-stage conventional biofilters had H_2S removal efficiencies of 99.6% and 99.4%, respectively. Data showed that the pH in the single-stage biofilter fell to 2.5 near the inlet by the end of the study. The pH of the second stage in the two-stage biofilter was between 7.9~8.1. The two-stage system presumably would have a longer bed life because the first stage bed was inert and the second stage was protected from acidification by removal of H_2S in the first stage. The weighted average removal of the VOCs was 74.2% in the AGB, 84.1% in the two-stage system and 81.3% in the single-stage biofilter.

Arja et al. (2001) developed a two-stage biotrickling filter for removing a mixture of H_2S, methanethiol (MeSH, CH_4S), and dimethyl sulfide (Me_2S, $(CH_3)_2S$) since the microorganisms for H_2S and Me_2S removal had different pH preferences. The first stage was filled with a 7cm layer of sludge and a 50cm layer of cylindrical ceramics. The second one had a packing material bed of saddle-shaped ceramics. GRT of the first stage varied from 61s to 132s and the second stage was 2min to 4min. The first stage mainly removed most of the H_2S and some of the MeSH at a pH of 2. The second filter removed the rest of MeSH and most of the Me_2S at a pH of 6.5. The maximum sulfur elimination capacity for H_2S in the first stage was 1008 g-S/m^3·day (removal efficiency 99.8%), for Me_2S it was 521 g-S/m^3·day (removal efficiency 43.5%), and for MeSH it varied greatly from 0 to 40 g-S/m^3·day (removal efficiency 0~100%). The maximum sulfur elimination capacity for H_2S in the second stage was 255 g-S/m^3·day (removal efficiency 99.6%), for Me_2S it was

521 g-S/m^3·day (removal efficiency 98.9%), and for MeSH it was 38 g-S/m^3·day (removal efficiency 98.4%).

Hebi et al. (2003) also studied the performance of a two-stage biofilter for a mixture of H_2S, MeSH, Me_2S and dimethyl disulfide (Me_2S_2) removal. H_2S had the highest overall removal efficiency (96%) followed by MeSH and Me_2S (90% and 91% removal, respectively) and Me_2S_2 (81%). Most of the removal of H_2S, MeSH, and Me_2S_2 occurred in the primary biofilter (72% H_2S, 66% MeSH, and 52% Me_2S_2) at a pH of 2.5, while most of the Me_2S removal occurred in the secondary biofilter (64% Me_2S) at a pH about 6.0~7.0.

From the above investigations, usually the first stage could achieve over 99% removal of H_2S at a low pH, and other pollutant compounds were removed chiefly during the second stage at a neutral pH. Therefore, two-stage bioreactors may thus provide a good solution to the problems encountered in the treatment of a mixture of air pollution emissions.

However, there have been reports of studies on co-treatment of a mixture gas of H_2S and VOCs in a single bioreactor where excellent pollutant removal had been obtained.

Ergas et al. (1995) conducted laboratory and field experiments using a pilot-scale compost biofilter to remove H_2S and VOCs from WWTPs. Inlet H_2S concentrations ranged from 1 to 80ppmV with a mean of 20ppmV. The filter bed pH was at 7 because of the available natural buffer. Removals of aromatic VOCs averaged greater than 80% during an 8.5-month field study and were typically greater than 90% to 95%, despite highly variable inlet concentrations (approximately 1000ppbV). Removals of chlorinated VOCs were inconsistent and ranged from none to more than 60%.

Todd et al. (1996) studied GAC and yard waste compost (YWC) biofilters with and without pH control. The contaminants included aromatics, chlorinated

hydrocarbons, aldehydes, and ketones in concentrations of 1 to 75ppbV and H_2S of 1 to 10ppmV. The 16-month field study reactors achieved 99% removal of H_2S, 53% to 98% removal of aromatic hydrocarbons, 37% to 95% removal of aldehydes and ketones, and 0 to 85% removal of chlorinated compounds. The GAC and YWC pilot reactors removed more than 80% and 65% of the total VOCs at the GRT of 17s and 70s. Declining pH had little negative effect on contaminant removals. The low pH GAC bench reactor was less effective in benzene removal, but overall compared well with the pH-controlled reactors. Benzene degrading microorganisms could adjust to slow pH declines.

Todd et al. (1997) conducted further studies to treat the off-gases from a wastewater treatment plant using biofilters. Three GAC biofilters and two yard waste compost biofilters were designed. One GAC biofilter among them was kept at a pH below 2.0. Gas retention time (GRT) was maintained at 1.15min. At the beginning of the experiment, microbial densities on the carbon were two to three orders of magnitude lower than those on the compost. However, by the end of the experiment, all five reactors supported similar microbial densities. At the end of the experiment, when pH values were lowest, microbial densities were at their highest values. They found that the declining pH had little effect on compound removal. The microbial community adjusted to difficult conditions, either through acclimation of individual species or through changing to dominance by low-pH-tolerant species. It might be that some of the low-pH inhibition previously observed by others was actually the result of sulfur toxicity.

Cox and Deshusses (2001) designed two single-stage biotrickling filters to determine the effectiveness of co-treatment of H_2S and toluene. The two identical biotrickling filters were operated with a GRT of 36s, one at pH 4.5 and the other at pH 7.0. The packing medium was polypropylene Pall rings. High concentrations of H_2S (up to 170ppmV) and toluene (up to 2.2 g/m^3) were supplied to investigate the influence of the pH on the maximum performance. A rapid startup (a few days) was observed for both toluene and H_2S removal in the neutral pH biotrickling filter. In the acidic biotrickling filter, toluene degradation started also immediately but at a

lower rate. However, after several weeks of operation the toluene elimination capacity at the low pH reached a steady value identical to that found in the neutral biotrickling filter. Overall, the results presented indicated that effective co-treatment of H_2S and VOCs could be obtained in a single-stage biotrickling filter.

Through their studies, effective co-treatment of H_2S and VOCs could be obtained in single-stage biofiltration. Comparing the performances between the controlled and uncontrolled pH biofiltration, no significant difference were found. The declining pH had little effect on compounds removal because the microbial community adjusted to difficult conditions.

Researchers have different opinions about whether a two-stage bioreactor or a single-stage bioreactor is the optimum one for co-treatment of H_2S and VOCs. In this study, the performances of three BAC biotrickling filters, one two-stage biotrickling filter and two single-stage biotrickling filters (neutral pH and low pH), were investigated not only to demonstrate the capabilities of the novel BAC but also to provide further insights on this issue.

2.4 Development of biofilter modeling

With the development of biofiltration technology, an important step is to derive and experimentally validate mathematical models for the predictive and scale-up calculations. The objective is to help us achieve a better understanding of relationships between pollutant removal, biological activity and packing material, etc. The model also serves as a tool for process engineering design and optimization.

Biofiltration unit can be classified into two categories: biotrickling filters and biofilters. In a biotrickling filter, water is applied continuously and forms a water layer surrounding the biofilm. In contrast, in a biofilter, water is either not applied or is only applied intermittently. The water layer is so thin that it can often be neglected. Accordingly, two mathematical models were developed as a III-phase

(air, water and biofilm) model that is appropriate for biotrickling filter and a II-phase model (air and biofilm) that is appropriate for biofilters (Hebi, 2002).

In this study, intermittent trickling was selected in the biotrickling filters' operation because it had been proven to be better than continuous trickling for the BAC operation during the two-stage biotrickling filter (Section 5.3.4) and by another researcher (Duan, 2005a). The BAC was trickled twice per day (0.8L/min for 30 minutes on each occasion) to complement water and nutrition (Section 3.6). Therefore, mostly the water phase in the packing bed is stationary, more like a biofilter. In many cases, the biofilm occupies the entire water volume, so there is no free water layer. Most of the water may exist as a water-saturated biofilm in the biofilter. According to the above considerations, only the biofilter model is introduced in this section and the model developed in this study is based on Shareefdeen's biofilter model (1994).

A number of researchers have attempted to model biofilters, with the majority of models developed only considering steady state conditions (Ottengraf et al., 1986; Shareefdeen et al., 1993; Ergas et al., 1995). Biofiltration is a technology for treating air emissions which are unlikely to be constant. Thus biofilters are more likely to operate under unsteady state conditions. Hence, questions such as how well a biofilter can respond to variations in volumetric flow rate and concentration are of paramount importance for commercial application of this technology. The existing models can be broadly classified into two groups: steady state models and transient models. Several selected model representatives are described here and the summary is shown in Table 2.8.

2.4.1 Steady state models

Biofilter modeling started in the early 1980s and was based on the earlier work on submerged biofilm models. The earliest extension of these submerged biofilm theories was done by Ottengraf (1986). Ottengraf's model is still most commonly referenced, and many other models were developed from it. In Ottengraf's model, intensive laboratory and pilot-scale experiments with several common VOCs (toluene, ethyl acetate, butyl acetate and butanol) were conducted to determine the overall kinetics of the biofiltration process. It is assumed that the gas phase is in plug flow and excess oxygen is available. The micro-kinetics for substrate elimination in the biofilm can be described by a Michaelis-Menten type expression. However, the model only considers two limiting cases: zero- and first-order kinetics and thus three operational regimes may generally be distinguished:

1. Zero-order kinetics with reaction limitation: the biofilm is fully saturated and fully active at high pollutant concentration, and no reaction free zone exists. The activity of the biofilm surrounding the packing particles is fully used and pollutant elimination is limited by the biological activity in the film. For this situation, the pollutant concentration with respect to filter height is given by:

$$\frac{C_G}{C_{Gi}} = 1 - \frac{hK_0}{C_{Gi}V_a} \tag{2.1}$$

2. Zero-order kinetics with diffusion limitation: the transition between the diffusion controlled and reaction limited regime occurs at the critical gas phase concentration C_{crit}. Below this critical concentration, reaction-free zone exists in the biofilm due to the first order character of the macro-kinetics of the elimination process. For this situation, the pollutant concentration with respect to filter height is determined by:

$$\frac{C_G}{C_{Gi}} = \left[1 - \frac{h}{V_a}\sqrt{\frac{K_0 D_{eff} a}{2mC_{Gi}\delta}}\right]^2 \tag{2.2}$$

3. First-order kinetics: at lower pollutant concentration the biofilm is not saturated. Diffusion in the biofilm will limit compound removal and the removal rate decreases with decreasing pollutant concentration in the off-gas.

The relationship of pollutant concentration with filter height is described using Equation 2.3 in this situation.

$$\frac{C_G}{C_{Gi}} = \exp\left(-\frac{hK_1}{mV_a}\right) \tag{2.3}$$

Where

C_G =gas concentration

C_{Gi}=inlet gas concentration

h =height in the biofilter

K_0=zero-order reaction rate constant

K_1 =first-order reaction rate constant

m =the gas liquid partition coefficient

V_a=the superficial velocity

D_{eff}=the effective diffusion coefficient

δ =the biolayer thickness

a=specific surface area of biofilter media

Based on Ottengraf's model, Ergas et al. (1995) arrived a model which assmed the biofilm had a pollutant concentration profile through its depth. Ergas's model assumed that dispersion was negligible and thus the contaminant rate in the gas phase was adequately described by advection and mass transfer into the biofilm. The mass balance in the gas phase was given by the following equation.

$$Gas: \frac{\partial C_g}{\partial t} = \upsilon \frac{\partial C_g}{\partial Z} + NA_s \tag{2.4}$$

The flux of the contaminant into the biofilm (N) was assumed to be proportional to the film contaminant concentration gradient at the gas/film interface shown in Equation 2.5.

$$N = -D_f \left(\frac{\partial C_f}{\partial X}\right)_{X=0} \tag{2.5}$$

The differential equation to describe the biofilm contaminant concentration shown in Equation 2.6 included expressions for diffusion and contaminant removal due to biodegradation. The biodegradation expression was represented by Monod equation, but simplified to a first-order expression.

$$\text{Film: } \frac{\partial C_f}{\partial t} = D_f \frac{\partial^2 C_f}{\partial X^2} - k' C_f \tag{2.6}$$

Only steady state condition was considered and thus the following analytical expression was obtained.

$$\ln\left(\frac{C_g}{C_{g0}}\right) = -\left(\frac{k' Z A_s \delta}{H_f V}\right)\frac{\tanh\phi}{\phi} \tag{2.7}$$

$$\text{Thiele number } \phi = \sqrt{\frac{k'\delta^2}{D_f}}$$

Where

C_g =gas concentration

C_{g0} =inlet gas concentration

H_f =gas/biofilm equilibrium partition coefficient in biofilm

Z =distance in the biofilter

N =contaminant flux from gas phase to biofilm

A_s =specific surface area of biofilter media

D_f =contaminant diffusivity in biofilm

k' =first-order reaction rate constant

δ =effective biolayer thickness

X =biofilm depth

The above models use simple kinetic models (zero- or first-order) to describe the pollutant biodegradation in the biofilm, which is assumed to have enough oxygen. However, there is now enough experimental evidence to prove that biodegradation kinetics for a compound are more complex than zero- or first-order type kinetics and are different when the compound is present alone or in a mixture with other organic compounds (Chang et al., 1993; Oh et al., 1994). Several studies also show that biofiltration of organic compounds are affected by availability of oxygen (Zarook et al., 1994a & b).

By eliminating some of the major assumptions of the model developed by Ottengraf (1986) and Ergas et al. (1995), like the presence of excess oxygen and simple biodegradation kinetics, Shareefdeen et al. (1993) developed an advanced steady

state model wherein the actual kinetic expressions from shake-flask experiments were used and took into account for the potential limiting effects of oxygen. Shareefdeen's model presented general equations for both the gas and liquid phases. The biodegradation term used did not distinguish between zero- and first-order, but rather used Monod and Andrews type dependence (Equation 2.8). Equations were developed for two compounds, methanol and oxygen. The differential equations were similar to Ergas'model except specific biomass growth rate in the biodegradation kinetic expression. The coupled equations were solved numerically.

$$\mu = \mu^{*}\left(\frac{C_f}{K_a + C_f + \left(C_f^2 / K_i\right)}\right)_{methanol}\left(\frac{C_f}{K_s + C_f}\right)_{oxygen} \qquad (2.8)$$

Where

μ=specific biomass growth rate

μ^{*}=maximum specific growth rate

K_a= constant

K_i=growth inhibition constant

C_f= pollutant concentration in the biofilm

K_s=constant in the specific grouth rate expression of a culture, expressing the effect of oxygen

2.4.2 Transient models

As discussed in the above, researchers have used simple models to describe the steady state of biofiltration system. However, this is not always the case. In practical applications, transient operation is more common than steady state conditions. To describe the transient aspects of biofiltration such as sudden changes in inlet concentration of flowrate, shut down and start-up conditions, etc., a theoretical model is essential. So far, research on the transient performance of biofilters has been rather limited.

Besides the biodegradation kinetics and oxygen limitation, pollutants can be involved in both kinetic interactions and physical interactions regarding their

adsorption on the packing material. The relationship between the adsorption and biodegradation of the gas pollutants by the filter material and microorganisms should be quantitatively taken into account to provide insights into the transient behavior of a biofilter. The model will be highly complex when these aspects are considered. However, it has been reported that kinetic interactions (Oh et al., 1994), oxygen limitations (Zarook et al., 1994a & b), and dispersion effects (Zarook et al., 1997) are very important and cannot be neglected.

Hodge and Devinny (1995) developed a transient model, which treated the porous medium as a two-phase system: the air phase and the water/solids phase. Treating the water and solids as a single phase ignored some important phenomena such as diffusion in the water/biofilm layer and details of the adsorption processes at the water-solid interface. The model separated the effects of contaminant adsorption and biological degradation processes. It also assumed that the pollutant biodegradation followed first-order kinetics and neglected potential effects caused by the availability of oxygen. The equation for the concentration of contaminant in the air included dispersion, advection and transfer to the biofilm/solids phase and could be modeled as:

$$\frac{\partial C}{\partial t} = D\frac{\partial^2 C}{\partial Z^2} - V\frac{\partial C}{\partial Z} - \left(\frac{1-\theta}{\theta}\right)\left[k\left(k_h C - C_{ads}\right)\right] \qquad (2.9)$$

Where

D=diffusivity in void space

V=interstitial velocity

k=transfer rate constant into biofilm

k_h=gas/biofilm partition coeffcient

θ=void fraction

t=time

Z=height of the packing bed

C=concentration in air phase

C_{ads}=concentration in solids/water phase

Deshusses et al. (1995) presented a transient biofiltration model which was also based on the assumptions of excess oxygen and plug flow for the gas phase. However, unlike Hodge and Devinny's model, Michaelis-Menten biodegradation kinetics was assumed to apply in the biofilm, and competitive inhibition was included for the simultaneous degradation of pollutants mixtures. The biofilter height was divided into layers, and within each layer three main sections existed: the gas phase, the biofilm and a liquid sorption volume. The sorption volume was assumed to be equal to the water content of the support material minus the biofilm volume, and no biological reaction took place here. This model was experimentally validated through biofiltration of methyl ethyl ketone (MEK) and methyl isobutyl ketone (MIBK) mixtures considering kinetic interactions.

Based on the earliest steady state model, Shareefdeen et al. developed a series of models for different situations, from a single component to gas mixture, from uniform biofilm to biomass patches, from steady state to transient conditions. Among these models, Shareefdeen's model with patches of biomass (1994) incorporates general mixing phenomena, oxygen limitation effects, adsorption phenomena and general biodegradation reaction kinetics. Significant improvement in the model prediction is observed in comparison to earlier simplified models. This model has been used in describing biofiltration under both transient and steady state conditions. Solutions of the model were presented with and without the assumption of pseudo-steady state for the biofilm leading to approximate and general models, respectively. Based on a thorough literature review, Shareefdeen's model with patches of biomass was found to be a better and more complete transient model to describe the biofilter process. Discussions on this will be provided in detail in Chapter Six.

Table 2.8 Summary of selected biofiltration models

Model		Characteristics	Biokinetics	Solution	Validation on
Steady state model	Ottengraf et al., 1986	Simple, excess oxygen, plug flow	Zero and first-order	Analytical	Compost/peat biofilter
	Ergas, 1995	Pollutant concentration gradient through biofilm depth	Zero and first-order	Analytical	Compost biofilter
	Shareefdeen, 1993	Oxygen limitation, substrate inhibition	Monod and Andrews type	Numerical	Peat/perlite biofilter
Transient model	Hodge and Devinny, 1995	Uniform solids/water phase assumption	first-order	Numerical	Carbon and compost biofilter
	Deshusses et al., 1995	Soption, pollutant cross-inhibition	Michaelis-Menten kinetics	Numerical	Compost biofilter
	Shareefdeen's model with patches of biomass (1994)	Patches of biomass, adsorption	Monod and Andrews type	Numerical	Peat/perlite biofilter

2.5 Conclusions

A thorough literature review, including gas properties, biofiltration system, bacteria for biodegradation, packing medium, the history of BAC, biofiltration application and biofiltration models, was reviewed in this chapter and the following conclusions can be drawn.

H_2S and toluene are excellent surrogates of odour and VOCs in WWTPs off gases, which cause severe odorous and toxic problems. Biological treatment is a promising, economic, and environment friendly technology for air pollution control. Among the bioreactors, the biotrickling filter has been widely applied because of its low cost and simple operation. The packing medium, as a support for microbial growth, is the crucial part of the biotrickling filter, which will determine the biotrickling filter performance. The existing materials have many drawbacks such as material degradation and hence require frequent replacement.

GAC is an interesting packing medium because it has a high adsorptive capacity. GAC colonized with microorganisms was found to combine the adsorption and biodegradation processes and to form a new packing medium (BAC) in wastewater treatment. However, the use of BAC in air pollution control is rarely reported, especially for gas mixture treatment.

The degradation of some pollutants produces acid, which decreases the pH of the biotrickling filter. However, VOCs are removed effectively at a neutral pH. Low pH also causes the degradation of the packing medium and it is difficult to maintain the biotrickling filter operation at a neutral pH. Because of this conflicting problem, many researchers have explored studies about single pollutant removal while limited reports are published for gas mixture treatment. There appears to be some disputes among practitioners on the use of either a single-stage biotrickling filter or a two-stage biotrickling filter at a neutral pH or a low pH, for the efficient removal of contaminants in odorous air mixtures.

Base on the above literature review, biofiltration of gas mixture using BAC might be a significant research topic and will be discussed in the following chapters.

Biofiltration modeling is also reviewed in this chapter. So far, biofiltration models have been developed from simple steady state models to complete transient models where many aspects like kinetic interaction, oxygen limitation and adsorption are considered. However, the model applicability for a complex two-stage biotrickling filter is still questionable. The parameter values for the novel packing medium of BAC remain uncertain. This study attempts to provide further insights on the modeling of the adsorption and biodegradation processes occurring in the novel BAC medium.

CHAPTER THREE

MATERIALS AND MEHODOLOGIES

3.1 Bacteria

3.1.1 Bacteria cultivation

3.1.1.1 Preparation of liquid medium

Biological utilization of organic compounds requires supplemental inorganic chemicals. Therefore, the addition of nutrients is necessary for biological treatment of H_2S and VOCs. The nutrients mainly consist of nitrogen and phosphorus as well as trace elements (such as potassium, sodium, calcium, etc.). In this study, mineral salts medium was prepared to provide the essential inorganic nutrients and vitamins for microbial metabolism. The composition of the medium for toluene and H_2S degraders are shown in Tables 3.1 and 3.2. The phosphate buffer, which was composed of potassium dihydrogen phosphate (KH_2PO_4) and di-potassium hydrogen orthophosphate (K_2HPO_4), was used to buffer the pH fluctuation. Nitrate in Table 3.1 was used as a nitrogen source to prevent the growth of nitrifying bacteria (Arcangeli and Arvin, 1992). The composition of the trace element solution is given in Table 3.3.

The procedure to make sterile liquid medium for toluene degraders was as follows. As Table 3.1 illustrated, the components with the respective weight were added to distilled water and the solution volume was brought to 1.0L. The medium was mixed thoroughly by a stirrer and then it was autoclaved for 15 minutes at a pressure of 15psi and a temperature of 121°C for the sake of sterilizing.

The procedure of the medium production for H_2S degraders was however different because sodium thiosulfate in H_2S medium was unstable at the high temperature of autoclaving. For this reason, sodium thiosulfate was dissolved separately using 100mL distilled water. Other components were mixed thoroughly with 900mL distilled water and were autoclaved just like what had been done to the toluene medium. After that, 100mL of sodium thiosulfate solution was filtered through a 0.22μm sterile filter and then mixed with the other autoclaved medium under a laminar flow chamber.

Table 3.1 Composition of mineral medium for toluene degraders

(Ehrhardt and Rehm, 1985)

Components	Weight (in g per liter of distilled water)
NH_4NO_3	1.0
$(NH_4)_2SO_4$	0.5
NaCl	0.5
$MgSO_4 \cdot 7H_2O$	0.5
K_2HPO_4	1.5
KH_2PO_4	0.5
$CaCl_2$	0.01
$FeSO_4 \cdot 7H_2O$	0.01
Trace element solution	0.2 mL

Table 3.2 Composition of mineral medium for H_2S degraders

(http://www.dsmz.de)

Components	Weight (in g per liter of distilled water)
NH_4Cl	0.4
KH_2PO_4	1.5
K_2HPO_4	1.5
$MgCl_2 \cdot 6H_2O$	0.8
$Na_2S_2O_3 \cdot 5H_2O$ (sodium thiosulfate)	10 g
Trace element solution	10.0mL

Table 3.3 Composition of the trace element solution

Components	Weight (in mg per liter of distilled water)
$MnCl_2 \cdot 4H_2O$	0.0992
$CoCl_2 \cdot 6H_2O$	0.1192
$CuCl_2 \cdot 2H_2O$	0.0852
$NaMoO_4 \cdot 2H_2O$	0.1208
$NiCl \cdot 6H_2O$	0.0476
KI	0.0168

3.1.1.2 Preparation of solid medium

The solid medium was prepared to conduct the bacterial counting. The procedure to make the solid medium for toluene degraders was as follows. Before autoclaving, a mass of 15g of Bacto™ agar was added into 1L liquid medium for toluene degraders, whereupon the mixture was autoclaved for 15min at a pressure of 15psi and a temperature of 121°C. After that, the autoclaved agar solution was cooled to 60°C in a water bath prior to the addition of 50mg of pure toluene liquid, which could prevent excess volatility of toluene at a high temperature and solidification of agar at a low temperature. The warm gel liquid medium was then poured into Petri dishes to make the agar plate. The agar solution was left to solidify in the agar plates under a laminar flow station. As soon as the agar solution was cooled and solidified, the agar plates with their covers facing down were stored in a refrigerator at 4°C prior to use. The preparation of the solid medium for H_2S followed a similar procedure as that described for toluene.

3.1.1.3 Flask culturing

A volume of 10mL returned activated sludge from a local wastewater treatment plant was mixed with 90ml H_2S liquid medium in a 500mL conical flask, which was sealed with a cotton-stopper and shaken on a rotary shaker at 120rpm

(revolutions per minute) and at a room temperature of 25°C. After 4~6 days, the medium turned turbid, which indicated the growth of the sulphur-utilising bacteria. A volume of 10mL of the turbid liquid was then transferred to mix with 90mL of fresh medium and the same procedure was repeated resulting in several generations of bacteria culture. After acclimatization for about three weeks, the bacteria seeds were ready for inoculation onto activated carbon granules. Acid production during bacteria growth induced low pH naturally. According to the pH investigation of bacteria for H_2S biodegradation (Section 2.2.2), *Thiobacillus sp.* are dominant in extremely acidic environment. This is also proved with Polymerase Chain Reaction (PCR) and DNA sequencing methods by another colleague researcher using the same inoculum (Duan, 2005a). If a neutral pH was required, the pH would be controlled by the addition of NaOH.

For toluene removal at a neutral pH environment, a pure bacterium (*Pseudomonas putida* F1) from American Type Culture Collection (ATCC, USA) was used. For the purpose of the low pH condition, returned activated sludge was used for flask culturing and 1g of $Na_2S_2O_3 \cdot 5H_2O$ was added initially to facilitate the acid environment through the growth of *Thiobacillus sp.* in the sludge. A volume of 5mL sludge was added to 95mL of toluene liquid medium held in a 500mL glass flask, into which 50mg/L of liquid toluene was added everyday to facilitate the growth of toluene degraders. The subsequent culturing procedure was also similar to that adopted for H_2S degraders.

3.1.2 Morphological characterization

The morphology of bacteria attached on the carbon surface was studied using a scanning electron microscope (SEM). At first, a carbon particle with bacteria was soaked in a beaker of 2% (volume/volume) glutaraldehyde for about 2 hours, after which the sample was washed for three times in 20 minutes with 0.1M sodium cacodylate buffer. The washed sample was then dehydrated in 50%, 70%, 85%, 95% and 100% ethanol respectively, each for 15 minutes. After dehydration, the

sample was dried with a critical point drying equipment (E3000 Serious). Later the dried sample was sputter-coated with gold at 20mA in a high vacuum and a low temperature cryo-chamber for 60 seconds, and then viewed with a SEM (Stereoscan 420, Leica, Cambridge Instruments) at 15KV. The cross section of the carbon samples was prepared by a sterile knife cutting the carbon particles into half.

3.1.3 Bacterial counting

Plate count is a method for estimating the number of live bacteria in a sample because a viable cell is capable of forming colonies on a suitable agar medium. The assumption made in this type of counting method is that each viable cell will yield one colony. There are two ways of performing a plate count: the spread plate method and the pour plate method (Brock and Madigan, 1991).

In this study, the spread plate method was adopted. A volume of 0.1mL diluted culture was spread over the surface of an agar plate with a sterile spreader. The plate was then incubated at 30°C for 2 to 3 days. Colonies on the plates were promptly counted after incubation. Statistically, the usual valid practice was only to count those plates that had colonies with number ranging from 30 to 300. To obtain the appropriate colony number, several ten-fold dilutions of the sample were used. A sterile solution of 0.8% NaCl was employed as the dilution liquid. At each dilution rate, three replicate plates were prepared to get the average counts. Since two or more cells in a clump will form only one single colony, plate counts are often expressed as the number of *colony-forming units (cfu)* obtained rather than as the number of viable cells. The details of the sample dilution are shown in Figure 3.1. Organisms per millilitre of the original sample (cfu/mL) were calculated by Equation 3.1.

$$\text{cfu/mL} = \frac{\text{Colonies counted, cfu}}{\text{Actual volume of original sample on agar plate, mL}} \qquad (3.1)$$

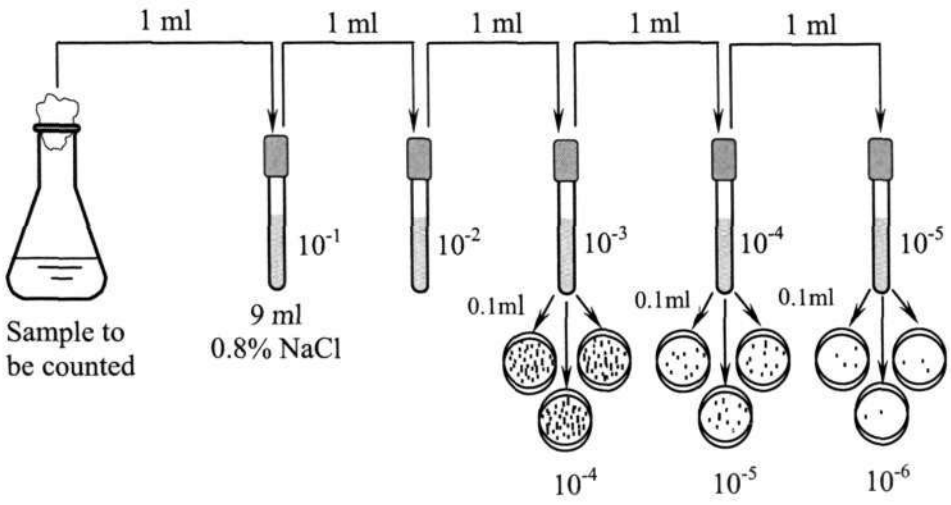

Figure 3.1 Procedure for plate count using serial dilutions

3.2 Packing material

3.2.1 Physical description of Calgon Carbon AP-460

The packing material selected for this study is GAC AP-460 of 4mm-diameter supplied by Calgon Co. (Pittsburgh, PA, USA). Figure 3.2 is the close-up of the packing material, which is a type of non-impregnated coal-based carbon of a neutral pH. The initial pH of the carbon should not be alkaline as the bacteria immobilized on it will not be able to grow well in a basic environment. This particular activated carbon with high surface area can provide a beneficial environment for bacteria growth. In order to test its feasibility and performance as a biotrickling filter medium, the properties of carbon were evaluated before and after the biotrickling filter operation. The analysis of changes in carbon properties provided a better understanding of the biochemical reactions occurring in the biotrickling filters as well.

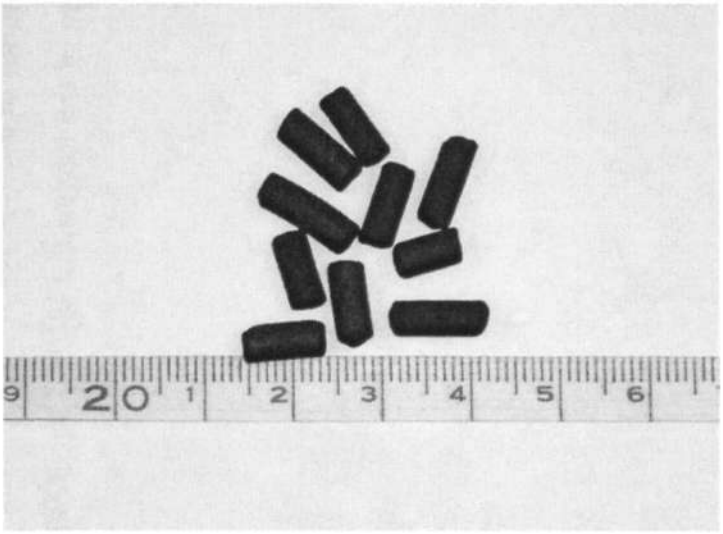

Figure 3.2 Close-up of Calgon Carbon AP-460

An ideal attachment medium used in biotrickling filters is characterized by having a high specific surface area as well as being able to provide an excellent surface for microbial growth. Preferably, the medium should have a high air and water permeability and also yield minimal pressure drop. Figure 3.3 shows a scanning electron microscope (SEM) image of the virgin carbon surface (Calgon AP-460) without bacteria. The particle surface is highly irregular including large rough zones and open cavities. The pitted surface of the GAC affords shelter from fluid shear forces and so enhances the attachment of microorganisms. The porous structure of the particle surface provides a good water-holding capacity as well.

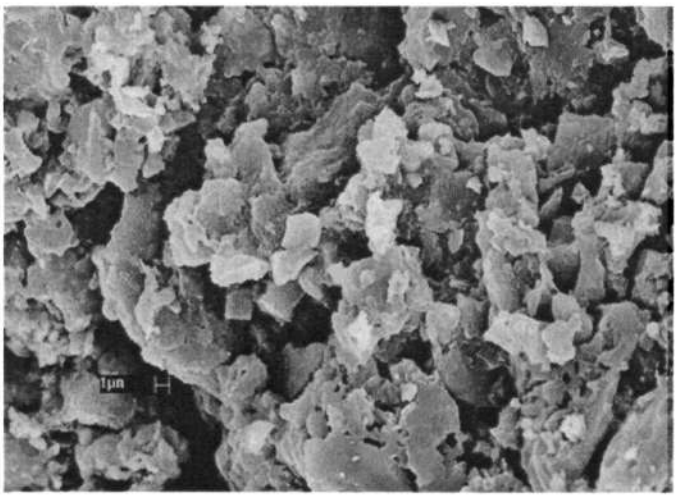

Figure 3.3 Carbon surface without bacteria

Table 3.4 Physical description of Calgon Carbon AP-460 from the supplier

Parameters	Value
Pellet diameter, mm	4
Hardness number, min	90
Mesh Size > US Mesh 6 (3.35mm), min %	95
Apparent density, kg/m^3	490
Ash Content, max % w/w	12
Moisture Content, max % w/w	5
pH	7.4

Table 3.4 shows the physical description of Calgon Carbon AP-460 from the supplier. The raw material of AP-460 is coal, which ensures a high density (490kg/m^3) and low ash content (max 12% w/w). GAC AP-460 has excellent structural properties and good resistance to crushing. The uniform particle size leads to even distribution of the gas flow (min 95%>3.35mm). The neutral pH (7.4) is suitable for microbial attachment. The alkali impregnated carbon was not selected in this study because the basic conditions on the carbon surface would be harmful for microorganims growth.

3.2.2 BET test

Different packing materials possess different surface features such as surface area, pore volume and micropore diameter. The Brumauer-Emmett-Teller (BET) method is the most widely used procedure for the determination of the surface area of solid materials. Nitrogen is used as the adsorbate gas. The surface area and pore volume of activated carbon were calculated from nitrogen adsorption/desorption isotherm measured by Autosorb 1C-MS. Carbon samples were first freeze vacuum dried for 24h and then degassed to 1.33Pa pressure at 70℃ prior to BET analysis. The operating procedures include: preparations for sample analysis; degassing samples prior to analysis purges impurities; computer set up for Degassing; sample testing; shut down.

Table 3.5 shows the BET data of the virgin carbon and exhausted carbons. As can be seen, AP-460 had a large external surface area (505.9m^2/g) that facilitated colonization by microorganisms. The micropore volume of the toluene or H_2S exhausted carbon was 0.093 cm^3/g and 0.078cm^3/g respectively, far smaller than that of the virgin carbon (0.276cm^3/g). This significant reduction in micropore volume demonstrated that the adsorption mainly took place in the micropores. The surface area of the toluene or H_2S exhausted carbon also decreased significantly when compared against that of the virgin carbon. For example, the total BET area of the virgin carbon was 1031.5m^2/g. However, it decreased to 614.3m^2/g after toluene exhaustion and to 579.2m^2/g after H_2S exhaustion. Average pore diameter of the toluene (2.015nm) or H_2S (2.024nm) exhausted carbon was larger than that of virgin carbon (1.980nm), which was caused mainly by pollutant adsorption in micropores. The adsorption processes of H_2S and toluene increasing the average pore diameter of the activated carbon also indicated that most of the adsorption took place in pores with very small diameters of below 1.98nm in the virgin carbon.

Table 3.5 BET data of virgin carbon and exhausted carbon

Carbon type	Micropore volume (cm^3/g)	Average pore diameter (nm)	Surface area (m^2/g)		
			External	Micropore	Total BET
Virgin carbon	0.276	1.980	505.9	525.6	1031.5
Toluene exhausted carbon	0.093	2.015	201.7	412.6	614.3
H_2S exhausted carbon	0.078	2.024	182.1	397.1	579.2

3.2.3 Breakthrough test

Breakthrough test was performed with the aim of evaluating the adsorption capacity of AP-460.

3.2.3.1 H_2S breakthrough test

The objective of this test is to determine the adsorptive capacity of activated carbon (Calgon AP4-60) by treating a 1% H_2S stream to a 50ppmV breakthrough. The breakthrough test was conducted according to the modified ASTM D28, which was designed to evaluate the performance of activated carbon against H_2S. The breakthrough test setup is given in Figure 3.4. In this method, the carbon sample was packed in a glass column with an internal diameter of 4.8 cm. The packing height was fixed at 22.9 cm and glass beads were packed both at the bottom and the top of the carbon bed in order to ensure a good mixing of H_2S gas stream.

The 1% H_2S (5% H_2S at 0.5 L/min + moist compressive air at 2 L/min) gas stream was introduced into the bottom of the carbon column. The H_2S concentration was monitored at the outlet of the carbon packed column by a Jerome 631-X Hydrogen Sulfide Analyzer (Arizona Instruments, Tempe, AZ) until a breakthrough of 50ppmV concentration was reached. The time taken for the breakthrough was recorded and the carbon breakthrough capacity in terms of weight (grams of H_2S per gram activated carbon sample) was calculated.

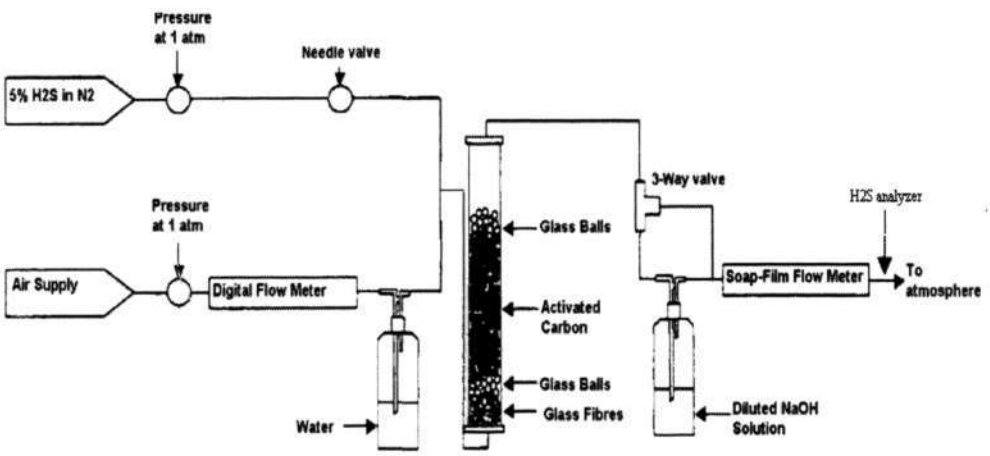

Figure 3.4 Schematic diagram of the H_2S breakthrough test

3.2.3.2 Toluene breakthrough test

The toluene breakthrough test was carried out with a bench system. The schematic of the bench biofilter is displayed in Figure 3.5. The reactor column was 3.6cm in internal diameter and 20cm in packing height with the total packing volume of 203mL. 98g of Calgon carbon AP-460 was packed in the reactor with glass beads in the inlet and outlet so as to facilitate the dispersal of gas flow. The column was sealed with two fitted rubber stoppers at the top and bottom. The toluene vapor was produced by passing ambient air through a bottle containing pure liquid toluene and toluene concentration in the toluene-rich air was varied by adjusting the bubble rate. Gas samples taken from inlet and outlet sampling port were measured according to the method described in Section 3.3. Inlet concentration of toluene gas was set at 50ppmV and the gas flowrate was regulated to yield a GRT of 30s for the bench system. Outlet concentration was monitored until it reached an equilibrium breakthrough concentration similar to the inlet concentration. The breakthrough curve was then obtained, from which the adsorption capacity was calculated.

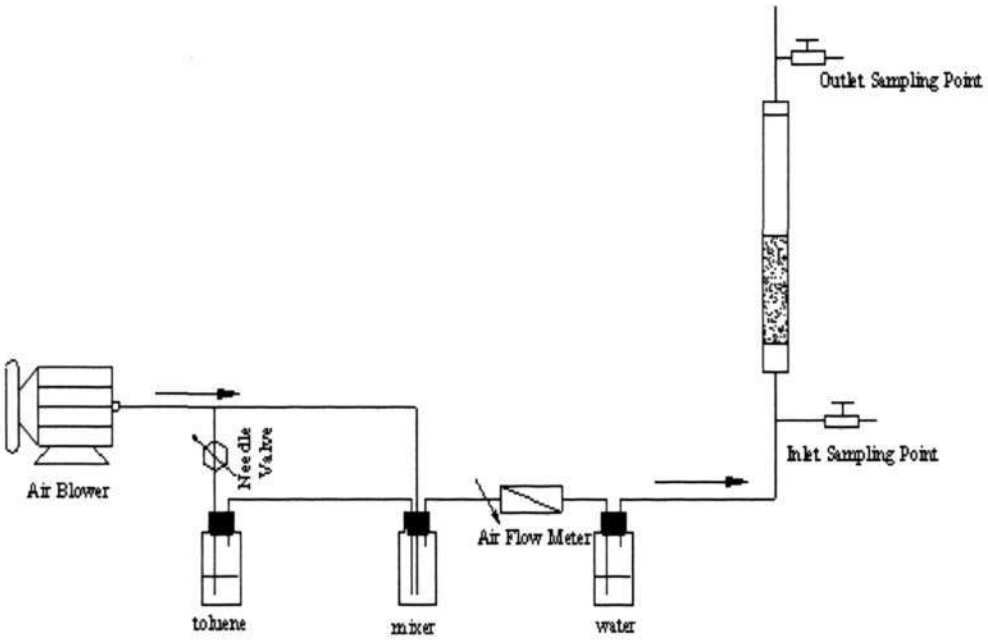

Figure 3.5 Schematic diagram of the toluene breakthrough test

3.2.3.3 Adsorption capacity of AP-460

According to the breakthrough test, the toluene adsorption capacity of AP-460 was 28.8g-toluene/100g-carbon, while the adsorption capacity of the H_2S was 5.4g-H_2S/100g-carbon. The carbon bed was exhausted completely by toluene after 15 days, while for H_2S, the carbon bed was exhausted after 26 days. The long breakthrough time reflected the high adsorption capacity of GAC Calgon AP-460, when compared against the breakthrough time of several hours which was usually associated with conventional packing media (Barona et al., 2005).

Researchers have observed slower adsorption kinetics and decreased capacity due to the development of the biofilm in GAC columns (Gauden et al., 2005). Although the adsorptive capacity of carbon will be reduced by the water and biomass on its surface, it still remains much higher than other media. During transient conditions, when microorganisms are unable to degrade large amounts of the incoming pollutants, this remaining GAC capacity may still be sufficient to remove the excessive pollutants as a buffer. Lower effluent concentration levels can be achieved by using this system under shock loading. Hodge and Devinny (1995) reported that the adsorptive capacity of the GAC could be maintained higher than the other two media (compost, a mixture of compost and diatomaceous earth), even if it was substantially reduced by water and microbial growth.

3.2.4 Thermal analysis

Thermal analysis, which evaluated the thermal desorption of different compounds adsorbed in carbon, was carried out by a Thermogravimetric Analyzer (PerkinElmer instruments, TGA7). The original and used carbon were heated from 30°C to 600°C at 10°C/min. Nitrogen gas as the carrier gas flowing into the system was regulated at 20.0mL/min.

Table 3.6 Boiling point of substances (1atm)

Substance	Water	Toluene	Sulphuric acid (98%)	Sulphur
Boiling point (℃)	100	110.7	338	444.6

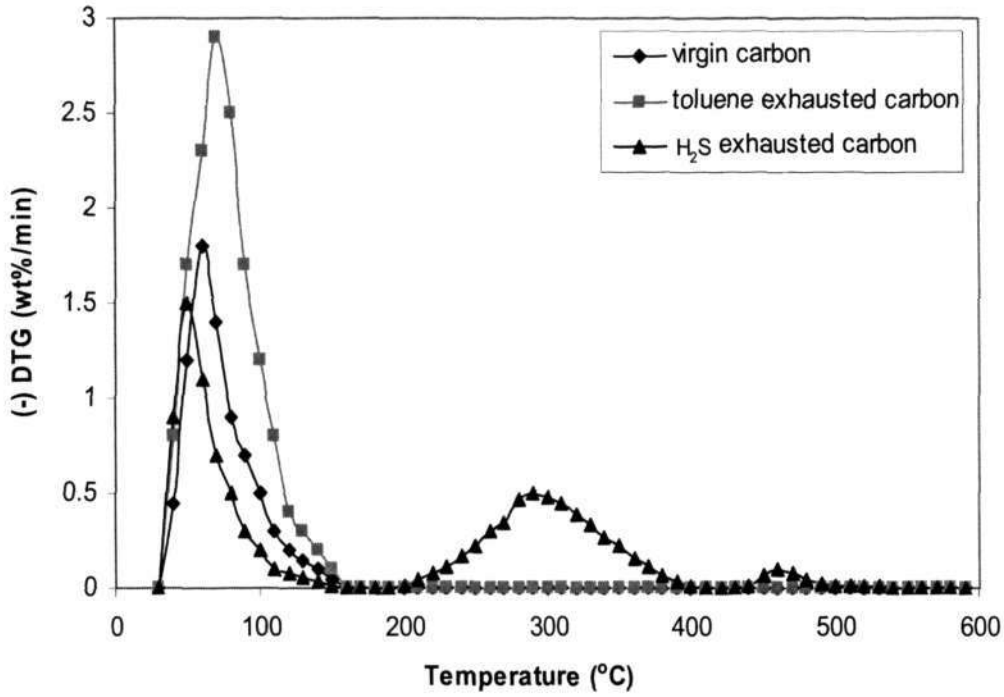

Figure 3.6 DTG curves of GAC before and after adsorption

In thermogravimetric analysis, each peak corresponds to the weight loss due to the desorption of the species from the activated carbon at the specific temperature. The taller the peak or the larger the area means the more weight loss.

Figure 3.6 shows the differential thermogravimetric (DTG) curves of the virgin and exhausted carbons. In the curve of the virgin carbon, one single peak was observed just before 100℃ when the virgin carbon sample was heated from 30℃ to 600℃. This peak close to 100℃ was attributed to the water evaporation. As for the toluene exhausted carbon, the DTG curve also had only one peak close to the value of 100℃. For the reason that the boiling points of water (100℃) and toluene (110.7℃) were very close to each other (illustrated in Table 3.6), the two peaks overlapped,

which resulted in one single peak being observed. This peak was higher than that of virgin carbon because of the additional toluene adsorption. As only one peak around toluene and water boiling point was found, this mass loss came from the desorption of physically adsorbed toluene and water. Peaks at higher temperatures, which indicated the occurrence of chemisorption in the impregnated activated carbon (Nestor et al., 2004), did not appear here because AP-460 was a non-impregnated carbon type. The results showed that the interaction between toluene and AP-460 was mainly a physical adsorption process.

In the DTG curve of the H_2S exhausted carbon, there were two other peaks around 300℃ and 450℃ in addition to the water peak. These two peaks were caused by H_2S adsorption/oxidation products because they were not present in the curve of the original virgin carbon. According to the boiling points shown in Table 3.6, the larger peak around 300℃ was brought on by the desorption of noncombustible oxidized sulfur species (SO_2, H_2SO_4, etc), while the smaller peak around 450℃ was attributed to the elemental sulfur components. The sulfur peak was very small in the exhausted carbon because most H_2S was oxidized to noncombustible oxidized sulfur species. Although the oxidation capacity of this carbon was too weak to cause toluene transformation, H_2S still could be oxidized easily. The exact locations of the two peaks may vary in temperature compared with the peak locations reported by other researchers owing to the different physical and chemical characteristics of the carbon in use (Yan et al., 2004). However, there is a general agreement that the peak relative to sulfur oxides emerges before the elemental sulfur peak.

As for H_2S adsorption on carbon surface, two mechanisms occuring are physical and chemical adsorption processes. Physical adsorption was a reversible process, involving only weak forces of van der Waals. Chemical adsorption involved a chemical reaction and formation of new chemical bonds between the gas molecules and the surface of the adsorbent. The following equations indicate the mechanisms involved in the virgin carbon adsorption (Yan et al., 2002).

Physical adsorption:

$H_2S\ (g) \longrightarrow H_2S\ (ads)$

$H_2S\ (ads) \longrightarrow H_2S\ (ads\text{-}liq)$

$H_2S\ (ads\text{-}liq) \longrightarrow HS^-\ (ads) + H^+$

Oxidation:

$HS^-\ (ads) + O^*\ (ads) \longrightarrow S\ (ads) + OH^-$

$HS^-\ (ads) + 3O^*\ (ads) \longrightarrow SO_2\ (ads) + OH^-$

$SO_2\ (ads) + O^*\ (ads) + H_2O\ (ads) \longrightarrow H_2SO_4\ (ads)$

$H^+ + OH^- \longrightarrow H_2O$

Where the species with (g), (ads), and (ads-liq) are in gas, adsorbed, and liquid phase. O* (ads) is dissociatively adsorbed oxygen.

3.2.5 Carbon surface pH

The pH of carbon suspension, which provides useful information about the average acidity/basicity of carbon surface, was measured using the method described by Foad et al. (2000): 0.4g of carbon sample was soaked in 20mL of ultra pure water and swirled in the auto-shaker (120rpm) for 16h so as to achieve equilibrium. The sample was then filtered and the pH of the filtrate was measured using a pH Meter (Jenway 4330, U.K.), which was calibrated with buffers (pH values of 4.0 and 7.0).

3.2.6 Sulfate analysis

Sulfate accumulated in the carbon was determined by transforming the sulfate into the aqueous phase. 0.4g of carbon sample was soaked in 20mL of ultra pure water and swirled in the auto-shaker (120rpm) for 16h in order to achieve equilibrium. The water sample was then filtered through a 0.2μm membrane filter to remove particles. Sulfate concentration in the solution was measured by gravimetry according to 4500-SO_4^{2-} Standard Method (Andrew and Lenore, 1995) and then converted to gram sulfate per gram carbon.

3.2.7 CNHS analysis

CNHS analysis provides information about the combustible elements of C, N, H and S in the carbon granules, which reflect element mass balances of the carbon bed before and after the biotrickling filter operation. It was determined by a CNHS/O Analyzer (PerkinElmer instruments 2400, Series II, USA). Three analyses of each carbon sample were conducted with the aim of minimizing experimental errors.

3.3 Gas sample collection and analysis

Gas samples were collected by Tedlar bags and measured immediately after sampling. To eliminate residual pollutants in the Tedlar bags, all sample bags were flushed by clean air as soon as the analysis was finished. H_2S concentration was measured by a Jerome 631-X Hydrogen Sulfide Analyzer (USA).

Toluene analysis was accomplished with a Hewlett Packard 5890 gas chromatograph (GC) with a capillary column. Gas samples were directly injected into the injection port of the GC with a gas tight syringe from Scientific Glass Engineering (SGE, Melbourne, Australia). The syringe was flushed using gas samples at leased twice before injection to remove background adsorption. Two measurements were carried out for each sample and the readings were averaged. GC-FID operating conditions were as follows:

Column: J&W Scientific DB-624 megabore column (30m-length × 0.53mm-ID × 3μm-film thickness)
Detector: Flame Ionization Detector (FID)
Carrier gas: Helium at 40mL/min
Temperature: Oven, 150°C (constant, 2.5min)
Injector, 180°C
Detector, 200°C
Pressure: 14psi

The calibration curve for toluene was prepared by injecting the known concentrations of toluene into the GC-FID unit. These toluene samples with known concentration were prepared by introducing 100μL of pure toluene liquid into a 62mL-sealed-glass bottle equipped with a Teflon rubber septum. The bottle was then set aside for about two days until the liquid evaporation and transformation into the gas phase reached the equilibrium state. Successive dilutions were then performed using other bottles with the same volume to get the required concentrations that were used for preparing the different data points for the calibration curve. The equation used to calculate the concentration in the gas phase of a liquid added to the closed system is:

$$C = 24.45 \times 10^6 \left(\frac{\rho V_L}{MV}\right)\left(\frac{T}{298}\right)\left(\frac{101.3}{P}\right) \qquad (3.2)$$

Where

C=pollutant concentration (ppmV)

V_L=volume of the liquid (mL)

V=system volume (L)

T=temperature (K)

M=molecular weight (g/mol)

ρ=liquid density of the compound (g/mL)

P= pressure (Kpa)

Figure 3.7 represents a sample of the toluene calibration curve.

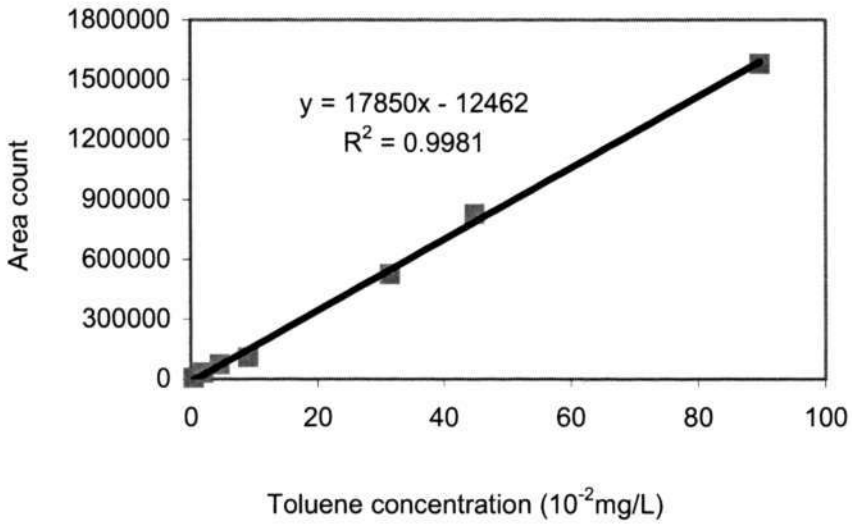

Figure 3.7 A sample of toluene calibration curve

3.4 BAC development

So far, BAC development for the purpose of H_2S or toluene treatment in a biofilter has rarely been reported. That is why bacteria immobilisation on carbon surface was tested before carbon applicaton in the biofilters. There are two ways for BAC development: offline immobilization and online immobilization. Activated carbon could be immobilized either before pollutant exhaustion or after exhaustion. The bacteria attachment on carbon surface was monitored by bacteria number measurement and confirmed by SEM images.

3.4.1 Offline immersed immobilization

A sample of 20g carbon was washed with ultra pure water prior to bacteria immobilisation. The washed carbon and 100mL of acidic inoculum (mainly *Thiobacillus sp.*) were added to an air-sparged glass bottle sealed with a Teflon rubber septum containing 900mL of liquid media. Ambient gas with H_2S or toluene

was respectively introduced into the bottle. The toluene vapor was produced by passing ambient air through a bottle containing pure liquid toluene and then mixed with the main air stream before entering the bottle with the inoculum. H_2S gas was produced through ambient air dilution of high concentration H_2S available from a standard gas cylinder. Inlet concentration of H_2S was regulated at about 20ppmV and the air flow rate was controlled by an air flow meter to produce a GRT of 15s in the liquid media. As for toluene, inlet concentration and GRT were set at 50ppmV and 60s. Solution pH and bacteria number attached on carbon were measured daily to monitor biofilm formation.

Both the virgin carbon and the exhausted carbon from the breakthrough test were inoculated with microorganisms in order to evaluate their attachment on the different carbon surface.

3.4.2 Online immobilization in a biofilter

Regarding a full-scale bioreactor, it is impractical to provide huge containers for BAC offline immersed immobilization. As a general rule, the online immobilization is selected to shorten the acclimatization period.

Online immobilization was studied in a bench biofilter operated for 15 days. The schematic diagram of the bench biofilter for online BAC development is shown in Figure 3.5. The reactor column was packed with GAC in a volume of 203mL. The detailed description of the reactor configuration and gas production can be found in Section 3.2.3.2. The inoculum was prepared separately and poured into the reactor packed with GAC. 5mL of concentrated microbial broth (*Thiobacillus sp.* or *P. putida*) was added into 45mL of fresh mineral medium. 50mL of bacteria solution with its bacteria concentration higher than 10^8cfu/mL was poured from the top of the column. After inoculation, synthetic polluted gas of H_2S or toluene was introduced immediately. When being soaked in the inoculum for 10 days, the excess solution was drained off from the biofilter. The bed was then irrigated twice a day

by submerging the bed in the culture medium for 20min to maintain the moisture and nutrition. After that the solution was released as the existence of a water layer around the medium would inhibit mass transfer of contaminants from the gas phase to the biofilm (Duan, 2005a). The concentration of H_2S and toluene was set at about 20ppmV (GRT: 15s) and 50ppmV (GRT: 60s), respectively.

3.5 Experimental set-up of the bench reactor

BAC capacity was firstly tested in a bench biofilter. The schematic diagram of the bench reactor used in this study is given in Figure 3.8. The reactor was made of a Perspex column, which was 3.6cm in internal diameter and 30cm in height, with a packing bed height of 20cm. The total packing volume was 203mL. GAC of Calgon AP-460 (98g) was packed in the reactor with glass beads in the inlet and outlet to facilitate the dispersal of gas flow. The column was sealed with two fitted rubber stoppers at the top and bottom. The top stopper was removable to add water and medium solution for sufficient moisture and mineral nutrient in the bed. All the gas pipelines were made of 6.35mm diameter Teflon tubing. The experiment was carried out at a room temperature of about 25℃. Physical properties of the biofilter are summarized in Table 3.7.

H_2S and toluene test were separately carried out using the bench biofilter. For the H_2S test the carbon was inoculated with *Thiobacillus sp.* while for toluene test, *P. putida* was used. The online inoculation of bacteria on the carbon medium followed the same procedure as described in Section 3.4.2. After being soaked in the inoculum for 10 days, the bed was irrigated twice a day by submerging the bed in the culture medium for 20min and then releasing the solution. The toluene vapor was produced by passing ambient air through a bottle containing pure liquid toluene and toluene concentration in the toluene-rich air was varied by adjusting the bubble rate. The toluene-rich air was then mixed with the main air stream before entering the reactor. H_2S gas was produced through ambient air dilution of high concentration H_2S in the gas cylinder (5% H_2S balanced in N_2, Linde Gas Singapore Pte Ltd).

Table 3.7 Physical properties of the biofilter

Dry carbon weight, W_1(g)	98
Wet carbon weight, W_2(g)	167
Moisture content, (W_2- W_1)/ W_2 (%)	41.3
Column diameter (cm)	3.6
Packing height (cm)	20
Packing volume (mL)	203
Diameter of carbon pellet (mm)	4
Apparent density of carbon (kg/m^3)	490
Initial pH of the bed (carbon pH)	7.4

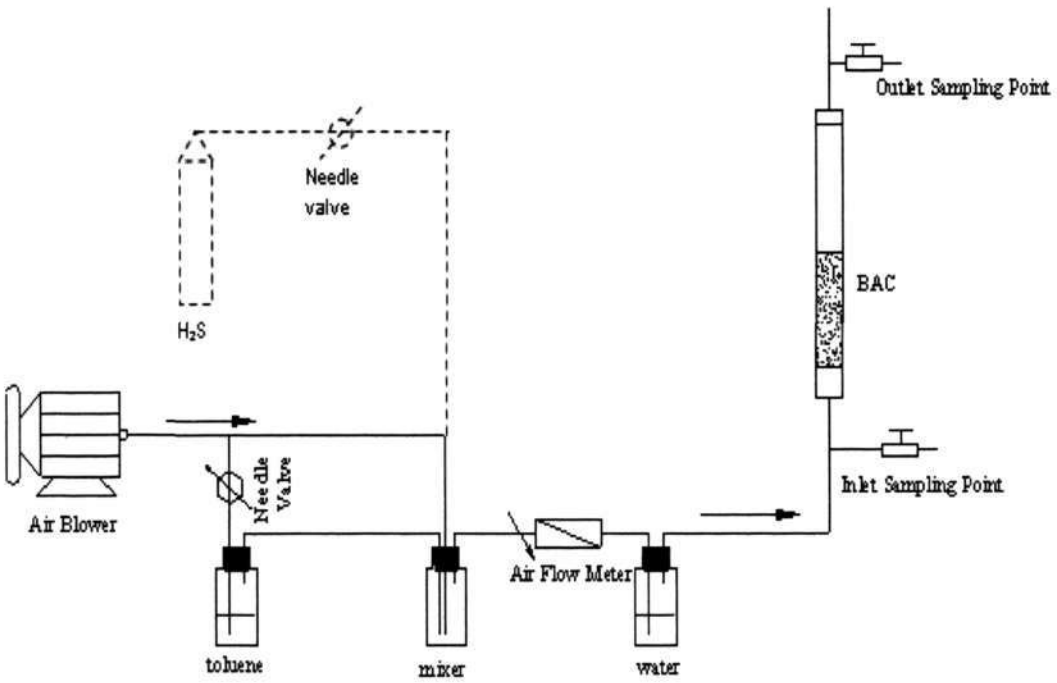

Figure 3.8 Schematic diagram of the bench reactor

A control test was operated to compare the performances of the BAC and virgin GAC which did not have bacteria immobilized on it. As for the GAC experiment, the same amount of carbon was packed in the column after the BAC test operation. Instead of bacteria solution, 50mL of distilled water was poured into the column. All the other parameters for both test runs were set under the same conditions.

The operating parameters of the bench biofilter are shown in Table 3.8. To evaluate the interaction of H_2S and toluene for BAC performance, 50-200ppmV of toluene gas was fed in from day 25 to 36 during the H_2S test, while 1-5ppmV H_2S was introduced from day 35 to 44 during the toluene test.

Table 3.8 Operating parameters of the bench biofilter

Parameter	H_2S	Toluene
Packing media volume (mL)	203	
Inlet gas concentration(ppmV)	20	50
GRT(s)	7	30
Gas flow rate (L/min)	1.74	0.4
pH of the carbon bed	1.0-3.0	6.0-8.0

3.6 Experimental runs with horizontal biotrickling filters

According to the literature review, earlier studies showed different results for co-treatment of H_2S and VOCs. Some agreed that a single-stage bioreactor was enough while others preferred a two-stage bioreactor (Ergas et al., 1995; Todd et al., 1997; Cox and Yang, 2002). Therefore, three BAC biotrickling filters—a two-stage biotrickling filter, a neutral pH biotrickling filter (single-stage) and a low pH biotrickling filter (single-stage), were designed to examine the performance of this novel packing medium (BAC) for gas mixture treatment. Through this study, the optimum reactor for co-treatment of gas mixture would be determined. Three phases of experiments in the following study were conducted with different objectives:

- Phase 1: to study the performance of a neutral pH biotrickling filter (single-stage)
- Phase 2: to study the performance of a low pH biotrickling filter (single-stage)
- Phase 3: to study the performance of a two-stage biotrickling filter

So far, vertical bioreactors for waste gas treatment had been widely reported by many researchers (Koe and Yang, 2000; Cox et al., 2002), while the horizontal style was rarely used. However, some Wastewater Treatment Plants (WWTPs) still use horizontal chemical scrubbers. Information about horizontal biotrickling filters performances will be useful when converting a horizontal chemical scrubber to a biotrickling filter. Also the pressure drop in the horizontal system is usually lower than that of the vertical one (Zhou, 2000). Therefore, the horizontal system requires less operation cost as a result of lower power consumption. Base on the above considerations, a horizontal system was installed to evaluate the single-stage and two-stage operation in this study.

3.6.1 Neutral pH single-stage biotrickling filter

3.6.1.1 Reactor configuration

The schematic diagram of the biotrickling filter is shown in Figure 3.9. The biotrickling filter consisted of six segments with the total volume of 13.5L. The size of each segment was 15cm x 15cm x 10cm (Width x Height x Length) with a volume of 2.25L. Five of them were packed with 5168g of Calgon carbon AP-460 and the remaining one was kept empty for flexibility in operation. The packed segments were named as I, II, III, IV and V (as shown in Figure 6.1) along the biotrickling filter bed with a volume of 11.25L. Figures 3.10 and 3.11 display photos of the biotrickling filter and one segment sample with wet carbon, respectively. The physical properties of the biotrickling filter are summarized in Table 3.9. To facilitate gas sampling, intermediate sampling ports were located between two adjacent segments. Only one tank was built in the single-stage biotrickling filter to hold the recirculation liquid.

Table 3.9 Physical properties of the horizontal biotrickling filter

Carbon commercial name	Calgon AP-460
Dry carbon weight, W_1(g)	5168
Wet carbon weight, W_2(g)	7491
Moisture content, (W_2- W_1)/ W_2 (%)	31
Packing bed dimensions (cm)	15 x 15 x 10 x 5
Packing segment length (cm)	10 x 5
Packing volume (mL)	11.25
Diameter of carbon pellet (mm)	4
Apparent density of carbon (kg/m^3)	490
Initial pH of the bed (carbon pH)	7.4

To maintain the pH of the biotrickling filter at the neutral level, caustic soda was added every day. The amount needed could be estimated from calculation of the sulfur balance in the biotrickling filter.

Biological reaction: $H_2S + 2O_2 \longrightarrow$ metabolic intermediates $\longrightarrow H_2SO_4$

Neutralization: $H_2SO_4 + 2NaOH \longrightarrow NaSO_4+2H_2O$

Reaction stoichiometry:

1mol H_2S:1mol H_2SO_4: 2moles NaOH

1g H_2S: 3.04g H_2SO_4: 2.48g NaOH

According to literature review, H_2SO_4 was the major end-product of H_2S biodegradation in the biotrickling filter and the formation of other metabolic intermediates was negligible (Anders and Colin, 1995). Results of later investigation in this study (Section 5.1.8.2) also lend support of this as well. Considering that a large amount of alkali would be consumed, H_2S concentration in the inlet was set at a low level (5ppmV) for most of the operation time.

Intermittent trickling was selected in the biotrickling filter operation because it had been proven to be better than continuous trickling for the BAC operation by another researcher (Duan, 2005a). The BAC was trickled twice per day (0.8L/min for 30

minutes on each occasion) to complement water and nutrition. In the single-stage biotrickling filter, the microorganisms in the whole reactor were set under the homogeneous nutrients liquid formula. The composition of mineral salts medium is shown in Table 3.10.

Table 3.10 Composition of mineral medium in the single-stage biotrickling filter (Chang, 2003)

Components	Weight (in g per liter of distilled water)
KNO_3	1.0
NaCl	1.0
KH_2PO_4	1.0
K_2HPO_4	1.0
$MgSO_4$	0.2
$CaCl_2$	0.02
Trace element solution	1mL

3.6.1.2 Synthetic foul air

Toluene and H_2S were chosen as the model VOC and odour compound, respectively. The toluene waste gas was produced by passing air through a bottle containing pure liquid toluene. High concentration standard H_2S in the gas cylinder (10% H_2S, Soxal Gas, Singapore) was controlled by a regulator and a flow meter to get the desired H_2S gas stream. With dilution of bulk ambient airflow, the combined gas stream was channeled through the packing reactor. The directions of gas flow and recirculation solution are shown in Figure 3.9 with solid and dotted arrows, respectively.

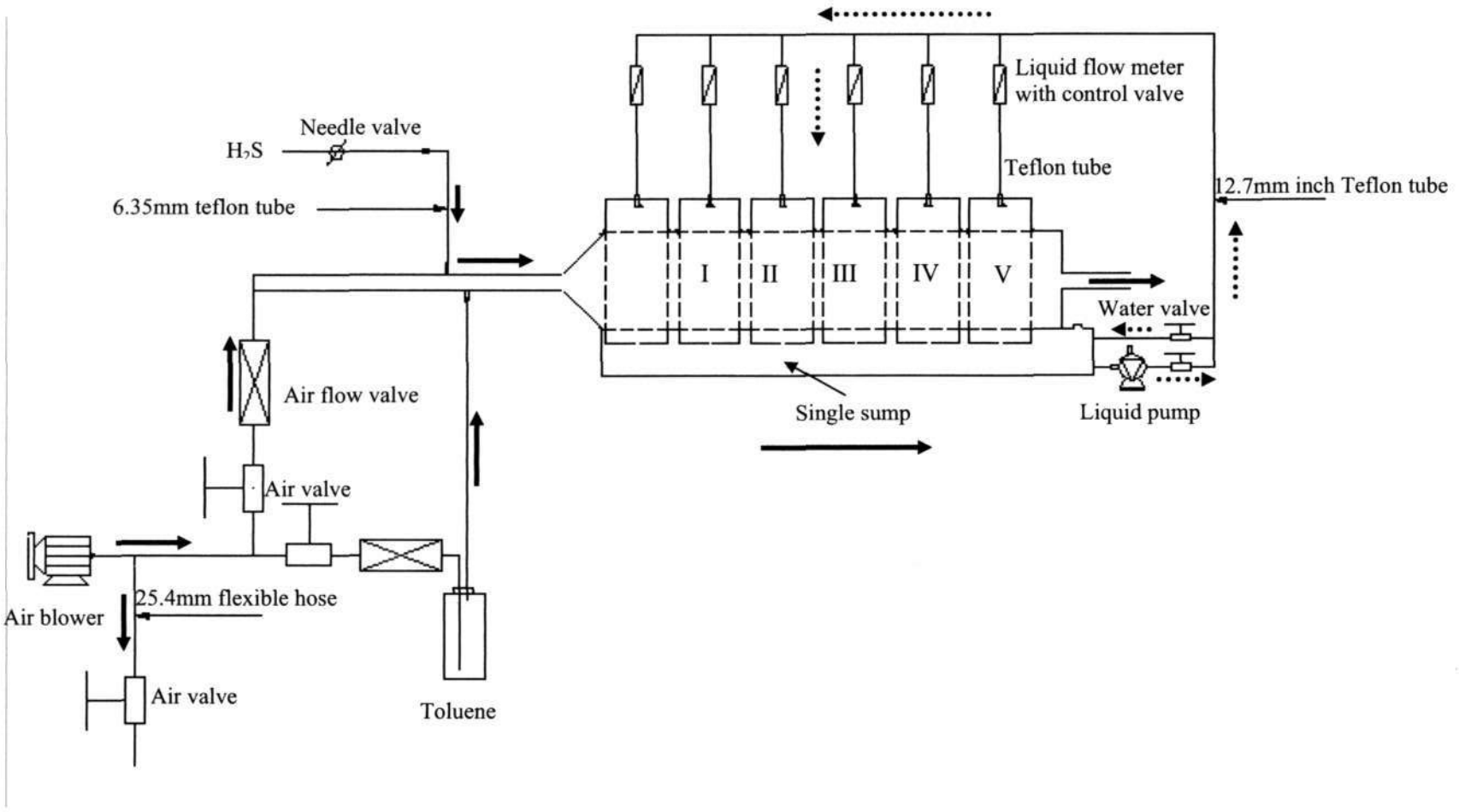

Figure 3.9 Schematic diagram of the single-stage biotrickling filter

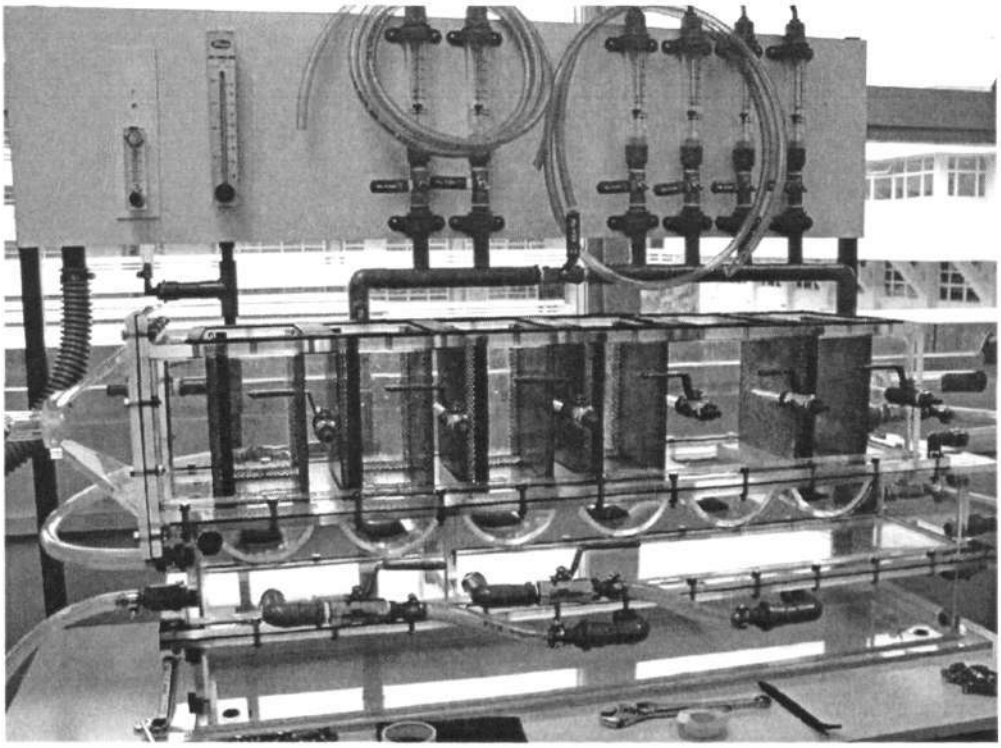

Figure 3.10 Photograph of the biotrickling filter

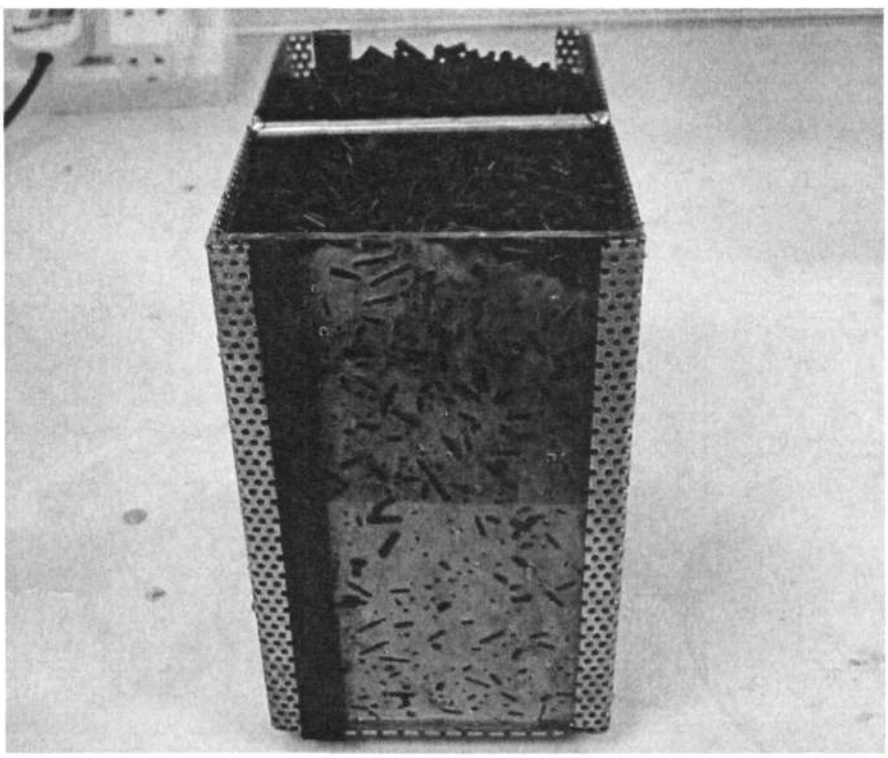

Figure 3.11 Segment sample with carbon

3.6.1.3 Experimental procedure

During the 90-day operation of the biotrickling filter, there were a series of continuous experimental runs exploring different situations such as different gas residence times and inlet gas concentrations. During the start-up period, H_2S and toluene concentration were set at about 5ppmV and 50ppmV and the air flowrate was regulated to yield a GRT of 60s for the biotrickling filter. Toluene gas was introduced firstly to prevent the adverse influence of H_2S. H_2S gas was delivered after toluene removal reached 95%. When the removal efficiencies of toluene and H_2S were stable at a high level (>95%), the system was assumed to be at the steady state. During the steady state, GRT was decreased from 60s to 7.5s and the inlet pollutants' concentrations were increased step by step to evaluate their influences on BAC performance. The parameters for operational runs are shown in Table 3.11.

Table 3.11 Operating parameters of the neutral pH single-stage biotrickling filter

Packing media volume (L)		11.25
Inlet gas concentration(ppmV)	H_2S	5-50
	Toluene	50-200
GRT(s)		60 (start-up) 7.5-60 (steady-state)
Gas flow rate (L/min)		11.25-90
pH of recirculation solution		6.0-8.0

3.6.1.4 Microorganisms used in the biotrickling filter

Unlike compost medium which has an indigenous microbial population, activated carbon needs to be inoculated with microorganisms. For easily biodegradable pollutants such as odours, or for complex waste gases, a general source of bacteria such as activated sludge is often sufficient. Activated sludge contains a wide

spectrum of bacteria, capable of degrading many different compounds. The use of adapted consortia or pure cultures with high biodegradation potential is favored when treating gases containing poorly biodegradable pollutants (Hanson, 2001). The neutral pH biotrickling filter (single-stage) was inoculated by a mixture of H_2S degraders and *Pseudomonas putida*.

3.6.1.5 Inoculation and biofilm

5168g of Calgon carbon AP-460 was rinsed out with distilled water to remove fines and dried at 100°C for 24h, and then it was randomly packed in the column. Microorganisms were online inoculated according to the procedure described in Section 3.4.2. The concentrated microbial broth (bacteria number>10^8cfu/mL, pH about 7) was added into the recirculation liquid. As a general rule, the broth volume is 1/10~2/10 of the trickling liquid volume (9L). The polluted gas was then introduced into the biotrickling filter for microorganisms' catabolism.

Monitoring of the viable cell adhesion onto activated carbon was done using the Centrifuge Method described by Yap (1999). In this method, about 1g of carbon sample was extracted from the bacteria-carbon mixture and placed in 10mL of 0.8% NaCl solution in a centrifuge tube. The bottle was then centrifuged at 10,000rpm for 5 minutes to dislodge the bacteria from the carbon surface. A bacteria count was then conducted using a direct counting method in the NaCl solution.

For activity measurements of the biofilm, carbon samples were suspended in the recycle liquid and analyzed for substrate-induced oxygen uptake rates (OURs). 2.5g of carbon sample was placed in the vessel fitted with an oxygen electrode (YSI) and saturated with air at room temperature. Substrate-induced OURs were measured after the addition of aqueous solutions of toluene (50mg/L) or $Na_2S_2O_3$ (the substitute for H_2S, 10g/L).

3.6.2 Low pH single-stage biotrickling filter

Operating a single-stage biotrickling filter at a neutral pH could be expensive in practice since large quantities of chemical were needed to maintain a neutral pH environment (see Appendix B). Todd et al. (1997) reported that a low pH single-stage biotrickling filter was also capable of realizing co-treatment of H_2S and VOCs. Therefore, a low pH single-stage biotrickling filter was investigated to evaluate the BAC performance under an acidic environment.

The reactor configuration and the volume of the low pH single-stage biotrickling filter were the same as those of the neutral pH single-stage biotrickling filter. The reactor was equipped with a single sump for the collection and recirculation of liquid nutrition. The same amount of GAC (AP-460) was also packed in Segment I to V. The physical properties of the biotrickling filter can be seen from Table 3.9. The synthetic foul air was produced similar to that produced in the operation of the neutral pH single-stage biotrickling filter. The recirculation water was also intermittently trickled through the packing bed and the composition of the solution is described in Table 3.10. The pH of the leachate was monitored every day.

3.6.2.1 Experimental procedure

Table 3.12 shows the operating parameters of the low pH single-stage biotrickling filter. As can be seen, the operation parameters of the low pH single-stage biotrickling filter were similar to those of the neutral pH single-stage biotrickling filter except that the pH of the recirculation solution was maintained from 1 to 3. During the 110 days of operation, H_2S and toluene concentration were set at about 20ppmV and 50ppmV and the air flowrate was regulated to yield a GRT of 60s during the start-up period. H_2S and toluene gas was introduced simultaneously to create the acid environment. After the start-up phase, GRT was decreased from 60s to 9s and the inlet pollutants concentrations were increased gradually to evaluate their influences on BAC performance.

Table 3.12 Operating parameters of the low pH single-stage biotrickling filter

Packing media volume (L)		11.25
Inlet gas concentration(ppmV)	H_2S	20-50
	Toluene	50-200
GRT(s)		60 (start-up) 9~60 (steady-state)
Gas flow rate (L/min)		11.25~75
pH of recirculation solution		1.0-3.0

3.6.2.2 Microorganisms used in the biotrickling filter

The low pH biotrickling filter (single-stage) was inoculated by the adapted consortium cultured from returned activated sludge (the flask culturing procedure has been described in Section 3.1.1.3) at the first day. The online inoculation procedure and biofilm measurement methods were similar to those of the neutral pH single-stage biotrickling filter. The pH of the inoculation microbial broth was about 3.

3.6.3 Two-stage biotrickling filter

The neutral pH single-stage biotrickling filter had the financial consideration of high operation cost (Appendix B), while the low pH single-stage biotrickling filter could not achieve good performance (low toluene removal efficiency, the results will be discussed in Chapter 5). The two-stage biotrickling filter was hence proposed to overcome the disadvantages of those two biotrickling filters.

Figure 3.12 shows the schematic diagram of the two-stage biotrickling filter, whose difference from the single-stage biotrickling filter was that the two-stage biotrickling filter had separated sump tanks for different recirculation liquids. Other parts of the two-stage reactor were similar to those of single-stage biotrickling filters. The solid and dotted arrows in Figure 3.12 represent the directions of gas flow and recirculation solution, respectively. The physical properties of the two-stage biotrickling filter could also be described using Table 3.9. Segment I was defined as the first stage with trickling liquid for the growth of *Thiobacillus sp.*. Segment II to V were defined as the second stage with trickling liquid for *Pseudomonas putida* growth. A total volume of 11.25L carbon was packed in the five biotrickling filter segments.

The consideration of pollutants interaction is very important for gas mixture removal. According to the experimental results of contaminant interaction in the bench biofilter study (Section 4.2.2), toluene gas in concentration of 50-200ppmV had no influence on H_2S removal. 5ppmV of H_2S decreased toluene removal efficiency while the low concentration of 1ppmV did not. Therefore, H_2S removal was arranged before toluene removal in the two-stage biotrickling filter. If toluene removal was before H_2S removal, the pH decrease of the first stage due to H_2S adsorption on the activated carbon would affect the activity of toluene-degraders (Andrey et al., 2001). This arrangement was to avoid the influence of H_2S on toluene removal efficiency.

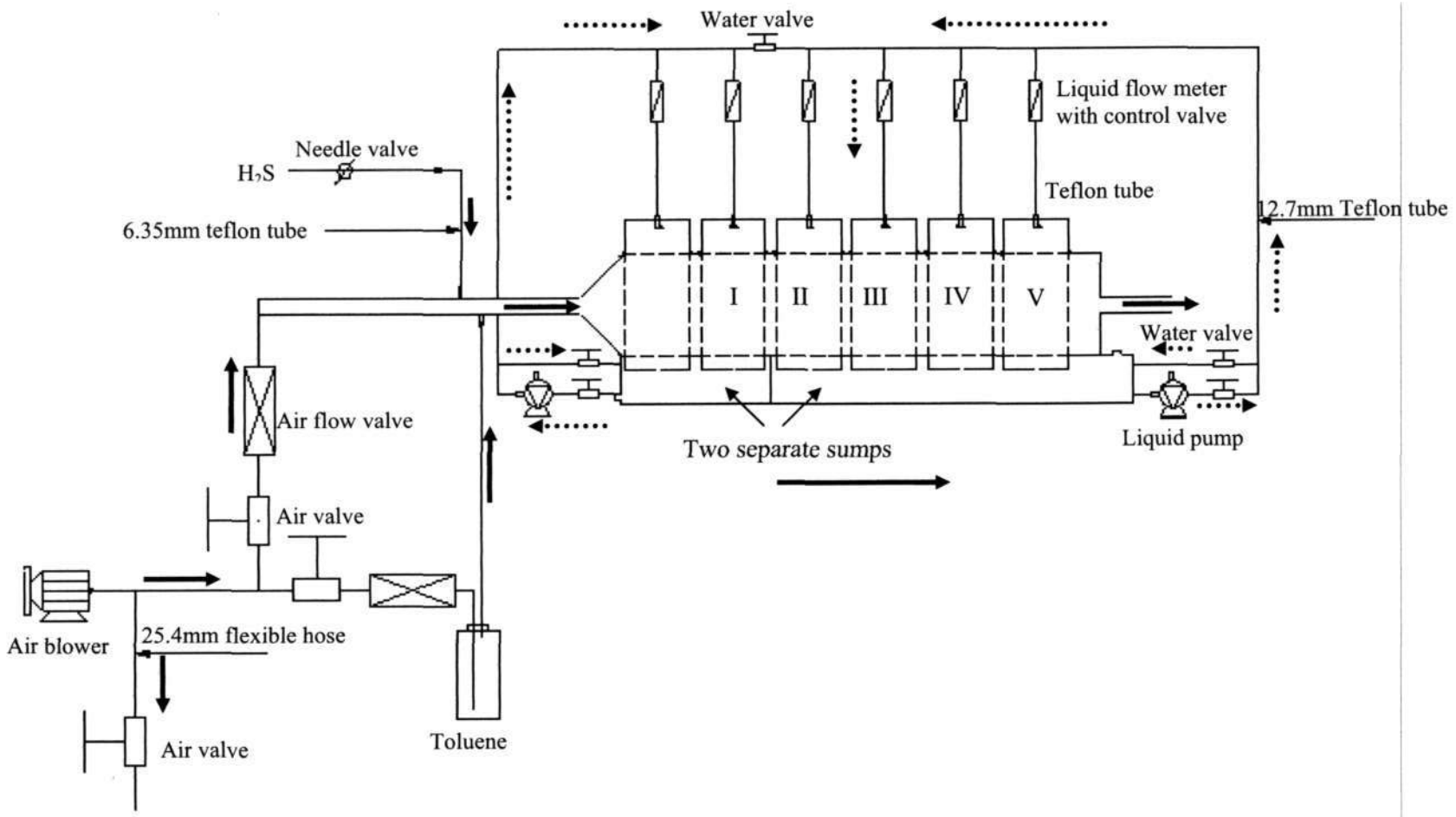

Figure 3.12 Schematic diagram of the two-stage biotrickling filter

3.6.3.1 Trickling style

To investigate the different reactions of the biotrickling filter to continuous trickling and intermittent trickling, these two styles were put into use during the two-stage biotrickling filter operation. The two-stage biotrickling filter was trickled continuously (0.4L/min) at the early stage of the operation. The liquid recirculation frequency was changed to twice per day (0.8L/min for 30 minutes on each occasion) after 72 days of operation. In the two-stage biotrickling filter, the compositions of the trickling medium for toluene and H_2S were different and they have been described in Tables 3.1 and 3.2. However, sodium thiosulfate, the surrogate of H_2S, should be excluded when the medium was used as the recirculation liquid for the biotrickling filter operation. The pressure drop of the carbon bed was measured about every ten days by connecting a water manometer with a minimum reading of 1mm water height to the inlet and outlet sampling ports.

3.6.3.2 Experimental procedure

Table 3.13 shows the operating parameters of the two-stage biotrickling filter. In the two-stage biotrickling filter, the first stage and the second stage had different operation parameters. The volume ratio and GRT ratio of the first and second-stage were set at 1:4 according to the literature review (Tables 2.6 and 2.7 show that GRT for H_2S was 3s-15s and GRT for toluene was 15s-60s, generally). The pH of the trickling water in the first-stage decreased quickly and naturally, and it was controlled at 1-3 eventually. The pH of the second-stage was maintained at 6-8 by the phosphorus buffer in the mineral salts solution. Initially only the second stage was packed with carbon and toluene gas was fed in to prevent the influence of H_2S like the neutral pH single-stage biotrickling filter. *Pseudomonas putida* was online inoculated when carbon bed adsorption capacity had reached breakthrough. H_2S gas was delivered after toluene removal reached 95%. During the 160 days of operation, GRT and inlet pollutant concentration were changed step by step as shown in Table 3.13 to test the performance of the BAC.

Table 3.13 Operating Parameters of the two-stage biotrickling filter

Operating Parameter		Two-stage biotrickling filter	
		First stage	Second stage
Packing media volume (L)		2.25	9
Inlet gas concentration(ppmV)	H_2S	5-50	
	Toluene	10-300	
GRT (s)		15 (start-up) 1.5~15 (steady-state)	60 (start-up) 6~60 (steady-state)
Gas flow rate (L/min)		9~90	
pH of recirculation solution		1.0-3.0	6.0-8.0

Note: The volume ratio of the first and second-stage in the two-stage biotrickling filter is 1:4.

3.6.3.3 Microorganisms used in the biotrickling filter

In the two-stage biotrickling filter, *Thiobacillus sp.* was inoculated at a low pH in the first stage while *Pseudomonas putida* was inoculated in the second stage at a neutral pH. It provided the optimum survival environment for bacteria growth thus enhancing the overall efficiency and effectiveness in the biotrickling filter system.

The inoculation procedure and biofilm measurement methods were the same as those of the neutral pH single-stage biotrickling filter. The pH of the microbial broth was about 7 for the second stage and about 3 for the first stage.

CHAPTER FOUR

APPLICATION OF BIOLOGICAL ACTIVATED CARBON IN A BENCH BIOFILTER

According to the physical characteristics, it is found that GAC Calgon AP-460 is not only an ideal packing medium with a large surface area for attachment of microorganisms, but also has a neutral pH and a rough surface for microbial attachment. It is of a porous structure for moisture holding and a uniform shape for even gas flow. Also, it has a good mechanical structure and a high adsorption ability to buffer concentration fluctuation. In this chapter, BAC was developed using offline and online immobilization methods, and then its capacity was tested in a bench biofilter.

4.1 BAC development

4.1.1 Offline immersed immobilization

The methodology is described in Section 3.4.1. Table 4.1 shows the variation of pH and bacteria number with time. The measurement of pH for *Thiobacillus sp.* gave evidence of the formation of microbial oxidation product, sulphuric acid. The faster pH decrease indicated higher degradation kinetics produced by *Thiobacillus sp.*. As illustrated in Table 4.1, the liquid pH decreased from 6.8 down to 2.4 within five days, during when the number of bacteria on the virgin carbon increased from 10^1cfu/mL to 10^4cfu/mL. However, the bacteria number on the virgin carbon was exceeded by that on H_2S exhausted carbon, which was 10^6cfu/mL (on the 5^{th} day), two orders of magnitude more than that on virgin carbon (10^4cfu/mL).

Table 4.1 Bacteria attachment on carbon surface (Offline immobilization)

Day		1	2	3	4	5	10	20
Thiobacillus sp. (log cfu/mL)	pH of virgin carbon	6.8	6.7	5.5	3.2	2.4	1.8	1.1
	Number on virgin carbon	1	2	3	4	4	7	9
	Number on H_2S exhausted carbon	1	2	4	5	6	9	9
P. putida (log cfu/mL)	pH	6.9	6.8	6.7	6.8	6.5	6.6	6.4
	Number on virgin carbon	1	2	4	5	5	8	10
	Number on toluene exhausted carbon	2	4	6	7	8	9	10

The neutral pH of *P. putida* enrichment showed little variation during 20 days of immobilization. The number of *P. putida* on the virgin carbon and toluene exhausted carbon was 10^5cfu/mL and 10^8cfu/mL on day 5, respectively. Making a comparison between the two different bacteria numbers, it was found that *P. putida* grew faster on the surface of exhausted carbon just like the case with *Thiobacillus sp.* for the reason that the exhausted carbon adsorbed a large amount of H_2S or toluene during the breakthrough test and hence attracted more bacteria attachment initially. But as time progressed, the bacteria density on these two carbons became fairly similar as shown by the numbers on day 20.

After 20 days of immobilization, carbon pellets were taken out and observed with SEM. The SEM pictures of the carbon granules on day 20 are shown in Figures 4.1 and 4.2. Figure 4.1 bears evidence that the BAC developed with a dense biomass of *Thiobacillus sp.* (short rods, 0.5 by 1.0-2.0μm) while Figure 4.2 shows clearly that thick biofilm layers of *P. putida* grew on the carbon surface as well. The bacteria counting and the SEM images indicated that both *Thiobacillus sp.* and *P. putida* were able to grow rapidly and were well attached on the carbon surface.

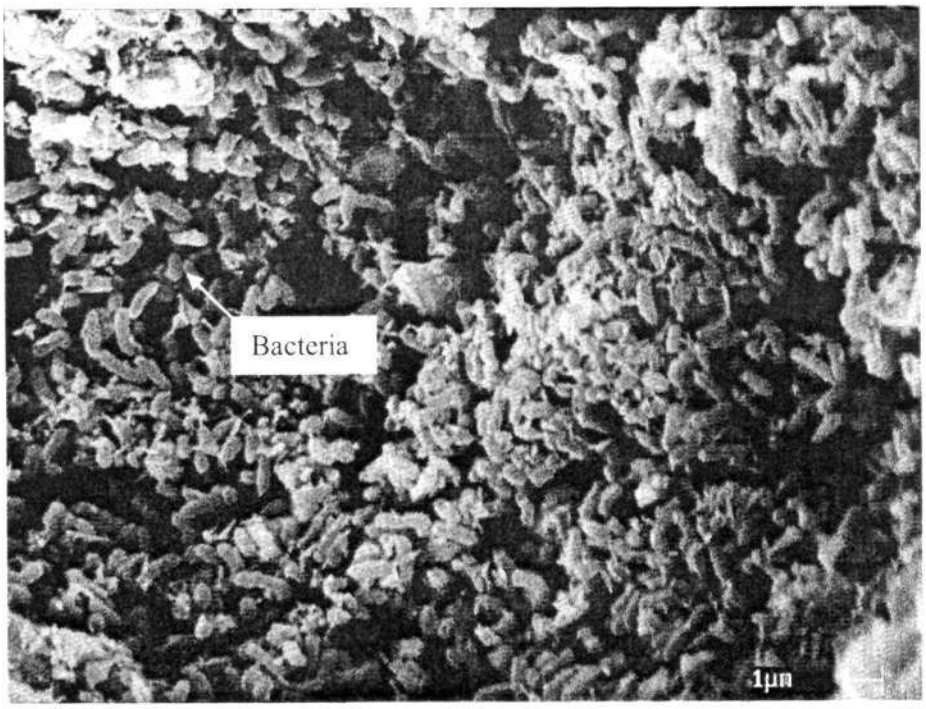

Figure 4.1 *Thiobacillus sp.* attachment on day 20

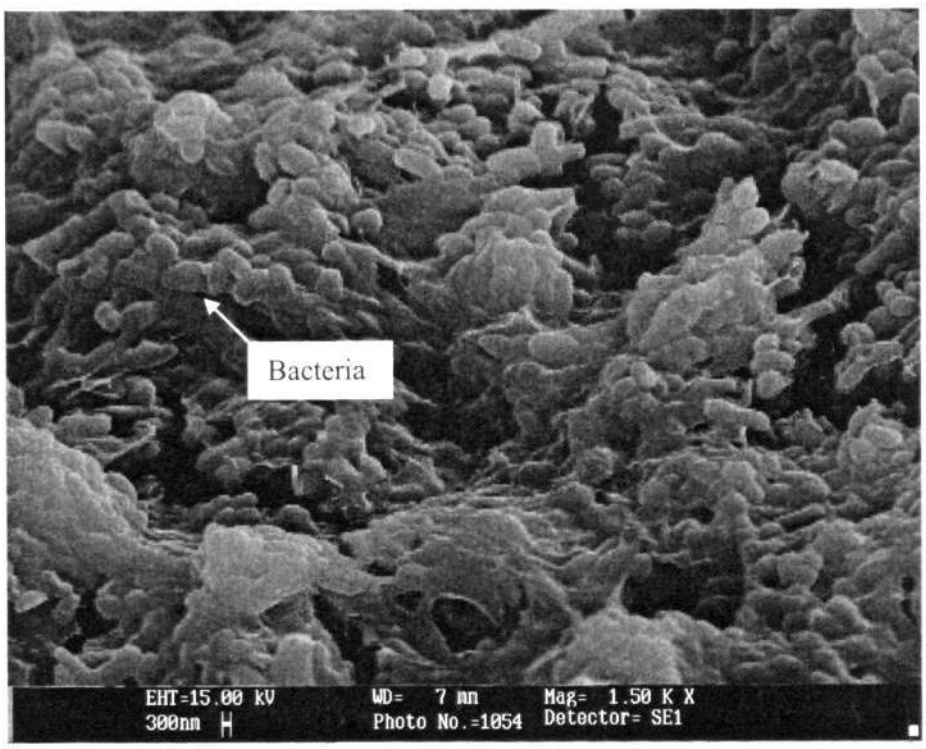

Figure 4.2 *P. putida* attachment on day 20

4.1.2 Online immobilization in a biofilter

Table 4.2 shows the results of the concentration of bacteria on the surface of carbon pellets which were subjected to online immobilization. The growth of bacteria was similar to that obtained in the offline immobilization, that the bacteria number increased with operating time and the exhausted carbon contained more bacteria than the virgin carbon did. For instance, on day 5, *Thiobacillus sp.* density was 10^6cfu/mL on the virgin carbon and 10^8cfu/mL on the H_2S exhausted carbon. For *P. putida*, the density was 10^7cfu/mL on the virgin carbon and 10^8cfu/mL for the toluene exhausted carbon on the same day.

Table 4.2 Bacteria attachment on carbon surface (Online immobilization)

Day		1	2	3	4	5	10	15
Thiobacillus sp. (log cfu/mL)	Number on virgin carbon	1	3	4	5	6	8	9
	Number on H_2S exhausted carbon	1	3	5	7	8	9	9
P. putida (log cfu/mL)	Number on virgin carbon	1	3	5	6	7	9	10
	Number on toluene exhausted carbon	2	4	6	7	8	9	10

After being operated for 15 days, carbon samples were taken out to observe the formation of the biofilm. Figures 4.3 and 4.4 illustrate the SEM images of BAC development during the online immobilization. As can be seen from the pictures, many layers of *Thiobacillus sp.* and *P. putida* were attached on the carbon surface, which evidenced that the production of BAC was successfully achieved by the online immobilization method.

Both offline and online immobilization tests exhibited a fast and excellent BAC development. *Thiobacillus sp.* and *P. putida* were easily attached on carbon surface to form a satisfactory biofilm.

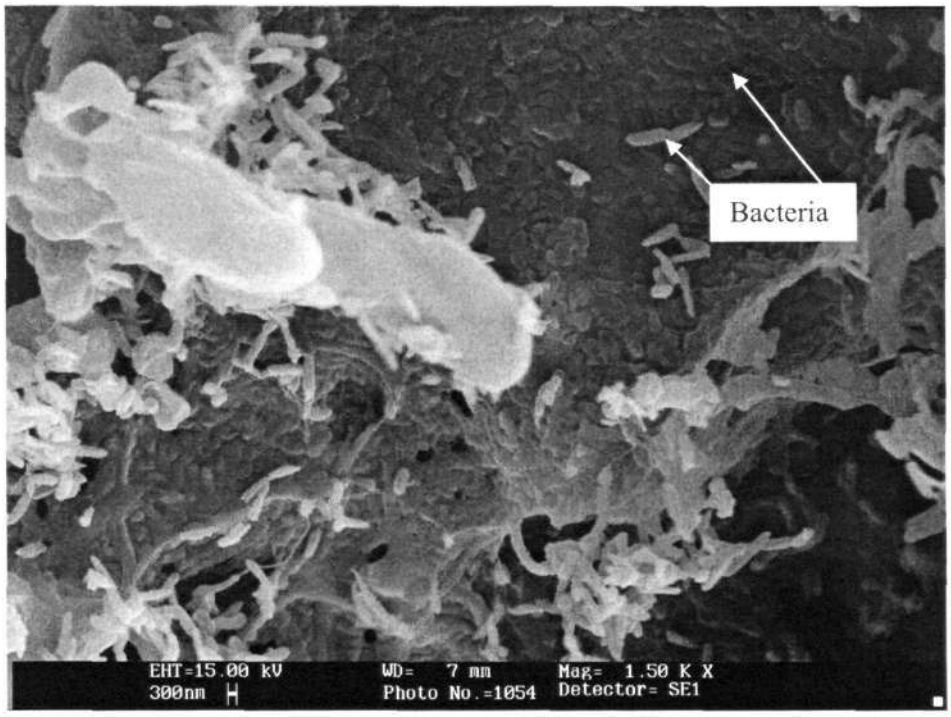

Figure 4.3 *Thiobacillus sp.* attachment on day 15

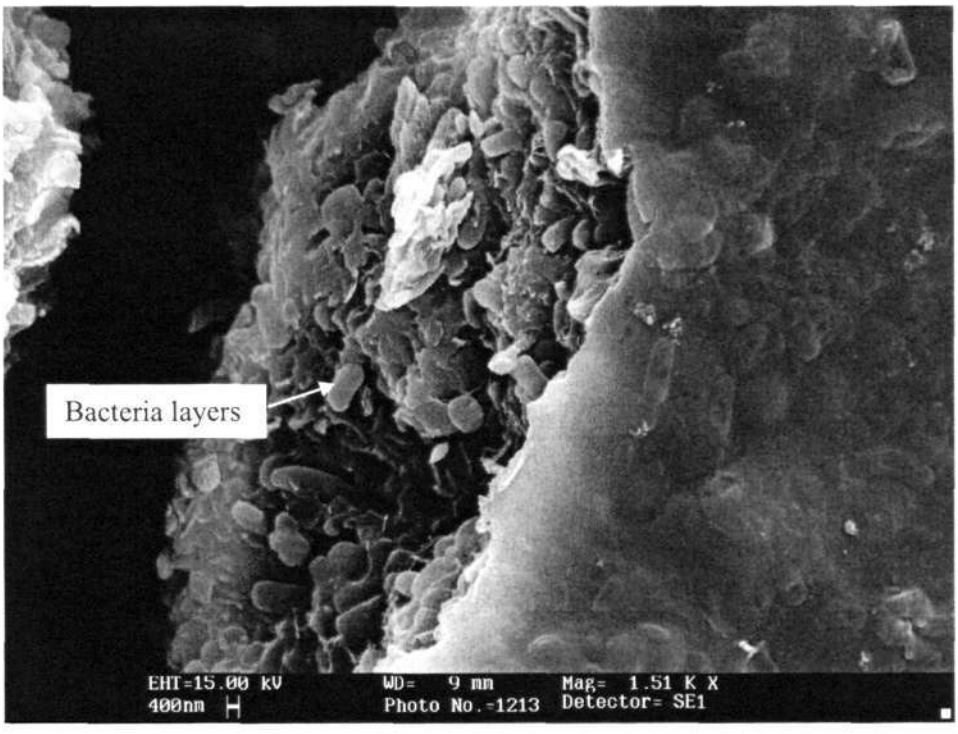

Figure 4.4 *P. putida* attachment on day 15

4.2 BAC test in a bench biofilter

A bench study was conducted firstly to study the performance of the BAC and to compare it against the performance of a non-biological activated carbon. The interaction of H_2S and toluene on the BAC was also explored in this bench biofilter. The characteristics of the carbon after exposure to H_2S or toluene were investigated as well. The methodology and experimental set-up for all the tests are described in Section 3.5.

4.2.1 BAC performance

The start-up period is the acclimation time required to establish optimal biological removal and to allow the system to have adequate time to stabilize. Depending on the properties of pollutants and microorganisms, this start-up procedure may last for a period ranging from a few days to a few months. Usually in the beginning, the pollutant removal is largely the result of the adsorption effects of the packing material. As time progresses, the removal efficiency will decline because the adsorptive capacity is gradually being exhausted, although some gas biodegradation will occur as the bacteria start to utilize the gaseous pollutant. Eventually, the performance of the bioreactor will improve as microbiological activity rises.

For conventional biofilter packing media such as compost and polypropylene rings, little adsorptive capacity is available and whatever available is used up very fast, possibly within a few hours (Ergas et al., 1995). However, an adequate microbial population cannot be established in such a short time. Therefore, a long start-up period (up to several months) with low removal efficiency (below 50%) is often seen in these biofilters' operation (Morales et al., 1998).

4.2.1.1 Toluene study

The toluene test was conducted with 50ppmV toluene gas at a GRT of 30s. Figure 4.5 shows the toluene removal during the start-up period using virgin GAC and

BAC. RE (BAC) is the removal efficiency of BAC combining adsorption and biodegradation, while RE (GAC) is the removal efficiency of GAC where biodegradation is not present due to the absence of bacterial film on the carbon granules.

Initially, BAC removal efficiency remained at 100% for a long period (day 0 to 4). The main mechanism for toluene removal was carbon adsorption. By this quick adsorption the immobilized cells avoided exposal to the toxic shock of toluene gas. Toluene was firstly adsorbed by the activated carbon and then slowly released for microbial degradation. Therefore, the GRT of a BAC biofilter, which was required for effective pollutant removal, could be much shorter than those of conventional biofilters. BAC biofilter could hence be designed as small as a carbon adsorption tower. It was also expected that a well-developed BAC could treat pollutants more completely with a higher efficiency than the conventional media.

On day 5, the removal efficiency decreased from 100% to 90%. Compared with the GAC curve (6 days of 100% removal), the breakthrough time of BAC was shorter (4 days of 100% removal). It demonstrated that adsorption capacity available in the BAC had declined under the influence of toluene adsorption and biomass obstruction when the biofilm was being formed. The delay and exhaustion of toluene adsorption by immobilized microorganisms might be caused by cells which narrowed or obstructed some pores and hindered the diffusion of toluene into the carbon. After only five days (day 5 to 10), the decreasing removal efficiency began to rise and reached 99% eventually. The main mechanism was believed to be biological oxidation now. However, GAC removal efficiency never recovered after decreasing to zero on day 15. Based on the high, stable removal efficiency of the BAC biofilter (day 14 to 20), the start-up period was considered to have been completed. During this BAC test, the removal efficiency remained at a high level (above 80%) all the time throughout the total start-up period.

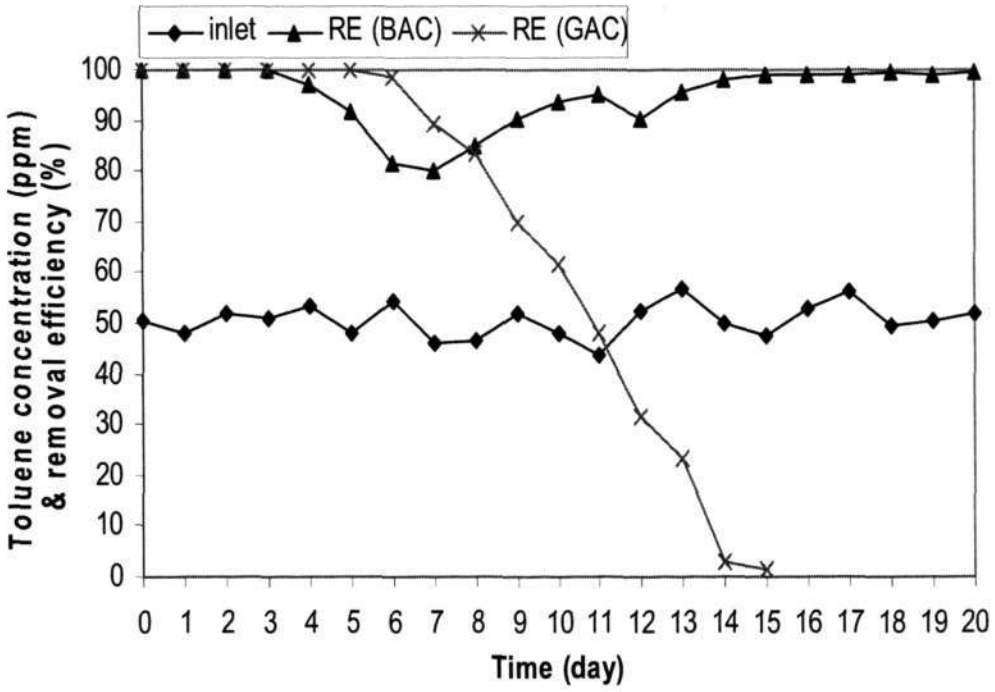

Figure 4.5 Toluene removal of BAC vs. GAC during the start-up period

4.2.1.2 H_2S study

Figure 4.6 shows H_2S removal during the start-up period. Inlet H_2S concentration was regulated at 20ppmV with a GRT of 15s. RE (BAC) is H_2S removal efficiency of BAC combining adsorption and biodegradation, while RE (GAC) is H_2S removal efficiency of GAC without biodegradation. The results of the H_2S test indicated a similar phenomenon to that obtained from the toluene test. After 17 days of 100% removal, RE (GAC) decreased to zero on day 26. During the initial 13 days, RE (BAC) was 100%. On day 14 RE (BAC) had a little decrease to 97% and recovered to 100% on day 16. The decrease was believed to be caused by the decrease in adsorption sites on the BAC due to biomass obstruction on the BAC granules. However, 16 days had been long enough for bacteria acclimation and that was why RE (BAC) returned to a high efficiency level quickly. During 30 days of operation, RE (BAC) remained stable at higher than 97%.

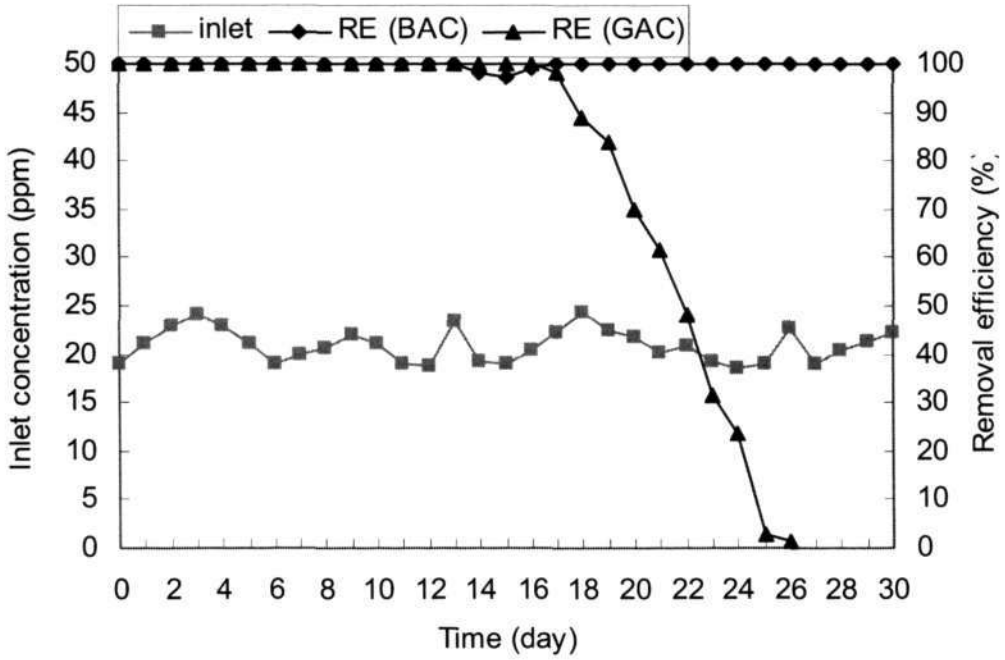

Figure 4.6 H_2S removal of BAC vs. GAC during the start-up period

All the results demonstrated that BAC achieved better performance than GAC without bacteria. The removal efficiency of GAC decreased to zero eventually and never recovered. BAC was hence a good packing material, which could achieve high performance during the start-up period and could shorten the acclimation time.

4.2.2 Contaminant interaction

Performance in a biofilter may be enhanced or inhibited by the interaction of the contaminants. It is often difficult to anticipate biofilter treatment success for mixed pollutants. Performance will depend on the interaction of the contaminant characteristics and the operating conditions of the system. Therefore, the interaction of H_2S and toluene was investigated to provide information on the performance of the biofilter when subjected to such a gas mixture.

4.2.2.1 Toluene influence on H_2S removal

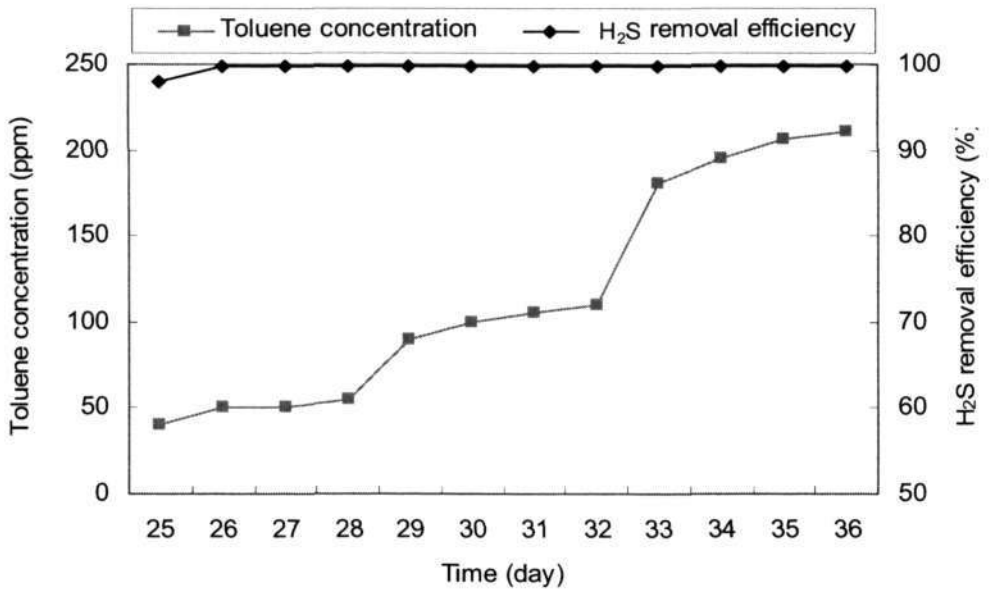

Figure 4.7 Toluene influence on H_2S removal

Toluene gas was introduced to the BAC column to test its influence on H_2S removal since day 25. The experimental results are shown in Figure 4.7. H_2S inlet concentration was controlled at about 20ppmV. Toluene concentration was increased from 50ppmV to 100ppmV, and then to 200ppmV. Experimental results showed that H_2S removal efficiency remained high at above 98% throughout the toluene concentration variation period, which demonstrated that toluene had no obvious influence on H_2S removal for the BAC.

In general, one compound can affect another one by changing the living environment of the latter degraders (such as pH, carbon source and etc.) or by impacting on the degraders themselves. During microbial degradation of multiple components, both beneficial and detrimental substrate interactions have been observed (Henderson, 2000; Song et al., 2003). If the optimum living environment of the contaminant degraders is changed, usually the removal efficiency tends to decrease. As for the impact of degraders themselves, one compound can stimulate

the transformation of another one by inducing the required catabolic enzymes needed for metabolism of the second pollutant, or by acting as a primary substrate to enhance cometabolism of another contaminant. In contrast, the presence of one compound can inhibit the degradation of another one by exerting toxicity, catabolite repression, competitive inhibition for enzymes or depletion of electron acceptor. In this study, toluene introduction did not change the living conditions of H_2S degraders in the biofilter. The low toluene concentration of up to 200ppmV did not promote or depress H_2S transformation, either.

4.2.2.2 H_2S influence on toluene removal

H_2S gas was introduced to investigate the changes of toluene removal by the BAC column since day 35. During this period, 50ppmV toluene gas at a GRT of 30s was controlled constantly and carbon pH was monitored everyday. Figure 4.8 reveals the influence of H_2S on toluene removal. From day 35 to 39, H_2S influent concentration was maintained at about 1ppmV by a needle valve. No significant fluctuation in toluene removal efficiency and in the carbon pH were observed, which could be attributed to the sufficient buffer capacity of the liquid medium to control the pH at a neutral level. When H_2S concentration was increased to 5ppmV, the behavior was found to be very different. During the five-day period (day 40 to 44), pH decreased from 6.7 to 2.4, meanwhile toluene removal efficiency decreased from 99% to 50%. A large amount of sulfuric acid, which resulted from H_2S adsorption, decreased the pH and destroyed the benign living environment of *P. putida* such that the biofilter performance was severely affected as indicated by the decrease in toluene removal.

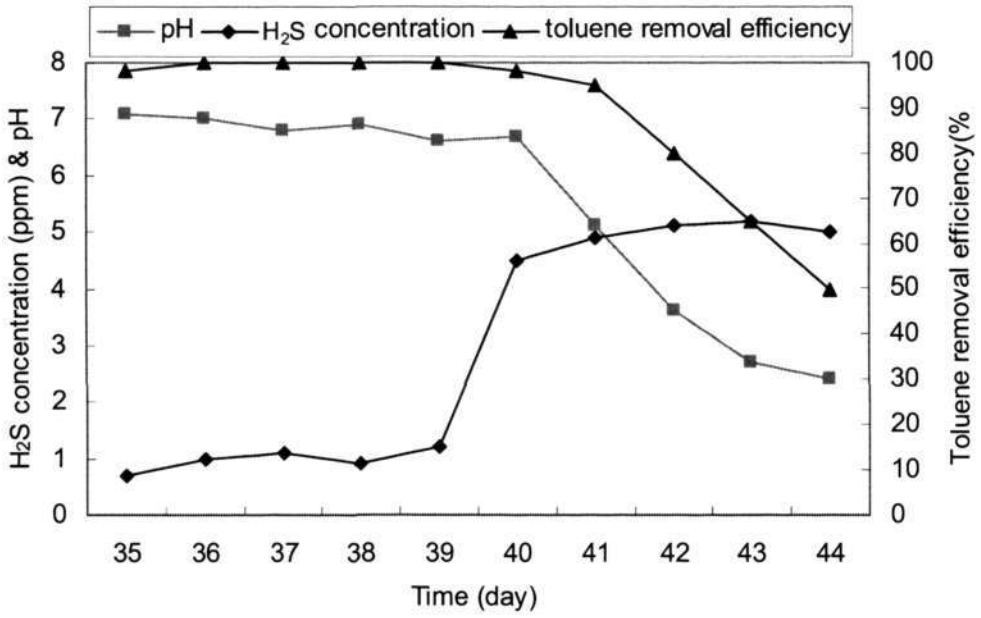

Figure 4.8 H_2S influence on toluene removal

4.2.3 Carbon characteristics

According to the International Union of Pure and Applied Chemistry (IUPAC) recommendations, the carbon pores are characterized based on their sizes.

1. Pores with opening exceeding 50nm in diameter are called "macropores".
2. The term "micropores" describes pores with diameters not exceeding 2nm.
3. Pores of intermediate size (2nm-50nm) are called "mesopores".

BAC samples were taken out for scanning electron microscope (SEM) analysis after the biofilter operation. Figure 4.9 is the SEM image of a big gap on the carbon surface from the toluene test. The right part in the photo is the biofilm layer while the left part is the carbon surface with several discrete bacteria. Theoretically, bacteria could not enter the micropores and mesopores, instead, most of them attached on the carbon surface and some large macropores. For example: The cell's diameter and length of *P. putida* are 0.7~1.1μm and 2.0~4.0μm, respectively. *Thiobacillus thiooxidans* is described to be short rods, 0.5 by 1.0~2.0μm. Both of them are bigger than mesopores. This was further supported by the SEM picture of

BAC cross section taken from the H_2S test. Figure 4.10 shows the cross section of a carbon granule, which was cut into half to observe its inner portion. Instead of bacteria, some undefined substances like metabolites or mineral salt were found to be attached on the carbon surface. Both of these two SEM images demonstrated that GAC particles allowed biological growth only on the surface and in pores sufficiently large for microbial cells, while the inner portion of the particle, which was a substantial portion of its volume, was inaccessible.

Salt accumulation could be observed in the inlet section of the biofilter column for the H_2S test run, but was absent at the outlet. Figure 4.11(a) shows that the surface of some carbon particles was coated by a white film. The white film part on the carbon surface was observed by SEM. It was found mostly in crystal shape (Figure 4.11(b)), which was very similar to the salt crystal reported by Acuña et al. (2002) in the biofilter system.

The pathway of sulfide biological oxidation by chemoautotrophs was suggested as: $H_2S \longrightarrow S^0 \longrightarrow S_2O_3^{2-} \longrightarrow S_4O_6^{2-} \longrightarrow S_3O_6^{2-} \longrightarrow SO_3^{2-} \longrightarrow SO_4^{2-}$ (Maier et al., 2000). High H_2S loading in the inlet area might cause the microorganisms to be overfed so that H_2S could not be completely biologically oxidized. As a result, the incomplete oxidation intermediates deposited on the carbon surface and formed a white film. In the outlet area, the bacteria degraded the remaining H_2S completely and the final product was sulfate, which was water soluble and could be washed away by the irrigation solution.

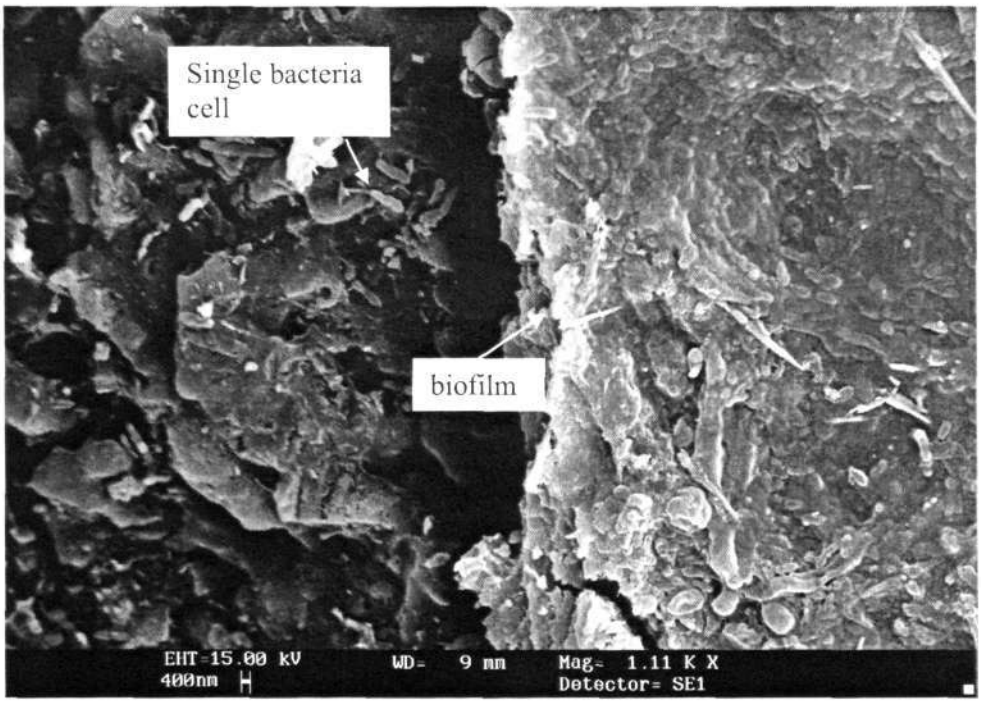

Figure 4.9 Biofilm gap from the toluene test

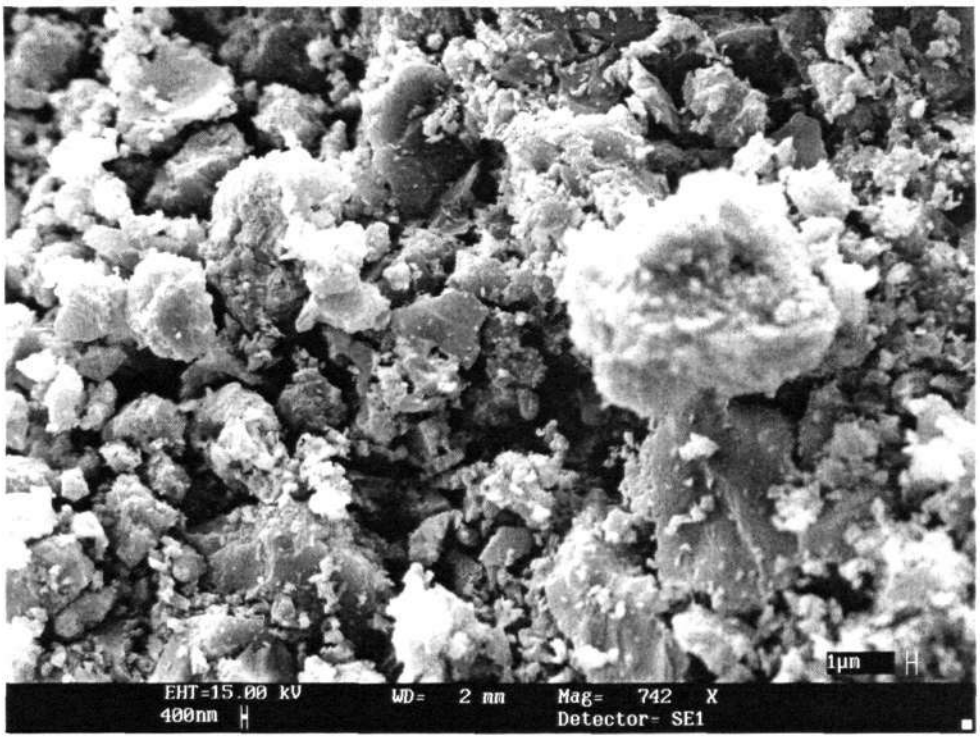

Figure 4.10 Cross section of BAC in the H_2S test

Figure 4.11(a) Activated carbon with the white film

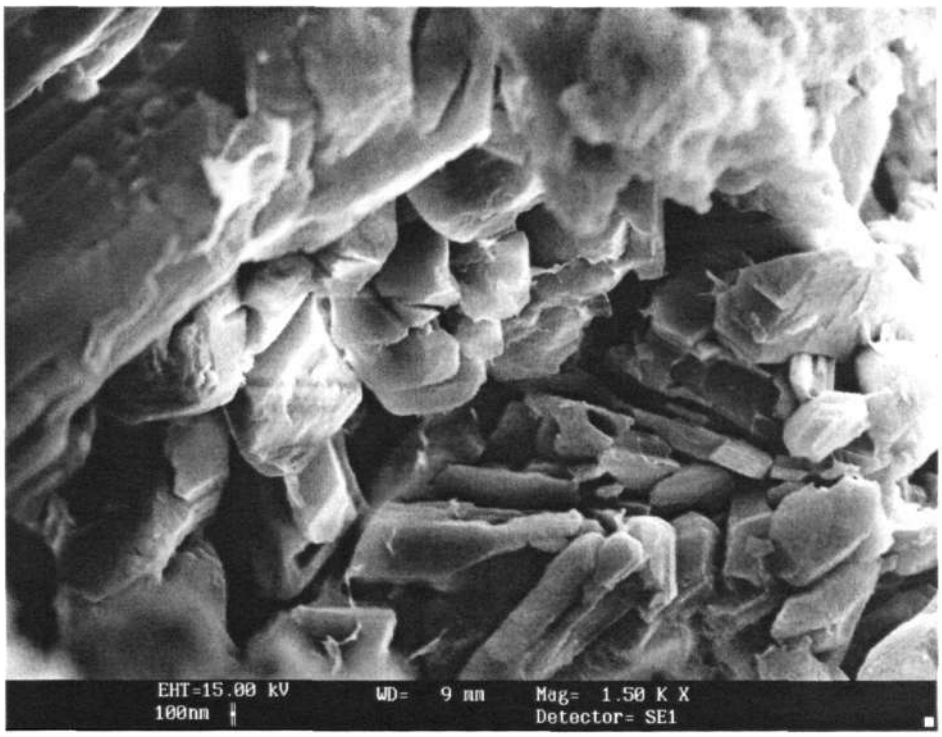

Figure 4.11(b) SEM image of the salt crystals

The bench study demonstrated the ability of the BAC to biodegrade as well as to adsorb H_2S and toluene compounds. This combination of physical adsorption and biological degradation seems to be applicable for the treatment of air streams containing high pollutant concentrations of a mixture of H_2S and toluene. The presence of toluene does not appear to affect H_2S removal by the BAC while the presence of H_2S does affect toluene removal significantly. Hence, it would be prudent to have a bioreactor system that firstly could remove H_2S in the influent air stream prior to toluene treatment. Such a dual bed system should be a better biosystem than conventional single bed systems.

CHAPTER FIVE

APPLICATION OF BIOLOGICAL ACTIVATED CARBON FOR GAS MIXTURE TREATMENT

To evaluate the capacity of the BAC as a biotrickling filter medium to treat a gas mixture containing toluene and H_2S, three biotrickling filters as described in Section 3.6 were set up and tested in a series of laboratory studies. Operating parameters such as GRT and inlet concentration were incrementally changed to test their influences on system performance. Results of the various tests are presented and discussed here.

5.1 Neutral pH single-stage biotrickling filter

5.1.1 Biotrickling filter performances

Figures 5.1(a) and (b) show the single-stage biotrickling filter performance on toluene and H_2S removal under the neutral pH condition, respectively. "Tol" represents the abbreviation for toluene. "RE I" in Figure 5.1(b) refers to H_2S removal efficiency of the first segment (Segment I). The first 20-day was considered the start-up period. In the first 15-day, toluene gas was introduced into the biotrickling filter bed packed with GAC. Inlet toluene concentration was modulated at about 50ppmV under a GRT of 60s. On day 4, the carbon bed was exhausted by toluene gas and toluene removal efficiency decreased from 100% to 3%. *Pseudomonas putida* was then inoculated immediately onto the carbon bed. The toluene removal efficiency increased quickly and reached 95% on day 11. On day 15, H_2S gas was delivered to the biotrickling filter after toluene removal efficiency remained stable at above 95%. Inlet H_2S concentration was set at 5ppmV and GRT was shortened to 30s. When H_2S removal efficiency decreased from 100% to 35% on day 17, H_2S degrading microorganisms were inoculated on the carbon bed to observe their effect on biotrickling filter performance. H_2S removal

efficiency was found moving up and achieved 100% on day 20. It was believed due to the combination effect of water absorption and biodegradation. However, water absorption was exhausted quickly in the initial several hours and biodegradation was dominant.

During the steady-state period from day 21 to 90, GRT and toluene inlet concentration were changed step by step to test the influences of these two important parameters on toluene removal efficiency as shown in Figure 5.1(a). When GRT was varied from 60s to 7.5s, the removal efficiency of toluene fell from about 100% to 80%. With the increasing inlet concentration of toluene from 50ppmV to 200ppmV (day 35 to 49), toluene removal efficiency decreased from 95% to 85% accordingly when the system was operated at a short constant GRT of 15s. From day 49 to 64, the H_2S inlet concentration was increased from 5ppmV to 10ppmV, and then to 20ppmV. During this period, the toluene removal efficiency was observed to decrease a little and then recovered to the initial level. Details of the interaction between H_2S and toluene will be decribed later in Section 5.1.4.

Figure 5.1(b) shows the H_2S removal performance of the single-stage biotrickling filter in the presence of toluene. As shown, inlet toluene concentration was varied from about 50ppmV to as high as 200ppmV during the 90-day operation of the biotrickling filter. During the steady-state operation, when GRT was decreased from 15s to 7.5s, the removal of H_2S by the first carbon segment (H_2S RE I) decreased from 99% to 80%, which indicated that Segment I was capable of removing most of the inlet H_2S. "Overall RE" represents the removal efficiency of H_2S for the whole reactor (Segment I~V). The overall removal efficiency was constantly at 100% because of the long overall GRT. When the inlet toluene concentration was increased from 50ppmV to 200ppmV (day 35 to 49), no significant fluctuation was observed in H_2S RE I (see Section 5.1.4). The presence of toluene in the system did not appear to have any impact on H_2S removal. It does appear that a neutral pH BAC biotrickling filter is capable of removing all H_2S loadings in spite of the presence of toluene gas.

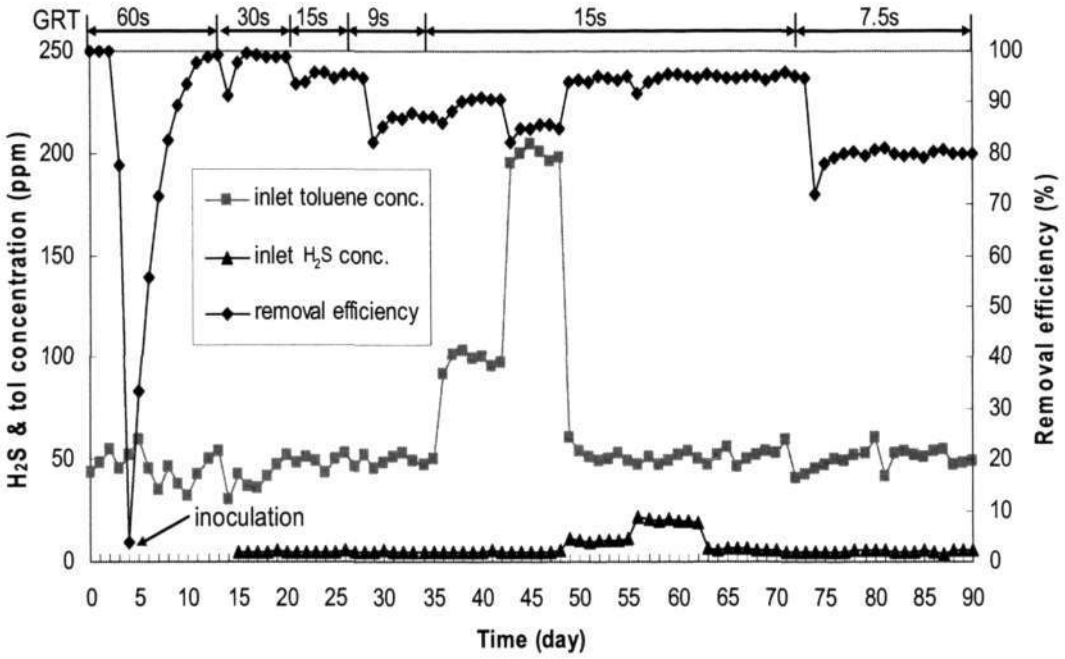

Figure 5.1(a) Toluene removal in the neutral pH single-stage biotrickling filter

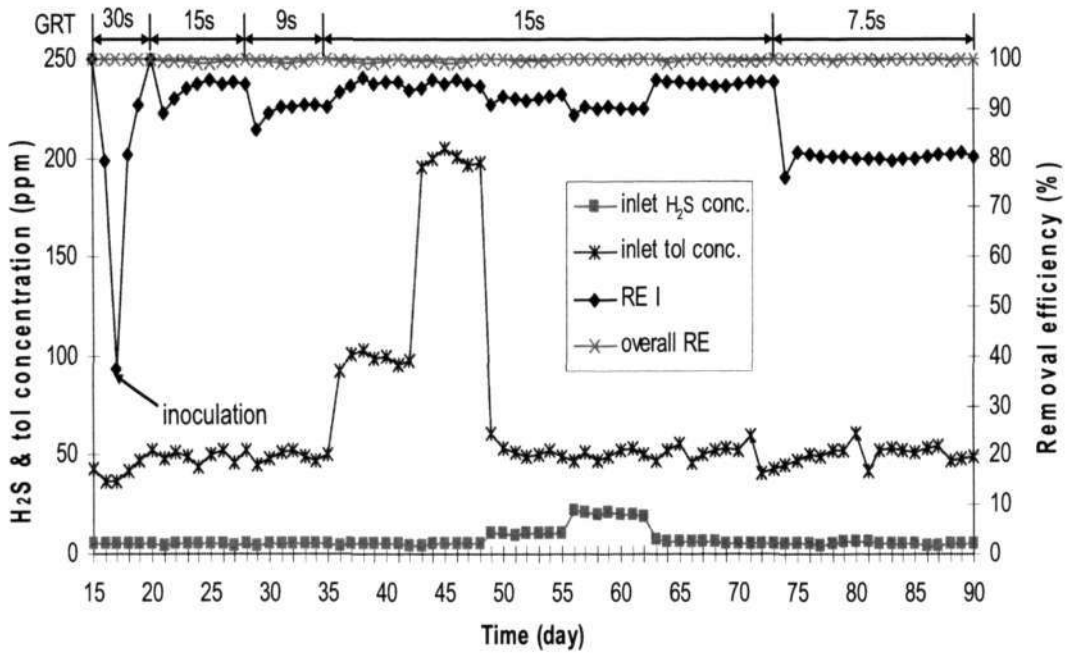

Figure 5.1(b) H_2S removal in the neutral pH single-stage biotrickling filter

5.1.2 Gas retention time

The effect of GRT on the removal efficiency was studied by changing the influent gas flow rate through the biotrickling filter bed. The GRT was controlled by the macrokinetics of the biofiltration process, which represented the interaction between the mass transfer phenomena and biodegradation by microorganisms (Ottengraf, 1986). When the GRT was sufficiently long, the pollutant was given the time to diffuse from the gas phase into the biofilm, and the microorganisms had enough time to utilize it.

Figures 5.2(a) and (b) show the variation of toluene and H_2S removal efficiency with GRT, respectively. The results reveal that toluene could be efficiently degraded (>94% removal) at a GRT of 15s or above. The further GRT reduction (<15s) led to the decrease of toluene removal. At a GRT of 9s, toluene removal efficiency was 86%. The H_2S removal efficiency decreased from 100% to 90% when the GRT was changed from 15s to 3.75s. In general, the decrease of GRT resulted in a lower removal efficiency. GRT appears to be an important factor in determining the removal efficiency. It appears that there is a minimal GRT below which the microorganisms on the biotrickling filter media will not have the sufficient time to utilize pollutant molecules efficiently.

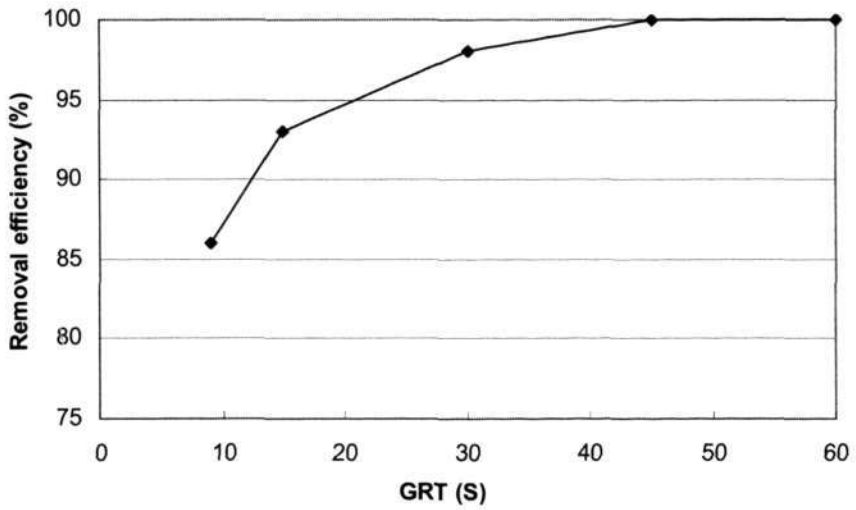

Figure 5.2(a) Toluene removal efficiency vs. GRT

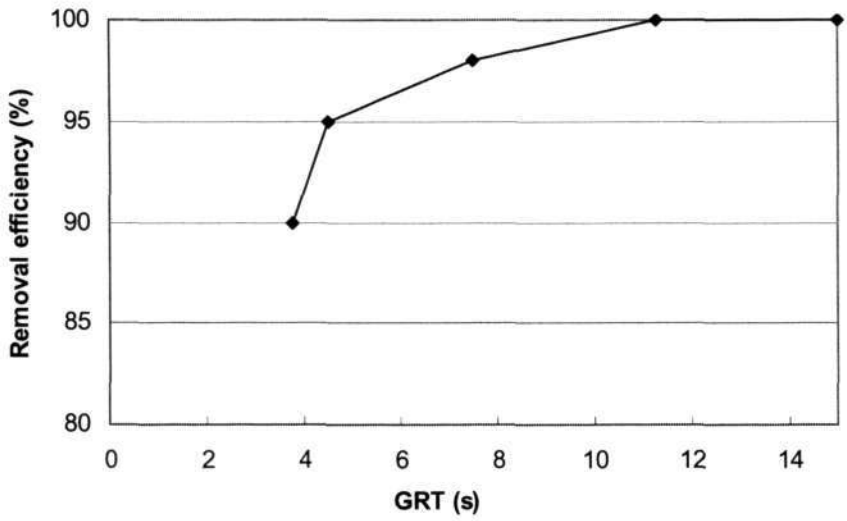

Figure 5.2(b) H_2S removal efficiency vs. GRT

5.1.3 Inlet concentration

Adjusting the inlet pollutant concentration, while maintaining a constant gas flow rate, allows the examination of the effects of different loading rates at a constant GRT on the performance of the biotrickling filter. According to Figures 5.1(a) and (b), usually at longer GRTs, the removal efficiencies remained stable for variations of inlet concentration. The effect of changing inlet concentration was minimal. For shorter GRTs, the removal efficiencies decreased with increasing inlet concentration. For example, at a short GRT of 15s, toluene removal efficiency declined from 95% to 85% with increasing toluene concentration from 50ppmV to 200ppmV. H_2S removal efficiency decreased from 95% to 90% with increasing concentration from 5ppmV to 20ppmV at a GRT of 4.5s. This phenomenon, that the removal efficiency decreased as the inlet concentration was increased, was also reported by Wan et al. (2004). In his study, the removal efficiency at the gas velocity of 15m/h decreased more rapidly than that of 6m/h, as input concentration was increased.

In Figures 5.1(a) and (b), minor reductions in removal efficiency was observed due to the sudden changes of the inlet concentration. When GRT was sufficiently long,

the removal efficiency was not very sensitive to the change of the inlet concentration since the microorganisms had sufficient time to oxidize the pollutants. When GRT was shorter, the time needed for recovery became longer correspondingly.

5.1.4 Contaminant interaction

In order to study the effects of contaminant interaction, the H_2S concentration in the inlet stream was held constant, while toluene concentration was increased gradually. According to Figure 5.1(b), toluene inlet concentration was increased from 50ppmV to 200ppmV during day 35 to 49. H_2S removal efficiency did not change and RE I was still performing at a high level of 95%. Therefore, it could be concluded that the fluctuation of toluene concentration (0~200ppmV) had little influence on H_2S removal in the neutral pH single-stage biotrickling filter. This was because low toluene concentration did not change the living environment of H_2S degraders, which had already been discussed in the bench biofilter (Section 4.2.2.1). Similar results had also been reported by Cox and Deshusses (2001).

Figure 5.3 plots the variation in toluene removal efficiency for the neutral pH single-stage biotrickling filter during a time period when inlet H_2S to the biotrickling filter was deliberately increased from 10 to 20ppmV. The results indicate that H_2S had an influence on toluene removal in the neutral pH single-stage biotrickling filter. When H_2S inlet concentration was increased suddenly from 10ppmV to 20ppmV on day 56, toluene removal efficiency decreased from 95% to 92%, but it then went back gradually to the initial level as the system acclimated to the H_2S change. The impact of pH was excluded because pH was maintained at 6-8 by the addtion of NaOH solution.

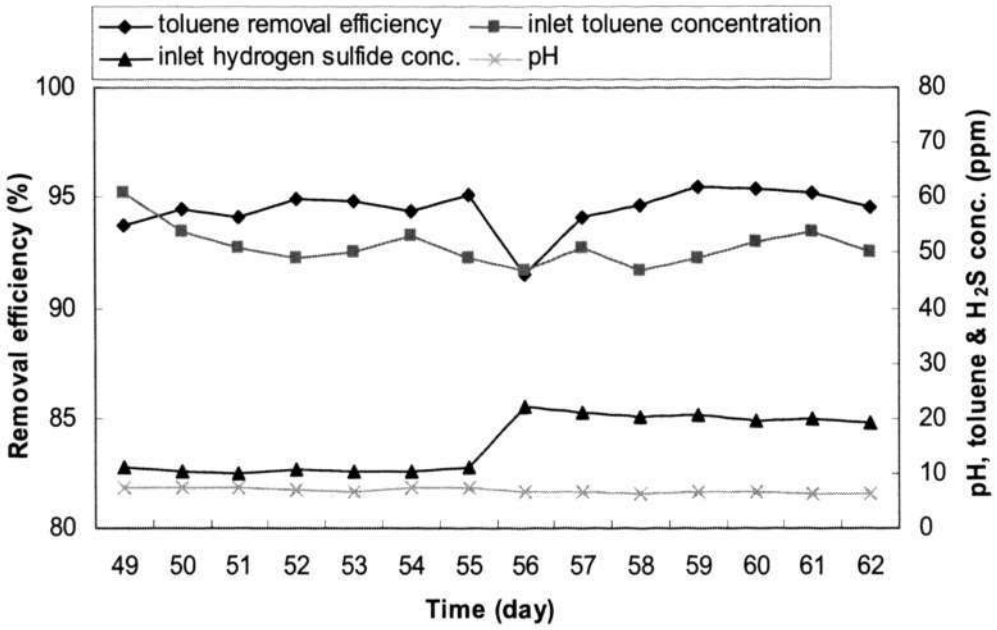

Figure 5.3 H_2S influence on toluene removal in the neutral pH single-stage biotrickling filter

To validate the reason of the decrease in toluene removal efficiency, variable sulfate concentrations were trickled through the carbon bed without the introduction of H_2S after the biotrickling filter operation. Sulfate sodium was dissolved in the recirculation liquid to produce sulfate solution in concentration of 0.1g/L, 0.5g/L, 1g/L and 5g/L. Toluene concentration was set at 50ppmV with a GRT of 30s. Figure 5.4 shows the effect of sulfate concentration on toluene removal efficiency. When sulfate concentration was varied from 0.1g/L to 0.5g/L, and then to 1g/L, toluene removal efficiency had reductions in performance due to the shock loading but then quickly recovered to the initial level. When sulfate concentration was increased to 5g/L, toluene removal efficiency decreased rapidly and did not recover at all. It appears that sulfate concentration should be limited below 5g/L for effective toluene removal.

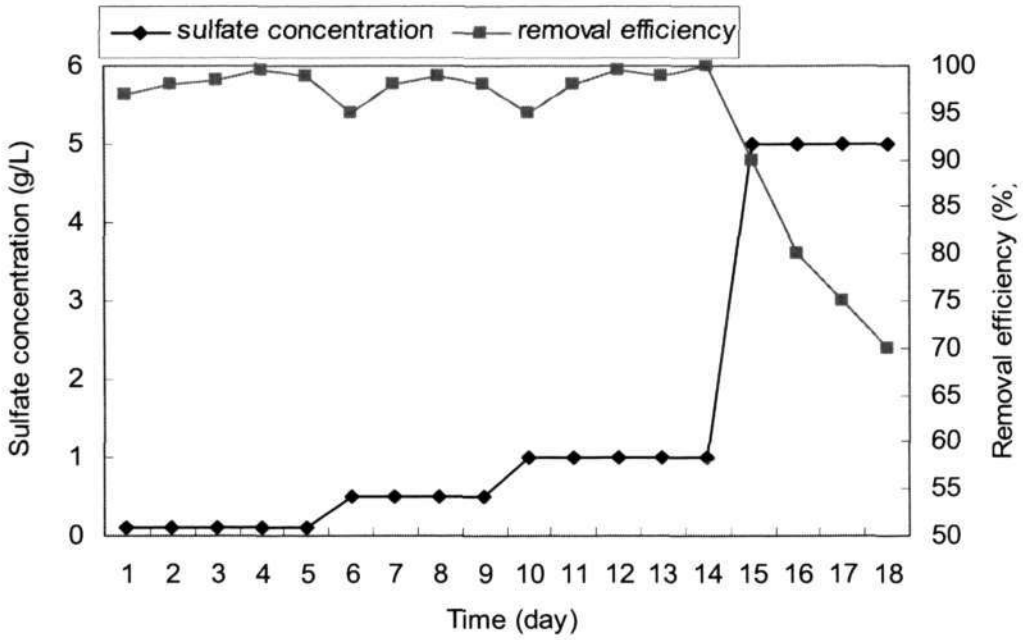

Figure 5.4 Effect of sulfate concentration on toluene removal efficiency

5.1.5 Elimination capacity

The elimination capacity is the capacity that the biosystem could bear without inhibiting its microbial activity. Figures 5.5(a) and (b) show the relationship of inlet loading and the elimination capacity of toluene and H_2S, respectively. The toluene elimination capacity increased linearly with increasing inlet loading until it reached an equilibrium value which was defined as the maximum elimination capacity of the biotrickling filter. It was of the same order of magnitude as found by Pedersen and Arvin (1995) and Kirchner et al. (1989). The maximum elimination capacity of toluene in the neutral pH single-stage biotrickling filter was 280g/m^3·h as shown in Figure 5.5(a).

The equilibrium state was not seen in Figure 5.5(b). It was due to the low inlet loading of the biotrickling filter. Therefore, H_2S degradation remained at first order kinetics so that the performance of the biotrickling filter was primarily limited by the H_2S diffusion rate in the biofilm. However, the elimination capacitiy of H_2S still followed the pattern of increasing linearly with increasing H_2S loading rate.

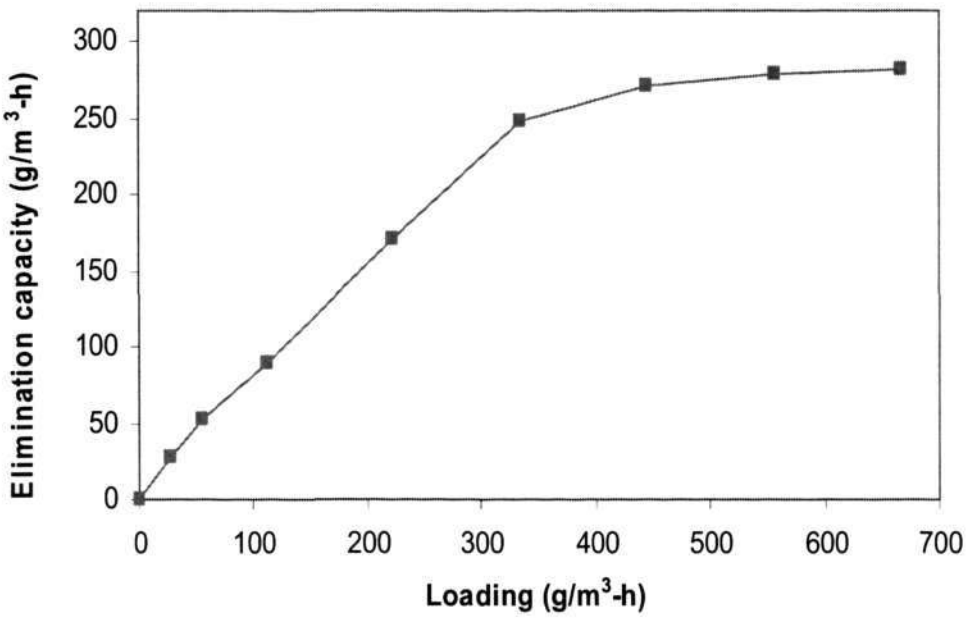

Figure 5.5(a) Inlet loading vs. toluene elimination capacity

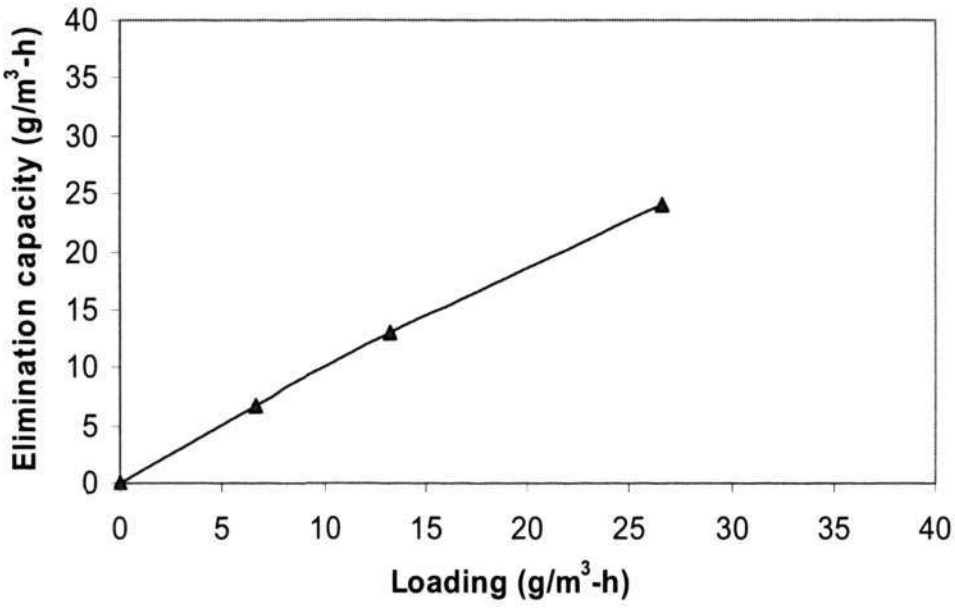

Figure 5.5(b) Inlet loading vs. H_2S elimination capacity

5.1.6 Concentration profile along the packing length

To understand the role of different sections along the packing bed length, the pollutant profiles along the packing bed were plotted here. Figure 5.6(a) shows the variation of H_2S concentration along the packing length in the neutral pH single-stage biotrickling filter. C/C_0 represents outlet concentration/inlet concentration, while h/H refers to packing length/the total packing length. Overall GRT was set at 15s which resulted in a GRT of 3s in Segment I. The inlet concentration was set at 5ppmV in the neutral pH single-stage biotrickling filter. 90% of the inlet H_2S was removed by Segment I (h/H=0~0.2) and the remaining 10% was removed by Segment II to Segment V (h/H=0.2~1). This was attributed to the longitudinal stratification of the biofilm in that the inlet area supported more biomass than the outlet area (Devinny et al., 1999). Therefore, more pollutant was removed in the first section of the packing bed due to higher microorganisms' concentration. Similar phenomena were also reported by Kim and Lee (2002) where in a carbon biotrickling filter with an inlet benzene concentration of 300ppmV, about 82% of the inlet benzene was degraded in the biotrickling filter height of 0~7.9cm, whereas 9.3% of benzene was degraded between 7.9 to 20.6cm.

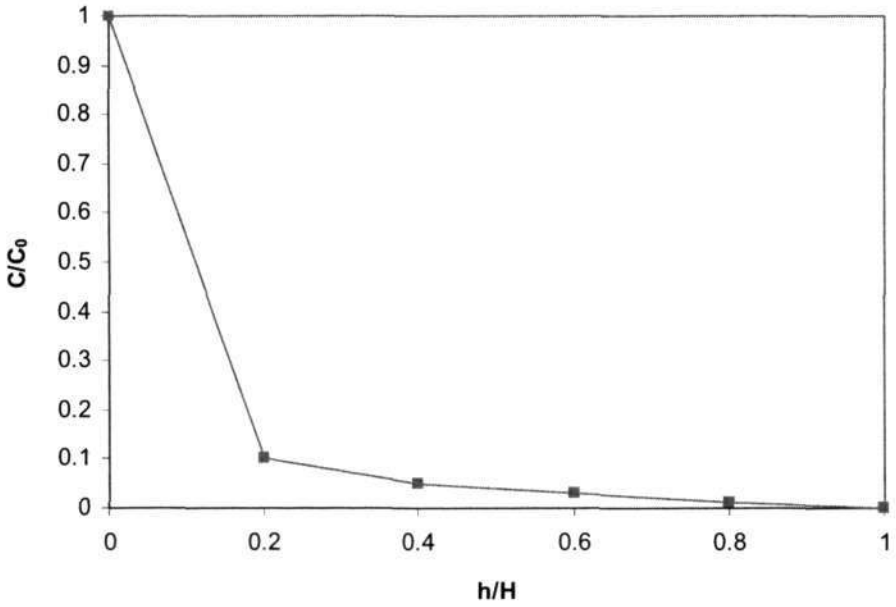

Figure 5.6(a) Variations of H_2S concentration along the packing length

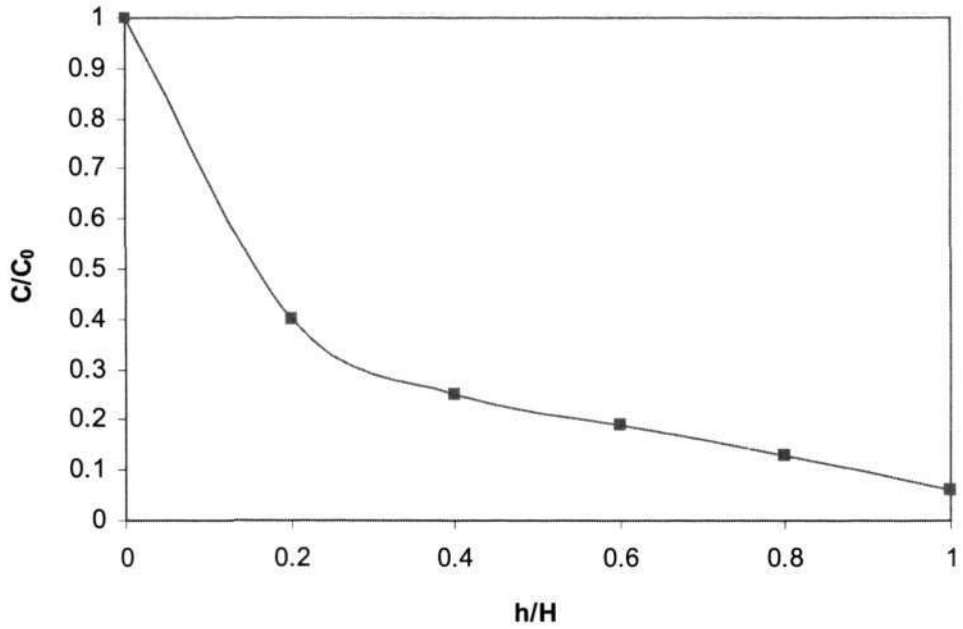

Figure 5.6(b) Variations of toluene concentration along the packing length

Figure 5.6(b), which was obtained at inlet toluene concentration of 50ppmV and a GRT of 15s, displays the toluene concentration profile along the packing bed in the neutral pH single-stage biotrickling filter. The profile of toluene was very similar to that of H_2S. Most of the inlet toluene (60%) was removed by only 1/5 of the packing bed length.

5.1.7 Biomass

The SEM image of a BAC sample was taken to observe the biofilm morphology on the carbon surface. Figure 5.7 shows the complex biofilm ecosystem of the single-stage system under the neutral pH condition. A complex microbial community was observed including numerous filamentous microorganisms, which illustrated that H_2S degraders together with toluene degraders grew among the filamentous branches. The system was not designed to maintain sterile conditions. Therefore, filaments were found in the biofilm but left no adverse effects on the reactor performance. On the contrary, it helped to bind the bacteria onto the surface of the packing medium.

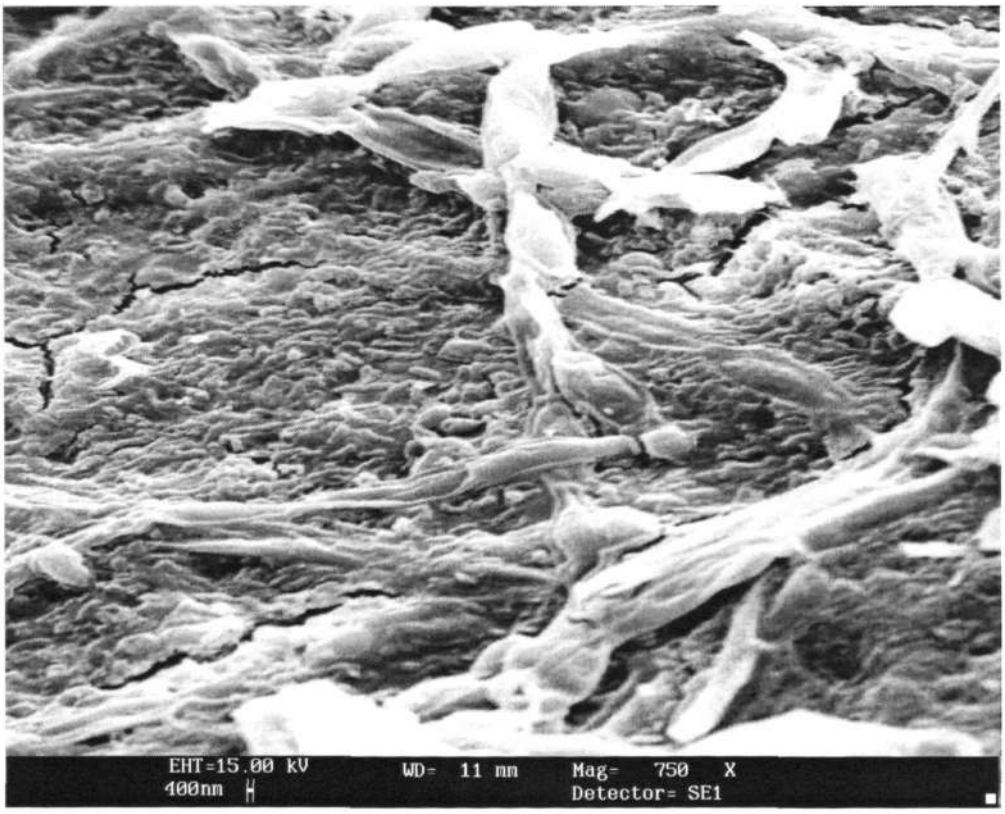

Figure 5.7 Biofilm in the neutral pH single-stage biotrickling filter

5.1.8 Removal mechanisms of BAC

The high removal capacity of BAC could be attributed to the degradation of the adsorbed contaminants through the biofilm, hence releasing the adsorption sites for futher pollutants uptake by carbon. This section attempts to evaluate the removal mechanisms of BAC to provide a better understanding of different contributions of adsorption and biodegradation. The virgin carbon refers to the unused carbon without bacterial film. The exhausted carbon was taken from the breakthrough test, which had been saturated by toluene or H_2S adsorption, without bacteria attachment. The BAC characteristics were caused by the combination of biodegradation and adsorption. The BAC samples were taken out after the biotrickling filter had operated for 90 days.

5.1.8.1 BET analysis

The BAC samples for the Brumauer-Emmett-Teller (BET) analysis, which provided the important pore and surface area information, were taken out from different points along the packing bed after the biotrickling filter operation. The BET data of the BAC are shown in Table 5.1. The data of the virgin and exhausted carbons are also shown here as reference. After the biotrickling filter operation, average pore diameter (1.966nm), average external surface area (413.5m^2/g), average micropore surface area (469.9m^2/g) and average total BET surface area (883.4m^2/g) of the BAC were close to those of the virgin carbon (1.98nm, 505.9m^2/g, 525.6m^2/g, 1031.5m^2/g). The experimental data demonstrated that the biofilm formation and adsorption did not significantly impact upon the carbon structure. Compared with the average micropore volume of virgin carbon (0.276cm^3/g) and the exhausted carbons (0.093cm^3/g for toluene, 0.078cm^3/g for H_2S), the average micropore volume of the BAC (0.214cm^3/g) was obviously close to that of the virgin carbon but was very different from those of the exhausted carbons even though the packing bed in this study was inoculated with microbial broth after the carbon bed was exhausted. It implied that most micropores of the BAC still remained empty at the end of the biotrickling filter operation, which proved that the spent activated carbon could be bioregenerated by microorganisms.

The regeneration of activated carbon by bacterial biofilms has been reported by several authors (Foad et al., 2000; Aizpuru et al., 2003; Gauden et al., 2005). The mechanism was believed to be the desorption of substances previously adsorbed on the activated carbon. The desorption took place because of the reverse concentration gradient between biofilm and carbon inside.

Some trends could be observed when the variance of BAC from inlet to outlet was studied in detail. Micropore volume (0.195-0.233cm^3/g) and micropore surface area (425.3-518.6m^2/g) increased along the packing length because most of the pollutants and degradation products in small molecules were concentrated in the inlet area. Average pore diameter (2.01-1.92nm) and external surface area (487.5-352.7m^2/g) decreased through the packing bed because more biomass near the inlet

could easily utilize the pollutants adsorbed in the external pores, and thus more empty places were released and pore diameter became larger at the inlet.

Table 5.1 BET data of the neutral pH single-stage biotrickling filter

Carbon type	Distance through packing bed (cm)	Micropore volume (cm^3/g)	Average pore diameter (nm)	Surface area (m^2/g)		
				External Surface area	Micropore surface area	Total BET surface area
BAC	5	0.195	2.01	487.5	425.3	912.8
	15	0.201	1.99	439.2	443.6	882.8
	25	0.217	1.96	413.8	467.1	880.9
	35	0.226	1.95	374.1	494.8	868.9
	45	0.233	1.92	352.7	518.6	871.3
	average	0.214	1.966	413.5	469.9	883.4
Virgin carbon		0.276	1.980	505.9	525.6	1031.5
Toluene exhausted carbon		0.093	2.015	201.7	412.6	614.3
H_2S exhausted carbon		0.078	2.024	182.1	397.1	579.2

5.1.8.2 Thermal analysis

The products of H_2S biodegradation include elemental sulphur, sulphate and thiosulphate, whereas toluene was converted to CO_2, H_2O, biomass and other intermediates. Thermal analysis provides the information about the thermal desorption of these products adsorbed in the carbon granules. Figure 5.8 shows the differential thermogravimetric (DTG) curves of the 5cm-45cm packing length in this BAC biotrickling filter. When water peak exists, other peaks of BAC are too small to be seen. Therefore, curves are plotted from 150℃ to avoid the adsorbed water interference although the tests were carried out starting from 30℃. The data are corrected accordingly so that the weight at 150℃ is considered as 100%. In all of the BAC curves, only the noncombustible sulfur peak around 300℃ was found,

even the small peak of sulfur found around 450℃ in the H_2S exhausted carbon (Figure 4.2) was not detected here, which indicated that the biofilm presence on the carbon might enhance the adsorbed H_2S oxidation to sulfate. It also demonstrated that the main final products of H_2S were H^+ and SO_4^{2-}, and the products of toluene biodegradation were CO_2, H_2O and biomass, respectively.

The curves from 5cm to 45cm of the packing length in Figure 5.8 show some trends along the medium bed. The peak height of 5cm-45cm decreased from 0.0039wt%/min to 0.0018wt%/min along the packing length in the single-stage biotrickling filter, which was because the inlet area received higher pollutant loading than the outlet area. As the pollutant was degraded along the packing length, the loading became less and less.

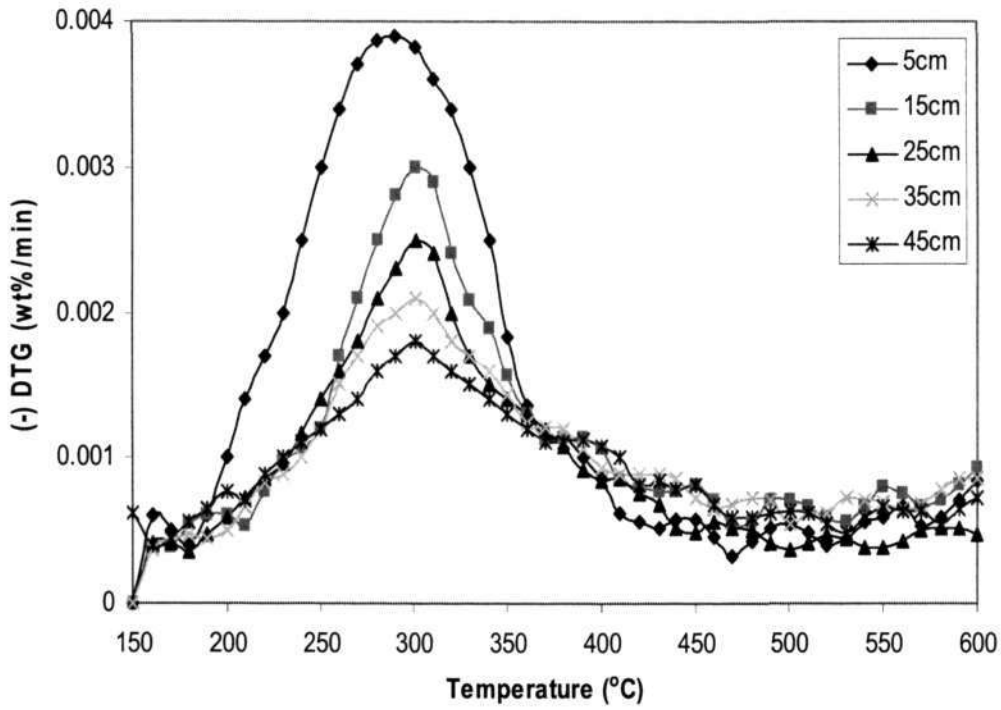

Figure 5.8 DTG curves of BAC in the neutral pH single-stage biotrickling filter

5.1.8.3 Sulfate accumulation

Sulphate was the principal final product of biological degradation of H_2S. Therefore, its accumulation in the biotrickling filter was unavoidable. The accumulation of sulphate in the carbon bed and recirculation liquid not only created a low pH environment, but also increased the ion concentrations (i.e. osmosis pressure), causing higher energy consumption for pumping substrate and nutrient through the cell membrane. Since it was closely related to pH, controlling the pH environment would also control the sulphate concentration at the same time.

Figure 5.9 illustrates the sulfate concentration diversification along the packing bed. In the single-stage biotrickling filter, sulfate accumulation (9-19.3mg/g-carbon) was much higher than that of the virgin carbon (0.014mg/g-carbon). As shown in Figure 5.9, sulfate concentration decreased along the packing bed because the inlet area removed more H_2S and so produced more sulfate than the outlet area.

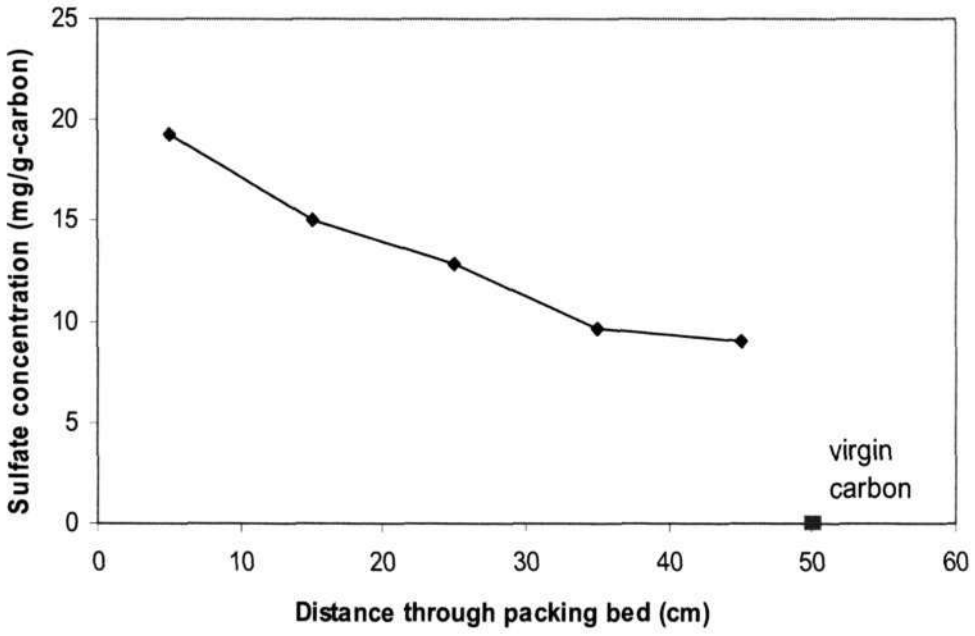

Figure 5.9 Sulfate concentration diversification along the packing bed

5.1.8.4 CNHS analysis

Thermal analysis evidenced that the dominant final product of H_2S oxidation was sulfate, which was non-combustible as the highest oxidation valence of sulfur. The combustible sulfur-bearing species could be any intermediate oxidation product that H_2S formed through either physical/chemisorption or biological oxidation. To obtain the possible content of sulfur-bearing species and the changes of other elements in the BAC, CNHS elemental analysis was conducted. Figure 5.10 shows the carbon (C), hydrogen (H), nitrogen (N) and combustible sulfur (S) content changes through the packing bed in the biotrickling filter. The element contents of the virgin carbon and the toluene or H_2S exhausted carbon were also included in Figure 5.10.

Compared with that of the virgin carbon (82.45%), the carbon content of the toluene exhausted carbon (85.21%) increased owing to toluene adsorption while that of the H_2S exhausted carbon (61.47%) decreased due to sulfur accumulation. The carbon content of the BAC (63.2-73.6%) was between that of the virgin carbon and that of the H_2S exhausted carbon. The hydrogen content of both exhausted carbon (0.83% for toluene and 1.64% for H_2S) and BAC (1.01-1.68%) increased a little when compared with that of the virgin carbon (0.57%). It was caused by toluene or H_2S adsorption and biodegradation. The nitrogen content of the virgin carbon was 0%, and the nitrogen contents of the exhausted carbon were 0.33% (H_2S) and 0.08% (toluene), which indicated relatively little changes. The nitrogen content of the BAC increased to 0.8-1.5%, which was mainly caused by the addition of nutrient liquid and the biomass accumulation. The changes of carbon, hydrogen and nitrogen content did not show any trend along the packing length as shown in Figure 5.10.

The changes of the combustible sulfur content were produced by H_2S because toluene had no sulfur element. The combustible sulfur content of the H_2S exhausted carbon (7.05%) was much higher than that of the virgin carbon (0.05%). The combustible sulfur content of the BAC (2.9-0.5%) was higher than that of the virgin carbon, but much less than that of the H_2S exhausted carbon because most H_2S was

oxidized completely to H_2SO_4. It was also observed that the combustible sulfur content in the biotrickling filter decreased along the packing length because the inlet area received higher H_2S loading.

In general, the element contents of the BAC at the end of biotrickling filter operation were close to those of the virgin carbon, which indicated that there was a constant mass balance of these elements during the biotrickling filter performance.

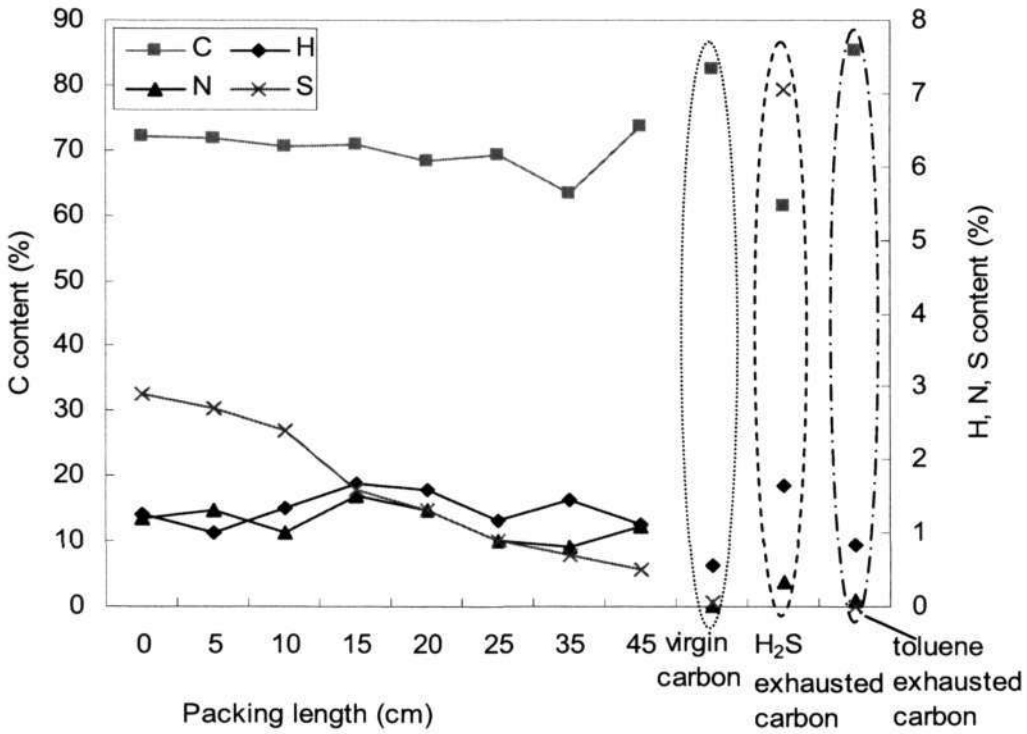

Figure 5.10 Element content of the BAC through the packing bed

According to BAC removal mechanisms investigation, the mechanisms of BAC for polluted gas treatment were different from those of pure GAC adsorption. For the GAC, carbon adsorption for gas removal was caused by physical and chemical adsorption, which mainly occurred in the micropores. While for the BAC, adsorption was integrated with biodegradation. In the beginning, the pollutant was removed largely by the adsorption effects. As time progressed, the adsorption capacity declined and biodegradation played the role gradually. Their relationship in the start-up period has been discussed in the bench biofilter (Section 4.2.1). At the steady state, biodegradation was dominant because all the BET data of the BAC were near to those of the virgin carbon but far different from those of the exhausted carbon caused by pure adsorption; the main final products of H_2S were H^+ and SO_4^{2-}; and the constant mass balance of element C, N, H, S during the system performance. The previously adsorbed pollutant was removed by the bioregeneration capacity of the BAC. During the transient conditions, the remaining adsorption capacity of the BAC had the ability to buffer the shock loading, which will be described in detail in Section 5.4.2.

5.2 Low pH single-stage biotrickling filter

5.2.1 Biotrickling filter performances

Figures 5.11(a) and (b) show the toluene and H_2S removal in the low pH single-stage biotrickling filter, respectively. The first 15 days was the start-up period and GRT was regulated at 60s. In the low pH single-stage biotrickling filter, 20ppmV of H_2S and 50ppmV of toluene were introduced simultaneously. Bacteria seed cultured from the returned activated sludge was inoculated on the first day. Toluene and H_2S removal efficiency increased and reached 100% in a short period (7 days). After the inoculation using the adapted consortium (pH around 3), the leachate pH was about 4.5 and remained uncontrolled. It decreased naturally and quickly to 2.7 on day 5 because the product of H_2S oxidation was sulphuric acid.

As shown in Figure 5.11(a), the toluene removal efficiency decreased as GRT was decreased. For a GRT longer than 30s, the removal efficiency was always above 94%. When GRT was reduced to 15s, the removal efficiency fell to about 86%, which meant that insufficient contact time between gas and liquid phase limited the mass transfer of toluene into the biofilm. From day 46 to 67, Toluene concentration was changed from 50ppmV to 200ppmV under a GRT of 15s to check its influence on toluene and H_2S removal efficiency. As a result, toluene removal efficiency decreased from 86% to 75% while H_2S removal efficiency had no changes.

"RE I" in Figure 5.11(b) refers to H_2S removal efficiency in Segment I. As GRT was changed from 60s to 9s, RE I decreased from 100% to 90% while overall removal efficiency (overall RE) of Segment I-V still remained at 100%. It indicated that most H_2S was removed by Segment I, which was similar to that observed in the neutral pH single-stage biotrickling filter. However, pH of the whole biotrickling filter was still acidic (1-3) because of the homogeneous recycling liquid. From day 75 to 95, the effect of H_2S concentration on the system performance was evaluated by increasing H_2S concentration from 20ppmV to 40ppmV at a GRT of 15s. As a result, H_2S RE I decreased from 92% to 88% while toluene removal efficiency had no changes.

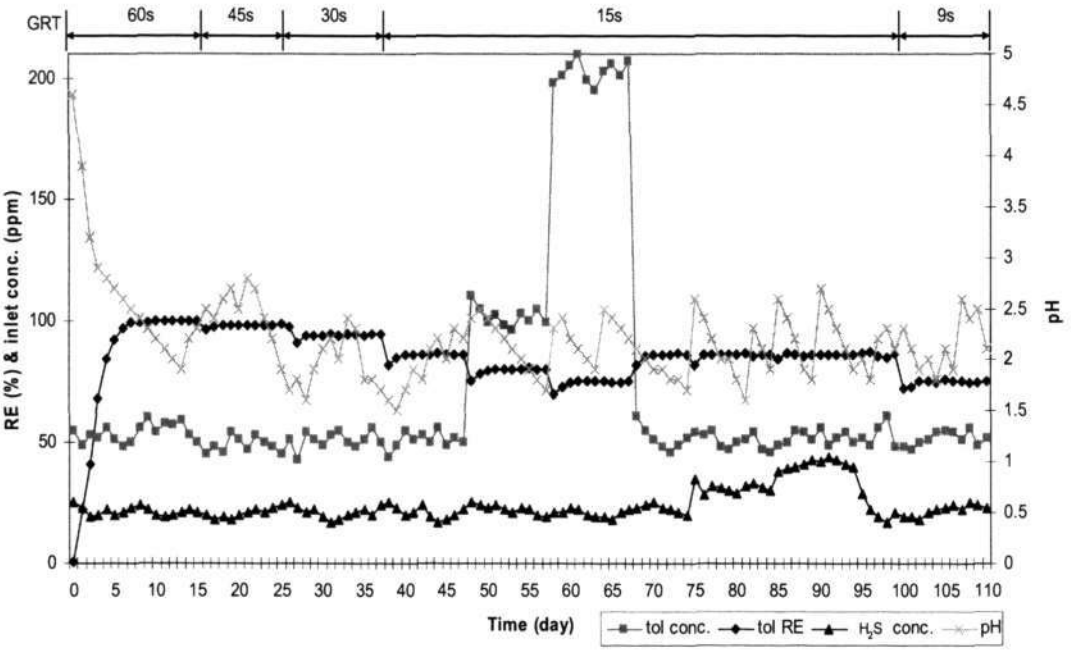

Figure 5.11(a) Toluene removal in the low pH single-stage biotrickling filter

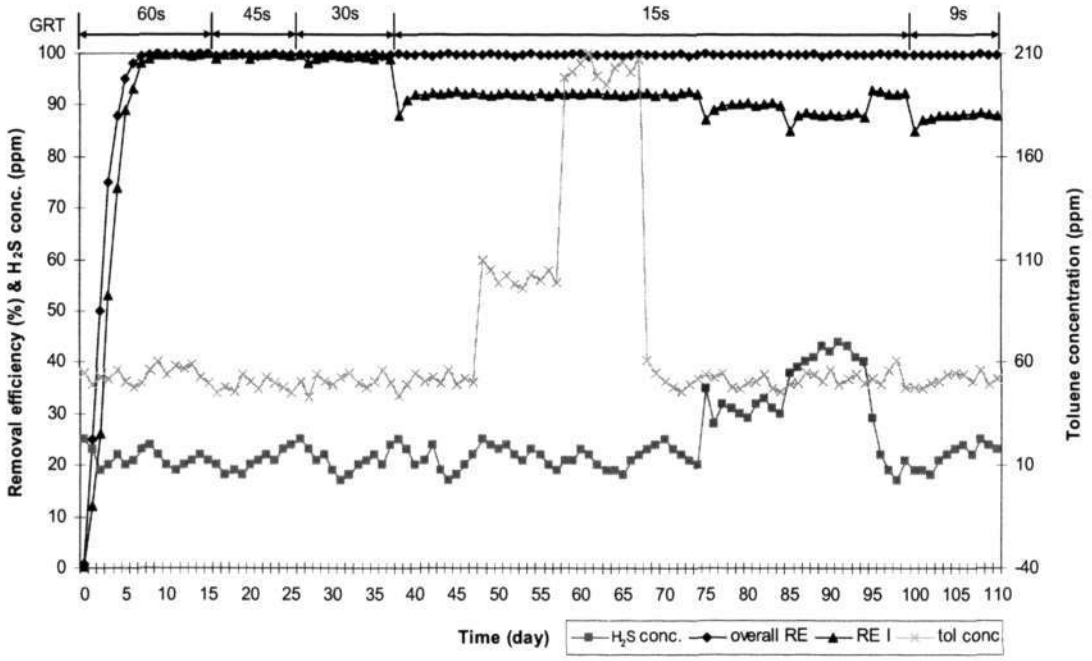

Figure 5.11(b) H_2S removal in the low pH single-stage biotrickling filter

5.2.2 Gas retention time

GRT is an important parameter in a biotrickling filter because it must be sufficiently long to obtain a high removal efficiency of pollutants. Figures 5.12(a) and (b) show the relationship of toluene and H_2S removal efficiency vs. GRT, respectively. A general pattern of decreasing removal efficiency with shortened GRT was also observed for both toluene and H_2S removal in the low pH single-stage biotrickling filter. When GRT was reduced from 60s to 15s, toluene removal efficiency decreased from 100% to 86%, which was lower than that of the neutral pH single-stage biotrickling filter (100% to 94%). H_2S removal efficiency declined from 100% to 92% as GRT was varied from 15s to 3.75s, which was because the microorganisms might not have sufficient time to degrade pollutant molecules when the GRT was shortened.

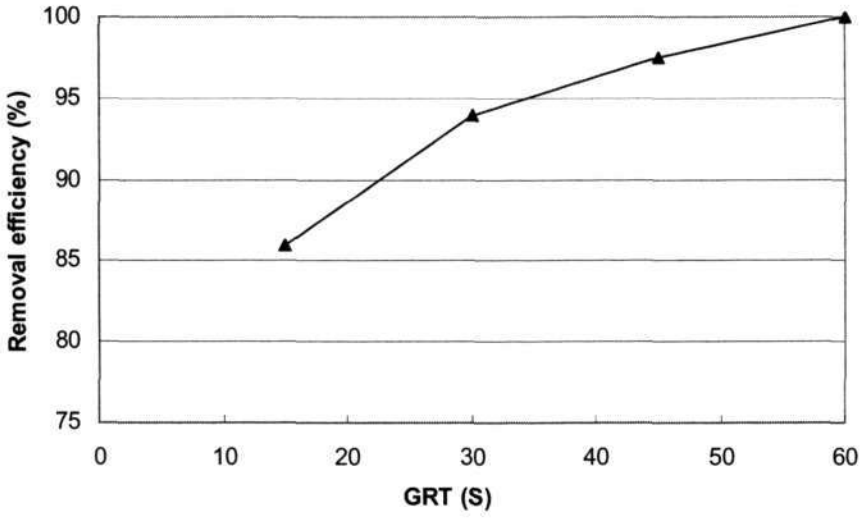

Figure 5.12(a) Toluene removal efficiency vs. GRT

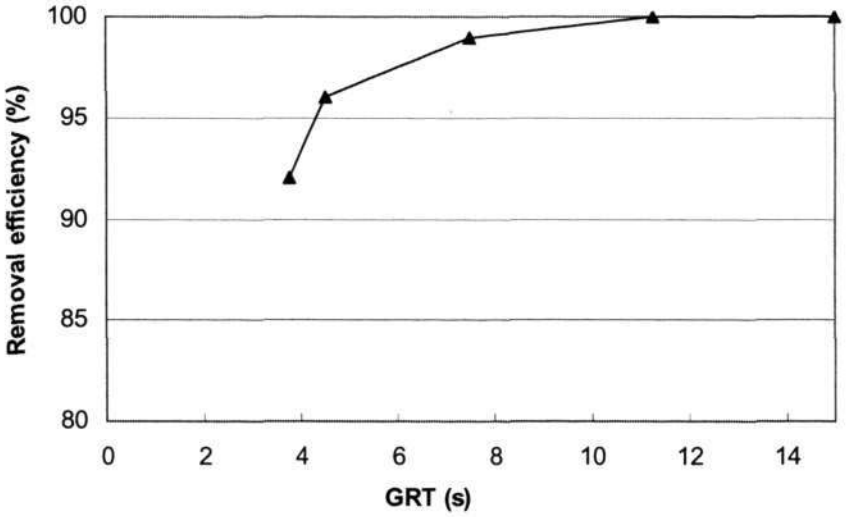

Figure 5.12(b) H_2S removal efficiency vs. GRT

5.2.3 Contaminant interaction

The contaminant interaction in gas mixture will influence the biotrickling filter performance. Therefore, the interaction study was carried out by changing the concentration of one compound while maintaining a constant concentration of another compound.

As seen from Figure 5.11(b), toluene concentration was increased from 50ppmV to 100ppmV, and then to 200ppmV from day 46 to 67. H_2S RE I remained at 90% during this period and no fluctuation was found, which demonstrated that the shock loading of 0-200ppmV toluene had no influence on the H_2S removal efficiency in the low pH single-stage biotrickling filter.

As shown in Figure 5.11(a), H_2S inlet concentration was increased from 20ppmV to 30ppmV, and then to 45ppmV during day 75 to 95. Although the toluene removal efficiency was kept at a low level of 86%, it remained constant. The negative or positive effect of increasing H_2S inlet concentration on the toluene removal efficiency was not observed in this study, which was because the acidophilic heterotrophs had acclimated to the extremely acidic environment in the low pH single-stage biotrickling filter.

5.2.4 Elimination capacity

Elimination capacity is one of the important parameters to evaluate the biotrickling filter performance. Figure 5.13(a) shows the variation of toluene elimination capacity with the inlet loading in the low pH single-stage biotrickling filter. There was a similar trend of increasing elimination capacity with increasing inlet loading and then reaching a constant level as was achieved in the neutral pH single-stage biotrickling filter. The maximum elimination capacity of toluene in the low pH single-stage biotrickling filter was 205g/m^3·h.

Figure 5.13(b) shows the relationship of the H_2S elimination capacity with the inlet loading. The H_2S loading was observed to be higher in the low pH single-stage biotrickling filter (0-70g/m^3·h) than that in the neutral pH single-stage biotrickling filter (0-28g/m^3·h). The elimination capacity curve still increased linearly but could not achieve the equilibrium value.

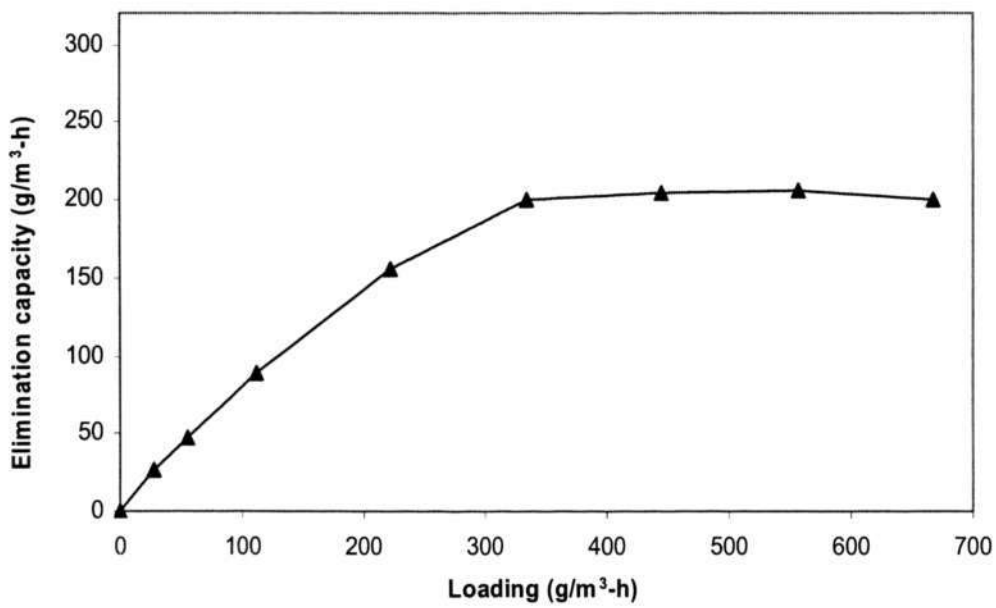

Figure 5.13(a) Inlet loading vs. toluene elimination capacity

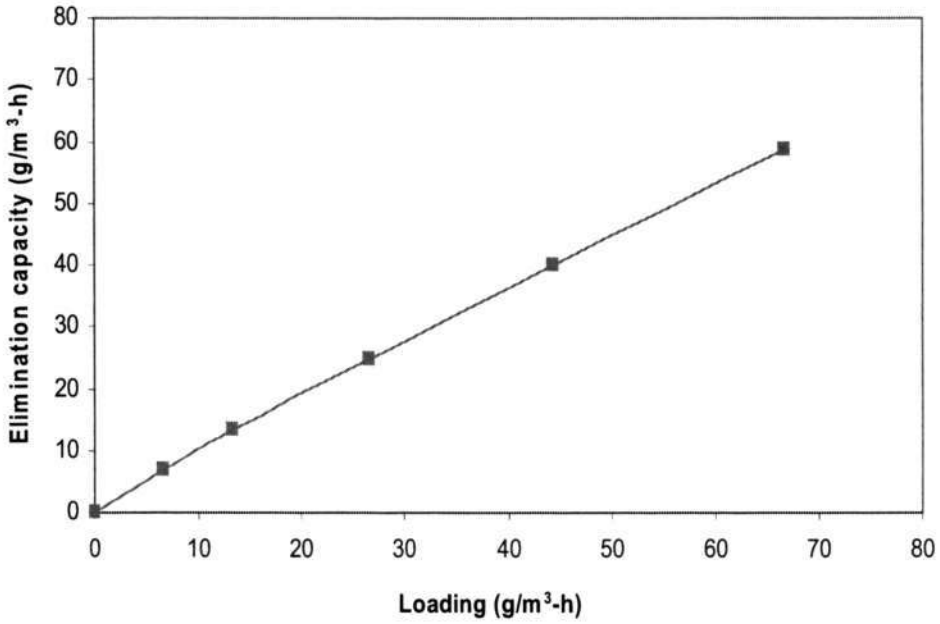

Figure 5.13(b) Inlet loading vs. H_2S elimination capacity

5.2.5 Concentration profile along the packing length

The concentration profile along the packing length provides the information about the function of different parts of the packing bed. Figure 5.14(a) is the variation of H_2S concentration along the packing length in the low pH single-stage biotrickling filter. The total GRT was set at 15s, and therefore the GRT of the first segment was 3s with an inlet H_2S concentration of 20ppmV. 93% H_2S was removed by Segment I (h/H=0~0.2) of the low pH single-stage biotrickling filter.

Figure 5.14(b), which is obtained at inlet toluene concentration of 50ppmV and a GRT of 15s, shows the toluene concentration profile along the packing bed in the low pH single-stage biotrickling filter. The results indicated that 45% of inlet toluene was removed by Segment I, which was similar to that of the neutral pH single-stage biotrickling filter, i.e., most pollutant was degraded in the inlet area of the bioreactor.

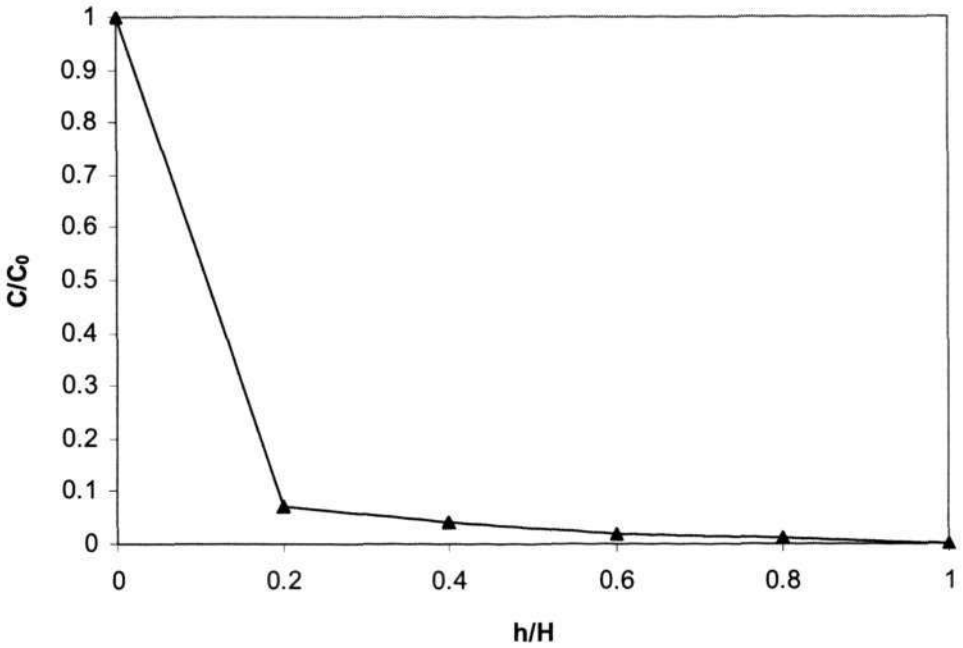

Figure 5.14(a) Variations of H_2S concentration along the packing length

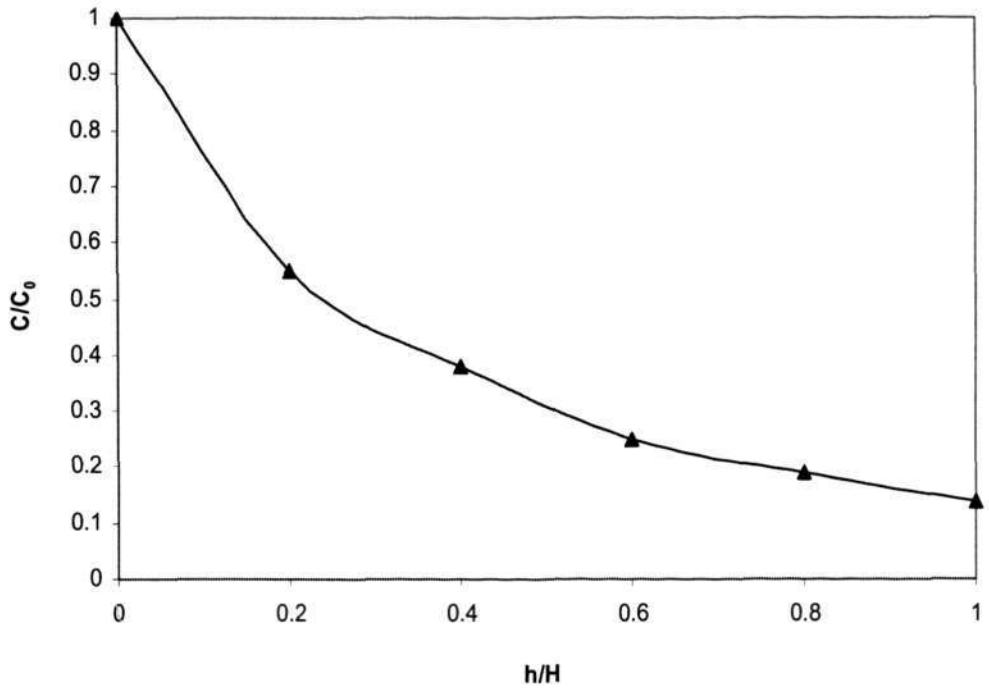

Figure 5.14(b) Variations of toluene concentration along the packing length

5.2.6 Biomass

The microbial growth on the carbon surface was observed using a scanning electron microscope (SEM). Figure 5.15 shows the SEM image of biofilm on the BAC in the low pH single-stage biotrickling filter. The carbon surface was covered by a well-formed biofilm, which was composed of bacteria, filamentous bacteria or fungus. The biofilm morphology was very similar to the biofilm in the neutral pH single-stage biotrickling filter shown in Figure 5.7. A mass of branches could be seen obviously in the following picture.

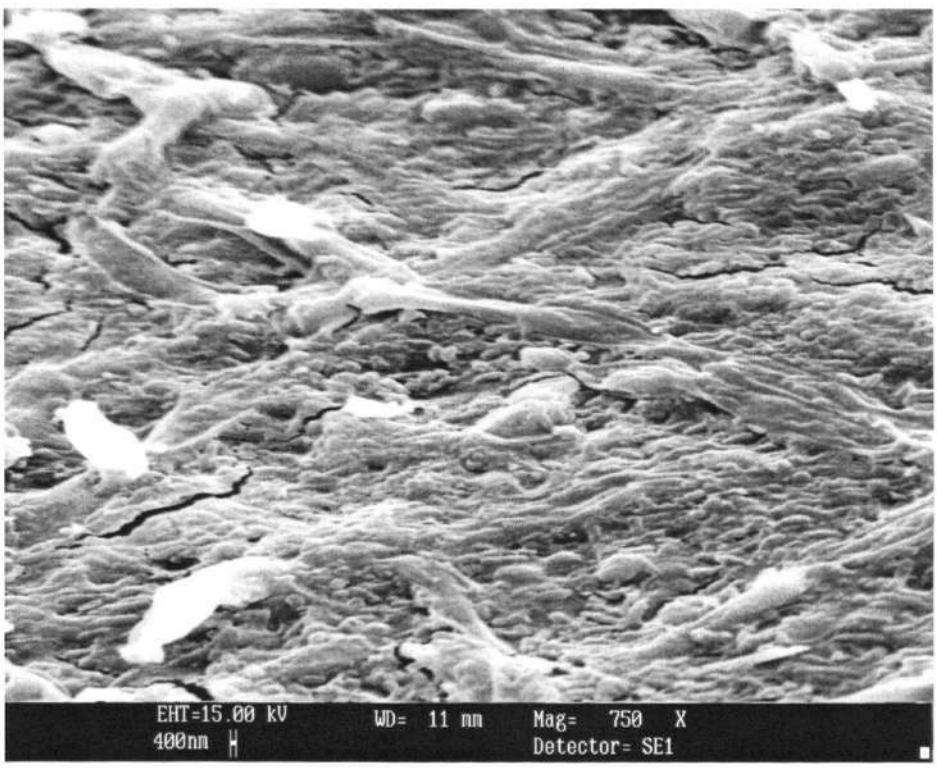

Figure 5.15 Biofilm in the low pH single-stage biotrickling filter

5.2.7 Removal mechanisms of BAC

This section attempts to evaluate the removal mechanisms of BAC. The BAC samples were taken out at the end of the biotrickling filter operation. The virgin carbon without bacterial film and the exhausted carbon taken from the breakthrough test were used for comparison.

5.2.7.1 BET analysis

The pore and surface characteristics of BAC were identified using the Brumauer-Emmett-Teller (BET) test. The BET data of the BAC in the low pH single-stage biotrickling filter, the virgin carbon and the exhausted carbons are shown in Table 5.2. The BAC sample taken from the low pH biotrickling filter had an average micropore volume of 0.205cm^3/g, average pore diameter of 1.97nm, average external surface area of 403.1m^2/g, average micropore surface area of 489.3m^2/g, and average total BET surface area of 892.4m^2/g. All these data of the BAC in the low pH single-stage biotrickling filter were close to those of the virgin carbon, far different from those of the exhausted carbon, which was already reported in the neutral pH single-stage biotrickling filter. It was because that biofilm only formed on the carbon surface and some of the macropores and thus had little effect on the pore and surface area. It also validated that the bioregeneration phenomena occurred in the BAC because the microorganisms were inoculated after the carbon bed exhaustion.

Speitel and DiGiano (1987) used radio labeled phenol to observe the mechanisms of the BAC. $^{14}CO_2$ in the effluent stream indicated that pre-adsorbed compounds had been desorbed and subsequently biodegraded in the biofilm. Although the size of the bacteria made them too large to colonise the mesopores and micropores of the carbon, enzymes produced by the bacteria could easily diffuse into them and react with the adsorbed substrate.

Along the packing bed, micropore surface area (459.5-519.7m^2/g) and micropore volume (0.186-0.223cm^3/g) increased while external surface area (478.4-339.2m^2/g) and average pore diameter (2.02-1.93nm) decreased. This phenomenon and its

occurring reason had already been discussed in detail in the neutral pH single-stage biotrickling filter (Section 5.1.8.1).

Table 5.2 BET data of the low pH single-stage biotrickling filter

Carbon type	Distance through packing bed (cm)	Micropore volume (cm^3/g)	Average pore diameter (nm)	Surface area (m^2/g)		
				External surface area	Micropore surface area	Total BET surface area
BAC	5	0.186	2.02	478.4	459.5	937.7
	15	0.194	1.99	445.8	476.2	922
	25	0.205	1.97	397.1	488.6	885.7
	35	0.218	1.94	354.9	502.3	857.2
	45	0.223	1.93	339.2	519.7	858.9
	average	0.205	1.97	403.1	489.3	892.4
Virgin carbon		0.276	1.980	505.9	525.6	1031.5
Toluene exhausted carbon		0.093	2.015	201.7	412.6	614.3
H_2S exhausted carbon		0.078	2.024	182.1	397.1	579.2

5.2.7.2 Thermal analysis

Thermal analysis was carried out to further analyze the oxidation products of pollutants in the BAC biotrickling filter. Figure 5.16 shows the differential thermogravimetric (DTG) curves of the BAC in different packing length of the low pH single-stage biotrickling filter. Only one peak (noncombustible sulfur) around 300℃ was detected in the low pH BAC biotrickling filter. The peak height from 5cm to 45cm in the low pH single-stage biotrickling filter showed the similar trend of decreasing along the packing length to that of the neutral pH single-stage biotrickling filter. The highest peak value of the low pH single-stage biotrickling filter was 0.0045wt%/min while it was 0.0038wt%/min in the neutral pH single stage biotrickling filter. Its accumulated noncombustible sulfur content was more than that of the neutral pH single-stage biotrickling filter because of higher H_2S inlet concentration (20ppmV vs. 5ppmV).

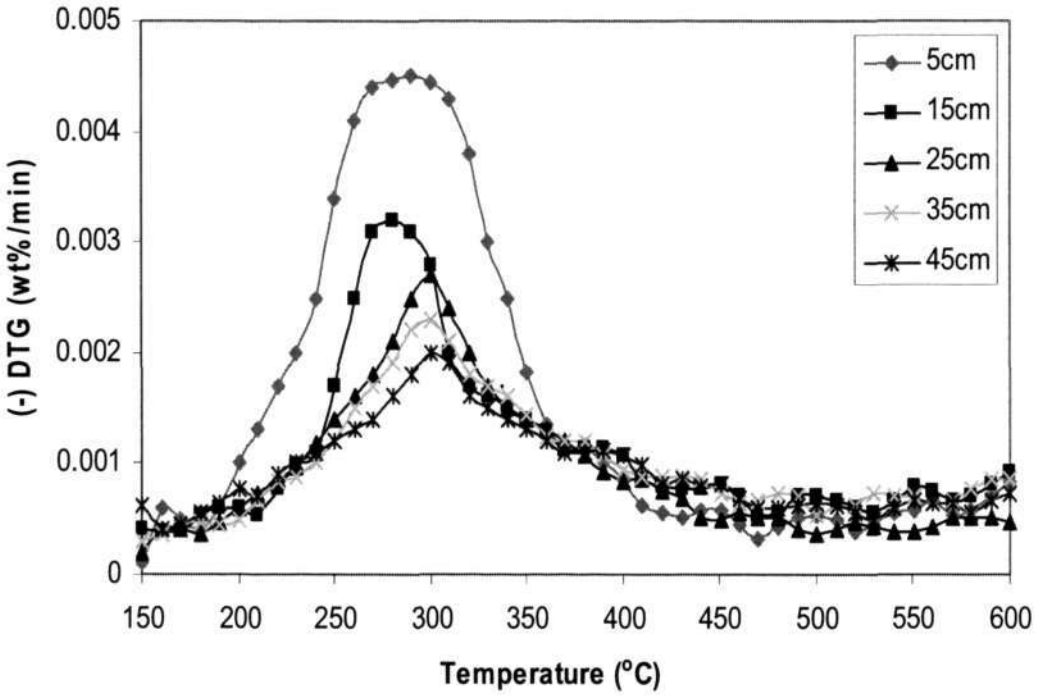

Figure 5.16 DTG curves of the BAC in the low pH single-stage biotrickling filter

5.2.7.3 Sulfate accumulation

Figure 5.17 shows the sulfate concentration diversification of the BAC along the packing bed in the low pH single-stage biotrickling filter. Sulfate concentration of the BAC was 25.4mg/g-carbon in 5cm and 18.55mg/g-carbon in 45cm, which were remarkably higher than that of the virgin carbon (0.014mg/g-carbon). The curve illustrated that sulfate accumulation decreased along the packing length for the reason that the inlet area was subjected to higher H_2S loading.

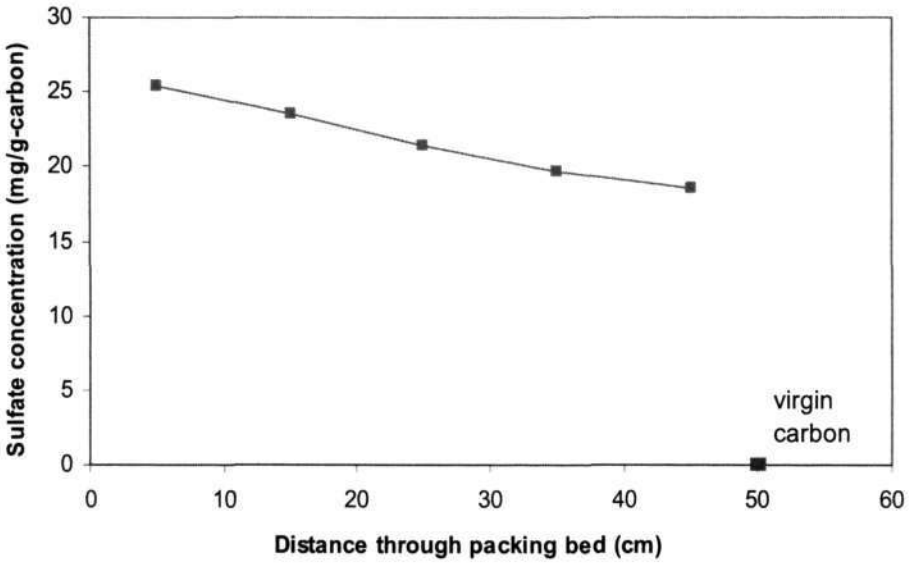

Figure 5.17 Sulfate concentration diversification along the packing bed

5.2.7.4 CNHS analysis

The element changes before and after the biotrickling filter operation were studied with a CNHS analyzer. Figure 5.18 introduces the changes of carbon (C) content, hydrogen (H) content, nitrogen (N) content, and combustible sulfur (S) content through the packing bed in the low pH single-stage biotrickling filter.

As can be seen, the carbon content of the BAC did not have many changes before (82.45%) and after the biotrickling filter operation (61.7-74.1%). The BAC values of hydrogen content (2.19-3.12%) were close to the original number (0.57%). The nitrogen content of the BAC (0.6-1.9%) increased considerably than that of the virgin carbon (0%) and exhausted carbon (0.33% for H_2S, 0.08% for toluene) owing to the addition of mineral nutrition. The carbon content, hydrogen content and nitrogen content did not show any increasing or decreasing trend along the packing length according to Figure 5.18. The little variation of elements content indicated the mass balance of the whole system and the benign operation of the biotrickling filter.

Combustible sulfur content of the BAC (0.31-2.1%) was more than that of the virgin carbon (0.05%) and the toluene exhausted carbon (0.008%), but much less than the H_2S exhausted carbon (7.05%). In the curve, combustible sulfur content of the BAC decreased along the packing bed for the reason that H_2S was largely transformed in the inlet area according to the concentration profile in Section 5.2.5 and so little H_2S remained in the subsequent carbon segments.

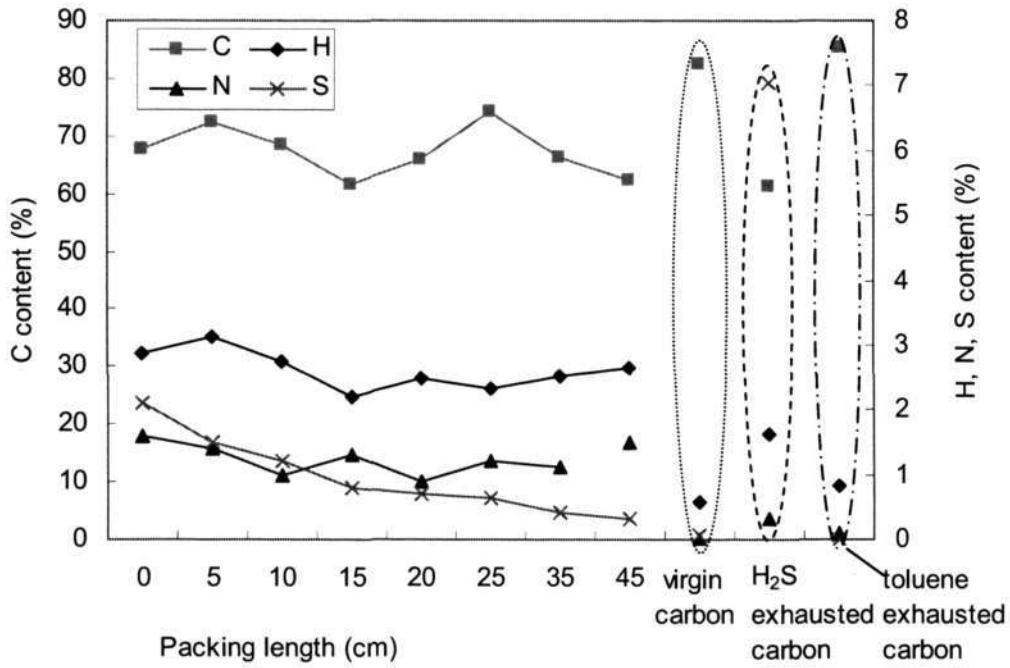

Figure 5.18 Element content of the BAC through the packing bed

5.3 Two-stage biotrickling filter

5.3.1 Biotrickling filter performances

The toluene removal in the two-stage biotrickling filter is shown in Figure 5.19(a), in which GRT and RE I refer to the second stage GRT (from Segment II to V) and the toluene removal efficiency of the first stage, respectively. H_2S removal in the two-stage biotrickling filter is shown in Figure 5.19(b), in which GRT, Outlet I and RE I refer to the first stage GRT, the H_2S outlet concentration from the first stage and H_2S first stage removal efficiency, respectively.

The first 40 days was considered as the start-up period of the two-stage biotrickling filter. During the first 28 days as shown in Figure 5.19(a), only the second stage was packed with carbon and toluene gas was fed in to prevent the influence of H_2S. Toluene inlet concentration was varied from 150ppmV to 50ppmV at a GRT of 60s. *Pseudomonas putida* was online inoculated on day 4 after carbon bed breakthrough to evaluate the bioregeneration capacity of the BAC biotrickling filter because microorganisms might degrade the previously adsorbed pollutant molecules in the carbon granules. The removal efficiency increased quickly from 0% to 80% with the action of microorgnisms. On day 8, the system was shut down for maintenance of the recirculation system. The performance (50% removal) of the reactor decreased compared with the removal efficiency two days ago and could not recover to its initial level, which was probably due to the death of the microorganisms during the two-day shutdown period. Therefore, the system was re-inoculated on day 12 and toluene removal efficiency increased accordingly. On day 29, when toluene removal stabilized above 95%, H_2S was introduced. Toluene removal had minor decrease, and then adapted to the new environment quickly.

In Figure 5.19(b), after the second stage had operated for 28 days, carbon was placed in Segment I of the biotrickling filter and 10-20ppmV of H_2S were introduced with a GRT for the first stage segment controlled at 15s. When the adsorption capacity of the first-stage carbon (RE I) decreased to 85%, *Thiobacillus*

sp. was inoculated to the first stage and biodegradation of H_2S commenced immediately. Instead of decreasing, the removal efficiency increased rapidly and reached a stable level of 100% after about 7 days.

5.3.1.1 Toluene removal during the steady-state period

During the steady-state period of day 41 to 160, the second stage GRT was decreased from 60s to 6s and toluene removal efficiency changed accordingly. The detailed discussion is described in Section 5.3.2. When the second stage GRT was changed, some reductions in performance were observed in toluene removal efficiency due to the shock loading. Nevertheless, toluene removal efficiency would recover quickly within 1 to 2 days.

On day 62, the toluene removal efficiency decreased to 50% and the pressure drop was up to 95mmH_2O/m-carbon, which indicated that the second stage biotrickling filter was clogged. The reason was suspected to be the overgrowth of biomass due to the continuous nutrition over-supply. The second stage was then washed continuously using tap water at 1L/min for two days and the performance recovered gradually after washing. From day 72 onwards, intermittent trickling style replaced earlier continuous trickling to prevent the biotrickling filter clogging. From day 113 to 118, no data were recorded because of GC malfunction. On day 154, inlet H_2S concentration was increased approximately to 50ppmV to test its effect on the biotrickling filter performance. The second stage was acidized quickly because of the high H_2S outlet concentration (>3ppmV) from the first stage. The pH of the second stage decreased from 6.8 to 2. Biofilm with carbon powder sloughed into the recirculating water and made it turbid.

According to Figure 5.19(a), VOC removal of the first stage was unstable (-13% to 50%). The outlet concentration from the first stage was found sometimes higher than the inlet concentration. BAC samples were taken out from the first stage to monitor the viable cell adhesion onto the carbon surface. No toluene degraders were found in the first stage during the bacteria counting. The removal mechanism was

hence believed having no bacteria degradation, but carbon adsorption and desorption. Therefore, most of the inlet toluene was removed by the second stage. When the second stage GRT was reduced from 60s to 6s, the removal efficiency decreased from 100% to 85%. With the increasing inlet concentration of toluene from 50ppmV to 300ppmV from day 120 to 150, the removal efficiency also decreased from 85% to 60% at the second stage GRT of 6s. In general, the overall removal efficiency was above 90% when the second stage GRT was controlled longer than 9s and toluene inlet concentration was less than 50ppmV.

5.3.1.2 H_2S removal during the steady-state period

GRT and RE I in Figure 5.19(b) refer to the first stage GRT and H_2S first stage removal efficiency, respectively. "Outlet I" represents H_2S outlet concentration from the first stage. When the first stage GRT was shortened from 15s to 1.5s during the steady-state period, RE I decreased. As the air flow rate was regulated to less than 40L/min corresponding to a first stage GRT of longer than 3s and H_2S inlet concentration was controlled to less than 20ppmV, the first stage removal efficiency remained higher than 95%. When the first stage GRT was decreased to 1.5s, the first stage still could get 88% removal efficiency. However, the overall removal efficiency (overall RE) always stayed above 98% in the two-stage bioreactor. Generally speaking, the first stage H_2S outlet concentration was less than 3ppmV indicating the effective removal of H_2S by the first stage BAC segment.

According to the above experimental results, inlet H_2S was mainly removed by the first stage and overall H_2S removal for the whole BAC biotrickling filter was very high (close to 100%). The leachate pH remained between 1.5 and 4. In a counting of the bacteria concentration of the reciculation solution on day 60, a number of H_2S degrading bacteria were observed in the second stage leachate. It showed that the second stage was contaminated by H_2S degraders. Therefore, it was possible that H_2S was removed in the second stage due to degradation by bacteria and carbon adsorption. From day 149 to day 158, inlet H_2S concentration was raised from 20ppmV to 50ppmV aiming to test its effect on H_2S and toluene removal efficiency.

As a result, H_2S RE I decreased from 88% to 85%, toluene removal efficiency decreased from 85% to 60% and pH of the second stage leachate decreased from 6.8 to 2 (the details are discussed in Section 5.3.3). To avoid the above acidification phenomenon in the second stage, the first stage H_2S outlet concentration should be controlled below 3ppmV to ensure normal operation of the whole BAC system. After changing to intermittent trickling on day 72, the removal efficiency of both toluene and H_2S increased (this will be discussed in Section 5.3.4). When the first stage GRT and the inlet concentration was changed, incremental reductions were also observed in H_2S RE I due to the shock loadings. As the BAC system adjusted to the new loadings, the H_2S removal efficiency slowly recovered.

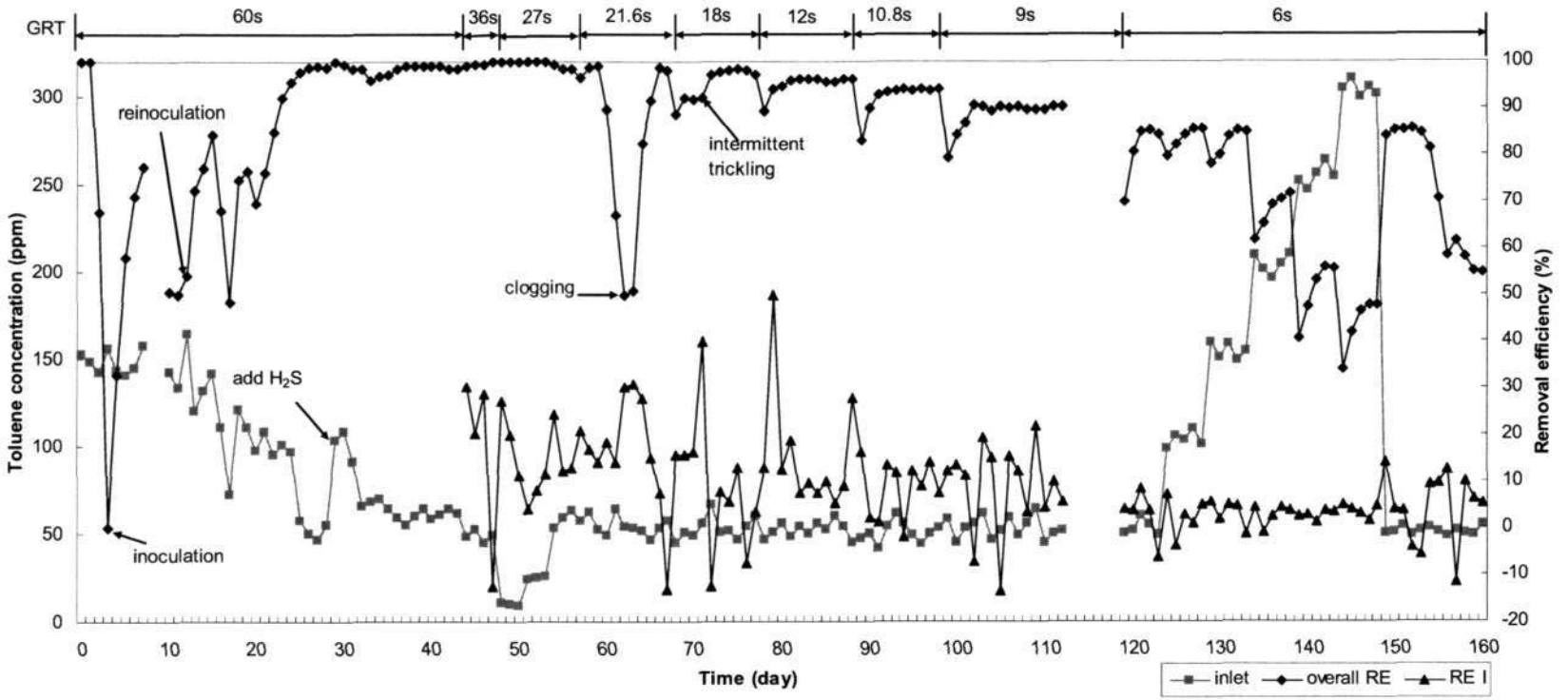

Figure 5.19(a) Toluene removal in the two-stage biotrickling filter

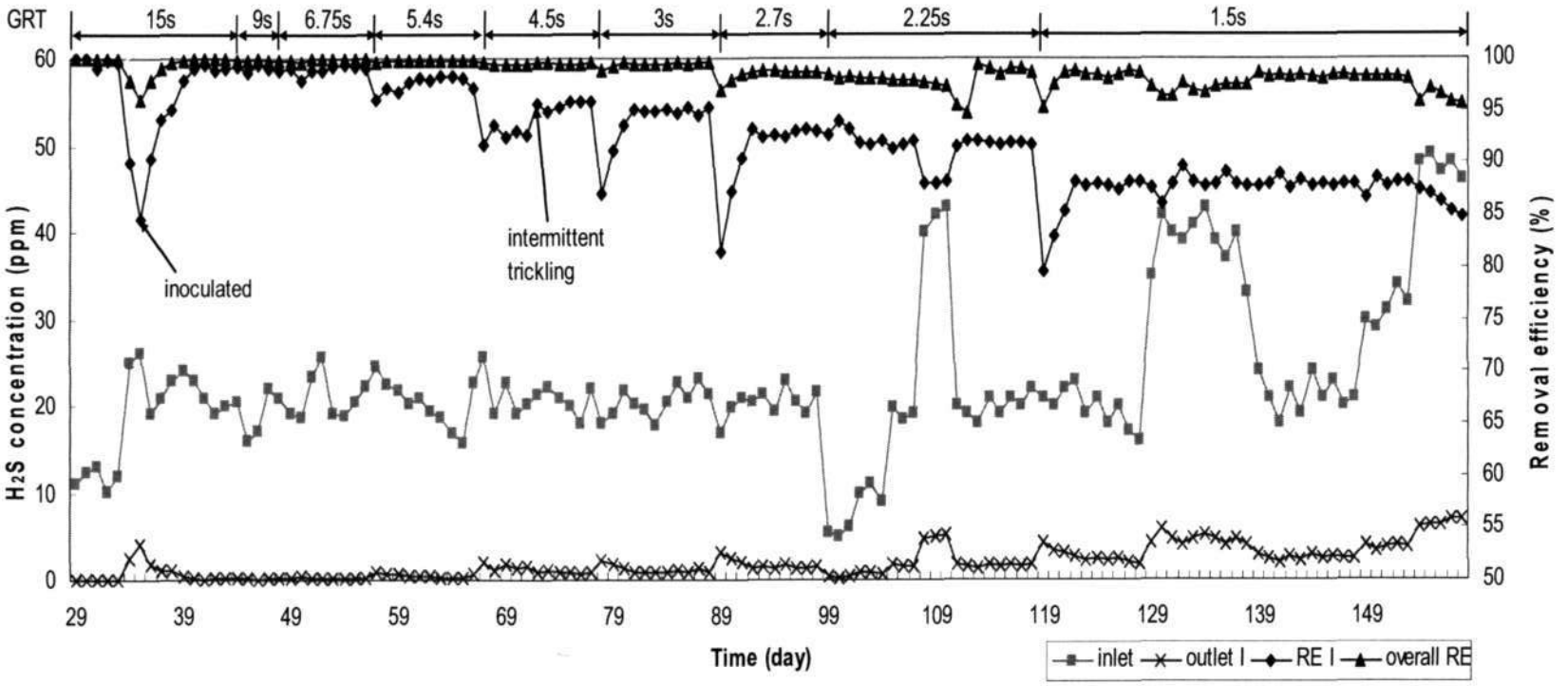

Figure 5.19(b) H_2S removal in the two-stage biotrickling filter

5.3.2 Gas retention time

To evaluate a successful biotrickling filter, a short GRT is always expected for high removal efficiency because it means a small reactor volume and thus low capital cost. Figures 5.20(a) and (b) show the changes of toluene and H_2S removal efficiency with GRT, respectively. Both toluene and H_2S removal efficiency decreased with decreasing GRT, which was consistent with the results obtained for both the neutral pH and low pH single-stage biotrickling filter. When the gas flow was regulated to yield a GRT from 60s to 30s, toluene removal efficiency could be maintained at a high level of 100%. However, when GRT was shortened to 9s, toluene removal efficiency was only about 90%. For H_2S, the removal efficiency decreased from 100% to 92% when GRT was changed from 15s to 2.25s. For both situations, the reason was that microorganisms could not degrade toluene and H_2S completely in such a short time. In the two-stage biotrickling filter, to achieve removal efficiency higher than 95% for both H_2S and toluene, the GRT should be longer than 3.75s for the first stage and 15s for the second stage, respectively.

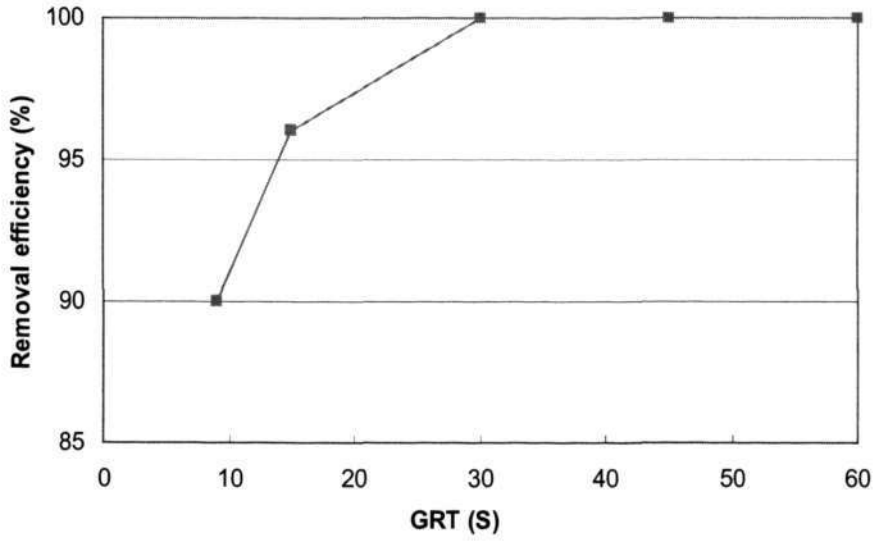

Figure 5.20(a) Toluene removal efficiency vs. GRT

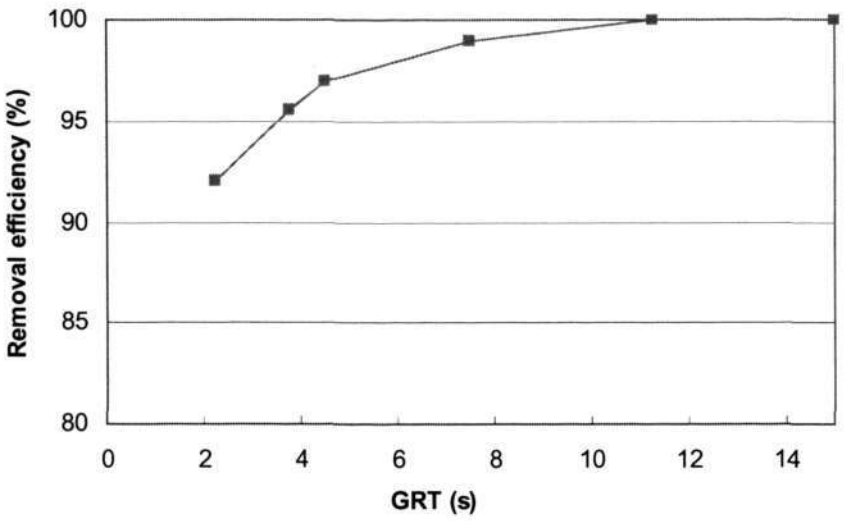

Figure 5.20(b) H_2S removal efficiency vs. GRT

5.3.3 Contaminant interaction

For the treatment of gas mixture containing H_2S and toluene, one important issue, which we should pay attention to especially, is that the acid production of H_2S oxidation reduces the pH in the biotrickling filter and may further cause poor removal efficiency of toluene. The influence of toluene on H_2S removal is also investigated here.

Figure 5.21(a) indicates an example of toluene influence on H_2S removal in the two-stage biotrickling filter. When toluene concentration was increased from 10ppmV to 70ppmV, H_2S RE I remained stable at above 98%. In Figures 5.19(a) and (b), toluene inlet concentration was changed from 50ppmV to 300ppmV during day 120 to 150, no significant fluctuation was observed on H_2S RE I, either. Based on these results, the increase of toluene concentration (0-300ppmV) had little influence on the H_2S removal.

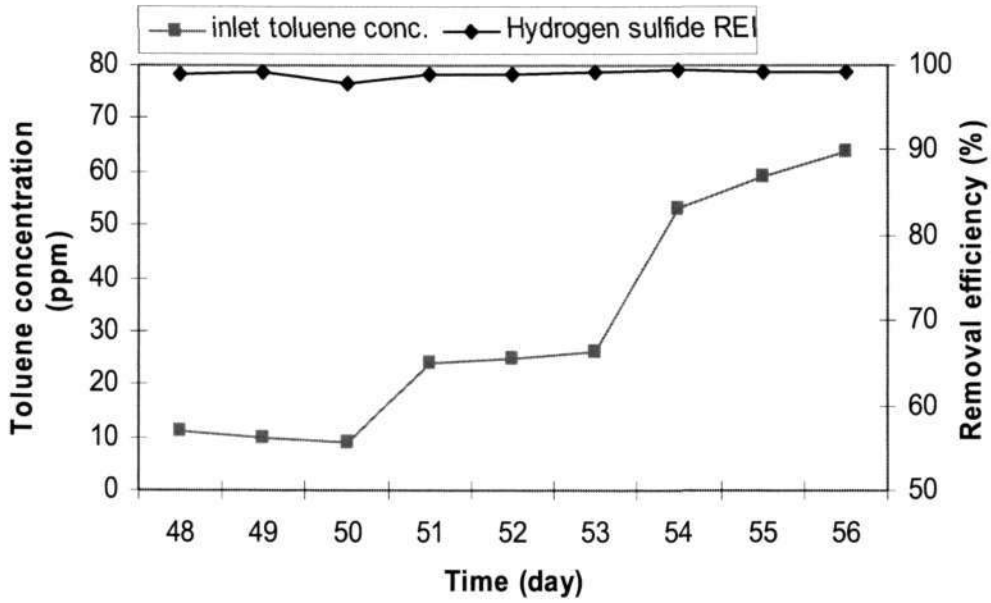

Figure 5.21(a) Toluene influence on H_2S removal in the two-stage biotrickling filter

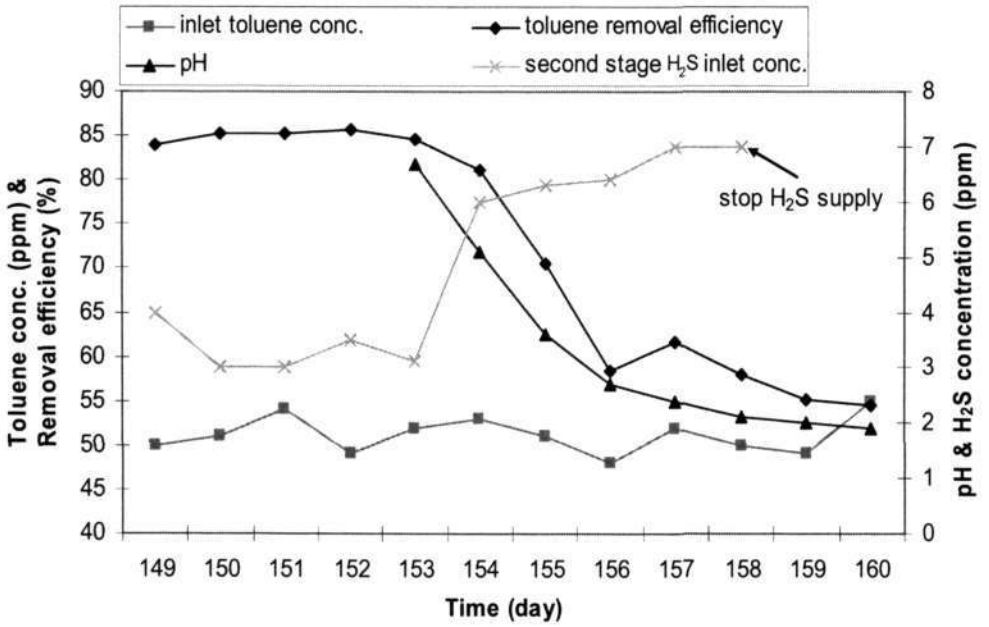

Figure 5.21(b) H_2S influence on toluene removal in the two-stage biotrickling filter

According to Figure 5.19(b), H_2S outlet I, i.e. the second stage H_2S inlet, was kept below 3ppmV until day 153. During this period, constant and high toluene removal efficiency at different GRTs is shown in Figure 5.19(a). Similar results were also obtained for the case with 1ppmV inlet H_2S in the earlier bench study (Section 4.2.2.2). The effect of H_2S on toluene removal was not found when H_2S concentration entering the second stage was below 3ppmV in the two-stage biotrickling filter. This was likely due to the high buffering capacity of the phosphate chemicals in the recirculation liquid which was sufficient to maintain a near neutral pH for the second stage BAC segments. The living environment of *Pseudomonas putida* was not changed by the small amount of remaining H_2S entering the second stage.

However, the situation changed when H_2S concentration was further increased. Figure 5.21(b) shows the acidification of the second stage in the two-stage biotrickling filter. From day 154 to day 158, inlet toluene concentration was controlled constant at 50ppmV and inlet H_2S concentration was raised from 20ppmV to 50ppmV to evaluate its effect on the toluene removal efficiency. The second stage H_2S inlet concentration increased from 3ppmV to 7ppmV accordingly. Toluene removal efficiency decreased from 85% to 60% and pH of the second stage leachate fell from 6.8 to 2. This adverse effect to toluene removal, which was caused by the acidification of the second stage as a result of high H_2S inlet concentration, was very obvious.

5.3.4 Continuous and intermittent liquid trickling

Water content is another important parameter for a biotrickling filter. Figure 5.22 shows the removal efficiency and pressure drop changes under different trickling conditions. In the two-stage biotrickling filter, water recirculation was maintained continuously at 0.4L/min initially. From day 72 onwards, the liquid recirculation frequency was changed to twice per day (0.8L/min for 30 minutes on each occasion) and pressure drop of the biotrickling filter decreased sharply from 10 to 2mm H_2O/m-carbon. The removal efficiency of H_2S and toluene was observed to increase from 92% to 95% and from 92% to 96% respectively, which might be attributed to

the following three factors. Firstly, the interference of the water film decreased, which was equivalent to increasing GRT because the mass transfer limitations of substrates in the aqueous phase were greater than those in the gas phase. Secondly, contaminants could contact the biofilm and be utilized directly. Thirdly, pollutant adsorption on the activated carbon was easier with less competition by water molecules for adsorption sites. This demonstrated that the existence of a water layer surrounding the biofilm lowered the removal efficiency because the mass transfer resistances at the gas-liquid and liquid-biofilm interfaces prevented pollutants from reaching the biofilm during the short contact time.

Intermittent recycling had more practical advantages than continuous recycling. Pressure drop decreased significantly and thus power supply was saved, which implied that the operation cost was reduced. The results obtained with the BAC biotrickling filter were different from those studies carried out with other packing materials such as polypropylene rings and polyurethane foam (Wu L., 2000). When the water supply was shut off, the removal efficiencies of those reactors decreased sharply. It does appear that activated carbon had a good water affinity and water holding capacity.

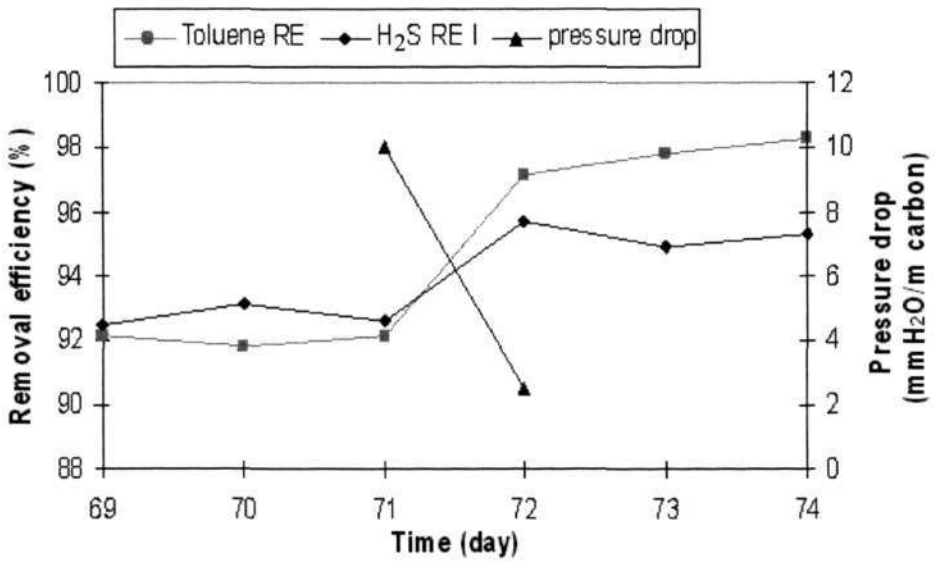

Figure 5.22 Continuous trickling vs. intermittent trickling in the two-stage biotrickling filter

5.3.5 Pressure drop

Resistance to the gas flow is the major factor that determines the amount of energy needed by the blowers to force the contaminated gas through the filter bed material. Pressure drop measurement is a valuable indicator of the changes in airflow resistance through the filter bed. Pressure drop across the biotrickling filter material depends on several factors: the nature of the carrier material, particle size and shape, superficial gas velocity, biomass growth and water content.

Pressure drop was measured about every ten days during the biotrickling filter operation. The variation of pressure drop with time in the two-stage biotrickling filter is shown in Figure 5.23. In the two-stage biotrickling filter, pressure drop increased continuously from 0 to 95mm H_2O/m-carbon on day 62 with the biofilm growth. The high pressure drop and low toluene removal efficiency (50%) indicated that the second stage was clogged. The second stage was then washed continuously using tap water at 1L/min for two days. The pressure drop decreased to 0 on day 63 and then increased as time progressed. When water was recycled intermittently on day 72, pressure drop (2.5mm H_2O/m-carbon) became much lower than before (10mm H_2O/m-carbon). The clogging phenomenon did not reappear during the subsequent operation and the pressure drop remained below 20mmH_2O/m-carbon.

Table 5.3 makes a comparison between the pressure drop of the BAC and that of another medium with a similar diameter (4mm carbon vs. 6mm celite). As can be seen, the pressure drop observed in this study (20mm H_2O/m-carbon) was significantly smaller than that cited from the literature (64mm H_2O/m-celite). The low pressure drop of the BAC profited from the even gas flow due to the uniform shape and porous structure of activated carbon.

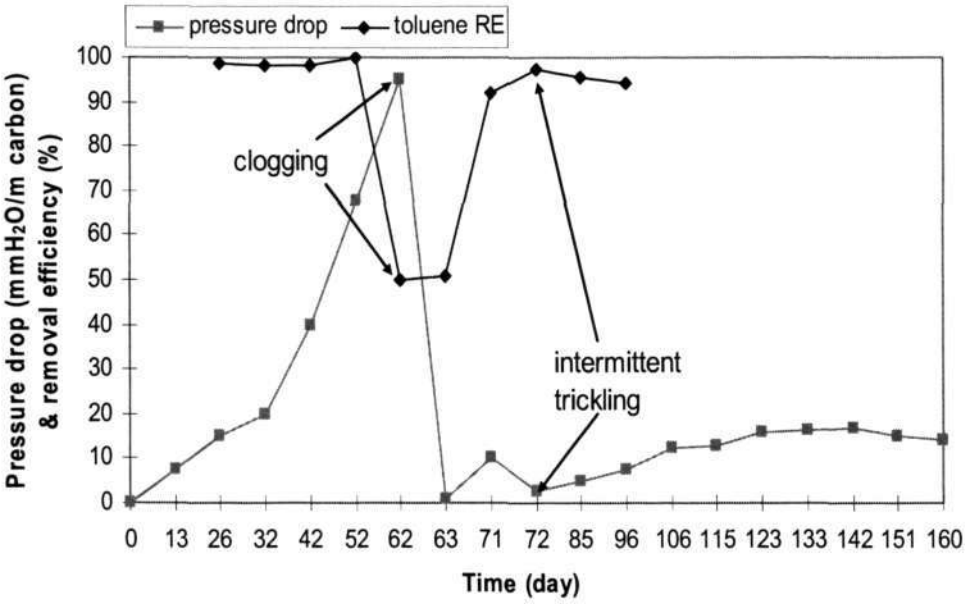

Figure 5.23 Variable-time pressure drop in the two-stage biotrickling filter

Table 5.3 Comparison of pressure drops

Surface area	Diameter of packing media	Superficial gas velocity	Pressure drop	Source
505.9 m^2/g	4mm	120m/h	20mm H_2O/m-carbon	This study
500 m^2/m^3	6mm	73m/h	64mm H_2O/m-celite	Sorial et al.,1995

5.3.6 Elimination capacity

An important parameter to measure the ability of a biotrickling filter for pollutant removal is elimination capacity, which should be as high as possible. Figure 5.24(a) shows inlet loading vs. toluene elimination capacity for the two-stage biotrickling filter. Elimination capacity for toluene increased linearly with increasing inlet loading and reached an equilibrium value, which was the maximum elimination capacity of the biotrickling filter. The maximum elimination capacity of toluene for the two-stage biotrickling filter was 310g/m^3·h.

Figure 5.24(b) shows inlet loading vs. H_2S elimination capacity for the two-stage biotrickling filter. The curve followed a linear increasing trend, but did not reach an equilibrium maximum value. A H_2S maximum elimination capacity of 140g/m^3·h was previously reported by Duan (2005a) using the same packing GAC (AP-460) in lab test. For the two-stage biotrickling filter in this study, an elimination capacity of 131g/m^3·h was obtained.

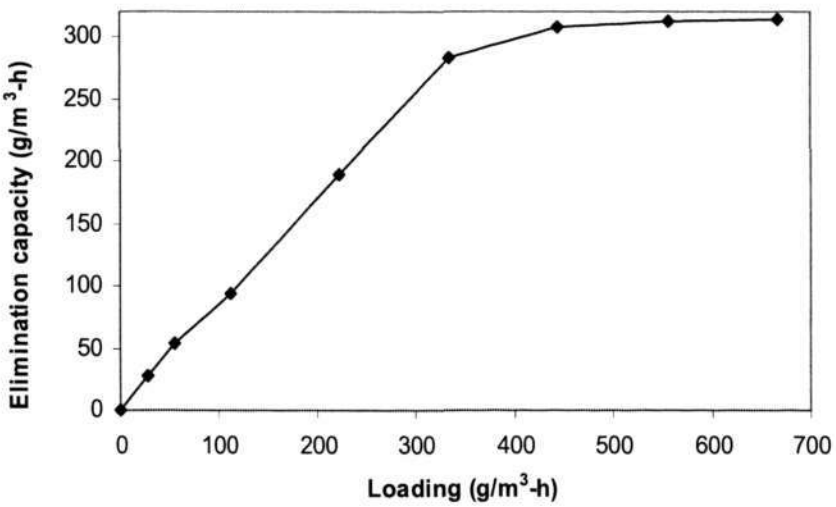

Figure 5.24(a) Inlet loading vs. toluene elimination capacity

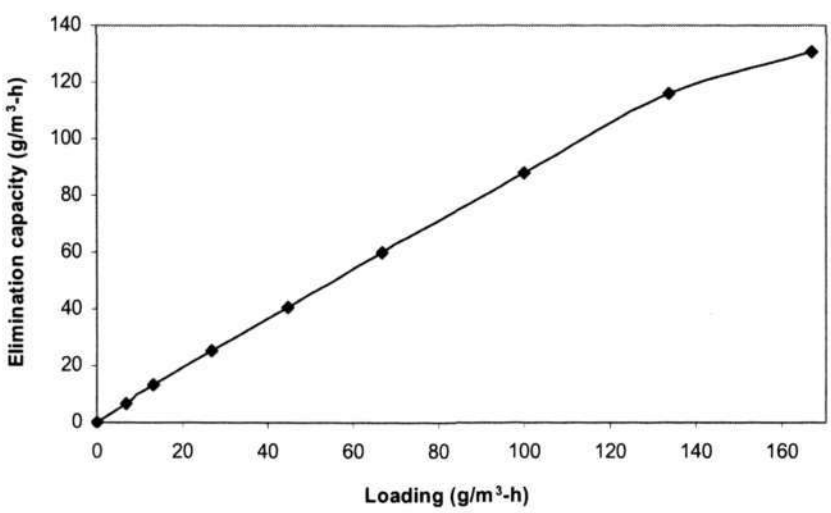

Figure 5.24(b) Inlet loading vs. H_2S elimination capacity

5.3.7 Concentration profile along the packing length

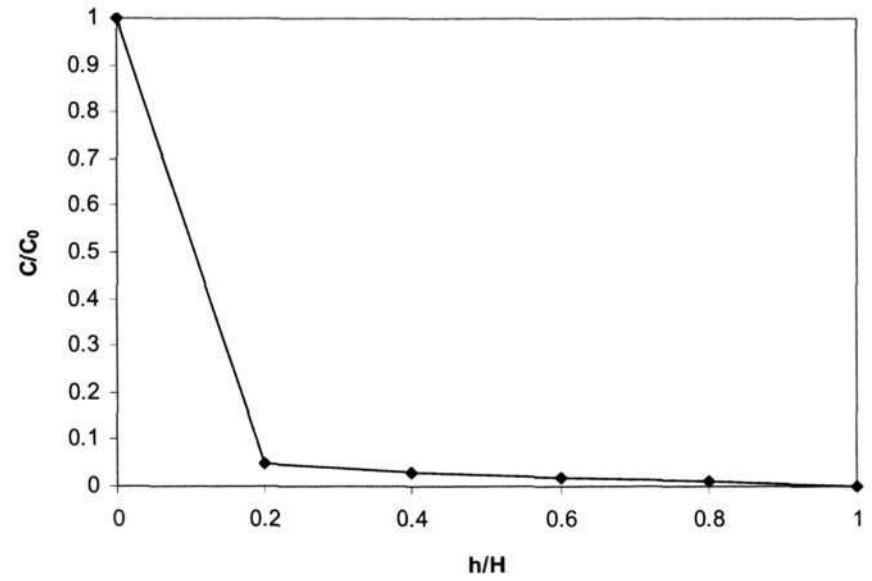

Figure 5.25(a) Variations of H_2S concentration along the packing length

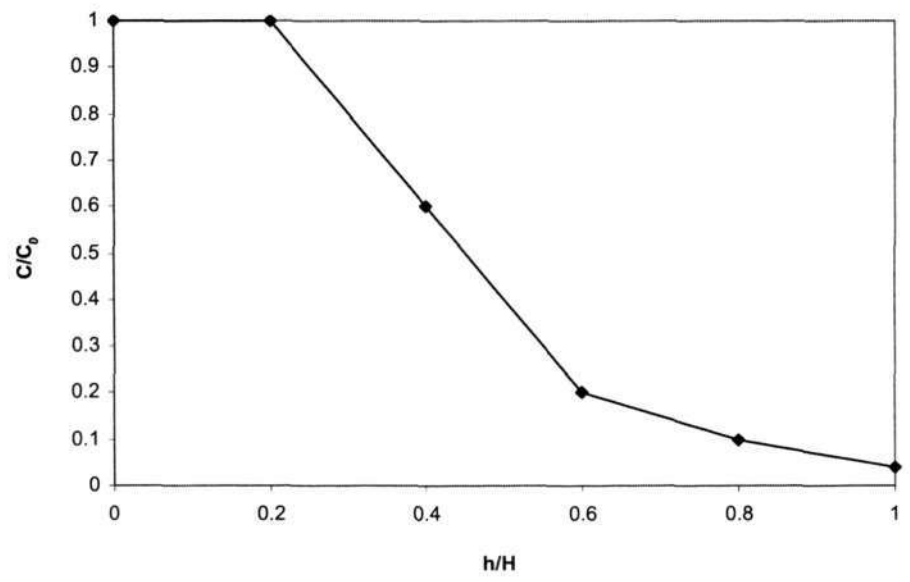

Figure 5.25(b) Variations of toluene concentration along the packing length

The pollutant concentration profile along the packing length reflects the functional part of the biotrickling filter for pollutant removal. Figure 5.25(a) shows the variation of H_2S concentration along the packing length in the two-stage biotrickling filter. Overall GRT was set at 15s and thus the GRT of the first segment was 3s. H_2S inlet concentration was controlled at 20ppmV and 95% of it was removed by Segment I (h/H=0~0.2). Similar to results obtained for the single-stage biotrickling filters, the inlet area of the two-stage BAC reactor degraded most of the incoming pollutants.

Figure 5.25(b), which is obtained at inlet toluene concentration of 50ppmV and a GRT of 15s, shows the toluene concentration profile along the packing bed in the two-stage biotrickling filter. As shown in the figure, the toluene profile of the two-stage biotrickling filter was quite different from the concentration profiles found in the previously reported single-stage biotrickling filters. C/C_0 remained constant at 1 during the first stage (h/H=0~0.2), which meant that the first segment of the packing length was useless for toluene removal because it was used for H_2S treatment. C/C_0 decreased from 1 to 0.6 in Segment II (h/H=0.2~0.4), and then to 0.2 in Segment III (h/H=0.4~0.6). The effective sections for toluene removal were found to be the first two sections of the second stage (Segment II and III) in this experiment. This was because the first section of the second stage (Segment II) was also required to treat the balance of H_2S coming out from Segment I. Although the amount of remaining H_2S was quite small, the lower pH (5.8) in Segment II than those (6.7~7.3) of Segment III, IV and V may have influence on the microbial activity of *P. putida* in Segment II as well.

5.3.8 Biomass

SEM allows observing the growth, structure and morphology of the microbial community on the carbon surface directly. Figure 5.26(a) shows a picture of the short rods H_2S degraders from the first stage of the two-stage biotrickling filter, dominated by *Thiobacillus sp.* at pH 1~3. Toluene degraders from the second stage of the two-stage biotrickling filter are illustrated in Figure 5.26(b). *Pseudomonas putida* was coated with sticky grume containing extracellular polymeric substances

(EPS) and dead cells. EPS was produced by the microorganisms and formed a polymer which trapped the microbial cells.

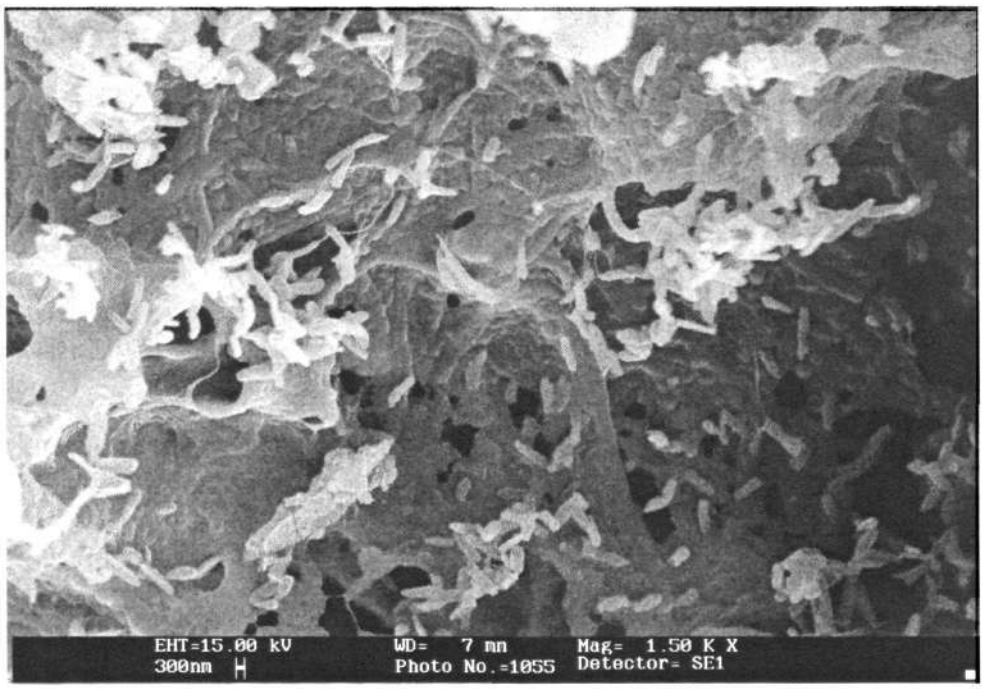

Figure 5.26(a) ***Thiobacillus sp.*** **in the first stage**

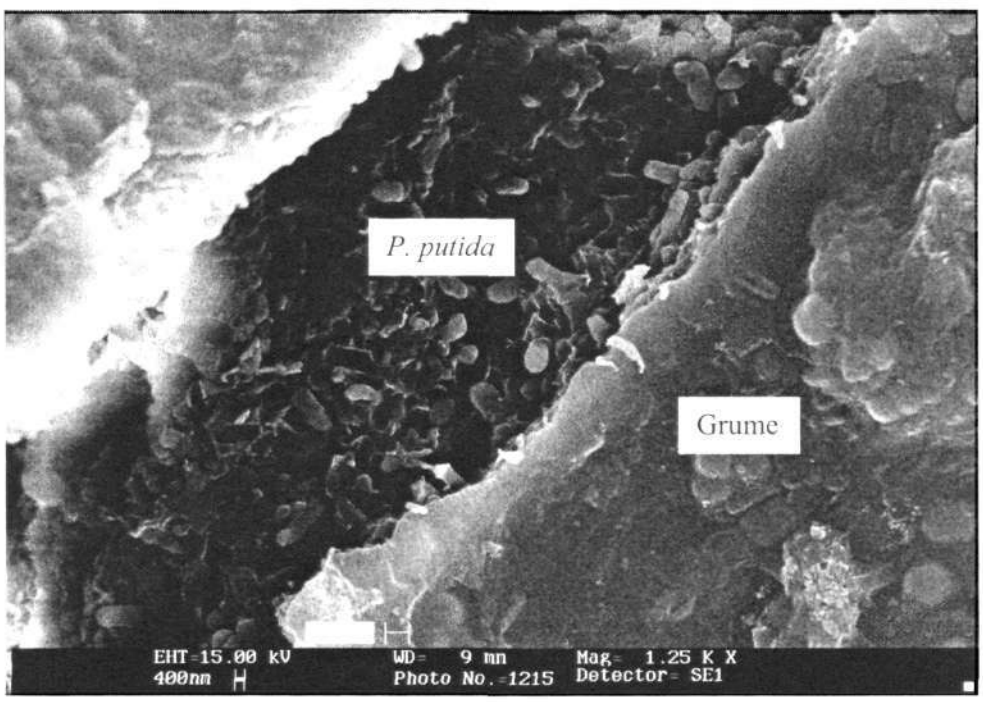

Figure 5.26(b) ***Pseudomonas putida*** **in the second stage**

5.3.9 Removal mechanisms of BAC

The removal mechanisms of BAC were studied in this section to provide a better understanding of different functions of adsorption and biodegradation. The BAC samples were taken out from different points along the packing bed after the biotrickling filter had normally operated for 150 days because the second stage was acidized since day 150. The virgin carbon without bacterial film and the exhausted carbon taken from the breakthrough test were used as reference.

5.3.9.1 BET analysis

The Brumauer-Emmett-Teller (BET) test provides information about the pore and surface of the carbon granules, which indirectly explains the effects of microbial growth on the carbon structure. The BET data of the BAC on day 150 from the two-stage biotrickling filter are shown in Table 5.4. The average micropore volume, average pore diameter, average external surface area, average micropore surface area, and average total BET surface area after the biotrickling filter operation were 0.213cm^3/g, 1.974nm, 402.12m^2/g, 445.2m^2/g and 847.32m^2/g, respectively. In general, these values of the BAC approached those of the virgin carbon (0.276 cm^3/g, 1.98nm, 505.9m^2/g, 525.6m^2/g, 1031.5m^2/g), but was different from those of the toluene or H_2S exhausted carbon (shown in Table 5.4). However, the packing bed was inoculated with microbial broth after the carbon bed exhaustion and the carbon properties before the biotrickling filter operation should be close to those of the exhausted carbon theoretically. This conflicting result demonstrated that the changes of carbon properties were caused by microorganisms' biodegradation of the adsorbed pollutant molecules. It verified the bioregeneration phenomena of the BAC and biodegradation was predominant in the steady state of the two-stage biotrickling filter.

With regard to the variation of the BET data along the packing length, some trend was observed. From 25cm to 45cm along the packing length of the two-stage biotrickling filter, micropore volume and micropore surface area increased from 0.213cm^3/g to 0.221cm^3/g and from 426.0m^2/g to 461.4m^2/g, respectively. It was attributed to the amount of the pollutants and their products mainly adsorbed in

micropores decreasing along the packing length. Along this packing length, average pore diameter and external surface area decreased from 2.015nm to 1.965nm and from 428.3m^2/g to 330.2m^2/g, respectively. This was because the pollutants adsorbed in the external pores were more easily utilized near the inlet due to more biomass accumulation there so that pore diameter and external surface area were larger near the inlet. The trend of the BET data from 5cm to 25cm could not be found. The difference of the BET data between 5cm-25cm and 25cm-45cm came from having different pollutants, heterogeneous microorganisms and diverse trickling solution along the packing bed. 5cm carbon bed (Segment I) was used for H_2S removal with *Thiobacillus sp.* under low pH trickling condition, 15cm carbon bed (Segment II) was employed to remove toluene and the remaining H_2S together with *Pseudomonas putida* and *Thiobacillus sp.* under neutral pH trickling condition, and 25cm-45cm carbon bed (Segment III-V) was used only to remove the toluene gas with *Pseudomonas putida* under neutral pH trickling condition.

Table 5.4 BET data of the two-stage biotrickling filter

Carbon type		Distance through packing bed (cm)	Micropore volume (cm^3/g)	Average pore diameter (nm)	Surface area (m^2/g)		
					External Surface area	Micropore surface area	Total BET surface area
BAC	First stage	5	0.223	1.930	378.1	486.0	864.1
	Second stage	15	0.189	1.985	484.3	407.1	891.4
		25	0.213	2.015	428.3	426.0	854.3
		35	0.218	1.973	389.7	445.3	835
		45	0.221	1.965	330.2	461.4	791.6
	average		0.213	1.974	402.12	445.2	847.32
Virgin carbon			0.276	1.980	505.9	525.6	1031.5
Toluene exhausted carbon			0.093	2.015	201.7	412.6	614.3
H_2S exhausted carbon			0.078	2.024	182.1	397.1	579.2

5.3.9.2 Thermal analysis

The degradation products were analyzed with thermal analysis. Figure 5.27 shows the differential thermogravimetric (DTG) curves of the BAC after 150 days of operation in the two-stage biotrickling filter. The curve of 5cm belongs to the first-stage while those of 15cm-45cm belong to the second-stage. One peak around 300 ℃, which was attributed to the desorption of non-combustible sulfur on the carbon granules, was detected. The peak height of 5cm was 0.0058wt%/min and the peak height of 15cm-45cm was 0.0022-0.0037wt%/min. It indicated that the non-combustible sulfur content of the first stage was much higher than that of the second stage in the two-stage biotrickling filter because H_2S was largely removed by the first stage. However, the noncombustible sulfur was detected available in the second stage, which demonstrated that the second stage could remove the remaining H_2S that exited from the first stage segment.

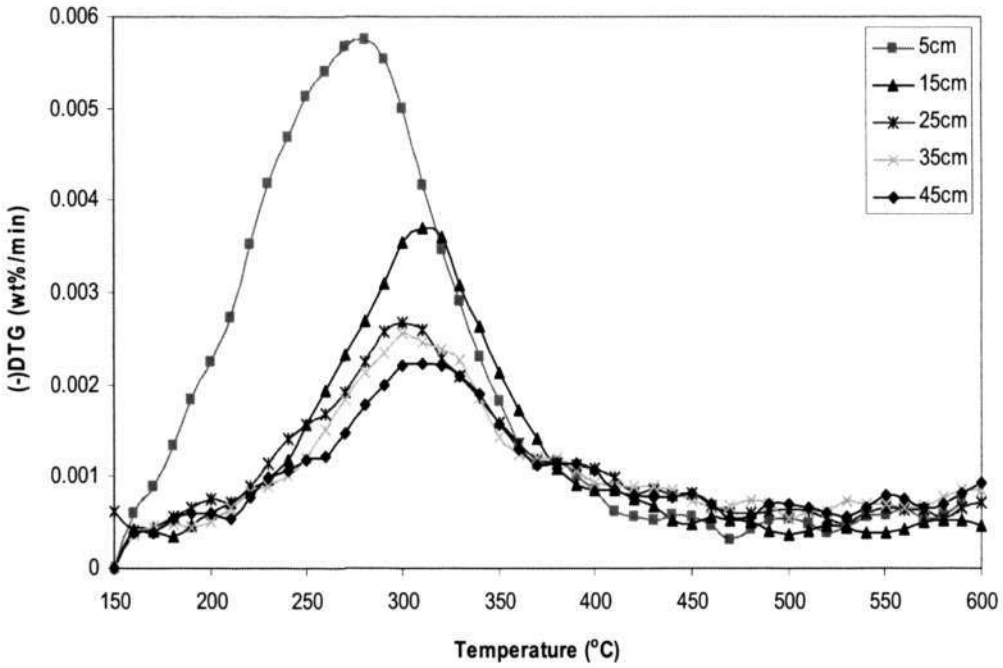

Figure 5.27 DTG curves of BAC in the two-stage biotrickling filter

5.3.9.3 Sulfate accumulation

Sulfate is the main final product of H_2S oxidation; therefore, its accumulation reflects H_2S removal capacity of different parts in the biotrickling filter. Figure 5.28 shows the sulfate concentration diversification along the packing bed after 150-day operation of the two-stage biotrickling filter. In the two-stage biotrickling filter, sulfate concentration in the first stage was as high as 27.5mg/g-carbon due to abundant H_2S oxidation while it was less than 2.0mg/g-carbon in the second stage. It was because most H_2S was removed by the first stage and the remaining H_2S entering the second stage was usually below 3ppmV. Sulfate accumulation of the second stage decreased significantly, but was still higher than that reported for the virgin carbon (0.014mg/g-carbon).

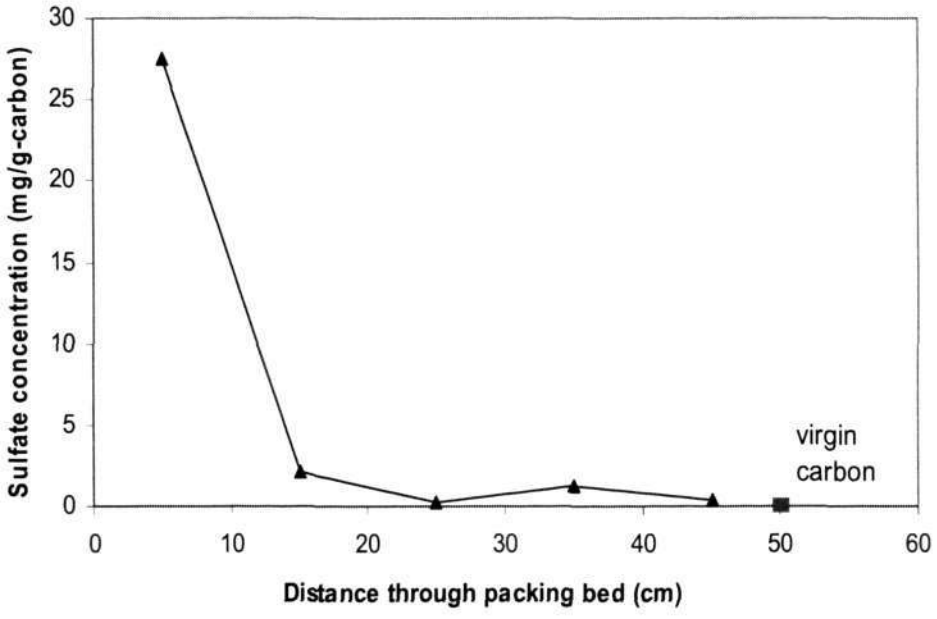

Figure 5.28 Sulfate concentration diversification along the packing bed

5.3.9.4 CNHS analysis

CNHS analysis provides information about the element changes before and after the biotrickling filter operation. Figure 5.29 shows the carbon (C) content, hydrogen (H) content, nitrogen (N) content and combustible sulfur (S) content of the BAC after the two-stage biotrickling filter was operated for 150 days.

In the two-stage biotrickling filter, the carbon content (63.8-75.7%) and hydrogen content (2.2-3.8%) of the BAC had little variance compared with those of the virgin carbon (C: 82.45%, H: 0.57%), which indicated that the composition of activated carbon remained stable during the biotrickling filter operation and activated carbon was not biodegraded. The benign element mass balance of activated carbon implied that it was a nondegradable packing medium. The nitrogen content of the BAC (0.2-1.8%) increased compared with that of the virgin carbon (0%) due to the addition of chemical nutrition. As for the carbon content, hydrogen content and nitrogen content, no increasing or decreasing trend was found along the packing bed as shown in the following figure.

The combustible sulfur content of the BAC (0.14-2.55%) was higher than that of the virgin carbon (0.05%) and that of the toluene exhausted carbon (0.008%), but much lower than that of the H_2S exhausted carbon (7.05%). As shown in the following figure, the combustible sulfur content of the BAC decreased along the packing length and the combustible sulfur content of the first stage (2.55%) was much higher than those of the second stage (0.14-1.32%) because H_2S degradation occurred mainly in the first stage.

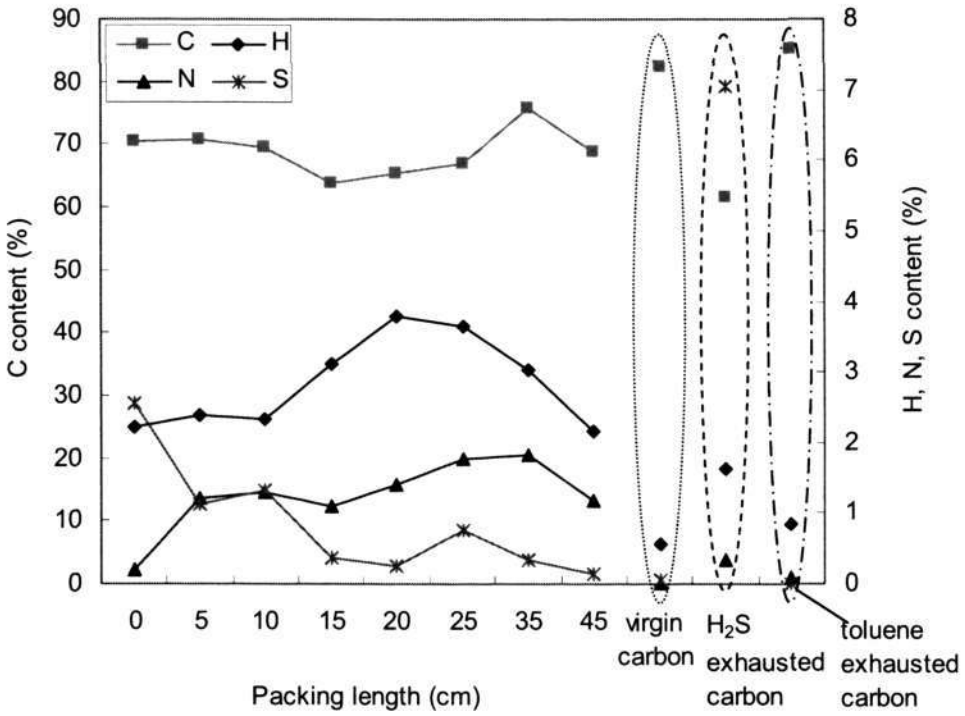

Figure 5.29 Element content of BAC through the packing bed

5.4 Comparison of the three biotrickling filters

5.4.1 Gas retention time

To compare the capacity of the three biotrickling filters, the curves of removal efficiency as a function of GRT are plotted together. Figures 5.30(a) and (b) show the toluene and H_2S removal efficiency vs. GRT in the three biotrickling filters, respectively. For comparison of toluene removal efficiency, the inlet toluene concentration was taken to be at 50ppmV. As for H_2S removal efficiency in Figure 5.30(b), the inlet H_2S concentration was set at 20ppmV in the two-stage biotrickling filter and the low pH single-stage biotrickling filter. However, the concentration in the neutral pH single-stage biotrickling filter was set at 5ppmV because H_2S concentration was kept at a low level during most of the operation period. If 20ppmV was assumed in the neutral pH single-stage biotrickling filter, one would expect the removal efficiency to be lower as the biotrickling filter tended to have poorer performance with the increasing inlet concentration. As can be seen, the three biotrickling filters show a similar behavior of removal efficiency decreasing with shorter GRT. However, they achieved different removal efficiency values at the same GRT.

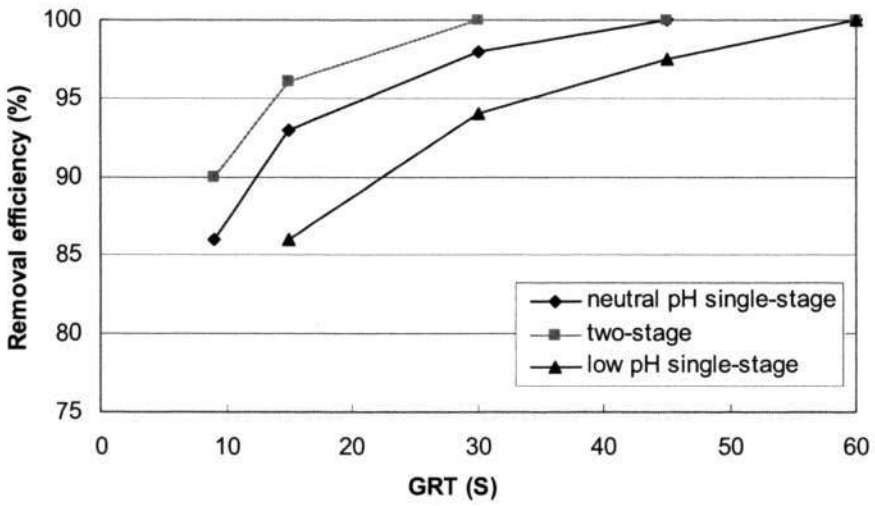

Figure 5.30(a) Toluene removal efficiency vs. GRT in the three biotrickling filters

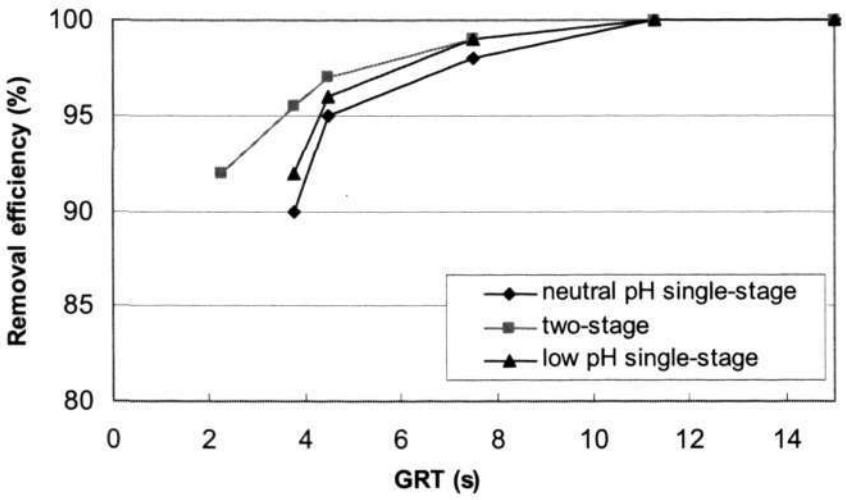

Figure 5.30(b) H_2S removal efficiency vs. GRT in the three biotrickling filters

5.4.1.1 Comparison of toluene removal efficiency in the three biotrickling filters

As shown in Figure 5.30(a), toluene removal efficiency was the highest in the two-stage biotrickling filter and the lowest in the low pH single-stage biotrickling filter. For instance, at a GRT of 15s, the removal efficiency of the two-stage biotrickling filter, the neutral pH single-stage biotrickling filter and the low pH single-stage biotrickling filter were 96%, 94%, 86%, respectively, higher than those of the reported media listed in Table 2.7. The difference was caused by many reasons such as pH and microbial activity, which would be discussed in detail in the following passages.

In the neutral pH single-stage biotrickling filter, pH had no effect on toluene removal because the range of 6-8 was optimum for the growth of *P. putida*. The decrease of the removal efficiency might be caused by the following reasons. Firstly, H_2S degraders shared a part of carbon surface area. Secondly, the removal efficiency might be adversely affected through the accumulation of high salt concentrations and increased ionic strength because a large quantity of alkali was added to maintain pH at a neutral level (Dolfing *et al.*, 1993). Sulfate concentration

in the second stage of the two-stage biotrickling filter was less than 2.0mg/g-carbon before acidification, while it went up to 19.3mg/g-carbon (neutral pH) and 25.4mg/g-carbon (low pH) in the single-stage biotrickling filters. Thirdly, maintaining the uniformity of the neutral pH in the whole medium might be difficult because the irrigation water might not trickle through it uniformly.

In the low pH single-stage biotrickling filter, the microbial communities adjusted to the tough environmental conditions through acclimation of the species present or by growth of low-pH tolerant species. The low removal capacity might be attributed to the low degradation activity of another microbial community different from that in neutral pH, or the low activity caused by the tough environmental effect. In the oxygen uptake rate (OUR) test, biofilm degraded toluene at 0.35mgO_2/L·min in the two-stage biotrickling filter while 0.28mgO_2/L·min (neutral pH) and 0.11mgO_2/L·min (low pH) in the single-stage biotrickling filters. In general, the consortium of the low pH single-stage biotrickling filter had lower activity than the other two biotrickling filters. However, it also demonstrated that some species could tolerate acid environment and degrade toluene at the low pH.

5.4.1.2 Comparison of H_2S removal efficiency in the three biotrickling filters

The relationships between H_2S removal efficiency and GRT in the three biotrickling filters shown in Figure 5.30(b) were different from those of toluene. At the same GRT, H_2S removal was the best in the two-stage biotrickling filter, followed by the low pH single-stage biotrickling filter and then the neutral pH single-stage biotrickling filter. For example, the removal efficiency of the two-stage biotrickling filter, the low pH single-stage biotrickling filter and the neutral pH single-stage biotrickling filter were 95.5%, 92% and 90% respectively at a GRT of 3.75s. The reasons were discussed as follows.

In the two-stage and single-stage biotrickling filters, different values of pH resulted in different dominant species of H_2S degraders, which had already been reviewed in Section 2.2.2. The removal rates of various microorganisms were different,

accordingly. Yang et al. (1989) reported H_2S removal at a rate of 0.73mmol/L·h using *Thiobacillus thioparus* TK-m in a neutral pH system, while *Thiobacillus thiooxidans* yielded a very high removal capacity of 396~428g-S/m^3·h (12.375~13.375mmol/L·h) in a low pH biotrickling filter (Cho et al., 2000).

Furtheremore, in the two-stage bioreactor, different microorganisms for H_2S and toluene degradation were under separate optimum living environment. While in the single-stage reactors, all kinds of organisms lived in a complex ecosystem together. At the same time, parts of the surface area were shared by the toluene degrading bacteria. Therefore, the microbial activities in the three biotrickling filters were different under different living environments. In the OUR experiments of this study, biofilm from the two-stage biotrickling filter oxidized $Na_2S_2O_3$ at 0.08mgO_2/L·min, while the value was 0.06mgO_2/L·min (low pH) and 0.03mgO_2/L·min (neutral pH) in the single-stage biotrickling filters.

5.4.2 Shock loading

When GRT and the inlet substrate concentration were changed, the biotrickling filter was subjected to shock loading. In reviewing the operation of the three biotrickling filters (shown in Figure 5.1(a) & (b), 5.11(a) & (b) and 5.19(a) & (b)); when the parameters were changed, H_2S and toluene removal efficiency had a slight decrease and then recovered quickly within one day. The quick response of the BAC biotrickling filters to shock loading demonstrated that BAC had an excellent buffering capacity.

The ability to buffer the shock loading is imperative for the proper and effective functioning of any bioreactor. Under the shock loading, short recovery time and lower effluent concentration levels can be achieved using this novel BAC system. This results from adsorption of a portion of the increase in the influent concentration and this portion can be subsequently desorbed and biodegraded when the pollutant concentration returns to pre-shock levels or reaches stable conditions.

Abumaizar et al. (1998) obtained similar results in his studies about biofiltration of BTEX using compost-activated carbon filter media. Compared with other conventional media such as ceramic and compost (Altaf et al., 1998b; Eldon et al., 2005), BAC presented a better buffering capacity at a short GRT.

Activated carbon allows the adsorption of gases onto the carbon itself and the biofilm, which could enhance the removal efficiency of hydrophobic gases pollutants. It has been proven that the mesopores and micropores can be accessible to the adsorption of substrate molecules through the biofilm (Walker et al., 1999; Alexander et al., 2001). It was also reported that the transfer rate in the carbon was faster than other packing materials due to adsorption (Chung et al., 2005).

5.4.3 Elimination capacity

The comparison of elimination capacity directly reflects different abilities of the three biotrickling filters. Figures 5.31(a) and (b) indicate the relationship of the inlet loading and the elimination capacity of H_2S and toluene, respectively. The three biotrickling filters showed a similar behavior for the toluene elimination capacity as a function of loading rate, i.e. the elimination capacity increased linearly with the increasing inlet loading until it reached the maximum elimination capacity of the biotrickling filter. The maximum elimination capacities of toluene in the three biotrickling filters were 310g/m^3·h (the two-stage biotrickling filter) > 280g/m^3·h (the neutral pH single-stage biotrickling filter) > 205g/m^3·h (the low pH single-stage biotrickling filter). These values of the BAC biotrickling filters were much higher than 15~165g/m^3·h of other reported media listed in Table 2.7.

Based on the results of Figure 5.31(b), all the H_2S elimination capacities of the three biotrickling filters increased linearly with the increasing inlet loading but could not achieve an equilibrium value because of the low inlet loading rate. Under a H_2S loading of 27g/m^3·h, the two-stage biotrickling filter, the low pH single-stage biotrickling filter and the neutral pH single-stage biotrickling filter achieved the elimination capacity of 25.5g/m^3·h, 24.8g/m^3·h and 24g/m^3·h, respectively. The H_2S

elimination capacities order of the three biotrickling filters was hence the two-stage biotrickling filter > the low pH single-stage biotrickling filter > the neutral pH single-stage biotrickling filter.

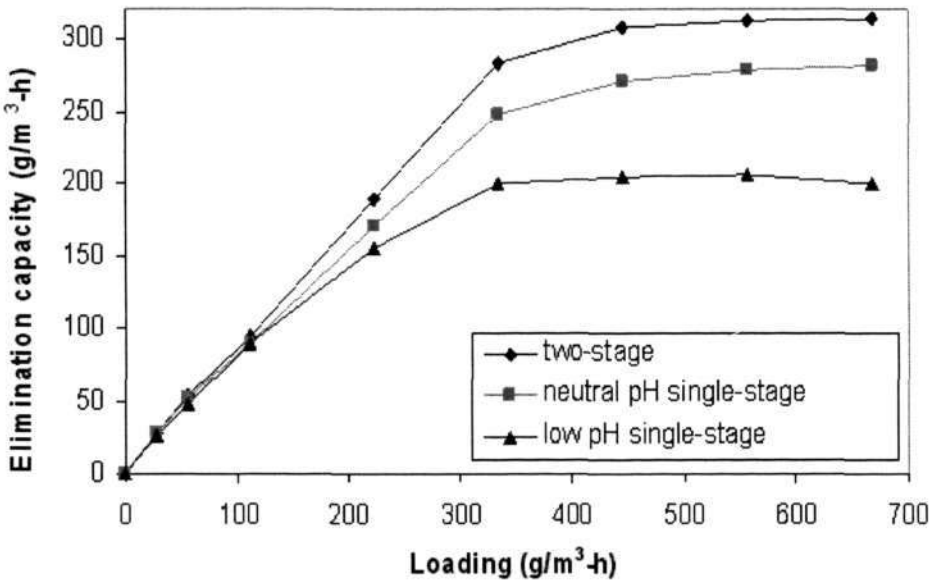

Figure 5.31(a) Inlet loading vs. toluene elimination capacity

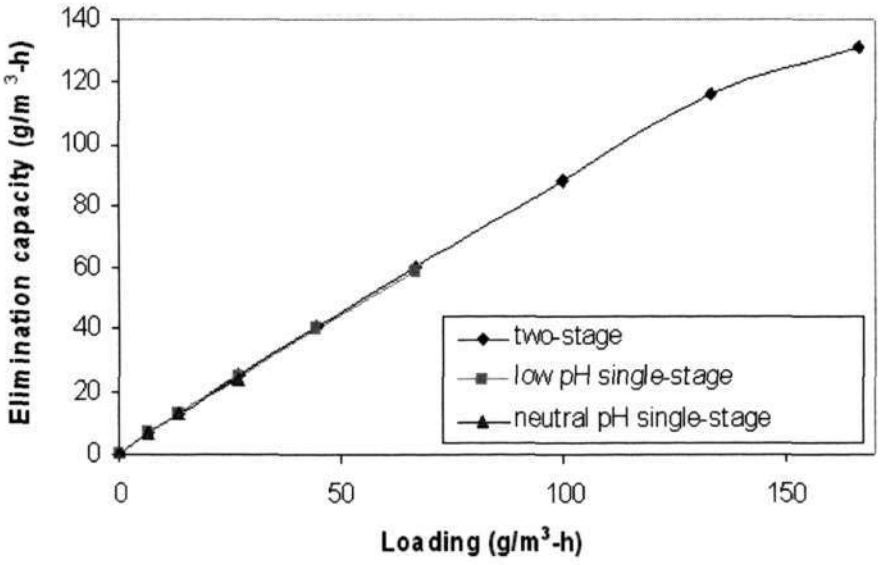

Figure 5.31(b) Inlet loading vs. H_2S elimination capacity

5.4.4 Concentration profile along the packing length

In different biotrickling filters, the fuctional locations for pollutant removal may be different. Figures 5.32(a) and (b) show the variations of H_2S and toluene concentration along the packing bed length of the three biotrickling filters. The variations of H_2S concentration in the three biotrickling filters show a similar behavior along the biotrickling filter packing length at the corresponding GRT. Overall GRT was set at 15s and hence the GRT of the first segment was 3s. H_2S inlet concentration was set at 20ppmV except 5ppmV in the neutral pH single-stage biotrickling filter. H_2S was removed by 95%, 93% and 90% in segment I (h/H=0~0.2) of the two-stage biofiter, the low pH single-stage biotrickling filter and the neutral pH single-stage biotrickling filter, respectively. Once again it proved that the removal efficiency of the two-stage biofitler was the best.

The difference between the toluene curves of the three biotrickling filters was obviously observed in Figure 5.32(b). GRT was regulated at 15s and toluene inlet concentration was controlled at 50ppmV. At h/H of 0.2, C/C_0 already decreased to 0.4 in the neutral pH single-stage biotrickling filter and 0.55 in the low pH single-stage biotrickling filter, which implied that the neutral pH and low pH single-stage biotrickling filters removed more pollutants in Segment I. However, the curve of the neutral pH single-stage biotrickling filter decreased faster than that of the low pH single-stage biotrickling filter.

The curve of the two-stage biotrickling filter was quite different from those of the single-stage biotrickling filters. C/C_0 remained at 1 during 0-0.2 of h/H, which indicated that the two-stage biotrickling filter had no toluene removal in Segment I. C/C_0 decreased to 0.6 at h/H of 0.4 (Segment II) and 0.2 at h/H of 0.6 (Segment III), which indicated that toluene was largely removed in Segment II and III. Nevertheless, C/C_0 of the whole two-stage biotrickling filter (0.04) was still smaller than those of the other two single-stage biotrickling filters (0.06 for neutral pH, 0.14 for low pH). The results showed that the two-stage biotrickling filter yielded better overall toluene performance than the other two single-stage biotrickling filters.

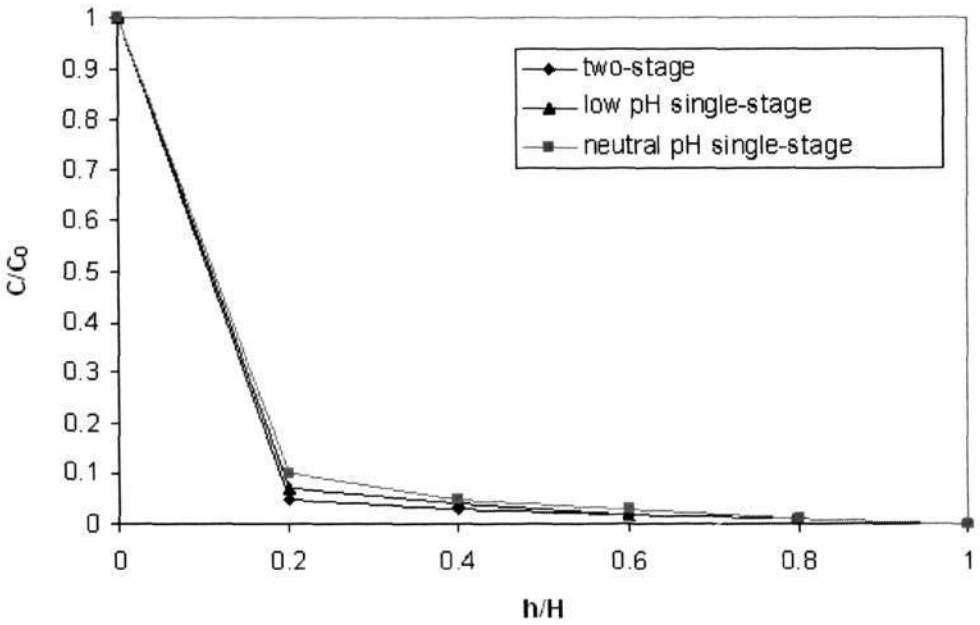

Figure 5.32(a) Variations of H_2S concentration along the packing length

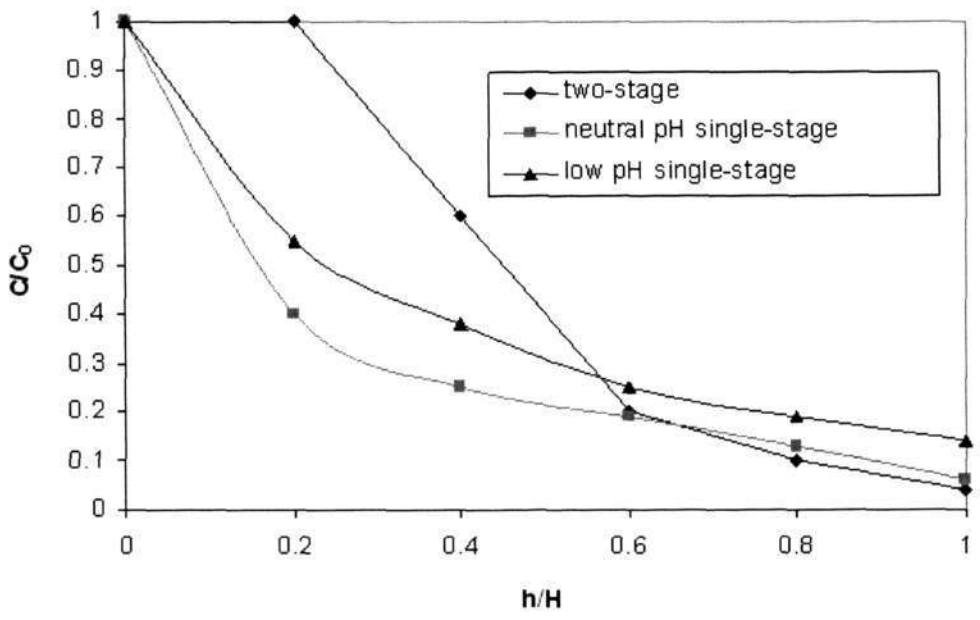

Figure 5.32(b) Variations of toluene concentration along the packing length

5.4.5 Summary

BAC capacity for gas mixture treatment was evaluated with three horizontal biotrickling filters, from which effective contaminants removal could be seen. The performances of these three biotrickling filters were compared taking into consideration different kinds of factors: GRT, elimination capacity, concentration profile along the packing bed length, and costs concern (Appendix B). All the results demonstrated that the two-stage biotrickling filter achieved better removal efficiencies than the other two single-stage biotrickling filters. The two-stage biotrickling filter was shown to be an effective and economical system superior to other biotrickling filters for gas mixture removal. The idea of placing microorganisms under separate optimum living environments should not be confined to the conflicting pH optima for microbial activity. Gas mixture of hydrophilic and hydrophobic pollutants can also be divided into several sections in order to obtain the best performance. The same idea can also be applied to gas mixture under aerobic and anaerobic biodegradation conditions.

CHAPTER SIX

BIOFILTRATION MODELING

A BAC biotrickling filter involves biodegradation, direct adsorption, oxygen limitation and transient conditions. In particular, a two-stage biotrickling filter has two separate stages under different operating environments. To describe these complex phenomena, a mathematical model is developed based on Shareefdeen's model in this chapter.

6.1 Shareefdeen's model with patches of biomass

Shareefdeen's model (1994) is a realistic transient biofilter model for mixed pollutants which incorporates general flow pattern by considering axial dispersion effects, oxygen limitations, interactive kinetics and multicomponent adsorption phenomena. Figure 6.1 shows the model concept for description of biofiltration. As foul gas passes through the biofilter, dispersion, advection, diffusion, bioreaction and adsorption will all affect the removal performance. It is difficult to consider every phenomenon that occurs in the biofilter so some simplifying assumptions are made in the theoretical model.

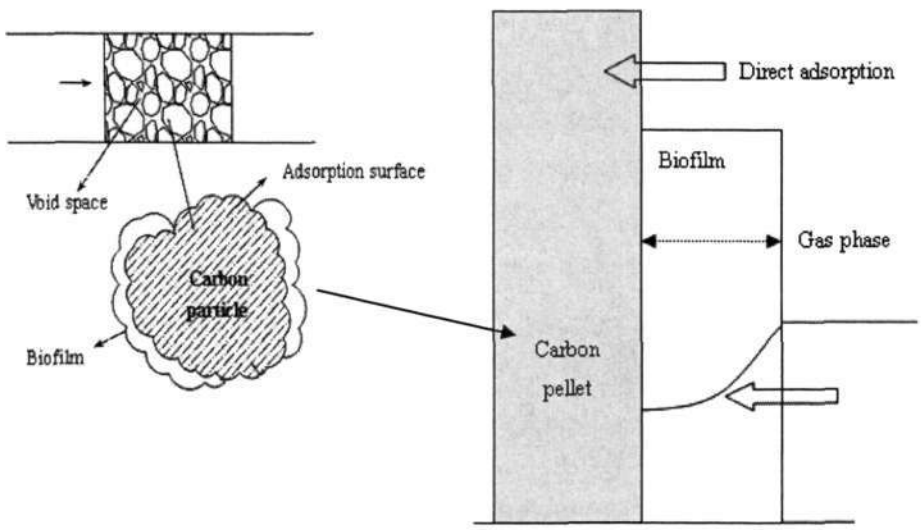

Figure 6.1 Model concept for description of biofiltration

In this model, a biofilter consists of three regions of phases:

1. A liquid biolayer where the substrates are transported and degraded.
2. A gas phase which carries the substrate and oxygen.
3. A solid surface where the substrate gets adsorbed.

6.1.1 The biofilm

The pollutants in the gas phase, as well as oxygen, are partially dissolved in the liquid phase of the biolayer and are degraded or consumed by the microorganisms. The transportation within the biofilm is by molecular diffusion. Concentration gradient of both oxygen and substrate exists in the biofilm. At some thickness, the diffusing oxygen and substrate is consumed by reaction before it penetrates through the entire biolayer. Most of the biological conversion occurs in the outer layers of the film, called the effective or active biolayer. During the start-up period of a biofilter, the biofilm formation is not fully completed and its thickness varies with time. This phenomenon cannot be easily described and is out of the scope of this model. Hence, the transient model here is really applicable only for the transition from one set of operation conditions to another, after the biolayer has been fully developed.

In developing a theoretical model in the biofilm, the following assumptions are made:

1. There are patches of biofilm on the solids leaving the bare surface of the solids in direct contact with the air stream. In these bare surfaces, the pollutants get adsorbed.
2. Biodegradation takes place only within the biofilm. No biological reaction occurs in the adsorption area.
3. The substrate and/or oxygen are depleted in a fraction of the actual biolayer. This fraction is called the effective biolayer.

4. The extent of the biofilm patch is much larger than its depth. Hence, the substrate and oxygen transported into the biolayer through the side surfaces of the biofilm patch can be neglected. And diffusion/reaction in the biofilm can be considered in a single direction only.

Based on the above assumptions, the mass balances of pollutant j and oxygen (O) in the biofilm are described using the following equations.

$$\frac{\partial S_j}{\partial t} = f(X_V) D_{jW} \frac{\partial^2 S_j}{\partial X^2} - \frac{X_V}{Y_j} \mu_j(S_j, S_O) \tag{6.1}$$

$$\frac{\partial S_O}{\partial t} = f(X_V) D_{OW} \frac{\partial^2 S_O}{\partial X^2} - \sum_{j=1}^{n} \frac{X_V}{Y_{Oj}} \mu_j(S_1, \ldots\ldots, S_n, S_o) \tag{6.2}$$

The initial and boundary conditions are as follows:

$t=0$	$h=0, X=0$	$S_j = \frac{C_{ji}}{m_j}$	(6.3)
$t=0$	$0<h\leq H, X=0$	$S_j = \frac{C_{j,0}(h)}{m_j}$	(6.4)
$t=0$	$0<X\leq\delta$	$S_j = S_{j,0}(X)$	(6.5)
$X=0$	$0<t<\tau; h>u_g t$	$S_j = \frac{C_{j,0}(h)}{m_j}$	(6.6)
$X=0$	$0<t<\tau; h<u_g t$	$S_j = \frac{C_j(h)}{m_j}$	(6.7)
$X=0$	$t>\tau; h>0$	$S_j = \frac{C_j(h)}{m_j}$	(6.8)
$X=\delta$	$h>0; t>0$	$\frac{\partial S_j}{\partial X} = 0$	(6.9)

Where

$C_{j,0}$ = Value of C_j at t=0 (g/m^3)

C_{ji} = Value of C_j at h=0 (g/m^3)

D_{jW} = Diffusion coefficient of substrates in water (m^2/s)

D_{OW} = Diffusion coefficient of oxygen in water (m^2/s)

$f(X_V)$ = Ratio of diffusivity of a compound in the biofilm to that in water

h = Position in the column (m)

H = Total height of the biofilter bed (m)

S_j = Concentration of pollutant j at a position x in the biolayer at a point h along the column (g/m^3)

$S_{j,0}$ = Value of S_j at $t=0$ (g/m^3)

S_O = Oxygen concentration at a position x in the biolayer at a point h along the column (g/m^3)

t = Time (h)

X_V = Biofilm density (kg/m^3)

X = Position in the biolayer (m)

Y_j = Yield coefficient of a culture on VOC j (g-biomass/g-compound j)

Y_{Oj} = Yield coefficient of a culture on oxygen (g-biomass/g-oxygen)

δ = Effective biolayer thickness (m)

6.1.2 Gas phase

The fundamental phenomena governing the transport of substrates in gas phase are dispersion, advection, diffusion, biodegradation in the biofilm and adsorption on the solid phase. In deriving the mass balance equation for the gas phase, the following assumptions are made:

1. The substrate and oxygen in the air are dissolved in water and assumed to be in equilibrium state as dictated by Henry's law.
2. The saturated concentration of substrate in the water is dictated by distraction coefficients.
3. The substrate and oxygen transferred from water to biofilm (biolayer) for biodegradation is dictated by diffusion coefficients.
4. Assume the ionic strength and operation temperature are constant. The interaction between oxygen and substrate with biofilm is dictated by biomass growth rate. The diffusion and dispersion processes are occurred on biofilm concurrently.

The mass balances of pollutant j and oxygen (O) in the gas phase can be modeled as:

$$\upsilon\frac{\partial C_j}{\partial t} = D_j\upsilon\frac{\partial^2 C_j}{\partial h^2} - u_g\frac{\partial C_j}{\partial h} + f(X_V)D_{jW}\alpha A_s^*(\frac{\partial S_j}{\partial X})_{X=0} - (1-\alpha)A_s^* k_j(C_j - C_j^*) \tag{6.10}$$

$$\upsilon\frac{\partial C_O}{\partial t} = D_O\upsilon\frac{\partial^2 C_O}{\partial h^2} - u_g\frac{\partial C_O}{\partial h} + f(X_V)D_{OW}\alpha A_s^*(\frac{\partial S_O}{\partial X})_{X=0} \tag{6.11}$$

With the following initial and boundary conditions:

$t=0$	$h=0$	$C_j=C_{ji,0}$	(6.12)
$t=0$	$0<h\leq H$	$C_j=C_{j,0}(h)$	(6.13)
$h=0$	$t>0$	$D_j\frac{\partial C_j}{\partial h} = -u_g(C_j\big\|_{0^-} - C_j\big\|_{0^+})$	(6.14)
$h=H$	$t>0$	$\frac{\partial C_j}{\partial h} = 0$	(6.15)

Where

A_S^* = Total surface area available for biolayer formation and adsorption per unit volume of biofilter (m^{-1})

C_j = Concentration of substance j in the air at a position h along the biofilter (g/m^3)

C_j^* = Equilibrium pollutant j concentration in the gas phase (g/m^3)

$C_{j,0}$ = Value of C_j at t=0 (g/m^3)

$C_{ji,0}$ = Value of C_j at $h=0$ and $t=0$ (g/m^3)

C_O = Oxygen concentration in the air at a position h along the biofilter (g/m^3)

D_j = Dispersion coefficient of substrates in air (cm^2/s)

D_O = Dispersion coefficient of oxygen in air (cm^2/s)

D_{jW} = Diffusion coefficient of substrates in water (m^2/s)

D_{OW} = Diffusion coefficient of oxygen in water (m^2/s)

$f(X_V)$ = Ratio of diffusivity of a compound in the biofilm to that in water

h = Position in the column (m)

H = Total height of the biofilter bed (m)

k_j = Mass transfer coefficient between the gas and the solid particle (m/h)

S_j = Concentration of pollutant j at a position x in the biolayer at a point h along the column (g/m^3)

S_O = Oxygen concentration at a position x in the biolayer at a point h along the column (g/m^3)

t = Time (h)

u_g = Superficial air velocity in the biofilter (m/h)

X_V = Biofilm density (kg/m^3)

X = Position in the biolayer (m)

a = Fraction of total surface area available for biofilm formation

υ = Packing material porosity

6.1.3 Solid phase

At the steady state conditions, the adsorption process is in equilibrium and thus it does not come into play. However, under transient conditions, adsorption process needs to be explicitly accounted for in the model development.

In deriving the mass balance equation for the solid phase, the following assumptions are made:

1. Adsorption of the pollutant occurs only through the direct bare solid/air interface. It does not occur in the biofilm.
2. Adsorption is a reversible process and its equilibrium characteristics are described through the use of adsorption isotherms.
3. Oxygen does not get adsorbed on the solid particles.

The mass balance of pollutant j in the solid phase is given by

$$(1-\upsilon)\rho_P \frac{\partial C_{jP}}{\partial t} = (1-\alpha)A_s^{\bullet} k_j (C_j - C_j^{\bullet}) \tag{6.16}$$

$$t=0 \qquad h \geq 0 \qquad C_{jp}=C_{jp,0}(h) \tag{6.17}$$

Where

$A_S^{\bullet}$ = Total surface area available for biolayer formation and adsorption per unit volume of biofilter (m^{-1})

C_j = Concentration of substance j in the air at a position h along the biofilter (g/m^3)

$C_j^{\bullet}$ = Equilibrium pollutant j concentration in the gas phase (g/m^3)

C_{jP} = Concentration of substance j on the solid particle (g of pollutant j-adsorbed/g particle)

k_j = Mass transfer coefficient between the gas and the solid particle (m/h)

t = Time (h)

a = Fraction of total surface area available for biofilm formation

υ = Packing material porosity

ρ_P = Density of the solid particles (g/m^3)

6.1.4 Degradation kinetics and adsorption isotherm

The specific growth rate of the pollutant j degrading biomass is determined through Andrews kinetics.

$$\mu_j(S_j) = \frac{\mu_j^* S_j}{(K_j + S_j + \frac{S_j^2}{K_{Ij}})} g(S_O) \tag{6.18}$$

The functional dependence of the specific growth rate on oxygen is given by

$$g(S_O) = \frac{S_O}{(K_O + S_O)} \tag{6.19}$$

Where

μ_j^* = Constant in the specific growth rate expression (h^{-1})

μ_j = Specific growth rate (h^{-1})

K_O= Constant in the specific growth rate expression of a culture, expressing the effect of oxygen (g/m3)

K_j= Constant in the specific growth rate expression of a culture growing on compound j (g/m3)

K_{IJ}= Inhibition constant in the specific growth rate expression of a culture growing on compound j (g/m3)

The adsorption for single pollutant j is given by the Langmuir isotherm.

$$C_{jP} = \frac{a_j C_j^*}{1 + b_j C_j^*} \tag{6.20}$$

For mixtures of two compounds 1 and 2, the Extended Langmuir Model (Gordon, 1996) is used.

$$C_{1P} = \frac{a_1 C_1^*}{1 + b_1 C_1^* + b_2 C_2^*} \tag{6.21}$$

$$C_{2P} = \frac{a_2 C_2^*}{1 + b_1 C_1^* + b_2 C_2^*} \tag{6.22}$$

Where a_j and b_j are the isotherm constants for each component j in its single-stage system.

The model has been solved by two approaches (approximate and general) and validated with biofiltration of benzene and toluene mixture data. The approximate model is based on the quasi-steady-state approximation in the biofilm to reduce the mathematical complexity, but the general model is solved without any simplification. The results show that the predictions obtained by the general model are closer to the actual experimental results. Both experimental data and model predictions have shown that transient conditions during the shuting down and restart-up period are not very long. Moreover, the theoretical predictions of responses to random variation in the operation conditions show that the biofilter is able to withstand extreme conditions commonly encountered in practical applications. To sum up, the results provide the evidence that the model is capable of qualitatively describing the transient aspects of the biofiltration process very well.

6.2 Two-stage biotrickling filter model

As for the single-stage biofiltration, the model for gas mixture has been studied in Shareefdeen's model. Therefore, only the complex model of the two-stage biotrickling filter is discussed here. In this two-stage biotrickling filter, the reactor is divided into three phases under different conditions: (I) the first stage (Segment I); (II) H_2S and toluene interaction phase in the second stage of the biotrickling filter (the removal of H_2S and toluene); (III) only toluene removal in the second stage of the biotrickling filter (toluene removal only).

- In phase I, toluene is only adsorbed. No toluene biodegradation is assumed. H_2S is removed by biodegradation and adsorption. Low toluene concentration has no influence on H_2S removal.
- In phase II, toluene and the remaining H_2S are removed simultaneously. In this study, this function was accomplished by Segment II.
- In phase III, no H_2S and only toluene is removed by biodegradation and adsorption. It refers to Segment III-V in this experiment.

The mass balances of H_2S (H), toluene (T) and oxygen (O) in the biofilm, in the gas phase and in the solid phase during the three phases are illustrated in the following equations.

Phase I: *H_2S: biodegradation+adsorption; Toluene: adsorption*

Mass balances in the biofilm:

$$\frac{\partial S_H}{\partial t} = f(X_V) D_{HW} \frac{\partial^2 S_H}{\partial X^2} - \frac{X_V}{Y} \mu_H (S_H, S_O) \tag{6.23}$$

$$\frac{\partial S_O}{\partial t} = f(X_V) D_{OW} \frac{\partial^2 S_O}{\partial X^2} - \frac{X_V}{Y_{OH}} \mu_H (S_H, S_o) \tag{6.24}$$

Mass balances in the gas phase:

$$\upsilon \frac{\partial C_H}{\partial t} = D_H \upsilon \frac{\partial^2 C_H}{\partial h^2} - u_g \frac{\partial C_H}{\partial h} + f(X_V) D_{HW} \alpha A_s^* (\frac{\partial S_H}{\partial X})_{X=0} - (1-\alpha) A_s^* k_H (C_H - C_H^*) \tag{6.25}$$

$$\upsilon \frac{\partial C_T}{\partial t} = D_T \upsilon \frac{\partial^2 C_T}{\partial h^2} - u_g \frac{\partial C_T}{\partial h} - (1-\alpha) A_s^* k_T (C_T - C_T^*) \tag{6.26}$$

$$\upsilon \frac{\partial C_O}{\partial t} = D_O \upsilon \frac{\partial^2 C_O}{\partial h^2} - u_g \frac{\partial C_O}{\partial h} + f(X_V) D_{OW} \alpha A_s^* (\frac{\partial S_O}{\partial X})_{X=0} \tag{6.27}$$

Mass balances in the solid phase:

$$(1-\upsilon) \rho_P \frac{\partial C_{HP}}{\partial t} = (1-\alpha) A_s^* k_H (C_H - C_H^*) \tag{6.28}$$

$$(1-\upsilon) \rho_P \frac{\partial C_{TP}}{\partial t} = (1-\alpha) A_s^* k_T (C_T - C_T^*) \tag{6.29}$$

Phase II: *H_2S: biodegradation+adsorption; Toluene: biodegradation+adsorption*

Mass balances in the biofilm:

$$\frac{\partial S_H}{\partial t} = f(X_V) D_{HW} \frac{\partial^2 S_H}{\partial X^2} - \frac{X_V}{Y_H} \mu_H (S_H, S_o) \tag{6.30}$$

$$\frac{\partial S_T}{\partial t} = f(X_V) D_{TW} \frac{\partial^2 S_T}{\partial X^2} - \frac{X_V}{Y_T} \mu_T (S_T, S_o) \tag{6.31}$$

$$\frac{\partial S_O}{\partial t} = f(X_V) D_{OW} \frac{\partial^2 S_O}{\partial X^2} - \frac{X_V}{Y_{OH}} \mu_H(S_H, S_o) - \frac{X_V}{Y_{OT}} \mu_T(S_T, S_O) \tag{6.32}$$

Mass balances in the gas phase:

$$\upsilon \frac{\partial C_H}{\partial t} = D_H \upsilon \frac{\partial^2 C_H}{\partial h^2} - u_g \frac{\partial C_H}{\partial h} + f(X_V) D_{HW} \alpha A_s^* (\frac{\partial S_H}{\partial X})_{X=0} - (1-\alpha) A_s^* k_H (C_H - C_H^*) \tag{6.33}$$

$$\upsilon \frac{\partial C_T}{\partial t} = D_T \upsilon \frac{\partial^2 C_T}{\partial h^2} - u_g \frac{\partial C_T}{\partial h} + f(X_V) D_{TW} \alpha A_s^* (\frac{\partial S_T}{\partial X})_{X=0} - (1-\alpha) A_s^* k_T (C_T - C_T^*) \tag{6.34}$$

$$\upsilon \frac{\partial C_O}{\partial t} = D_O \upsilon \frac{\partial^2 C_O}{\partial h^2} - u_g \frac{\partial C_O}{\partial h} + f(X_V) D_{OW} \alpha A_s^* (\frac{\partial S_O}{\partial X})_{X=0} \tag{6.35}$$

Mass balances in the solid phase:

$$(1-\upsilon)\rho_P \frac{\partial C_{HP}}{\partial t} = (1-\alpha) A_s^* k_H (C_H - C_H^*) \tag{6.36}$$

$$(1-\upsilon)\rho_P \frac{\partial C_{TP}}{\partial t} = (1-\alpha) A_s^* k_T (C_T - C_T^*) \tag{6.37}$$

Phase III: *Toluene: biodegradation+adsorption*

Mass balances in the biofilm:

$$\frac{\partial S_T}{\partial t} = f(X_V) D_{TW} \frac{\partial^2 S_T}{\partial X^2} - \frac{X_V}{Y_T} \mu_T(S_T, S_o) \tag{6.38}$$

$$\frac{\partial S_O}{\partial t} = f(X_V) D_{OW} \frac{\partial^2 S_O}{\partial X^2} - \frac{X_V}{Y_{OT}} \mu_T(S_T, S_O) \tag{6.39}$$

Mass balances in the gas phase:

$$\upsilon \frac{\partial C_T}{\partial t} = D_T \upsilon \frac{\partial^2 C_T}{\partial h^2} - u_g \frac{\partial C_T}{\partial h} + f(X_V) D_{TW} \alpha A_s^* (\frac{\partial S_T}{\partial X})_{X=0} - (1-\alpha) A_s^* k_T (C_T - C_T^*) \tag{6.40}$$

$$\upsilon \frac{\partial C_O}{\partial t} = D_O \upsilon \frac{\partial^2 C_O}{\partial h^2} - u_g \frac{\partial C_O}{\partial h} + f(X_V) D_{OW} \alpha A_s^* (\frac{\partial S_O}{\partial X})_{X=0} \tag{6.41}$$

Mass balances in the solid phase:

$$(1-\upsilon)\rho_P \frac{\partial C_{TP}}{\partial t} = (1-\alpha)A_s^* k_T (C_T - C_T^*) \tag{6.42}$$

6.2.1 Simplification of the model

In order to simplify the mathematical complexity of the above model, several non-dimensional groups, which are illustrated in the following equations, are derived.

$$\overline{C}_j = \frac{C_j}{C_{jI}} \qquad \overline{C}_O = \frac{C_O}{C_{OI}} \qquad \overline{S}_j = \frac{S_j}{K_j}$$

$$Z = \frac{h}{H} \qquad \theta = \frac{x}{\delta} \qquad \xi = \frac{u_g t}{H}$$

$$Pe_j = \frac{u_g H}{\upsilon D_j} \qquad Pe_O = \frac{u_g H}{\upsilon D_O} \qquad \chi_j = \frac{H(1-\alpha)A_s^* k_j}{\upsilon u_g}$$

$$\beta_{1j} = \frac{D_{jW} H\alpha A_s^* f(X_V) K_j}{\upsilon u_g C_{ji}\delta} \qquad \beta_2 = \frac{D_{OW} H\alpha A_s^* f(X_V) K_O}{\upsilon u_g C_{Oi}\delta}$$

$$\phi_{1j} = \frac{D_{jW} H f(X_V)}{u_g \delta^2} \qquad \phi_2 = \frac{D_{OW} H f(X_V)}{u_g \delta^2}$$

$$\eta_{1j} = \frac{H\mu_j^* X_V}{Y_j K_j u_g} \qquad \eta_{2j} = \frac{H\mu_j^* X_V}{Y_{Oj} K_O u_g}$$

$$\overline{C}_{jP} = \frac{C_{jP}(1-\upsilon)\rho_P}{u_g \upsilon} \qquad \lambda_{1j} = \frac{a_j \rho_P (1-\upsilon)}{\upsilon} \qquad \lambda_{2j}=b_j C_{ji}$$

$$\psi_j = \frac{1}{C_{ji}}\left[\frac{\upsilon C_{ji}}{(1-\upsilon)\rho_P k_{dj}}\right]^{\frac{1}{n_j}} \qquad \varepsilon_j = \frac{C_{ji}}{K_j m_j}$$

After introducing the dimensionless parameters, the model can be reduced to the following:

Phase I:

$$\frac{\partial \overline{S}_H}{\partial \xi} = \phi_{1H} \frac{\partial^2 \overline{S}_H}{\partial \theta^2} - \eta_{1H} g_1(\overline{S}_H, \overline{S}_o) \tag{6.43}$$

$$\frac{\partial \overline{S}_O}{\partial \xi} = \phi_2 \frac{\partial^2 \overline{S}_O}{\partial \theta^2} - \eta_{2H} g_1(\overline{S}_H, \overline{S}_o) - \eta_{2T} g_2(\overline{S}_T, \overline{S}_O) \tag{6.44}$$

$$\frac{\partial \overline{C}_H}{\partial \xi} = \frac{1}{Pe_H} \frac{\partial^2 \overline{C}_H}{\partial Z^2} - \frac{1}{\upsilon} \frac{\partial \overline{C}_H}{\partial Z} - \beta_{1H} (\frac{\partial \overline{S}_H}{\partial \theta})_{\theta=0} - x_H (\overline{C}_H - \overline{C}_H^{\bullet}) \tag{6.45}$$

$$\frac{\partial \overline{C}_T}{\partial \xi} = \frac{1}{Pe_T} \frac{\partial^2 \overline{C}_T}{\partial Z^2} - \frac{1}{\upsilon} \frac{\partial \overline{C}_T}{\partial Z} - x_T (\overline{C}_T - \overline{C}_T^{\bullet}) \tag{6.46}$$

$$\frac{\partial \overline{C}_O}{\partial \xi} = \frac{1}{Pe_O} \frac{\partial^2 \overline{C}_O}{\partial Z^2} - \frac{1}{\upsilon} \frac{\partial \overline{C}_O}{\partial Z} - \beta_2 (\frac{\partial \overline{S}_O}{\partial \theta})_{\theta=0} \tag{6.47}$$

$$\frac{\partial \overline{C}_{HP}}{\partial \xi} = x_H (\overline{C}_H - \overline{C}_H^{\bullet}) \tag{6.48}$$

$$\frac{\partial \overline{C}_{TP}}{\partial \xi} = x_T (\overline{C}_T - \overline{C}_T^{\bullet}) \tag{6.49}$$

$$\overline{C}_H^{\bullet} = \frac{\overline{C}_{HP}(1 - \lambda_{2T} \overline{C}_T^{\bullet})}{\lambda_{1H} - \lambda_{2H} \overline{C}_{HP}} \tag{6.50}$$

$$\overline{C}_T^{\bullet} = \frac{\overline{C}_{TP}(1 - \lambda_{2H} \overline{C}_H^{\bullet})}{\lambda_{1T} - \lambda_{2T} \overline{C}_{TP}} \tag{6.51}$$

$$g_1 = \frac{\overline{S}_H \overline{S}_O}{(1 + \overline{S}_H)(1 + \overline{S}_O)} \tag{6.52}$$

Phase II:

$$\frac{\partial \overline{S}_H}{\partial \xi} = \phi_{1H} \frac{\partial^2 \overline{S}_H}{\partial \theta^2} - \eta_{1H} g_1(\overline{S}_H, \overline{S}_o) \tag{6.53}$$

$$\frac{\partial \overline{S}_T}{\partial \xi} = \phi_{1T} \frac{\partial^2 \overline{S}_T}{\partial \theta^2} - \eta_{1T} g_2(\overline{S}_T, \overline{S}_o) \tag{6.54}$$

$$\frac{\partial \bar{S}_O}{\partial \xi} = \phi_2 \frac{\partial^2 \bar{S}_O}{\partial \theta^2} - \eta_{2H} g_1(\bar{S}_H, \bar{S}_o) - \eta_{2T} g_2(\bar{S}_T, \bar{S}_O) \tag{6.55}$$

$$\frac{\partial \bar{C}_H}{\partial \xi} = \frac{1}{Pe_H} \frac{\partial^2 \bar{C}_H}{\partial Z^2} - \frac{1}{\upsilon} \frac{\partial \bar{C}_H}{\partial Z} - \beta_{1H} \left(\frac{\partial \bar{S}_H}{\partial \theta}\right)_{\theta=0} - x_H (\bar{C}_H - \bar{C}_H^*) \tag{6.56}$$

$$\frac{\partial \bar{C}_T}{\partial \xi} = \frac{1}{Pe_T} \frac{\partial^2 \bar{C}_T}{\partial Z^2} - \frac{1}{\upsilon} \frac{\partial \bar{C}_T}{\partial Z} - \beta_{1T} \left(\frac{\partial \bar{S}_T}{\partial \theta}\right)_{\theta=0} - x_T (\bar{C}_T - \bar{C}_T^*) \tag{6.57}$$

$$\frac{\partial \bar{C}_O}{\partial \xi} = \frac{1}{Pe_O} \frac{\partial^2 \bar{C}_O}{\partial Z^2} - \frac{1}{\upsilon} \frac{\partial \bar{C}_O}{\partial Z} - \beta_2 \left(\frac{\partial \bar{S}_O}{\partial \theta}\right)_{\theta=0} \tag{6.58}$$

$$\frac{\partial \bar{C}_{HP}}{\partial \xi} = x_H (\bar{C}_H - \bar{C}_H^*) \tag{6.59}$$

$$\frac{\partial \bar{C}_{TP}}{\partial \xi} = x_T (\bar{C}_T - \bar{C}_T^*) \tag{6.60}$$

$$\bar{C}_H^* = \frac{\bar{C}_{HP}(1 - \lambda_{2T} \bar{C}_T^*)}{\lambda_{1H} - \lambda_{2H} \bar{C}_{HP}} \tag{6.61}$$

$$\bar{C}_T^* = \frac{\bar{C}_{TP}(1 - \lambda_{2H} \bar{C}_H^*)}{\lambda_{1T} - \lambda_{2T} \bar{C}_{TP}} \tag{6.62}$$

$$g_1 = \frac{\bar{S}_H \bar{S}_O}{(1 + \bar{S}_H)(1 + \bar{S}_O)} \tag{6.63}$$

$$g_2 = \frac{\bar{S}_T \bar{S}_O}{(1 + \bar{S}_T)(1 + \bar{S}_O)} \tag{6.64}$$

Phase III:

$$\frac{\partial \bar{S}_T}{\partial \xi} = \phi_{1T} \frac{\partial^2 \bar{S}_T}{\partial \theta^2} - \eta_{1T} g_2(\bar{S}_T, \bar{S}_o) \tag{6.65}$$

$$\frac{\partial \bar{S}_O}{\partial \xi} = \phi_2 \frac{\partial^2 \bar{S}_O}{\partial \theta^2} - \eta_{2H} g_1(\bar{S}_H, \bar{S}_o) - \eta_{2T} g_2(\bar{S}_T, \bar{S}_O) \tag{6.66}$$

$$\frac{\partial \overline{C}_T}{\partial \xi} = \frac{1}{Pe_T}\frac{\partial^2 \overline{C}_T}{\partial Z^2} - \frac{1}{\upsilon}\frac{\partial \overline{C}_T}{\partial Z} - \beta_{1T}\left(\frac{\partial \overline{S}_T}{\partial \theta}\right)_{\theta=0} - x_T(\overline{C}_T - \overline{C}_T^{\bullet}) \tag{6.67}$$

$$\frac{\partial \overline{C}_O}{\partial \xi} = \frac{1}{Pe_O}\frac{\partial^2 \overline{C}_O}{\partial Z^2} - \frac{1}{\upsilon}\frac{\partial \overline{C}_O}{\partial Z} - \beta_2\left(\frac{\partial \overline{S}_O}{\partial \theta}\right)_{\theta=0} \tag{6.68}$$

$$\frac{\partial \overline{C}_{TP}}{\partial \xi} = x_T(\overline{C}_T - \overline{C}_T^{\bullet}) \tag{6.69}$$

$$\overline{C}_T^{\bullet} = \psi_T\left(\overline{C}_{TP}\right)^{\frac{1}{n}} \tag{6.70}$$

$$g_2 = \frac{\overline{S}_T \overline{S}_O}{(1+\overline{S}_T)(1+\overline{S}_O)} \tag{6.71}$$

The initial and boundary conditions are as follows

$\xi = 0$	$Z=0,\ \theta = 0$	$\overline{S}_j = \varepsilon_j$	(6.72)
$\xi = 0$	$0<Z\le 1,\ \theta = 0$	$\overline{S}_j = \varepsilon_j \overline{C}_{j,0}(Z)$	(6.73)
$\xi = 0$	$0< \theta \le 1$	$\overline{S}_j = \overline{S}_{j,0}(\theta)$	(6.74)
$\theta = 0$	$Z>0$	$\overline{S}_j = \varepsilon_j \overline{C}_j(Z)$	(6.75)
$\theta = 1$	$Z>0;\ \xi>0$	$\frac{\partial \overline{S}_j}{\partial x} = 0$	(6.76)

$\xi = 0$	$Z=0$	$\overline{C}_j = 1$	$\overline{C}_{jP} = \overline{C}_{jP,0}(0)$	(6.78)
$\xi = 0$	$0<Z\le 1$	$\overline{C}_j = \overline{C}_{j,0}(Z)$	$\overline{C}_{jP} = \overline{C}_{jP,0}(Z)$	(6.79)
$Z=0$	$\xi>0$	$\frac{\partial \overline{C}_j}{\partial Z} = -Pe_j(\overline{C}_j\big\|_{Z=0^-} - \overline{C}_j\big\|_{Z=0^+})$		(6.80)
$Z=1$		$\frac{\partial \overline{C}_j}{\partial Z} = 0$		(6.81)

6.2.2 Solution of the model equations

The transient model constitutes a problem of coupled second order partial differential equations (PDEs) in three dimensions: time, biolayer and bed length. The equations form a system of highly non-linear complex set of equations. Therefore, the problems were solved using finite element method and arrived at a system of linear equations. A computer program was developed using MATLAB, which has a professional toolbox employing the finite element method to solve PDE problems.

6.2.3 Model parameters estimation

In order to facilitate data analysis and modeling, it is necessary to estimate a number of parameters for the substrates and the biofiltration system. These parameters can be determined from the literature or experiments. A summary of the parameter values used in the current work is given in Table 6.1.

The parameters involved in the adsorption isotherm can be determined from independent kinetic experiments. H_2S or toluene polluted air was passed through the bench reactor in the breakthrough test. The inlet and outlet concentration was monitored until the system reached the equilibrium level. It was assumed that pollutants were not adsorbed on the walls of column. The results of these experiments are shown in Figures 6.2(a) & (b). Plotting $1/C_{jP}$ vs. $1/C_j^*$, a_j and b_j can be obtained from the slope and intercept, respectively.

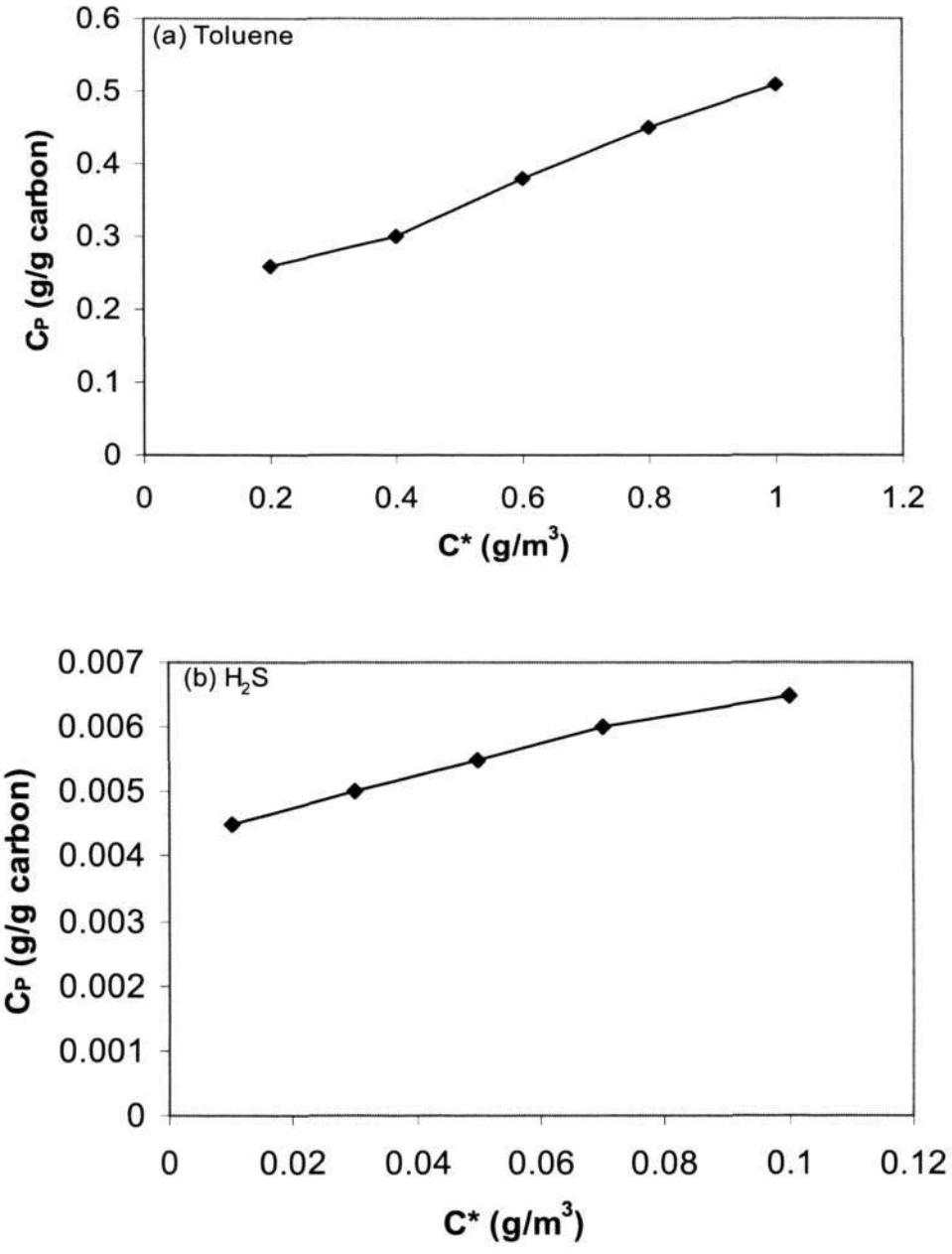

Figure 6.2(a) & (b) Adsorption isotherm of toluene and H_2S on carbon AP-460

Table 6.1 Summary of parameter values

Symbol	Unit	Value	Source
a	-	0.7	Abumaizar et al., 1997
μ_H^*	h^{-1}	0.87	Cosma et al., 1999
μ_T^*	h^{-1}	1.50	Zarook and Baltzis, 1994a
υ	-	0.37	This study
ρ_P	g/m^3	4.9×10^5	This study
C_{Oi}	g/m^3	275.0	Zarook and Baltzis, 1994a
D_{HA}	cm^2/s	0.0338	Hsieh et al., 1993
D_{TA}	cm^2/s	0.0792	Hsieh et al., 1993
D_{OA}	cm^2/s	0.2132	Hsieh et al., 1993
D_{HW}	m^2/s	1.89×10^{-9}	Hebi Li, 2002
D_{TW}	m^2/s	1.03×10^{-9}	Zarook and Baltzis, 1994a
D_{OW}	m^2/s	2.41×10^{-9}	Zarook and Baltzis, 1994a
$f(X_V)$	-	0.195	Zarook and Baltzis, 1994a
X_V	kg/m^3	100	Zarook and Baltzis, 1994a
m_H	-	0.42	Perry and Green, 1999
m_T	-	0.27	Zarook and Baltzis, 1994a
m_O	-	34.4	Zarook and Baltzis, 1994a
k_H	m/h	3.0×10^{-3}	Hsieh et al., 1993
k_T	m/h	6.04×10^{-3}	Zarook and Baltzis, 1994b
K_O	g/m^3	0.26	Zarook and Baltzis, 1994a
K_H	g/m^3	28.8	Hsieh et al., 1993

K_T	g/m^3	11.03	Zarook and Baltzis, 1994a
Y_H	-	0.904	This study
Yo_H	-	1.398	This study
Y_T	-	0.708	Zarook and Baltzis, 1994a
Yo_T	-	0.341	Zarook and Baltzis, 1994a
R_P	m	0.004	This study
a_H	m^3/g	8.38×10^{-5}	This study
a_T	m^3/g	2.34×10^{-5}	This study
b_H	m^3/g	0.03	This study
b_T	m^3/g	0.02	This study
γ_1	-	0.7	Zarook and Baltzis, 1994a
γ_2	-	0.5	Zarook and Baltzis, 1994a

6.3 Results and discussion

Experimental data from the two-stage horizontal biotrickling filter are used to verify the mathematical model.

6.3.1 Pollutant concentration in the gas phase

Figure 6.3 shows the experimental and model predicted transient concentration profiles in two different operating conditions. "H_2S model (I) and experimental data (I)" refer to the H_2S model and data for the first stage, while "H_2S model and experimental data" stand for the H_2S model and data of the total biotrickling filter. The inlet concentrations of toluene and H_2S were regulated at 50ppmV and

20ppmV, respectively. The biotrickling filter operation was changed from state A (GRT=18.75s) to state B (GRT=11.25s). C_j/C_{ji} model and experimental data of toluene and H_2S (I) were higher in stage B than those in state A because GRT was shortened. Two peaks in C_j/C_{ji} curves of toluene and H_2S (I) appeared on day 10 due to the sudden change of GRT and then the curves became stable. However, for state A or B, the H_2S model and experimental data of the total biotrickling filter remained at 100% due to sufficient GRT for H_2S degraders. In general, it was obvious that the model fit the experimental data very well. The experimental data of H_2S and toluene fluctuated a little with the model lines as time progressed.

Figure 6.4 shows the experimental data and model predictions of H_2S and toluene concentration profiles along the packing length. H_2S model line and experimental data decreased dramatically in h/H of 0-0.2, where 98% H_2S was removed. In contrast, toluene model line and experimental data were unchanged in this stage, but declined gradually in h/H of 0.2-1, i.e. the second stage. As can be seen, the model lines had little departure from the experimental data. That is to say, the model predictions are in very good agreement with the experimental results.

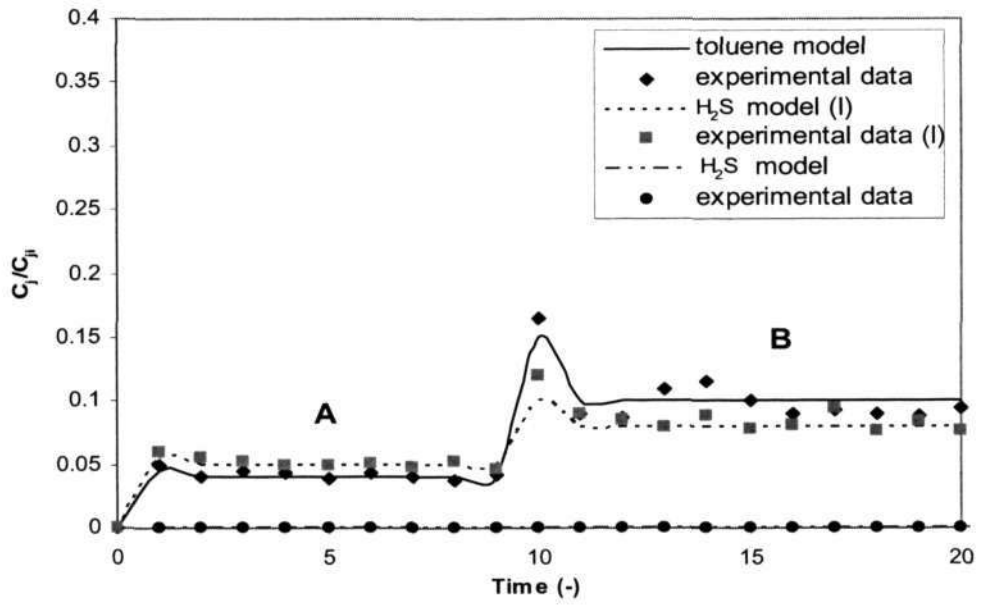

Figure 6.3 Experimental data and model predictions with time

(C_{Ti}=50ppmV, C_{Hi}=20ppmV; **A**: GRT=18.75s, **B**: GRT=11.25s)

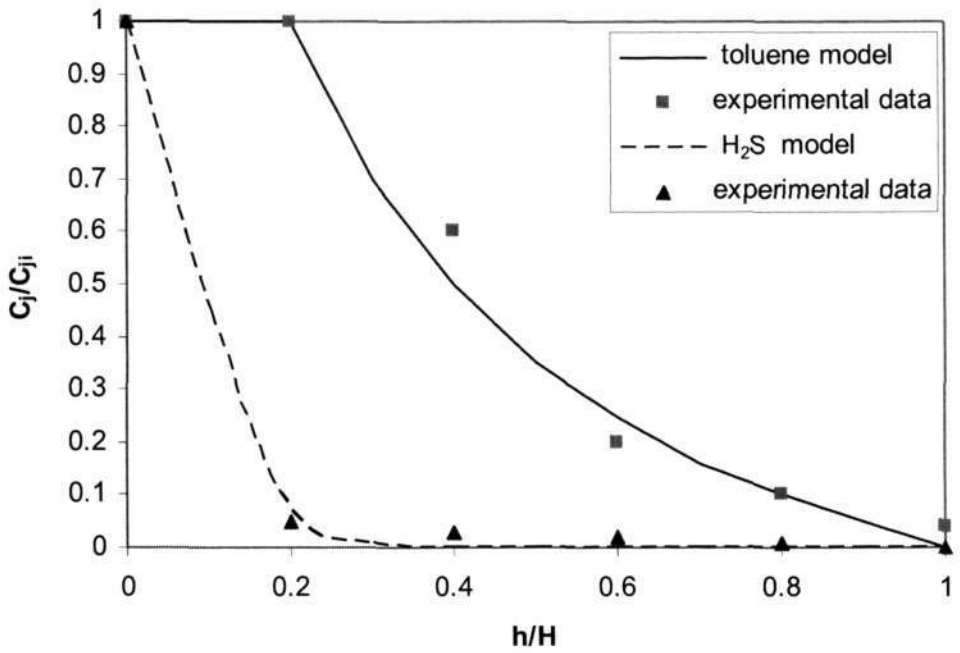

Figure 6.4 Experimental data and model predictions of H_2S and toluene concentration profiles along the packing length

(C_{Ti}=50ppmV, C_{Hi}=20ppmV; GRT=18.75s)

6.3.2 Substrate variation in the biofilm

Figure 6.5 offers the detailed concentration profiles with the biofilm thickness. Toluene and H_2S were depleted at biofilm depth of around 50μm and 20μm respectively. However, oxygen concentration was still left at 6.4g/m^3, which shows the same result as that of Shareefdeen's model (1993). H_2S and toluene were consumed before oxygen. The explanation is given in the model that at lower substrate concentrations, oxygen was available in plenty and might even be ignored in the model and the effective thickness of the biofilm was governed by the faster depleting substrate.

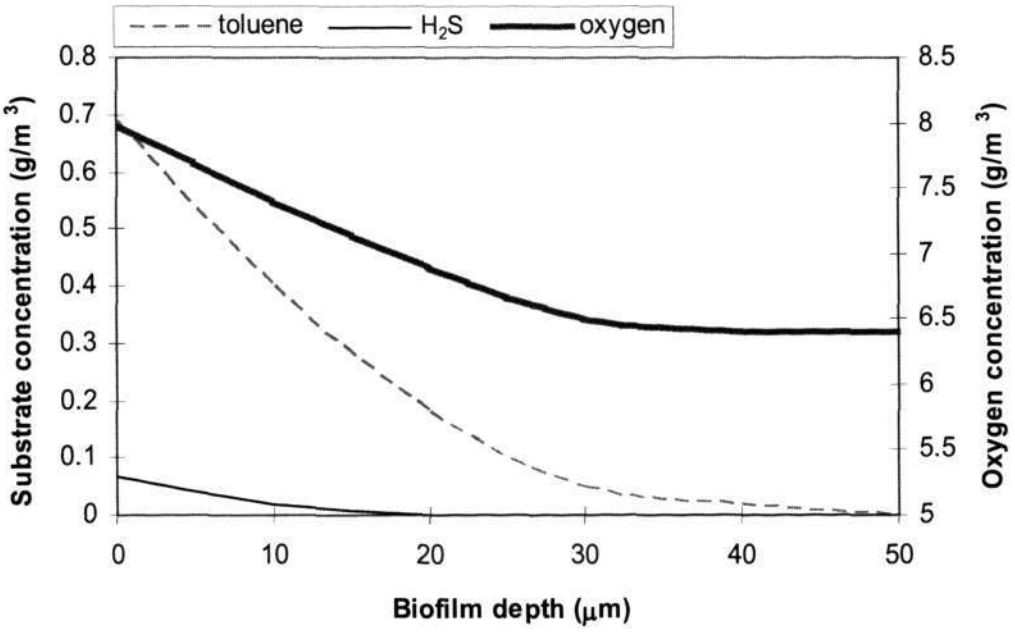

Figure 6.5 Variation profiles of low substrate concentration in the biofilm

(C_T=0.186g/m^3, C_H=0.027 g/m^3)

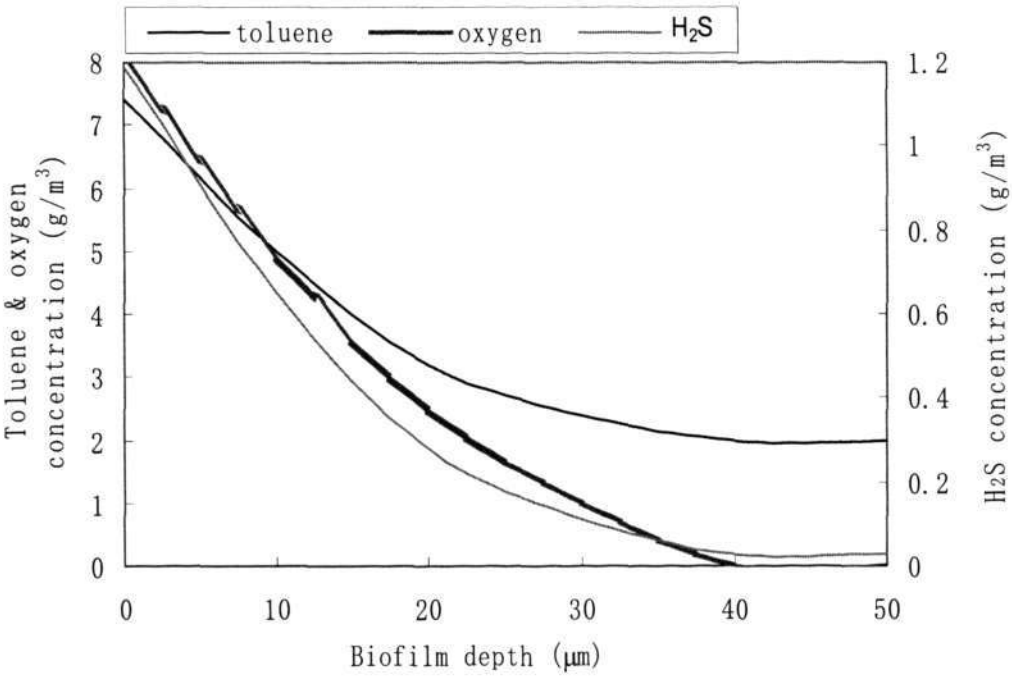

Figure 6.6 Variation profiles of high substrate concentration in the biofilm

(C_T=2g/m^3, C_H=0.5 g/m^3)

While the inlet pollutant concentration increases, oxygen is consumed rapidly and dictates the effective biofilm thickness. Figure 6.6 shows substrate variation in the biofilm at a high concentration. Oxygen was used up at 40μm thickness, while toluene and H_2S had not been degraded completely. These results imply that oxygen needs to be explicitly taken into account in the modeling of biofiltration process under the steady state or transient conditions. Oxygen plays a very crucial role and has potential limiting effects in the biofiltration process especially as the process is aerobic. Thus in a practical biofiltration operation, the inlet air should contain enough oxygen. Operations at lower oxygen concentrations will result in poor conversions and low removal efficiencies.

6.3.3 Sensitivity studies

A thorough investigation of the model's sensitivity is performed to find out the dependency of system performance on the model parameters. The parameters considered for sensitivity study include eight biofilm parameters (ϕ_{1T} and ϕ_{1H}, ϕ_2, η_{1T} and η_{1H}, ε_T and ε_H, ε_O) and four gas phase parameters (β_{1T} and β_{1H}, Pe_T and Pe_H)

6.3.3.1 Biofilm parameters

The effect of ϕ_{1T} and ϕ_{1H} on the outlet concentrations can be seen in Figures 6.7 (a) & (b). A high value of ϕ_{1T} and ϕ_{1H} indicates large pollutant diffusion coefficient into the biofilm. A large pollutant concentration would result in reaction limitation in the biofilm and also possible substrate inhibition. Therefore, an increase in the value leads to lower pollutant degradation and higher outlet concentration. However, a change in the value of this parameter for one compound has very little or no effect on the other.

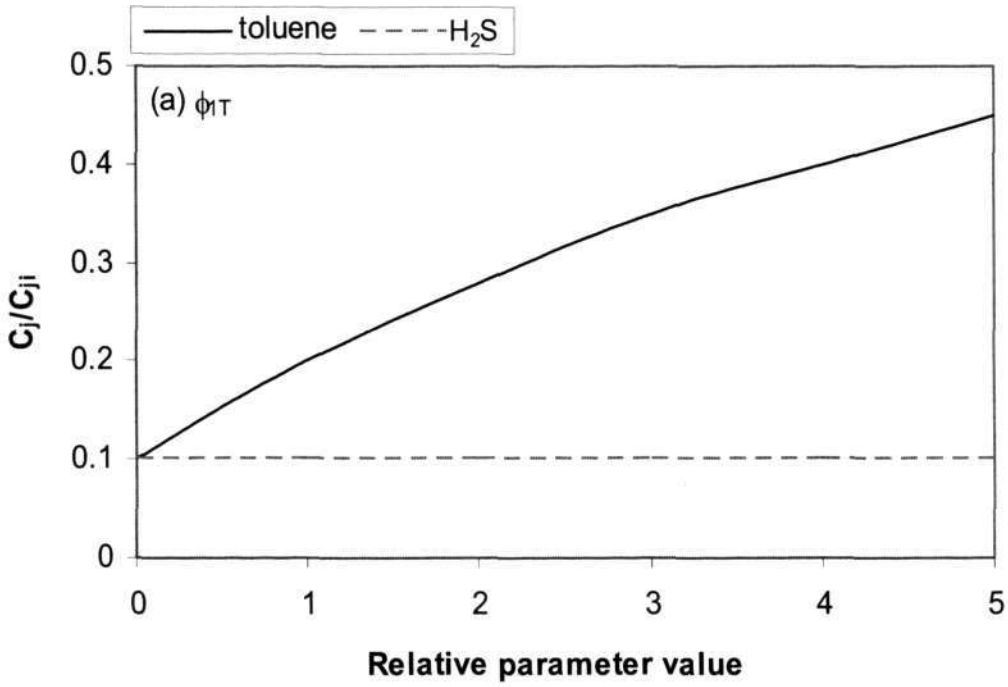

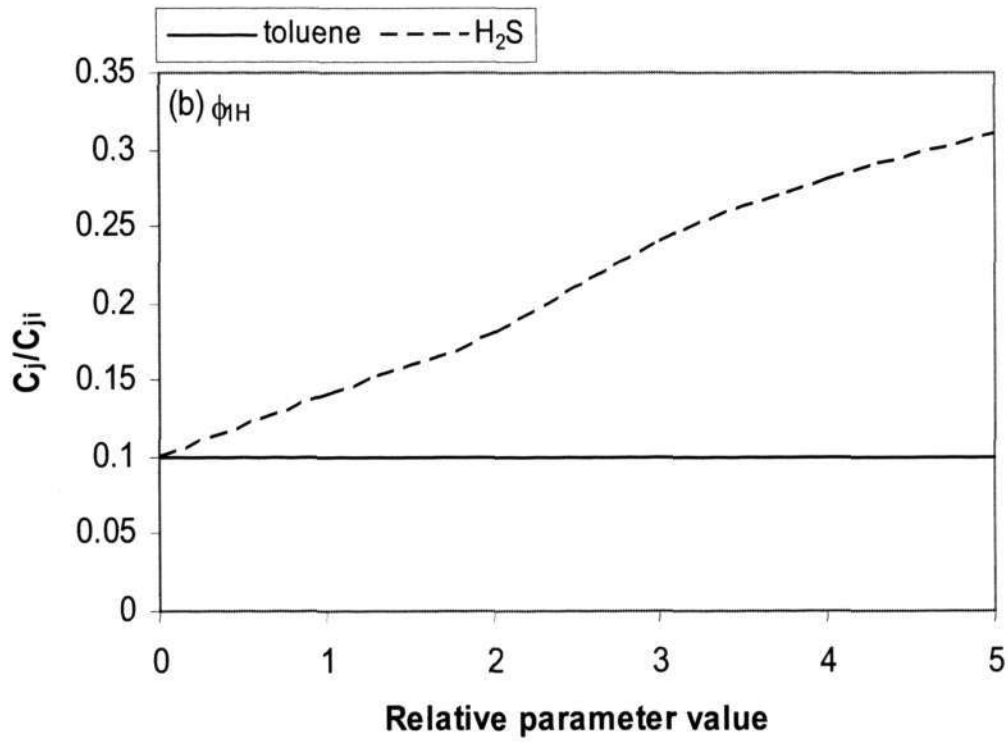

Figure 6.7 (a) & (b) Effect of ϕ_{1T} and ϕ_{1H} on the outlet concentrations

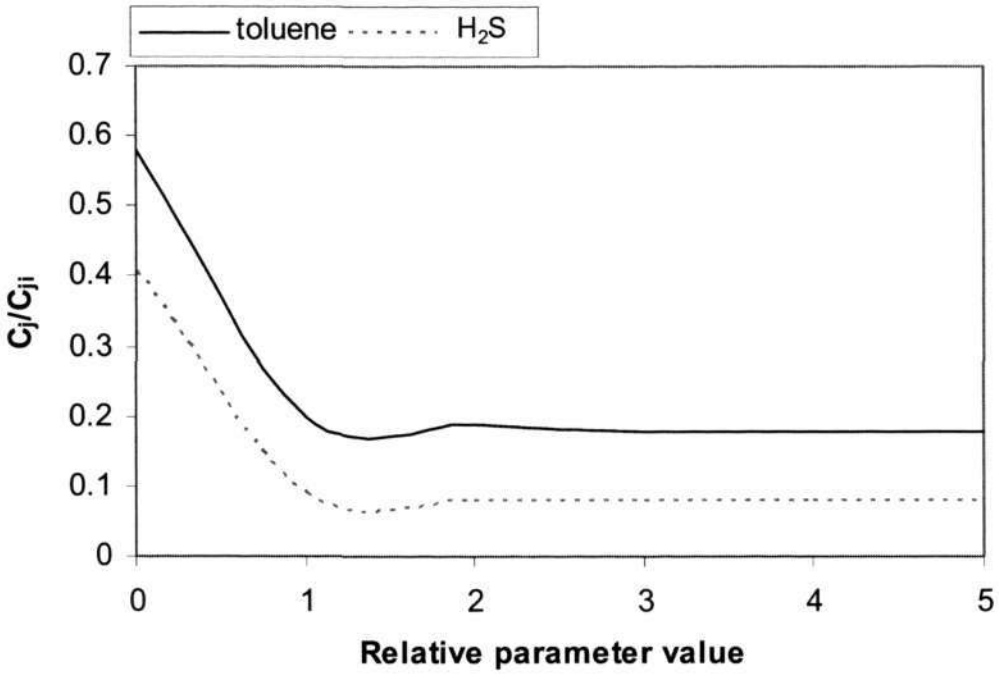

Figure 6.8 Effect of ϕ_2 on the outlet concentrations

Figure 6.8 shows the influence of the oxygen parameter ϕ_2 on the pollutant removal. As the relative parameter value is less than one, the outlet concentration of both H_2S and toluene decrease with the increase of ϕ_2, which is expected as greater diffusion of oxygen in the biofilm results in better substrate conversion. However, the performance is not sensitive for larger values.

As shown in Figures 6.9 (a) & (b), H_2S and toluene outlet concentration is very sensitive to η_{1T} and η_{1H}. C_j/C_{ji} of toluene decreases with the increasing value of η_{1T}. However, the variation of η_{1T} has no impact on H_2S removal. C_j/C_{ji} of H_2S remains constant. A large value of η_{1T} implies a large amount of toluene degradation in the biofilm and less convection in the gas phase. Similar effect can be seen due to changes in the value of η_{1H}.

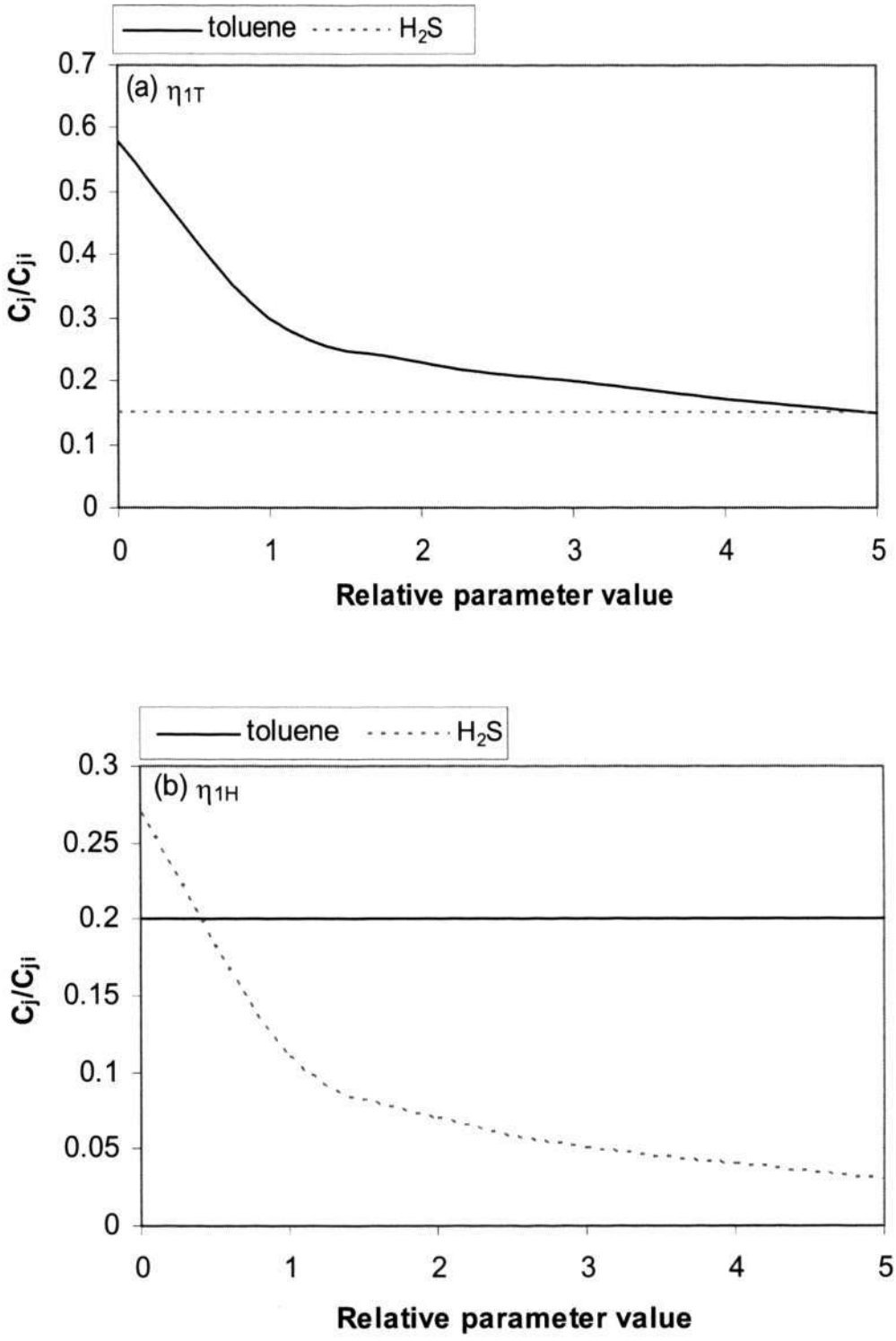

Figure 6.9 (a) & (b) Effect of η_{1T} and η_{1H} on the outlet concentrations

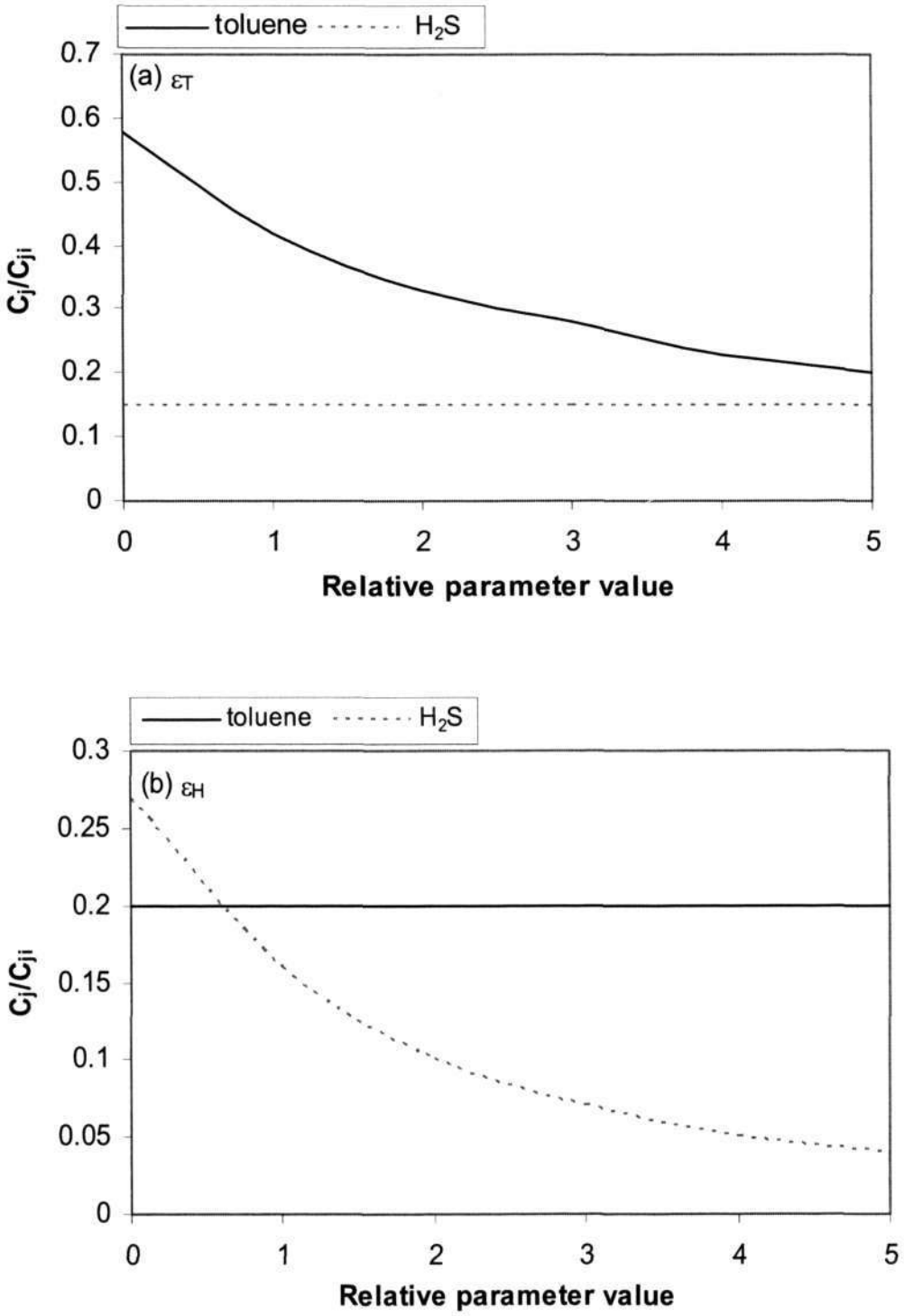

Figure 6.10 (a) & (b) Effect of ε_T and ε_H on the outlet concentrations

Figures 6.10 (a) & (b) show the effects of parameters ε_T and ε_H on the outlet concentrations. A large value of ε_T and ε_H indicate low Henry's law constant and so low volatility of pollutants, which will lead to greater diffusion in the biofilm, thus better removal efficiency. The tendency can be seen in the figures. As the value of ε_T increases, the outlet concentration of toluene decreases. However, there is no observable effect of ε_T on H_2S.

The effect of ε_O on the outlet concentrations was also investigated, as shown in Figure 6.11. As ε_O increases, the outlet concentration falls sharply. This only happened at low relative parameter value. When the value is larger than one, there is no effect at all. This behavior could be explained as ε_O is proportional to the oxygen inlet concentration which has important influence on the biodegradation. But when the amount of oxygen is adequate, there is no relationship found between the conversion and oxygen concentration.

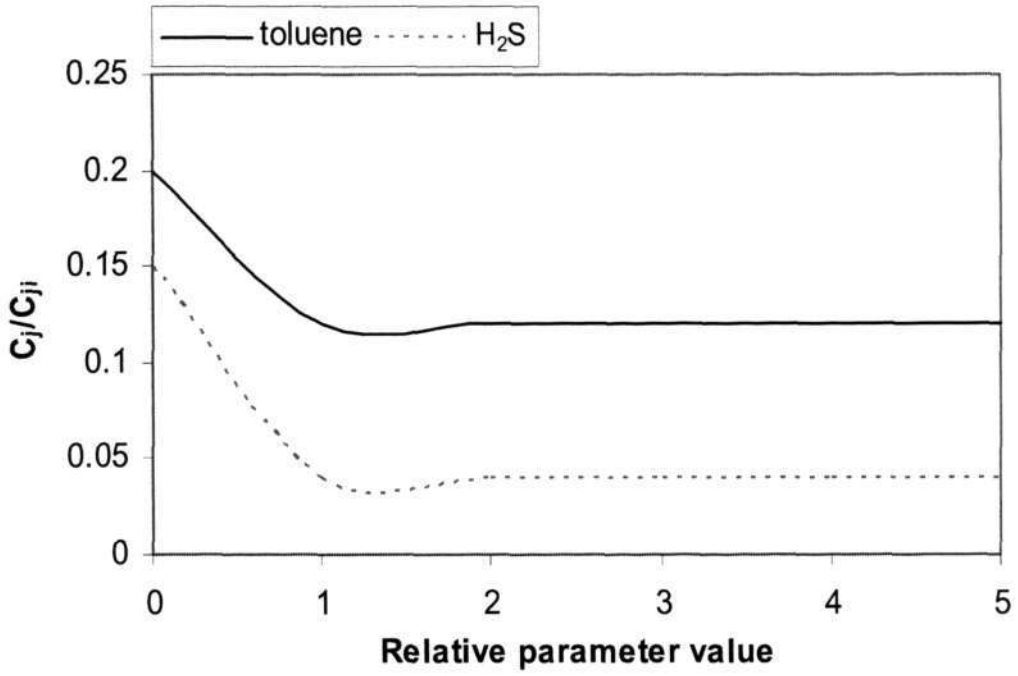

Figure 6.11 Effect of ε_O on the outlet concentrations

6.3.3.2 Gas phase parameters

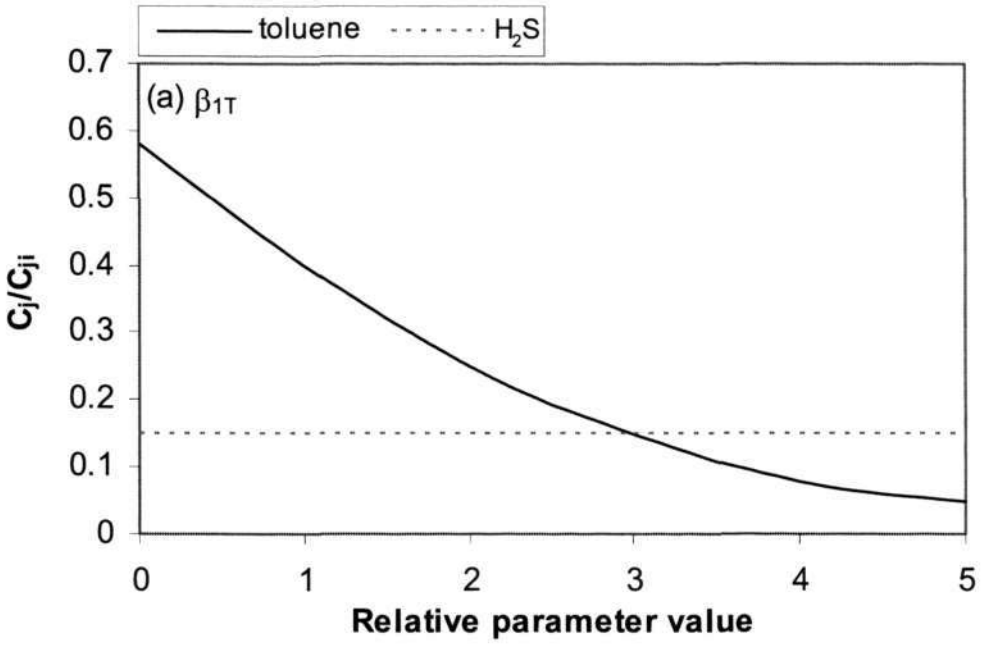

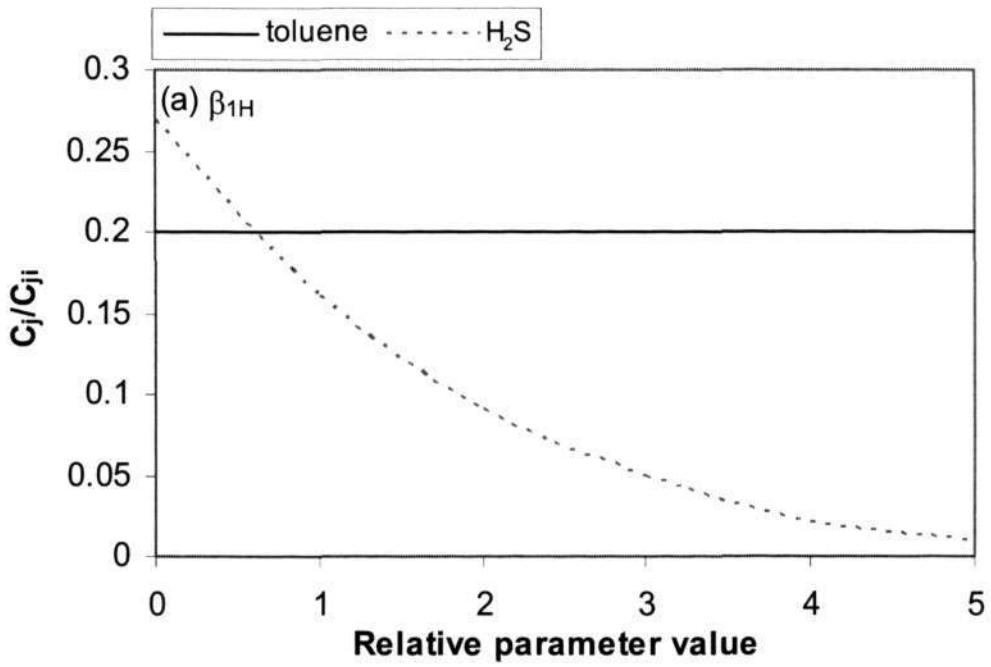

Figure 6.12 (a) & (b) Effect of β_{1T} and β_{1H} on the outlet concentrations

Figures 6.12 (a) & (b) show the effects of parameters β_{1T} and β_{1H} on the outlet concentrations. As can be seen, the model is very sensitive to these parameters. An increase in the value of β_{1T} and β_{1H} leads to a significant decrease in the outlet concentration of toluene and H_2S respectively. β_{1T} and β_{1H} can be interpreted as the ratios of substrate consumption in the biofilm to convection in the gas phase. Hence, high values of β_{1T} and β_{1H} cause greater substrate degradation in the biofilm and less partition in the gas phase.

The system performance is very sensitive to Peclet number, as shown in Figures 6.13 (a) & (b). A high value of Pe_T and Pe_H result in the increase of outlet concentration. These conditions prevail more at the inlet of the reactor where the concentration levels are higher. But a change in the value of Pe_T does not affect the concentration of H_2S at all and vice versa. A large value for Peclet number denotes plug flow and small value indicates well-mixed flow in the reactor. A drop in Peclet number expresses a transition from plug flow to mixed flow (the concentration profile becomes flatter), leading to better mass transfer and conversion.

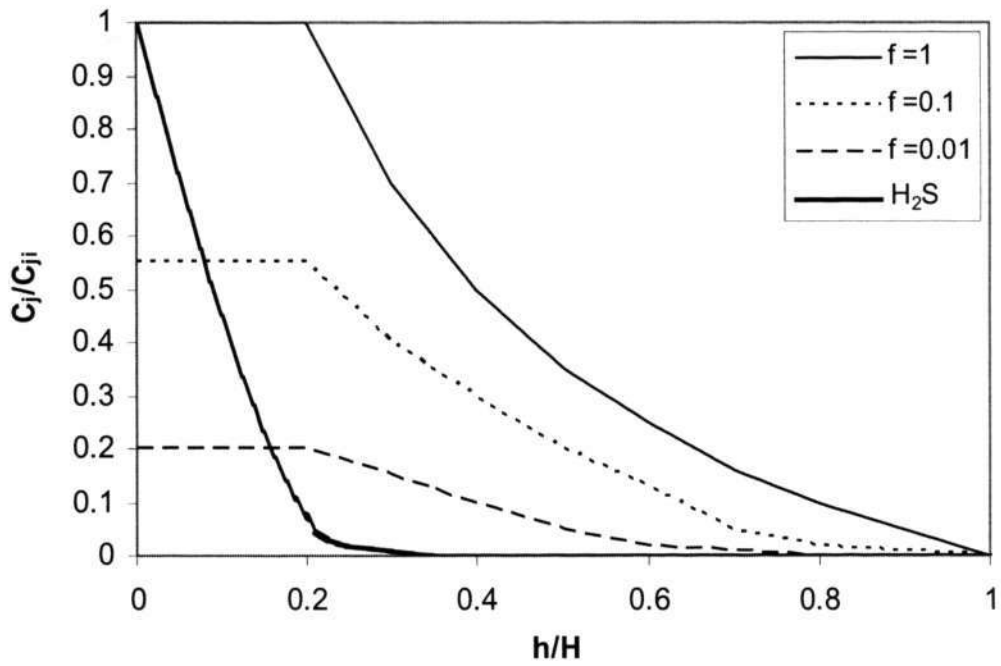

Figure 6.13 (a) Effect of Pe_T on the outlet concentrations of H_2S and toluene

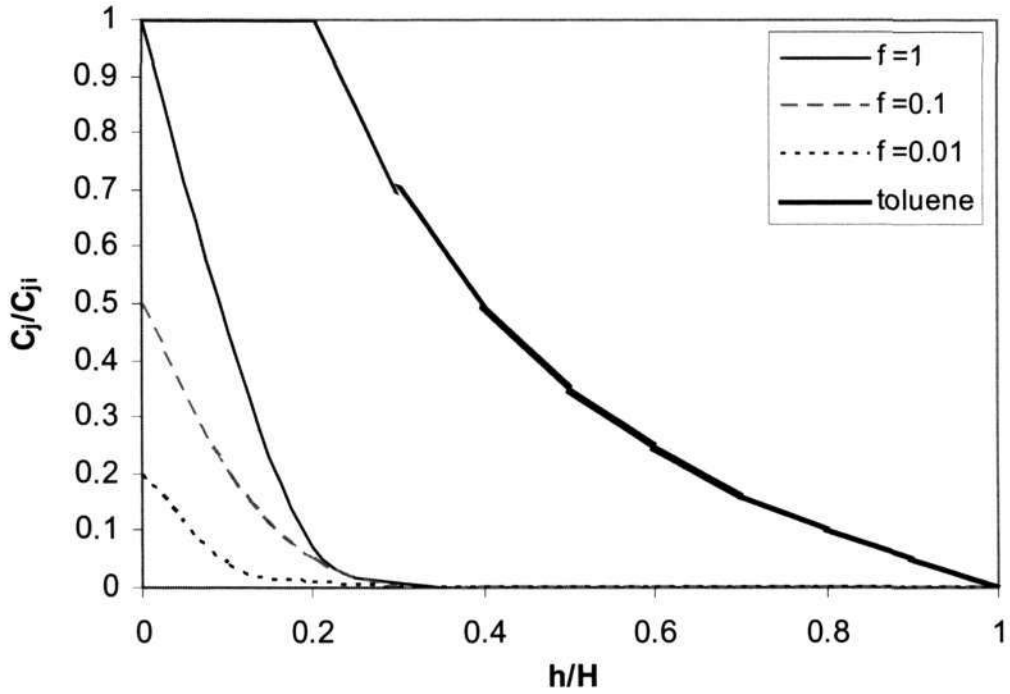

Figure 6.13 (b) Effect of Pe_H on the outlet concentrations of H_2S and toluene

CHAPTER SEVEN

CONCLUSIONS AND RECOMMENDATIONS

7.1 Conclusions

This research explores the use of BAC, a novel packing medium, for the biofiltration of gas mixture. Two major tasks were accomplished in this dissertation: (1) the feasibility of creating BAC; (2) the application of BAC as the biotrickling filter packing medium for gas mixture treatment. In order to perform the first task, the characteristics of virgin carbon were investigated to evaluate its feasibility of being a packing medium and the BAC production was experimentally studied. The application of BAC was first investigated in a bench reactor to compare the performance of BAC vs. GAC and the interaction of H_2S and toluene. The removal capacity of BAC for gas mixture was then tested in three horizontal biotrickling filters—a neutral pH single-stage biotrickling filter, a low pH single-stage biotrickling filter and a two-stage biotrickling filter. The performances of the biotrickling filters were evaluated and compared under various operating conditions. The degradation kinetics was also described using a complex mathematical model based on Shareefdeen's model. The detailed results obtained had been presented and discussed in the previous chapters. According to those results, the following conclusions were made.

7.1.1 Feasibility of BAC as a packing medium and BAC production

The scanning electron microscope (SEM) image indicated that the pitted and porous structure of carbon granules was easy for microbial attachment and provided a good water holding capacity. The Brumauer-Emmett-Teller (BET) test demonstrated that large external surface area (505.9m^2/g) gave enough space for microbial growth.

The breakthrough test confirmed the high adsorption capacity of activated carbon (28.8g-toluene/100g-carbon and 5.4g-H_2S/100g-carbon). Activated carbon also had uniform particle size and good resistance to crushing. A series of tests confirmed that activated carbon was a perfect packing medium and provided a benign environment for microorganisms.

The experiments of BAC development validated that microorganisms could be immobilized and grew well on carbon surface and so produced a novel packing medium—BAC. Both *Thiobacillus sp.* and *P. putida* could form a satisfactory biofilm for efficient removal of toluene and H_2S through the method of either offline immobilization or online immobilization.

7.1.2 Application of BAC in a bench biofilter

The performance of the bench scale biofilter trial illustrated that the BAC presented a better performance than the non-biological GAC as a gas pollutant adsorbent. The adsorption capacity of GAC for H_2S and toluene was exhausted eventually; however, the performance of BAC was kept at a high and stable level during the operation. Microorganisms immobilized on actived carbon were capable of extending the life span of carbon. Toluene gas at a low concentration of 0-200ppmV did not have an impact on H_2S biodegradation. 1ppmV of H_2S would not influence toluene removal but 5ppmV decreased toluene removal efficiency due to much acid accumulation. The SEM images showed that carbon surface was covered by many layers of biofilm. GAC particles allowed biological growth only on the surface and in pores sufficiently large for microbial cells. The inner portion of the particle, which was a substantial portion of its volume, was inaccessible. The mineral salt accumulation was also observed in the biofilm images of the H_2S test.

7.1.3 Application of BAC for gas mixture treatment in three horizontal biofilters

The removal capacity of BAC for gas mixture was studied in three biotrickling filters—a neutral pH single-stage biotrickling filter, a low pH single-stage biotrickling filter and a two-stage biotrickling filter. Biodegradation and adsorption interacted in the biotrickling filters and led to excellent performance for pollutants removal. In general, BAC was more efficient than GAC and also more successful than simple biological oxidation systems without a great adsorption surface. Biodegradation was the final transformation pathway of pollutants. Adsorption can be an important removal mechanism during transient or perturbation conditions. Therefore the adsorption and biodegradation successfully supplemented each other in the various schemes of air pollution control.

In the neutral pH single-stage biotrickling filter, H_2S and toluene removal achieved 90% at a GRT of 3.75s and 94% at a GRT of 15s, respectively. The biotrickling filter showed a behavior relating the toluene elimination capacity as a function of loading rate, i.e. the elimination capacity increased linearly with increasing inlet loading until it reached an equilibrium value—the maximum elimination capacity of the biotrickling filter. Toluene maximum elimination capacity was 280g/m^3·h. As for H_2S elimination capacity, it also increased linearly with the increasing inlet loading but did not reach an equilibrium value due to the low inlet loading tested in this study. The contaminant interaction was very important for mixture gases removal. The fluctuation of toluene concentration (0~200ppmV) had little influence on H_2S removal, while under H_2S shock loading, toluene removal decreased and then recovered to the original level as the biotrickling filter acclimated to the new environment.

In the low pH single-stage biotrickling filter, H_2S and toluene removal efficiency was 92% at a GRT of 3.75s and 86% at a GRT of 15s, respectively. Toluene maximum elimination capacity was 205g/m^3·h. When toluene inlet concentration

was increased to 200ppmV, no significant variation was found on H_2S removal efficiency. In this study, no negative or positive effect of increasing H_2S inlet concentration was observed on toluene removal efficiency because the acidophilic heterotrophs had acclimated to the extremely acidic environment.

The single-stage biotrickling filters set the whole reactor under the same operating conditions with the trickling water of a neutral pH or low pH. In contrast, the two-stage biotrickling filter divided the system into two stages. H_2S was removed in the first stage at a low pH, while toluene was degraded in the second stage at a neutral pH. H_2S and toluene removal efficiency in the two-stage biotrickling filter was 95% at a GRT of 3.75s and 96% at a GRT of 15s, respectively. Toluene maximum elimination capacity was 310g/m^3·h. When toluene inlet concentration was increased to 300ppmV, no significant variation was found on H_2S removal efficiency. When H_2S concentration entering the second stage was controlled below 3ppmV, the effect of H_2S on toluene removal was not found either. However, both toluene removal efficiency and pH of the second stage leachate decreased when H_2S concentration was further increased.

All three biotrickling filters could remove gas mixture of H_2S and toluene to a certain extent. However, their performances were very different. Comparing the three biotrickling filters, the two-stage biotrickling filter yielded the highest removal efficiency for H_2S and toluene at the same GRT and the highest toluene maximum elimination capacity. The results demonstrated that the two-stage biotrickling filter performance was better than the other two single-stage biotrickling filters. This was attributed to the presence of suitable degrading microorganisms growing in different environments. The two-stage bioreactor allowed for separate media beds that hosted different microorganisms. A simple cost comparison also indicated that the two-stage biotrickling filter was the most economical one (Appendix B).

7.1.4 Removal mechanisms of BAC

The BET test data of virgin carbon and H_2S/toluene exhausted carbon denoted that the adsorption mainly took place in the micropores. However, most micropores of BAC in all three horizontal biotrickling filters still remained empty at the end of operation even though the packing bed was inoculated with microorganisms after the carbon bed exhaustion, which proved that the spent activated carbon could be bioregenerated through the desorption of previously adsorbed substances on the activated carbon.

As for carbon adsorption, the two mechanisms were physical and chemical adsorption. With regard to BAC, the mechanisms were relatively different. Adsorption was integrated with biodegradation. Biodegradation and adsorption were independent processes only during the initial phase of the BAC process. With the biofilm accumulation and after achieving the adsorption equilibrium, the total removal mechanism is likely to be the synergetic effect of adsorption and microbial activity. Biodegradation was dominant in the steady state while adsorption provided good buffer for shock loading. Adsorption could be an important removal mechanism during the transient or perturbation conditions. The adsorbed pollutant could be eventually removed by bioregeneration. At the same time, adsorptive capacity enhanced the pollutant transfer rate in the biofilm.

Thermal analysis indicated that the main degradation product of H_2S was sulphuric acid, while most toluene was converted to carbon dioxide, water and biomass. The elemental changes were analyzed in detail. The carbon content and hydrogen content of BAC in the three biotrickling filters had little variance compared with those of virgin carbon, which was attributed to the benign mass balance of the BAC. The nitrogen content of BAC is higher when compared against that of virgin carbon (0%) due to chemical medium addition. The combustible sulfur content of BAC was higher than that of virgin carbon because of H_2S transformation, but much lower than that of H_2S exhausted carbon (7.05%).

In conclusion, BAC is an excellent packing material for its special physico-chemical properties, which can achieve high performance during both the start-up and the steady state period, and shorten the acclimation time. In summary, the BAC system, which combines adsorption and biodegradation, has the following advantages: faster development of the biomass; resistance to shock loading; stable and good performance; and allow for the treatment of hydrophobic biodegradable gases.

7.1.5 Mathematical model

Based on the literature review, Shareefdeen's model was found to be a complete and systematic model to describe the biofiltration process. The two-stage biotrickling filter was a complex system including two stages where different compounds were removed. A mathematical model was developed based on Shareefdeen's model. The reactor was divided into three phases under different conditions: (1) the first stage (Segment I), (2) H_2S and toluene interaction phase (Segment II), (3) only toluene removal (Segment III-V). By comparing the values predicted by the model with the experimental data obtained in this study, it is shown that the model offered a good approximation of the removal kinetics. A thorough sensitivity analysis of the model parameters was also performed. It was found that the process was very sensitive to some of these parameters. An increase in the value of ϕ_{1T} or Pe_T leads to lower pollutant degradation, while C_j/C_{ji} of toluene decreases with the increasing value of η_{1T}, ε_T or β_{1T}. However, the variation of these parameters has no impact on H_2S removal. Similar effect can be seen due to changes in the value of ϕ_{1H}, Pe_H, η_{1H}, ε_H or β_{1H}. As the relative parameter value of ϕ_2 or ε_O is less than one, the outlet concentration of both H_2S and toluene decrease with the increase of ϕ_2 or ε_O.

7.2 Recommendations for future research

BAC presents a number of exciting possibilities for future study. Although BAC biotrickling filters can achieve excellent performances and last for many years, the cost of activated carbon is still a little higher than those of other materials. It may be useful to study the incorporation of carbon with other packing materials such as polyethylene pall rings and polyurethane foam. The cost will be reduced; at the same time, the removal efficiency can still be fairly high. The volume ratio of different packing materials and some operating parameters such as liquid trickling rate are required to be tested.

So far only laboratory experiments of this novel packing medium have been carried out. In the real sewage gas, the air composition and shock loading conditions are different and so the pressure drop, liquid trickling style and other operation parameters may be different. Therefore, full-scale, large BAC biotrickling filters are still required to be investigated to provide the real operationg parameters. The findings from this laboratory study may have provided some useful information for future full-scale investigation.

The current study was limited to the removal of H_2S and toluene mixture gas at different values of pH. The theory of separating microorganisms under different environments also can be applied to other mixture conditions such as hydrophilic and hydrophobic pollutants. This theory can be extended to multi-stage systems as well, where every stage can have its own packing media, microorganisms, operation conditions such as moisture content, pH. Research in this area will certainly be of great interest to wastewater plant managers.

The improvement of the low pH single-stage biotrickling filter is another interesting topic. Microbial studies need to be conducted to enhance microorganisms' activity or to develop new species for VOCs degradation at a low pH. The new species or their combination can be investigated through microbiological methods such as denaturing gradient gel electrophoresis (DGGE), PCR and DNA sequencing. VOC

degradation pathway and effectiveness are also required to be studied. If the effective species or their combination can be found, the fast removal of VOCs and H_2S can be realized simultaneously at extremely low pH. If a microbial breakthrough can be discovered, the low pH single-stage biotrickling filter will be a promising success for practical use.

To reduce the complexity of the mathematical model, many assumptions have been made: substrate and oxygen diffusion/reaction in the biofilm can be considered in a single direction only; the airstream passes through the reactor in plug flow; and etc. In the real operation of the reactor, they may not be true. In future, these building blocks of mathematical model are required to be eliminated. This may be a worthwhile area for future research.

REFERENCES

Abumaizar R. J., Walter K., Edward H. S. (1998) "Biofiltration of BETX Contaminated Air Streams Using Compost-activated Carbon Filter Media". J. Hazardous Material, Vol. 60, pp.111-126.

Acuña M. E., Villanueva C., Cardenas B., Christen P., Revah S. (2002) "The Effect of Nutrient Concentration on Biofilm Formation on Peat and Gas Phase Toluene Biodegradation under Biofiltration Conditions", Process Biochemistry, Vol. 38, pp. 7-13.

Aizpuru A., Malhautier L., Roux J. C., Fanlo J. L. (2003) "Biofiltration of a Mixture of Volatile Organic Compounds on Granular Activated Carbon", Biotechnology and Bioengineering, Vol. 83, No.4, pp. 479-488.

Alexander S. S., Larisa Y. K.and Konstantin G. I. (2001) "The BAC-Process for Treatment of Waste Water Containing Non-ionogenic Synthetic Surfactants", Wat. Res., Vol. 35, No. 13, pp. 3265–3271.

Altaf H. W., Richard M. R. B., and Anthony K. L. (1998a) "Degradation Kinetics of Biofilter Media Treating Reduced Sulfur Odors and VOCs", Journal of the Air & Waste Management Association, Vol. 48, pp. 1183-1190.

Altaf H. W., Richard M. R. B. and Anthony K. L. (1998b) "Effects of Periods of Starvation and Fluctuating Hydrogen Sulfide Concentration on Biofilter Dynamics and Performance", Journal of Hazardous Materials, Vol. 60, No. 3, pp. 287-303.

Anders B. J. and Colin W. (1995) "Treatment of H_2S-containing Gases: a Review of Microbiological Alternatives", Enzyme Microb. Technol., Vol. 17, January, pp. 2-10.

Andrea R. H. P. (2004) "Biological Activated Carbon: the Relative Role of Metabolism and Cometabolism in Extending Service Life and Improving Process Performance", Thesis for Doctor of Philosophy, the University Of Texas at Austin

Andrey B., Foad A., Teresa J. B. (2001) "pH of Activated Carbon Surface as an Indication of its Suitability for H_2S Removal from Moist Air Streams", Carbon, Vol. 39, pp.1897–1905.

Arcangeli J. P. and Arvin E. (1992) "Toluene Biodegradation and Biofilm Growth in an Aerobic Fixed-film Reactor", Appl. Microbiol. Biotechnol, Vol. 37, pp. 510-517.

Arja R., Juhani R., and Petti J. M. (2001) "Oxidation of Gas Mixtures Containing Dimethyl Sulfide, Hydrogen Sulfide, and Methanethiol Using a Two-stage Biotrickling Filter", Journal of the Air & Waste Management Association, Vol. 51, No. 1, pp. 11-16.

ASCE (American Society of Civil Engineering) (1989) Manuals and Reports on Engineering Practice No. 69, Sulfide in Wastewater Collection and Treatment Systems, New York, American Society of Civil Engineers, pp. 4-15.

Barona A., Elias A., Amurrio A., Cano I., Arias R. (2005) "Hydrogen Sulphide Adsorption on a Waste Material Used in Bioreactors", Biochemical Engineering Journal, Vol. 24, pp. 79–86.

Bowker R.P.G., Smith J. M. and Webster N. A. (1989) Odour and Corrosion Control in Sanitary Sewerage Systems and Treatment Plants, Hemisphere Publishing Corporation, pp. 3-5, 29.

Brock T. D. and Madigan M. T. (1991) Biology of Microorganisms. Prentice-Hall International Editions, 6th edition.

Card T. R. (1998) Fundamentals: Chemistry and Characteristics of Odours and VOCs. In Odour and VOC Control Handbook, Chapter 2, ed by H.J. Rafson, The McGraw-Hill Companies, Inc., USA.

Chang M. K., Voice T. C. and Criddle C. S. (1993) "Kinetics of Competitive Inhibition and Cometabolism in the Biogdegradation of Benzene, Toluene, and *p*-Xylene by Two *Pseudomonas* isolates". Biotechnol. Bioeng. Vol. 41, pp.1057-1065.

Chang A. N., (2003) "Biofiltration of Petroleum Hydrocarbon Wapors and Co-Treatment of Volatile Organic Compounds in Low-pH Sulfide Biofilters". Thesis for Doctor of Philosophy, University of Southeren California.

Cho K., Ryu H. W., and Lee N. Y. (2000) "Biological Deodorization of Hydrogen Sulfide Using Porous Lava as a Carrier of *Thiobacillus thiooxidans*". Journal of Bioscience and Bioengineering. Vol. 1, pp. 25-31.

Chung Y. C., Huang C., Pan J. R. and Tseng C. P. (1998) "Comparison of Autotrophic and Mixotrophic Biofilters for H_2S Removal", Journal of Environmental Engineering, April, pp. 362-367.

Chung Y. C., Lin Y. Y. and Tseng C. P. (2005) "Removal of High Concentration of NH_3 and Coexistent H_2S by Biological Activated Carbon (BAC) Biotrickling Filter", Bioresource Technology, Vol. 96, No. 16, pp. 1812-1820.

Cosma J., Balaguer M., Poch M. and Rigola M. (1999) "Pilot Plant Evaluation for Hydrogen Sulfide Biological Treatment: Determination of Optimal Conditions Linking Experimental and Mathematical Modeling", Environ. Technol., Vol. 20, pp. 53.

Cox H. H. J. and Deshusses M. A. (1999) "Biomass Control in Waste Air Biotrickling Filters by Protozoan Predation" Biotechnology and Bioengineering, Vol. 62, No.2, pp. 216-224.

Cox H. H. J and Deshusses M. A. (2000) "Biotrickling Filters for Air Pollution Control", In G. Bitton (Editor-in-Chief), The Encyclopedia of Environmental Microbiology. J. Wiley & Sons.

Cox H. H. J. and Deshusses M. A. (2001) "Co-treatment of H_2S and Toluene in a Biotrickling Filter", Chem. Eng. J., Vol. 3901, pp. 1-10.

Cox H. H. J., Deshusses M. A., Converse B. M., Schroeder E. D., and Iranpour R. (2002) "Odor and Volatile Organic Compound Treatment by Biotrickling Filters: Pilot-scale Studies at Hyperion Treatment Plant", Water Enviro. Res., Vol. 74, No.6, pp.557-563.

Cox H. H. J., Nguyen T. T. and Deshusses M. A. (1998) "Elimination of Toluene Vapours in Biotrickling Filters: Performance and Carbon Balances", Proc. Annual Meeting and Exhibition of the Air and Waste Management Association.

de Nevers N. (1995) Air Pollution Control Engineering, Chapter 10, *McGraw*-Hill International Editions, Civil Engineering Series, McGraw-Hill, Inc.

Deshusses M. A., Hamer G., Dunn I. J. (1995) "Behaviour of Biofilters for Waste Air Biotreatment. 1. Dynamic Model Development", Environ. Sci. Technol, Vol. 29, pp.1048-1058.

Derek E. C. and Joseph S. D. (1999) "Evaluation of a Two-stage Biofilter for Treatment of POTW Waste Air", Environmental Progress, Vol. 18, No.3, pp. 212-221.

Devinny J. S., Deshusses M. A. and Webster T. S. (1999) Biofiltration for Air Pollution Control. Lewis Publishers

Dolfing J., Xan W. A. J. and Janssen D. B. (1993) "Microbiological Aspects of the Removal of Chlorinated Hydrocarbons from Air". Biodegradation. Vol. 4, pp. 261-282.

Duan H. Q., Koe L. C. C. & Yan R. (2005a) "Treatment of H_2S using a Horizontal Biotrickling Filter Based on Biological Activated Carbon: Reactor Setup and Performance Evaluation". Appl. Microbiol. Biotechnol., Vol. 67, pp.143-149.

Duan H. Q., Yan R. & Koe L. C. C. (2005b) "Investigation on the Mechanism of H_2S Removal by Biological Activated Carbon in a Horizontal Biotrickling Filter". Appl. Microbiol. Biotechnol., Vol. 69, No. 3, pp. 350-357.

Ehrhardt H. M. and Rehm H. J. (1985) "Phenol Degradation by Microorganisms Adsorbed on Activated Carbon", Appl. Microbiol Biotechol., Vol. 21, pp. 32-36.

Eldon R. R., Murthy D. V. S. and Swaminathan T. (2005) "Performance Evaluation of a Compost Biofilter Treating Toluene Vapours", Process Biochemistry, Vol. 40, No. 8, pp. 2771-2779.

Ergas S. J., Schroeder E. D., Chang D. P. Y., Robert L. M. (1995) "Control of Volatile Organic Compound Emissions Using a Compost biofilter", Water Environ. Res., Vol. 67, No. 5, pp. 816-821.

Foad A., Andrey B., and Teresa J. B. (2000) "Analysis of the Relationship between H_2S Removal Capacity and Surface Properties of Unimpregnated Activated Carbons", Environmental Science & Technology, Vol. 34, No. 4, pp. 686-692.

Forst L. and Conroy L. M. (1998) Health Effects and Exposure Assessments of VOCs. In Odour and VOC Control Handbook. Chapter 3, ed by H. J. Rafson, The McGraw-Hill Companies, Inc., New York.

Frank R. K. and Peter A. W. (1997) "Activated Carbon Sequencing Batch Biofilm Reactor to Treat Industrial Wastewater", Wat. Sci. Tech., Vol. 35, No. 1, pp. 169-176.

Gauden P. A., Szmechtig-Gauden E., Rychlicki G., Duber S., Garbacz J. K., Buczkowski R. (2005) "Changes of the Porous Structure of Activated Carbons Applied in a Filter Bed Pilot Operation", Journal of Colloid and Interface Science, In Press, Available online 28 September 2005.

Gordon M. (1996) Use of Adsorbents for the Removal of Pollutants from Wastewaters, Boca Raton, CRC Press.

Groenestijn J. W. and Hesselink P. G. M (1993) "Biotechniques for Air Pollution Control", Biodegradation, Vol. 4, Kluwer Academic Publishers, Netherlands, pp. 283-301.

Hanson J. R. (2001) "Biodegradation of Toluene and Methyl Tert-butyl ether (MTBE) by Pure Bacterial Cultures", Thesis for Doctor of Philosophy, University of California, Davis.

Hebi L. (2002) "Modeling and Optimization of Biofiltration for Odor Control", Thesis for Doctor of Philosophy, Michigan Technological University

Hebi L., James R. M., John C. C., and Keith A. A. (2003) "Field Measurements and Modeling of Two-Stage Biofilter that Treats Odorous Sulfur Air Emissions", Journal of Environmental Engineering, Volume 129, No.8, pp. 684-692.

Henderson L. M. H. (2000) "Propane-induced Biofiltration of TCE-contaminated Air", Thesis for Master of Engineering, Mississippi State University.

Hodge D. S. and Devinny J. S. (1995) "Modelling Removal of Air Contaminants by Biofiltration", J. Environ. Engin., ASCE, Vol. 121, No. 1, pp. 21-32.

Holden P. A., Hunt J. R. and Firestone M. K. (1997) "Toluene Diffusion and Reaction in Unsaturated *Pseudomonas putida* Biofilms", Biotechnology and Bioengineering, Vol. 56, No. 6, pp. 656-670.

Hsieh C. K. S. and Stenstrom M. K. (1993) "Estimating Emissions of 20 VOCs I. Surface Aeration", J. Environ. Eng, Vol. 119, pp. 1077.

Hutchinson D. H. and Robinson C. W. (1988) "Kinetics of the Simultaneous Batch Degradation of *p*-cresol and Phenol by *Pseudomonas putida*", Appl. Microbiol. Biotechnol., Vol. 29, pp. 599-604.

Islander R. L., Devinny J. S., Mansfield F., Postyn A., and Shih H. (1990) "Microbial Ecology of Crown Corrosion in Sewers", J. Environ. Eng., Vol. 117. pp. 751-770.

Ivana I. T., Bozo D., Zagorka T. and Elvira K. (1998) "Reuse of Biologically Regenerated Activated Carbon for Phenol Removal", Water Research, Vol. 32, No. 4, pp. 1085-1094.

Kennes C. and Veiga M. C. (2001) Bioreactors for Waste Gas Treatment. Kluwer Academic Publishers.

Kim J. O. and Lee W. B., (2002) "Biodegradation of Gaseous Benzene with Microbial Consortium in a Biofilter". Environmental Technology, Vol. 23, pp. 437-444.

Kirchner K., Schlachter U. and Rehm H. J. (1989) "Biological Purification of Exhaust Air Using Fixed Bacterial Monocultures", Appl. Microbiol. Biotech., Vol. 31, pp. 629-632.

Koe L. C. C., Wu L., Loo Y. Y. and Wu Y. (2001) "Field Trial Testing of a Biotrickling Filter for Sewage Odor Control". Proceedings of the air & waste

management association's 94th conference and exhibition, Orlando, Florida, Abstract No. 902 Session No. AE-2a-C2.

Koe L. C. C., Wu L., Loo Y. Y., Koh Y. M. and Wu Y. (2002a) "Pilot-scale Experiences in Convering a Chemical Scrubber to a Biotrickling Filter for the Treatment of Sewage Air", the 2nd International Meeting on Odour Management and Treatment, ODOUR 2, Cranfield University, Bedford, UK.

Koe L. C. C., Wu L., Loo Y. Y., Koh Y. M. and Wu Y. (2002b) "A Successful Conversion of a Chemical Scrubber to a Biotrickling Filter—Some Experiences", Enviro 2002 Convention & Exhibition, Melbourne, Australia.

Koe L. C. C., Wu L., Loo Y. Y., Koh Y. M. and Wu Y. (2002c) "A Fixed-film Biotrickling Filter for Treatment of Odorous Air", International Conference on Wastewater Management & Technologies for Highly Urbanized Coastal Cities, Hong Kong.

Koe L. C. C and Yang, F.H. (1999) "Development of a Fixed-film Biocrubber for Hydrogen Sulphide Removal", Water Environment Federation Conference and Expositions, WEFTEC'1999.

Koe L. C. C and Yang F. H. (2000) "A Bioscrubber for Hydrogen Sulphide Removal", Water Science and Technology, Vol. 41, No. 6, pp. 141-145.

Li G. W., Hu H. Y., Hao J. M. and Zhang H. Q. (2002) "Biological Treatment Characteristics of Benzene and Toluene in a Biofilter Packed with Cylindrical Activated Carbon", Water Science and Technology, Vol. 46, No. 11, pp. 51-56.

Liu P. K. T., Sabol G., Sabol H. K. and Barkley N. (1994) "Engineered Biofilter for Removing Organic Contaminants in Air", Journal of the Air & Waste Management Association, Vol. 44, No. 3, pp. 11-16.

Maier R. M., Pepper I. L. and Gerba C. P. (2000) Environmental Microbiology. Academic Press, San Diego.

Marie C. D., Louise B., Nathalie B., Sébastien R., Sophie B., Ryszard B., Jack L. K. and Michèle H. (2002) "Biofiltration of Air Contaminated with Toluene on a Compost-based Bed", Advances in Environmental Research, Vol. 6, No. 3, pp. 239-254.

Mason C. A., Ward G., Abu-Salah K. and Dosoretz C. G. (2000) "Biodegradation of BTEX by Bacteria on Powdered Activated Carbon", Bioprocess Engineering, Vol. 23, pp331-336.

Medina V. F., Devinny J. S. and Ramaratnam M. (1995) "Biofiltration of Toluene Vapors in a Carbon Medium Biofilter", Third International In Situ and On-site Bioreclamatio Symposium, San Diego.

Michal K., Mietek J. and Kishor P. G. (1997) "Nitrogen Adsorption Studies of Novel Synthetic Active Carbons", Journal of Colloid and Interface Science, Vol. 192, No. 1, pp. 250-256.

Morales M, Auria R, Perez F, Revah S. (1998) "Start-up and Ammonia Additons to Biofiter for Removal Toluene", Biotechnol. Bioeng., Vol. 60, pp. 483-491.

Nestor T., Natalia M., Fabiana M., Javier P., Carina P. and Tomás C. (2004) "Phenol Adsorption onto Powdered and Granular Activated Carbon Prepared from Eucalyptus Wood", Journal of Colloid and Interface Science, Vol. 279, No. 2, pp. 357-363.

Oh Y. S., Zarook S. M., Baltzis B. C. and Bartha R. (1994) "Interactions between Benzene, Toluene, and p-xylene (BTX) during their Biodegradation", Biotechnol. Bioeng., Vol. 44, pp. 533.

Ottengraf S. P. P. (1986) "Exhaust Gas Purification", Biotechnology, ed by Rehm, H.J. and Reed, G., Vol. 8, Chapter 12, pp. 426-452, VCH Verlagsgesellschaft: Weinheim, Germany.

Ottengraf S. P. P. and Diks R. M. M. (1992) "Process Technology of Biotechniques", In Biotechniques for Air Pollution Abatement and Odour Control Policies. Elsevier Science Publishers B.V., pp. 17-31.

Padival N. A.; Weiss J. S. and Arnold R. G. (1995) "Control of *Thiobacillus* by means of Microbial Competition: Implications for Corrosion of Concrete Sewers", Water Environment Research, Vol. 67, No. 2, pp. 201-205.

Patricio O., Fernando A., Christian C. and Germán E. A. (2003) "Biofiltration of High Concentration of Hydrogen Sulphide Using *Thiobacillus thioparus*", Process Biochemistry, Vol. 39, No. 2,pp. 165-170.

Pedersen A. R. and Arvin E. (1995) "Removal of Toluene in Waste Gases Using a Biological Trickling Filter", Biodegradation, Vol. 6, pp. 109-118.

Perry R. H. and Green D. W. (1999) Perry's Chemical Engineers' Handbook, McGraw-Hill, New York.

Raymond D. S., Dwayne C. S., Gary S. S., and Gary S. (1998) "Biodegradation of Aromatic Hydrocarbons in an Extremely Acidic Environment", Applied and Environmental Microbiology, Vol. 64, No. 11, pp. 4180-4184.

Reardon K. F.; Mosteller D. C. and Bull R. J. D. (2000) "Biodegradation Kinetics of Benzene, Toluene, and Phenol as Single and Mixed Substrates for *Pseudomonas putida* F1", Biotechnology and Bioengineering, Vol. 69, No.4, pp. 385-400.

Rice R. G and Robson C. M. (1982) Biological Activated Carbon Enhanced Aerobic Biological Activity in GAC System, Ann Arbor Science.

Scholz M. and Martin R. J. (1997) "Ecological Equilibrium on Biological Activated Carbon", Water Research, Vol.31, No. 12, pp. 2959-2968.

Shareefdeen Z. M., Baltzis B. C., Oh Y. S., Bartha R. (1993) "Biofiltration of Methanol Vapor", Biotechnol. Bioeng., Vol. 41, pp. 512-524.

Shareefdeen Z. M. (1994) "Engineering Analysis of a Packed-bed Biofilter for Removal of Volatile Organic Compound (VOC) Emissions", Thesis for Doctor of Philosophy, New Jersey Institute of Technology

Speitel G. E. and DiGiano F. A. (1987) "The Bioregeneration of GAC Used to Treat Micropollutants", J. AWWA, Vol. 1.

Smet E., P. L. and Langenhove H. V. (1998) "Treatment of Waste Gases Contaminated with Odorous Sulfur Compounds", Crit. Rev. Environ. Sci. Technol., Vol. 2. pp. 89-117.

Smith F. L., Sorial G. A., Suidan M.T., Breen A. W. and Biswas P. (1996) "Development of Two Biomass Control Strategies for Extended, Stable Operation of Highly Efficient Biofilters with High Toluene Loadings", Environ. Sci. Technol., Vol. 30, No.5, pp. 1744-1751.

Song J., Kerry A. K., and Paul J. (2003) "Influence of Nitrogen Supply and Substrate Interactions on the Removal of Paint VOC Mixtures in a Hybrid Bioreactor", Environmental Progress, Vol. 22, No. 2, pp. 137-144.

Sorial G. A., Smith F. L., Pandit A., Suidan M. T., Biswas P., Brenner R. C. (1995) "Performance of Trickle Bed Biofilters under High Toluene Loading" Proceedings, 88th Annual Meeting & Exhibition, Air & Waste Management Association, San Antonio, TX, June 18-23.

Swanson W. J. and Loehr R. C. (1997) "Biofiltration: Fundamentals, Design and Operations Principles, and Applications", Journal of Environmental Engineering, pp. 538-546.

Tang H. M. and Hwang S. J. (1997) "Transient Behavior of the Biofilters for Toluene Removal", Journal of the Air & Waste Management Association, Vol. 47, No. 11, pp. 1142-1151.

Thomas C. V., Pak D., Zhao X., Hickey R. F. (1992) "Biological Activated Carbon in Fluidized Bed Reactors for the Treatment of Groundwater Contaminated with Volatile Aromatic Hydrocarbons", Water Res., Vol. 26, No.10, pp. 1389–1401.

Tong D. J. (2005) "Use of Activated Carbon as Biofiltration Packing Material", Thesis for Master of Engineering, Nanyang Technological University.

Villaverde S., Mirpuri R. G., Lewandowski Z. and Jones W.L. (1997) "Physiological and Chemical Gradients in a *Pseudomonas putida* 54G Biofilm Degrading Toluene in a Flat Plate Vapour Phase Bioreactor", Biotechnology and Bioengineering, Vol. 56, No.4, pp. 361-371.

Walker G. M. and Weatherley L. R. (1999) "Biological Activated Carbon Treatment of Industrial Wastewater in Stirred Tank Reactors", Chemical Engineering Journal, Vol. 75, No. 3, pp. 201-206.

Wan N., Joon-Seok P., Jean S. V. G. (2004) "Effect of Gas Velocity and Influent Concentration on Biofiltration of Gasoline Off-Gas from Soil Vapor Extraction", Chemosphere, Vol. 57, pp. 721–730.

Weber F. J. and Hartmans S. (1995) "Use of Activated Carbon as a Buffer in Biofiltration of Waste Gases with Fluctuating Concentrations of Toluene", Appl. Microbiol Biotechnol, Vol. 43, pp. 365-369.

Webster S. T., Joseph S. D., Edward M. T. and Shabbir S. B. (1996) "Biofiltration of Odors, Toxics and Volatile Organic Compounds from Publicly Owned Treatment Works", Environmental Progress, Vol. 15, No. 3, pp. 141-147.

Webster S. T., Joseph S. D., Edward M. T., Shabbir S. B. (1997) "Microbial Ecosystems in Compost and Granular Activated Carbon Biofilters", Biotechnol Bioeng., Vol. 53, pp. 296–303.

Wu L. (2000) "Using Biotrickling Filter to Treat Odorous Off-Gas from Municipal Wastewater Treatment Facilities", Thesis for Master of Engineering, National University of Singapore.

Wu L., Koe L. C. C., Loo Y. Y. (2001). "A Pilot Study of Biotrickling Filter for the Treatment of Odours Sewage Air". Journal of Water Science & Technology, Vol 44, No.9, pp 295–299.

Wu Y. (2000) "Treatment of Toluene in Waste Gases Using a Biotrickling Filter", Thesis for Master of Engineering, National University of Singapore.

Yan R., Liang D. T., Leslie T. and Tay J. H. (2002) "Kinetics and Mechanisms of H_2S Adsorption by Alkaline Activated Carbon", Environmental Science & Technology, Vol. 36, No. 20, pp. 65-74.

Yan R., Ng Y. L., Chen X. G., Geng A. L. (2003) "Batch Experiment on H_2S degradation by Bacteria immobilized on Activated Carbons", 2nd IWA International Workshop & Conference on Odour & VOCs, Singapore.

Yan R., Chin T., Ng Y. L., Duan H. Q., Liang D. T. and Tay J. H. (2004) "Influence of Surface Properties on the Mechanism of H_2S Removal by Alkaline Activated Carbons", Environmental Science & Technology, Vol. 38, No. 1, pp.316-323.

Yang F. H. (1999) "Development of Fixed-film Bioscrubber for H_2S Control", Thesis for Master of Engineering, National University of Singapore.

Yang T. J., Takahiro K. and Eiichi M. (1989) "Removal of Dimethyl Sulfide, Methyl Mercaptan and Hydrogen Sulfide by Immobilized *Thiobacillus thioparus* TK-m". J. Ferm. Bioeng. Vol. 67, pp. 280-285.

Yang Y. H. and Allen E. R., (1994a) "Biofiltration Control of Hydrogen Sulfide 1. Design and Operational Parameters". J. Air & Waste Manage. Assoc., Vol. 44, pp. 863-868.

Yang Y. H. and Allen E. R., (1994b) "Biofiltration Control of Hydrogen Sulfide 2. Kinetics, Biofilter Performance and Maintanance". J. Air & Waste Manage. Assoc., Vol. 44, pp. 1315-1321.

Yap P. A. (1999) "Use of Spent Carbon as a Biofiter Medium", Thesis for Master of Engineering, National University of Singapore.

Zarook S. M. and Baltzis, B. C. (1994a) "Biological Removal of Hydrophobic Solvent Vapors from Airstreams". In Advances in Bioprocess Engineering, eds E. Galindo and O. T. Ramirez, pp. 397-404. Kluwer Academic Publishers, Dordrecht, The Netherlands.

Zarook S. M. and Baltzis B. C. (1994b) "Biofiltration of Toluene Vapor under Steady-state and Transient Conditions: Theory and Experimental Results". Chem. Eng. Sci, Vol 49, pp. 4347.

Zarook S. M., Shaikh A. A. and Ansar Z. (1997) "Development, Experimental Validation, and Dynamic Analysis of a General Transient Biofilter Model". Chem. Eng. Sci., Vol 52, pp. 759.

Zhao X., Robert F. H. and Thomas C. V. (1999) "Long-term Evaluation of Adsorption Capacity in a Biological Activated Carbon Fluidized Bed Reactor System", Water Res., Vol. 33, No.13, pp. 2983–2991.

Zhou D. Z. (2000) "Biological Treatment of Sewage Air Using a Horizontal Biotrickling Filter", Thesis for Master of Engineering, National University of Singapore.

Zilli M., Converti A., Del B. M. and Ferraiolo G. (1993) "Phenol Removal from Waste Gases with a Biological Filter by *Pseudomonas putida*", Biotechnol. Bioeng., Vol. 41, pp. 693-699.

Appendix A

Definition of performance parameters

Operation and performance of a biotrickling filter for air pollution control is generally reported in terms of removal efficiency (RE) or pollutant elimination capacity (EC) as a function of the pollutant loading (L) and gas retention time (GRT). These terms are defined as follows (Cox and Deshusses, 2000):

$$RE = \frac{C_{in} - C_{out}}{C_{in}} \times 100\% \quad \text{(A.1)}$$

$$EC = \frac{C_{in} - C_{out}}{V} \times Q \quad \text{(A.2)}$$

$$GRT = \frac{V}{Q} \quad \text{(A.3)}$$

$$L = \frac{C_{in}}{V} \times Q \quad \text{(A.4)}$$

Where

C_{in}=inlet pollutant concentration (ppmV or g/m^3)

C_{out}=outlet pollutant concentration (ppmV or g/m^3)

V=volume of packing bed (L)

Q=air flow rate (L/min)

It should be stressed that the elimination capacity, the pollutant loading and GRT are calculated using the volume of the packing bed but not the total volume of the reactor. Pollutant concentration is usually reported as mass per volume; conversion of volumetric concentration to mass concentration is done using the ideal gas law which reduces to Equation A.5 at room temperature.

$$C(g/m^3) = \frac{C(ppmV) \times MW(g/mol)}{24{,}776} \quad \text{(A.5)}$$

Where

C=pollutant concentration

MW=molecular weight of pollutant

For H_2S, to convert ppmV to g/m^3, multiply by 0.00137

For H_2S, to convert g/m^3 to ppmV, multiply by 728

For toluene, to convert ppmV to g/m^3, multiply by 0.00371

For toluene, to convert g/m^3 to ppmV, multiply by 269

The relationship between elimination capacity and pollutant loading in a biotrickling filter is shown in Figure A.1 (Cox and Deshusses, 2000). It is usual to report the performance as a function of the pollutant load rather than the concentration, which enables comparison of systems with different sizes operated under different conditions. One underlying assumption is that the performance depends only on the pollutant load, therefore, that low concentration-high flowrate conditions lead to similar elimination capacities as high concentration-low flowrate. This assumption is generally valid because the pollutant concentration commonly encountered in biotrickling filters is high enough for the micro-kinetics to be of zero order. This is no longer true at very low pollutant concentration (typically below 0.05~0.1 g/m^3) because mass transfer kinetics will prevail in the biofilm resulting in a reduction of the maximum elimination capacity.

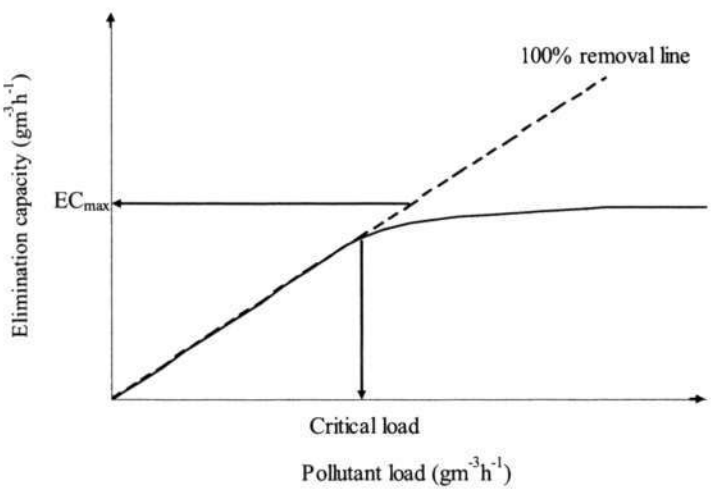

Figure A.1 Elimination capacity vs. load curve for a biotrickling filter

Examination of Figure A.1 reveals that there are essentially three operating regimes (Cox and Deshusses, 2000):

1. Low loading, also called first order regime. The elimination capacity and the loading are identical and the pollutant is completely removed. The biotrickling filter is operated well below its maximum elimination capacity. The performance increases proportionally with the loading.
2. Intermediate range. Breakthrough of the pollutant occurs. With higher inlet concentration or higher air flow rate, the elimination capacity increases, but to a lesser extent than the loading.
3. High loading, also called zero order regime. The biotrickling filter is operated at its maximum elimination capacity. Increases in pollutant concentration or of the air flow rate do not result in further increases in elimination capacity, and the removal efficiency decreases.

For the evaluation of biotrickling filter performance, both the maximum elimination capacity and the removal efficiency should be considered.

Appendix B

Costs concern

The ultimate measure for the potential success of the vapor phase biotreatment of off-gases is whether the technique will be competitive in terms of overall costs or not. Consequently, the difference among the costs concern of the three biotrickling filters was compared here. The overall costs consist of capital costs and operation costs. Capital costs comprise all system equipment and labor to build and install the reactor, including costs attributed to depreciation and interest. Operation costs arise from energy consumption, water consumption and disposal, monitoring, maintenance, and medium replacement.

Assuming that a $500m^3$ biotrickling filter is installed, the capital cost will be \$250k ($\$500/m^3$ x $500m^3$). One more water pump must be provided in the two-stage biotrickling filter; in the neutral pH single-stage biotrickling filter, chemical cost is required and the biotrickling filter volume should be larger; due to the poor removal efficiency, the volume of the low pH single-stage biotrickling filter must be much larger than those of the other two biotrickling filters. All the other parameters are set to be the same to compare the cost of the three biotrickling filters. The extra costs of the three biotrickling filters are roughly estimated here.

The two-stage biotrickling filter:

The cost for one water pump is estimated at \$1.0k. It is assumed that the equipment life would be 20 years. The cost of one year is \$0.05k. Electricity to run the recycle pump is estimated at 10kWh, so energy cost will be \$4.4k per year ($\$0.05\ kWh^{-1}$). The whole extra cost is \$4.4k/y + \$0.05k/y = \$4.45k/y.

The neutral pH single-stage biotrickling filter:

If caustic soda use is assumed to maintain the pH at neutral level, the amount will be about 40 gallons per day at \$1 per gallon = \$14.6k per year. The volume is assmed to be $700m^3$ to remain the same performance as that of the two-stage

biotrickling filter. As systems increase in volume, the increasing rate of construction cost declines. This is partly because the cost of materials will be reduced through large quantity discount purchases. The capital cost is assumed to be \$315k (\$450/m^3 x 700m^3). The capital cost added is \$315k - \$250k = \$65k (\$3.25k/y for 20 years use). The whole extra cost is \$14.6k/y + \$3.25k/y = \$17.85k/y

The low pH single-stage biotrickling filter:
To get the same performance, GRT of the low pH single-stage biotrickling filter must be about twice longer than that of the two-stage biotrickling filter according to the experimental results in Section 7.4.1. Thus, its volume will be twice larger (1000m^3). The capital cost is assumed to be \$400k (\$400/m^3 x 1000m^3). The balance is \$400k - \$250k = \$150k (\$7.5k/y for 20-year use).

The cost for extra land occupation is neglected here because it is difficult to be estimated (some WWTPs are in urban areas where the land is expensive while others have plenty of space available in rural areas). The order of the cost is \$17.85k/y (the neutral pH single-stage biotrickling filter) > \$7.5k/y (the low pH single-stage biotrickling filter) > \$4.45k/y (the two-stage biotrickling filter). A successful biotrickling filter should meet a performance level while minimizing capital and operation costs. Therefore, considering the economic cost, the two-stage biotrickling filter is still the best one compared with the other two single-stage biotrickling filters.

To reduce the operation costs, the secondary effluent from Wastewater Treatment Plants is recommended to be used as the trickling liquid for the biotrickling filter. The nutrients in the effluent water are enough for microorganisms' growth. The excess recirculation solution can be discharged directly to the influent flow of the Wastewater Treatment Plants. The normal pH of activated sludge is slightly basic (6.5~8.5). High quantity of wastewater can neutralize the waste sump water and dilute the sulphate to safe levels. Thus, the waste recirculation solution can easily be treated by the plant without any additional cost.

Appendix C

Computer program for solving the two-stage model

```
%***************************** Main ****************************
m = 0;
xs =  [0:0.01:1];
ts= [0:0.01:1.01];

solS = pdepe(m,@pdeS,@pdeicS,@pdebcS,xs,ts);
save solS;

xc= [0:0.01:1];
tc =  [0:0.01:1];

solC = pdepe(m,@pdeC,@pdeicC,@pdebcC,xc,tc);

solS(102,:,:)=[];

SH=solS(:,:,1);
ST=solS(:,:,2);
SO=solS(:,:,3);
CH=solC(:,:,1);
CT=solC(:,:,2);
CO=solC(:,:,3);
CHP=solC(:,:,4);
CTP=solC(:,:,5);

figure
surf(xs,ts,SO)
title('SO(x,t)')
xlabel('Distance x')
ylabel('Time t')
```

```
%**************************** gas phase*****************************
function [c,f,s] = pdeC(xc,tc,u,DuDx)

load solS
du1=diff(solS(:,1,1));
du2=diff(solS(:,1,2));
du3=diff(solS(:,1,3));

%*************************constants*****************************
CHi=0.1855;
CTi=0.0274;
ug=120;
AS=820.9;
H=0.5;
alpha=0.7;
muH=0.87;
muT=1.50;
v=0.37;
rohP=4.9*105;
COi=275.0;
CHi=0.1855;
CTi=0.0274;
ug=120;
AS=820.9;
H=0.5;
alpha=0.7;
muH=0.87;
muT=1.50;
v=0.37;
rohP=4.9*105;
COi=275.0;
DHA=0.0338;
```

```
DTA=0.0792;
DOA=0.2132;
DHW=1.89e-9;
DTW=1.03e-9;
DOW=2.41e-9;
fxv=0.195;
XV=100;
mH=0.42;
mT=0.27;
mO=34.4;
Kh=3.0e-3;
Kt=6.04e-3;
KO=0.26;
KH=28.8;
KT=11.03;
YH=0.925;
YOH=0.462;
YT=0.708;
YOT=0.341;
RP=0.004;
aH=8.38;
aT=2.34;
bH=0.03;
bT=0.02;
gamma1=0.7;
gamma2=0.5;

delta=3e-4;

DH=gamma1*DHA+ gamma2*2*RP*ug/v;
DT=gamma1*DTA+ gamma2*2*RP*ug/v;
DO=gamma1*DOA+ gamma2*2*RP*ug/v;
```

```
PeH=ug*H/v/DH;
PeT=ug*H/v/DT;
PeO=ug*H/v/DO;
XH=H*(1-alpha)*AS*Kh/v/ug;
XT=H*(1-alpha)*AS*Kt/v/ug;
beta1H=DHW*H*alpha*AS*fxv*KH/v/ug/CHi/delta;
beta1T=DTW*H*alpha*AS*fxv*KT/v/ug/CTi/delta;
beta2=DOW*H*alpha*AS*fxv*KO/v/ug/COi/delta;
phi1H=DHW*H*fxv/ug/delta^2;
phi1T=DTW*H*fxv/ug/delta^2;
phi2=DOW*H*fxv/ug/delta^2;
eta1H=H*muH*XV/YH/KH/ug;
eta1T=H*muT*XV/YT/KT/ug;
eta2H=H*muH*XV/YOH/KO/ug;
eta2T=H*muT*XV/YOT/KO/ug;
lambda1H=aH*rohP*(1-v)/v;
lambda1T=aT*rohP*(1-v)/v;
lambda2H=bH*CHi;
lambda2T=bT*CTi;

eposilonH=CHi/KH/mH;
eposilonT=CTi/KT/mT;
eposilonO=COi/KO/mO;
%-----------------------------------------------------------------------
tc
number=int8(tc/0.01+1);

DS1=du1(number,1);
DS2=du2(number,1);
DS3=du3(number,1);

g7= XH*(u(1)-u(5)*(2*lambda2H*u(4)-lambda1H)
```

```
/(-lambda1H*lambda1T+lambda1H*lambda2T*u(5)+lambda2H*lambda1T*u(4)));

g8= XT*(u(2)-u(4)*(2*lambda2T*u(5)-lambda1T)...
/(-lambda1H*lambda1T+lambda1H*lambda2T*u(5)+lambda2H*lambda1T*u(4)));

g4=-g7-beta1H*DS1*u(1);

g5=-g8-beta1T*DS2*u(2);

g6=-beta2*DS3*u(3);

c = [1; 1; 1; 1; 1];
f = [1/PeH; 1/PeT; 1/PeO; 0; 0].* DuDx+[-1/v; -1/v; -1/v; 0; 0].*u;
s = [g4; g5; g6; g7; g8];

%****************** Boundary conditions (gas phase) ******************
function [pl,ql,pr,qr] = pdebcC(xl,ul,xr,ur,t)

load parameters

pl = [(1/v-1)*ul(1); (1/v-1)*ul(2); (1/v-1)*ul(3); 0; 0];
ql = [1; 1; 1; 1; 1;];
pr = [ur(1)/v; ur(2)/v; ur(3)/v; 0; 0];
qr = [1; 1; 1; 1; 1];

%****************** Initial conditions (gas phase) **********************
function u0 = pdeicC(x);

load parameters

u0 = [eposilonH*(1-x); eposilonT*(1-x); eposilonO*(1-x); eposilonH*CHi;
eposilonT*CTi;];
```

```
%************************** Biofilm ******************************
function [c,f,s] = pdeS(xs,ts,u,DuDx)

g1 =u(1)*u(3)/((1+u(1))*(1+u(3)));

g2 =u(2)*u(3)/((1+u(2))*(1+u(3)));

g3 =eta2H*g1+eta2T*g2;

c = [1; 1; 1];
f = [phi1H; phi1T; phi2].* DuDx;
s = [-g1; -g2; -g3];

%********************** Boundary conditions (biofilm) ******************
function [pl,ql,pr,qr] = pdebcS(xl,ul,xr,ur,t)

load parameters

pl = [0; 0; 0];
ql = [1; 1; 1];
pr = [0; 0; 0];
qr = [1; 1; 1];

%********************** Initial conditions (biofilm) *******************
function u0 = pdeicS(x);

load parameters

u0 = [eposilonH*(1-x); eposilonT*(1-x); eposilonO*(1-x)];
```